UNIVERSITEIT GENT

FACULTY OF **SCIENCES**

Department of **Biology**

Evolutionary Morphology of Vertebrates

Structural diversity in the cranial musculoskeletal system in Anguilliformes: an evolutionary-morphological study

Part 1 - Text

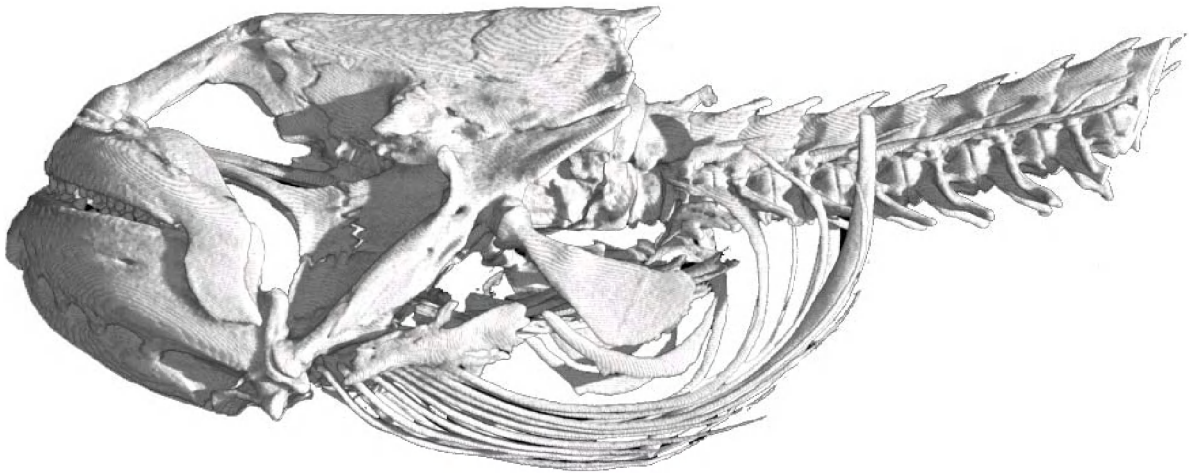

Soheil Eagderi

Thesis submitted to obtain the degree of Doctor in Sciences (Biology)

Academic year 2009-2010
Rector: Prof. Dr. Paul van Cauwenberge
Dean: Prof. Dr. Herwig Dejonghe
Promoter: Prof. Dr. Dominique Adriaens

FACULTY OF SCIENCES

DEPARTMENT OF BIOLOGY

EVOLUTIONARY MORPHOLOGY OF VERTEBRATES

Structural diversity in the cranial musculoskeletal system in Anguilliformes: an evolutionary morphological study

Part 1 - Text

Soheil Eagderi

Thesis submitted to obtain the degree of Doctor in Sciences (Biology)

Academic year 2009-2010
Rector: Prof. Dr. Paul van Cauwenberge
Dean: Prof. Dr. Herwig Dejonghe
Promoter: Prof. Dr. Dominique Adriaens

Cover image: CT scan image of the skull of *Simenchelys parasiticus*

Members of the Examination Committee

Prof. Koen Sabbe, Chairman	(Ghent University)
Prof. Dr. Dominique Adriaens, Promoter	(Ghent University)
Dr. Eric Parmentier	(University of Liège)
Dr. Natalie De Schepper	
Dr. Sam Van Wassenbergh	(University of Antwerp)
Prof. Dr. Ann Huysseune	(Ghent University)
Dr. Tom Geerinckx	(Ghent University)
Dr. Emmanuel Vreven	(Royal Museum for Central Africa)
Prof. Dr. Luc Lens	(Ghent University)

Reading committee

Dr. Eric Parmentier	(University of Liège)
Dr. Natalie De Schepper	
Dr. Sam Van Wassenbergh	(University of Antwerp)

TABLE OF CONTENTS

Acknowledgments

Acknowledgments

I wish to express my genuine and sincere gratitude to those who contributed to the process that led to this dissertation, as without their help I could not have fulfilled this task.

Infinite thanks go to my supervisor and promoter Prof. Dr. Dominique Adriaens, who gave me the opportunity to start and complete my doctoral thesis in his research group. He not only greatly increased my insight in biology, especially in the wonderful world of vertebrate morphology, but he also is a truly inspiring scientist and person. His corrections and comments, that filled all spaces between my double-lined manuscripts with different colors, not only brought my writing to a higher level, but also gave more color to my personal and scientific experience. His unfailing enthusiasm and patience could always motivate me and I truly find it hard to find proper words to express my gratitude to him.

"Thank you very much, best teacher I ever had."

I am deeply indebted to Prof. Dr. Walter Verraes for his help, especially when I arrived in Belgium.

I wish to express my thanks to Prof. Dr. Ann Huysseune for increasing my knowledge of histology.

My sincere thanks go to my colleagues in the research group 'Evolutionary Morphology of Vertebrates', Dr. Tom Geerinckx, Dr. Natalie De Schepper, Dr. Frank Huysentruyt, Dr. Stijn Devaere, Barbara De Kegel, Joachim Christiaens, Marleen Brunain, Heleen Leysen, Fatemeh Tabatabaei, Paul Van Daele, Tim Tkint, Annelies Genbrugge, Celine Ide, Emilie Descamos and Niels De Smet. They were not only colleagues, but also good friends of mine, who were always ready to help.

Several of these deserve an additional word of thank, as their assistance had an enormous and positive impact on this work:

Tom Geerinckx; thank you for your assistance, correcting my writings, providing critical comments, and helping me enthusiastically and patiently to understand morphology and experimental methods whenever I needed help.

Natalie De Schepper; thank you for your help in starting my PhD, teaching experimental methods and providing part of my material.
Frank Huysentruyt, Stijn Devaere and Heleen Leysen; thank you for sharing your time with me for answering my questions.
Barbara, Joachim and Marleen; thank you for all the practical help.
Of course, I thank all people of the third floor, especially Hilde Van Wynsberge for her assistance so often during my doctorate.
I am profoundly indebted to the members of my PhD jury: Prof. Dr. Koen Sabbe, Dr. Eric Parmentier, Dr. Natalie De Schepper, Dr. Sam Van Wassenbergh, Prof. Dr. Ann Huysseune, Dr. Tom Geerinckx, Dr. Emmanuel Vreven, and Prof. Dr. Luc Lens.
I acknowledge the following international scientists for their very useful comments: R.S. Mehta (UcDavis, USA), D.G. Smith, (Smithsonian, USA), D. Johnson (National Museum of Natural History-Smithsonian Institution) and J.G. Nielsen (Natural History Museum of Denmark, Copenhagen University).
I also acknowledge P. Pruvost (Paris Natural History Museum, MNHN), R.H. Robins and A. Lopez (Florida Museum of Natural History), M. McGrouther (Australian Museum), D. Johnson (National Museum of Natural History-Smithsonian Institution) and P.R. Møller (Natural History Museum of Denmark, Copenhagen University) for making museum specimens available to me.
I appreciate the support of my colleagues at Tehran University during my study in Belgium.
And of course my parents I can't thank enough for everything they have done to me. They did support and motivate me throughout my studies. So again mum, dad... THANKS!
Also I thank my daughter Sania for understanding that her papa should work and not to be disturbed from time to time.
And, last but not least, a huge thanks to my wife, Aram, and her family. Without Aram's help it would have been very difficult to finish this work. She kept supporting me at all times. Thank you again for everything.

Chapter 1

Introduction

Chapter one

General Introduction

1.1. General Context

1.1.1. Adaptation and diversity

A vast body of scientific effort is concerned with clarifying the evolution in various groups of organisms, with natural selection being the fundamental driving force behind it (Darwin, 1859). Survivorship is related to adaptations that can be measured as the performance of functions in the context of the interaction between an organism and its environment, such that survivorship is maintained over generations (Brock, 2000). In this process, aspects of form and function of organ (or organ system) can change. Systems that display a constant function may reflect relatively little change in its composing structures or may just change function with a new adaptation arising (Ridley, 2004). As such, many structures may arise that can be described as evolutionary novelties. Something that we recognize as novelties can arise even through the modification of existing structures (Ridley, 2004). Hence, the evolutionary origin of adaptations consists of the gradual accumulation of new or modified anatomical structures, physiological processes or behavioral traits (Solomon et al., 2005).

The head musculoskeletal system and its integration in the functioning of the skull can be considered as a highly important pattern for giving rise to evolutionary specializations by means of natural selection. The head of fishes is quite complex, with over 30 individual bony elements that can be moved by their associated muscles. Throughout evolution quite some variation originated in the cranial musculoskeletal system of fishes. Judging from that, it can be expected that many combinations of muscles and bones are possible to perform a certain function, such as those for mouth opening and closing. The head bones and relevant muscles are important elements composing the feeding and respiration apparatus.

In contrast, some characteristics of an organism are not necessarily the result of adaptative evolution but rather represent evolutionary constraints, phylogenetic predispositions or just random phenotypic variation that has no effect on

performance. Evolutionary constraints can be defined as limits to the direction, nature, rate or amount of change that is possible (Carroll, 1997a). A phylogenetic predisposition can be defined as a retained ancestral character that is shared by all members of that phylogenetic group (Mishler, 2003). For instance, body elongation of Anguilliformes can be expected to be the result of adaptive evolution, whereas this feature is to be considered a phylogenetic predisposition within the Anguilliformes families.

Body elongation has evolved many times independently and in different environmental and ecological circumstances (Ward and Brainerd, 2007), which is considered adaptive for a large range of life styles (De Schepper, 2007). The elongated body in all members of the eel families is the basic Anguilliformes body plan, but variation exists. In some eels, for example body elongation is quite extreme, e.g., the tropical moray *Strophidon sathete* (Muraenidae) (Castle, 1968).

The Anguilliformes is an order that still needs to be fully explored. Many new species of Anguilliformes are described each year (Smith and Kanazawa, 1977; Castle and McCosker, 1999; Chen and Mok, 2001; Smith and Karmovskaya, 2003; Smith, 2004), and more are expected to be recognized as various habitats are examined more closely, especially those of the deep sea.

There are a number of adaptations which may have evolved from eels with a relatively sedentary life style (Castle, 1968). Mesopelagic eels, such as Nemichthyidae, Serrivomeridae and Nettastomatidae, which inhabit the ocean depths between surface and bottom, have their own set of adaptations (such as elongated jaws and increased dentigerous areas by the forward prolongation of the snout and associated tooth-bearing bones (Böhlke, 1989a)).

As an example of trophic adaptations in eels, a few have become plankton feeders, where a predatory lifestyle represents the primitive condition of Anguilliformes (Gosline, 1971; Smith, 1989a). The so-called garden eels, of the congrid subfamily Heterocongrinae, live in colonies in fine coral sand, usually in reef areas where there is a relatively strong current. A tube is excavated in the sediment by the tail so that the animal may sink out of sight in its burrow, or hold a portion of its body out into the food-bearing current (Castle, 1968) (Fig. 1.1). The jaws of

heterocongrines are much shortened and the large eyes are placed on the tip of the snout (Castle and Randall, 1999; De Schepper et al., 2005).

Although the eel-like body form allows sustained swimming (Aarestrup et al., 2009), it is not efficient for sustained movement at high swimming speeds. This body shape allows eels wedging itself into crevices or into bottom sediments, their favorite habitats (Castle, 1968). In burrowing species, like *Moringua edwardsi* (Moringuidae) a number of adaptations of cranial structures have appeared in relation to this mode of life (De Schepper et al., 2005). For example, small gill openings positioned more ventrally may assist in preventing sediment from entering into the gill cavity (De Schepper et al., 2005).

Most eels are rapacious feeders and many display a considerable enlargement of the teeth and jaws (Castle, 1968). For example, moray eels that are found living in holes, under rocks and crevices, possess large pointed teeth on their oral jaws. In addition, they use a second set of dentigerous jaws, i.e. the pharyngeal jaws to grab and pull the prey down towards their esophagus (Mehta and Wainwright, 2007a). Also, some eels display peculiar and unique teeth, like those of *Simenchelys parasiticus* (Synaphobranchidae). In this deep water species, which is claimed to spend some of its life feeding parasitically on the tissues of other fishes, the mouth gape is reduced and is considered to be modified into an effective sucking mechanism, with chisel-like teeth on the jaws (Nelson, 2006; Robins and Robins, 1989).

Another deep water species, the gulper eel (*Eurypharynx pelecanoides:* Eurypharyngidae), is probably one of the most bizarre looking creatures within the Anguilliformes that bears extremely enlarged gapes at the tip of its eel-like body (Fig.1.1).

The diversity of eels is astounding and structural diversity in their cranial musculoskeletal system is thus to be expected. The study of such a diversity will provide information on how their structures have changed through adaptive (or non-adaptive) evolution and this may contribute to a better understanding of Anguilliformes classification and evolution.

1.1.2. Taxonomical history of Anguilliformes

The Anguilliformes, an order of teleosts, belongs to the superorder of the Elopomorpha (Nelson, 2006). The members of the Elopomorpha live in a highly diverse range of habitats, going from freshwater to saltwater and at depths ranging from the shallow continental shelf to the deep sea. The common feature of this group is the distinct pelagic larval stage, termed leptocephalus (Helfman et al., 1997; Wang et al., 2003).

Regan (1909) recognized the Anguilloides (Apoda) as distinct from other eel-like fishes because of separate premaxillaries being absent and the vomer being sutured to the ethmoid. Regan (1912) and Nelson (1966) provided more features to justify the monophyly of the Anguilliformes, including a reduced number of hyopalatine bones (hyomandibula, quadrate, and palatopterygoid remaining), elongate branchiostegals, a single pair of upper dentigerous pharyngeal tooth plates, and absence of an orbitosphenoid, posttemporal and mesocoracoid. Latter other characters such as the bone-enclosed ethmoidal commissure (Gosline, 1961), the initial fusion of the angular and retroatricular bones in the lower jaw (Forey, 1973) and crescentic nucleus in the spermatozoa (Jamieson, 1991) were presented to support monophyly of the Elopomorpha.

Greenwood et al. (1966) recognized a relationship between Anguilliformes and other members of Elopomorpha, based on the leptocephalus larval stage. These included three orders: Elopiformes (with Elopidei and Albuloidei suborders), Anguilliformes (Anguilloidei and Saccopharyngoidei suborders) and Notacanthiformes (Fig. 1.2). Although leptocephalus larvae have a forked caudal fin (resembling whitebait-like larvae) in *Megalops* and *Elops*, Tsukamoto and Okiyama (1997) opposed considering them as being derived from whitebait larvae (as occurs commonly in clupeomorphs). Hulet and Robins (1989) pointed out that the leptocephalus larval stage should be considered as an important evolutionary step in delaying or avoiding osmotic problems by fish undergoing metamorphosis in the course of their upstream migration. However, alternative hypotheses have been suggested (Pfeiler and luna, 1986; Pfeiler, 1986; Pfeiler, 1997; Pfeiler, 1999).

Nelson (1973), Forey (1973), Patterson and Rosen (1977) and Forey et al. (1996) proposed different hypothetical interrelationships among elopomorph fishes (Fig.

1.3). Also, recently published phylogenetic studies examined the elopomorph/anguilliform relationships and using molecular evidence, confirmed the monophyly of the Elopomorph fishes. They also represented the Elopomorpha to include the orders Elopiformes (Megalopidae + Elopidae), Albuliformes (Albulidae + Notacanthidae), and Anguilliformes (Anguilloidei + Saccopharyngoidei) (Obermiller and Pfeiler, 2003; Wang et al., 2003; Inoue et al., 2004; Lopez et al., 2007; Inoue et al., 2010) (Figs, 1.4, 1.5, 1. and 1.7).

Inoue et al (2004) pointed out that mitogenomic data strongly supported the monophyly of Elopomorpha, indicating the validity of the leptocephalus as an elopomorph synapomorphy. They also mentioned that the fork-tailed type of leptocephalus had originated as the common ancestor of the Elopomorpha whereas filament-tailed and round-tailed types have diversified separately in two more derived major clades.

The current classification of the anguilliform families is mostly based on the superficial (external) characters. There are few comparative studies of eels (mostly based on osteological features), such as Nelson (1966), Böhlke (1989a), Belouze (2001) and De Schepper (2007) that provide many musculoskeletal features of Anguilliformes, but they are rare dealing with this specious order. Also, the Saccopharyngoidei that include the deep sea gulper eels, are poorly known and little detailed osteological information is available. Bertin (1934), Tchernavian (1947), Bertelsen and Nielsen (1987) and Bertelsen et al. (1989) provided good accounts of the external morphology of the Saccopharyngoidei.

1.1.3. Introduction of studied taxa

The superorder Elopomorpha is the most diversified group of basal teleosts and comprises 856 species placed in three orders (Elopiformes, Albuliformes, Anguilliformes), 24 families, and 156 genera (Nelson, 2006; Inoue et al., 2004) (Table 1.1). As an introduction and background to the studied species, a brief overview is given here of the families to which they belong.

1.1.3.1. Anguillidae

The family Anguillidae or freshwater eels comprises 15 species within one genus *Anguilla* (Nelson, 2006). Representatives are found in tropical and temporal seas, except in the eastern Pacific and southern Atlantic (Nelson, 2006). This family is-

Table 1.1. Systematic overview of the superorder Elopomorpha (Nelson, 2006; Inoue et al., 2010)

Order Elopiformes (8 species):
1- Elopidae (Lady Fishes)
2- Megalopidae (Tarpons)
Order Albuliformes (29 species):
1- Albulidae (Bone Fishes)
2- Halosauridae (Freshwater Eels)
3- Notacanthidae (Spiny Eels)
Order Anguilliformes
-Suborder Anguilloidei (738 species):
1- Anguillidae (Freshwater Eels)
2- Heterenchelyidae (Mud Eels)
3- Moringuidae (Spaghetti Eels)
4- Chlopsidae (False Morays)
5- Myrocongridae (Thin Eels)
6- Muraenidae (Morays)
- Uropterygiinae (Morays)
-Muraeninae (Morays)
7- Synaphobranchidae
- Ilyophinae (Arrowtooth Eels)
- Synaphobranchinae (Cutthroat Eels)
- Simenchelyinae (Pugnose Eels)
8- Ophichthidae (Snake eels and Worm Eels)
-Myrophinae
-Ophichthinae
9- Colocongridae (Colocongers)
10- Congridae (Conger Eels)
- Congrinae
- Bathymyrinae
- Heterocongrinae (Garden Eels)
11- Muraenesocidae (Pike conger Eels)
12- Derichthyidae (Longneck Eels)
13- Nemichthyidae (Snipe Eels)
14- Serrivomeridae (Sawtooth Eels)
15- Nettastomatidae (Duckbill Eels)
-Suborder Saccopharyngoidei (26 species):
1- Cyematidae (Bobtail Snipe Eels)
2- Saccopharyngidae (Swallowers or Whiptail Gulpers)
3- Eurypharyngidae (Pelican or Umbrella-mouth Gulpers)
4- Monognathidae (Monognathids)

considered morphologically to comprise the most generalized eels of all Anguilliformes (Smith, 1989a), despite the fact that the phylogeny suggests that they are a group derived from deepwater eels (Inoue et al., 2010). Based on the following characters, freshwater eels can be distinguished (Nelson, 2006): minute scales present; gill opening crescentic, lateral; lateral line complete on body and head; pectoral fins well developed. Adult anguillids live in freshwater or in estuaries. They stop feeding at maturity, when they move from freshwater out to sea. The leptocephali move back to coastal areas, undergo metamorphosis, and enter freshwater as elvers.

1.1.3.2. Nettastomatidae

The family Nettastomatidae or duckbill eels comprises six genera, *Facciolella*, *Hoplunnis*, *Nettastoma*, *Nettenchelys*, *Saurenchelys*, and *Venefica*, with about 38 species (Smith, 1989b; Nelson, 2006). The Nettastomatidae is a family of long-snouted, eels found mainly on the outer continental shelf and continental slope of the world's tropical and warm-temperate seas (Smith, 1989b). The following characters are used to define Nettastomatidae representatives (Nelson, 2006): head and snout elongate and narrow; mouth enlarged; tail greatly attenuated; pectoral fin usually absent in adults; vertebrae usually 190–280; maximum length about 1 m. This family is poorly known.

1.1.3.3. Heterenchelyidae

The family Heterenchelyidae or mud eels comprises eight species within two genus (*Panturichthys* and *Pythonichthys*) (Nelson, 2006). These eels are found in tropical areas of the Atlantic and eastern Pacific (Nelson, 2006). Based on the following characters, mud eels can be distinguished (Nelson, 2006): pectoral fin absent; mouth large; scales absent; gill openings low on body; dorsal fin origin over gill opening; lateral line obsolete. Members of this family appear to burrow (head-first).

1.1.3.4. Synaphobranchidae

The Synaphobranchidae or cutthroat eels are found in Atlantic, Indian and Pacific oceans. This family comprises 10 genera and about 32 species within three subfamilies (Ilyophinae, Synaphobranchinae and Simenchelyinae). A brief overview of the morphological features of this family is given below (Nelson, 2006): gill openings low on body, at or below insertion of pectoral fin (this fin is absent in a

few species); vertebrae 110–205; third hypobranchial directed forward from midline, meets third ceratobranchial at a sharp angle.

Ilyophinae: Lower jaw shorter than upper; body scaleless (except in some *Ilyophis*); pectoral fin absent in some species of *Dysomma* and the monotypic *Thermobiotes*; head shape depressed and relatively rounded; some teeth relatively long.

Synaphobranchinae: Lower jaw longer than upper; body scaled (usually naked in *Haptenchelys texis*); head shape compressed and relatively pointed; teeth small and needle-like; branchial apertures confluent or only slightly separated in most; two genera, *Haptenchelys* and *Synaphobranchus*.

Simenchelyinae: Body especially slimy, with scales embedded in skin; snout blunt and rounded with terminal slit-like mouth; pectoral fin moderate in size; palatopterygoid arch (arcade) complete; one species, *Simenchelys parasiticus*. It is essentially worldwide from tropical to temperate latitudes. Little is known of its feeding habits and food.

1.1.3.5. Muraenidae

The Family Muraenidae or moray eels are found in tropical and temperate seas but some species occasionally enter freshwater. The Muraenidae comprises about 185 species classified in two subfamilies (Uropterygiinae and Muraeninae) and 15 genera (Nelson, 2006). Based on the following characters, mud eels can be distinguished (Nelson, 2006): gill openings restricted to small roundish lateral openings; lateral line pores on head but not on body; two branchial pores; gill arches reduced; fourth branchial arch strengthened and supporting pharyngeal jaws; pectorals absent; posterior nostril high in head; most with long fanglike teeth; vertebrae usually 110–200.

Uropterygiinae: Ossified hypobranchials in first and second arches; vertical fins reduced; rays confined to tip of tail; four genera, *Anarchias*, *Channomuraena*, *Scuticaria*, and *Uropterygius*.

Muraeninae: No ossified hypobranchials; vertical fins not confined to tip of tail (usually the dorsal fin origin is above the gill opening or forward); about 11 genera, *Echidna*, *Enchelycore*, *Enchelynassa*, *Gymnomuraena*, *Gymnothorax*, *Monopenchelys*, *Muraena*, *Rhinomuraena*, *Siderea*, *Strophidon*, and *Thyrsoidea*.

1.1.3.6. Congridae

The Congridae are one of the largest and most divers anguilliform family (Smith, 1989c). This family comprises three subfamilies (Heterocongrinae, Bathymyrinae and Congrinae) with 32 genera and roughly 160 species (Nelson, 2006). The Congridae are found worldwide in tropical and subtropical latitudes and occur in the Atlantic, Pacific and Indian Oceans. The following characters can be used to define the Congridae (Nelson, 2006): body shape variable; moderately stout to elongate; lateral line complete; pectoral fin usually present; branchiostegal rays 8–22; vertebrae 105–225.

Hetrocongrinae: Dorsal and anal fin rays unsegmented; pectoral fin minute or absent; body very elongate and slender; mouth short and lower jaw projecting beyond upper; two genera, *Gorgasia* and *Heteroconger*, with 25 species.

Bathymyrinae: Dorsal and anal fin rays unsegmented; pectoral fin well developed; posterior nostril below mid-eye level; five genera, *Ariosoma*, *Bathymyrus*, *Chiloconger*, *Parabathymyrus*, and *Paraconger*.

Congrinae: Dorsal and anal fin rays segmented; pectoral fin well developed; posterior nostril at or above mid-eye level; about 25 genera, e.g., *Acromycter*, *Conger*, *Gavialiceps*, *Gnathophis*, *Hildebrandia*, *Lumiconger*, *Macrocephenchelys*, *Rhechias*, *Rhynchoconger*, *Uroconger*, and *Xenomystax*.

1.1.3.7. Eurypharyngidae

The monotypic Eurypharyngidae or pelican eel is found in the bathyal zone of the tropical and temperate areas of all oceans (Böhlke, 1966; Nelson, 2006). The following characters can be used to define the Eurypharyngidae (Nelson, 2006; Bertelsen, 1989): skin black; gill openings small, closer to anus than to end of snout; only teleost with five gill arches and six visceral clefts; mouth enormous; jaws with numerous minute teeth; pectoral fins minute; caudal fin absent; caudal part compresses and less deep than trunk; vertebrae 100–125.

1.2. Aims and thesis outline

1.2.1. General aim of this study

The general aim of this work is to provide a comparative anatomical study on the structural diversity in the cranial musculoskeletal system of several representatives

of the order Anguilliformes. Hence, the goal is to document the structural patterns and evolutionary changes in their head musculoskeletal system, especially those reflecting specializations towards feeding. Regarding the common elongated body plan of these fishes, it is expected that most adaptive changes within this order may be concentrated at the level of their head musculoskeletal system.

An eel-like body form is seen in approximately 45 other fish families where it is considered a convergent feature (Gans, 1975; Lindell, 1994; Carroll, 1997b; Renous et al., 1998; Cohn and Tickle, 1999; Caldwell, 2003; Adriaens et al., 2002, Ward and Brainerd, 2007). An elongated body can be considered highly advantageous for wedging through small openings, or for burrowing. The study of De Schepper (2007) proposed that it is not body elongation but rather other morphological modifications (i.e. at the level of the cranium, sensory system etc.) that reflect the diversity of adaptation to the environment where Anguilliformes can be found. Hence, the order Anguilliformes provides an opportunity to better understand the evolutionary changes in the cranial musculoskeletal system, of which some are the adaptations to different modes of life, within a taxon with a single evolutionary origin of an eel-like body.

One of the themes of this comparative study is a consideration of the functional significance of structures in relation to different life styles. Demonstrating that traits of organisms are the result of adaptive evolution has been one of the major focuses in evolutionary biology since the time of Darwin (Mayr, 1983). For this purpose, we first need to determine what the function of a specific trait is and then it is necessary to show that individuals possessing those traits take advantage of having them. In a comparative method, it can be hypothesized that the presence of a different form of a feature from that of a closely related species may be the result of adaptive evolution (Brock, 2000). Also, a given morphological character that is advantageous for one species in a specific environment may not be an adaptive feature in another species, but rather a retained ancestral one. In addition, many organs or organ systems are able to perform more than one function (Dullemeijer, 1991); where one of these functions may arise as a new adaptation, without a marked structural change.

As many biologists advocated the explicit use of a phylogenetic framework in all comparative studies (Lauder, 1981, 1982, 1990; Felsenstein, 1985; Rieppel, 1988), also in this study the observations are discussed within a phylogenetic framework where evolutionary transformations of homologous structures can be traced (Böhlke, 1989b; Belouze, 2001; Obermiller and Pfeiler, 2003; Wang et al., 2003; Lopez et al., 2007).

In this study, those anguilliform clades considered as case studies are those that have undergone substantial changes in their head morphology, as well as those of which hardly anything was known concerning their musculoskeletal morphology. Such apparent pronounced morphological specializations can be expected to improve the potential to become adapted to a specific environment (Fisher, 1930). Also, this information can help to understand at what structural level, changes may have occurred in relation to a specific life style.

Therefore taxa were selected exhibiting marked levels of cranial specializations or specialized behavior in which the head is strongly involved. These include jaw elongation in the duckbill eel, *Hoplunnis punctata* (Nettastomatidae), head-first burrowing in *Pythonichthys macrurus* (Heterenchelyidae), parasitic feeding in *Simenchelys parasiticus* (Simenchelyinae: Synaphobranchidae), pharyngeal system for mechanical transport of captured prey in muraenids, and the extraordinarily modified cephalic system in *Eurypharynx pelecanoides* (Eurypharyngidae).

1.2.2. Outline of thesis

The body text of this thesis is divided into eight chapters.

CHAPTER 1: A general introduction is provided, followed by the goals of the study itself, in which the general aim and outline (including research questions) of this research are formulated.

CHAPTER 2: The second chapter presents an overview of the material and applied methods. More details of the methods and material for each of the specific topics studied are then listed within the corresponding chapters.

CHAPTER 3: The third chapter is the first chapter in which results are presented. The skull morphology of the poorly studied *Hoplunnis punctata* (Nettastomatidae) is described and changes in the cranial musculoskeletal associated with jaw elongation were examined. Particularly the implication for the functioning of the feeding apparatus is discussed. The central question of this part was:

- What implications may jaw elongation in *H. punctata* have had on the overall head musculoskeletal system, particularly the feeding apparatus?

CHAPTER 4: The fourth chapter focuses on the cephalic morphology of *Pythonichthys macrurus* (Heterenchelyidae).
The cranial morphology of this highly specialized fossorial eel was examined. Specializations in relation to head-first burrowing were characterised. The results are discussed in a context of adaptations to head-first burrowing in different lineage of Anguilliformes, by comparing with Moringuidae and Ophichthidae. Therefore this study tries to deal with the following questions:

- What kind of cranial specializations are related to the fossorial life style in *P. macrurus*?
- Is head-first burrowing in eels associate with a converging morphology or are there different ways to be a head-first burrower?

CHAPTER 5: In chapter five, the head musculoskeletal morphology of an alleged parasitic eel, *Simenchelys parasiticus* (Synaphobranchidae), was examined.
The cephalic features of this species show marked differences from other members of the family Synaphobranchidae, to which it is compared. These differences are described in order to evaluate to what degree the cranial morphology reflect adaptations to parasitism. Hence, this case study attempts to answer:

- What kinds of specializations define the head of the parasitic pugnose eel, *S. parasiticus*?
- And can these specializations be related to their parasitic lifestyle?

CHAPTER 6: In chapter sixth, the cephalic morphological changes in relation to the highly specialized pharyngeal jaws in muraenids is explored. The muraenids bear an

innovative feeding mechanisms that allow them to transport large prey items from the oral jaw all the way back towards the esophagus, using the pharyngeal jaws (Mehta and Wainwright, 2007a). Hence, comparing their head musculoskeletal features with a closely-related outgroup may help to reveal to what degree trade-offs may have arisen in the oral feeding apparatus, in relation to this pharyngeal transport system. As such, we would like to know:

- How may a highly specialized pharyngeal mechanical transport system in morays have affected the evolutionary changes in the head musculoskeletal system?

CHAPTER 7: The chapter seven focuses on the osteology and myology of *Eurypharynx pelecanoides* (Eurypharyngidae). This pelican eel is a enigmatic deep-sea fish that occurs at bathypelagic depths throughout the world's oceans. It's bizarre appearance results from extremely enlarged jaws, exhibiting an enormous gape. The cranial osteology and myology of *E. pelecanoides* presents a splendid example of the extreme level of changes that may have occured in the musculoskeletal system in Anguilliformes. Hence, our central questions in this case study are:

- How have the cranial musculoskeletal elements become modified during evolution in order to form that of *E. pelecanoides*?
- How can the cephalic features function in relation to its feeding behavior?

CHAPTER 8: The final chapter forms the general discussion. In this chapter, the results obtained from this thesis are integrated with data from literature, where it is attempted to explore the structural patterns of the evolutionary changes in the head musculoskeletal system in relation to different specializations, as well as showing the structural diversity in the cranial musculoskeletal system of the Anguilliformes. It is also discussed how the results of this comparative study may help to better understand evolutionary transformations as the result of adaptive and non-adaptive changes of head characteristics in Anguilliformes. Finally, based on this study, some insights for further research are discussed.

Chapter 2

Material and Methods

Chapter two

Material and Methods

2.1. Material examined

A total of 68 specimens, representing 10 species and 7 families, have been examined in this dissertation study. In addition, 8 specimens and their data, representing 4 species; *Conger conger* (Congrinae: Congridae), *Heteroconger hassi* (Heterocongrinae: Congridae), *Moringua edwardsi* (Moringuidae), and *Pisodonophis boro* (Ophichthidae), were obtained from the thesis project of De Schepper (2007) (Table 2.1). Museum specimens was examined as well as commercially obtained specimens.

The specimens used for the anatomical descriptions in chapters III-VII are listed in Table 2.1. Additional information, such as total length, method (and staining) used to study the specimens are presented in the material and methods section of the chapters III-VII.

Five specimens of *Anguilla anguilla* (Anguillidae) were commercially obtained from wild catch. The museum materials were obtained from the following collections:

USNM: Smithsonian National Museum of Natural History.
UF: Florida Museum of Natural History.
ANS: Australian Museum.
MNHN: Musée National d'Histoire Naturel of Paris.
MCZ: Harvard University, Museum of Comparative Zoology.
UGMD: Zoological Museum of the Ghent University.
NHMD: Natural History Museum of Denmark.

Table 2.1: Specimens used in chapters III-VII (CS: Cleared and stained; Ds: Dissected).

species	Source	collection nr	Number of species	Methods	chapter
Hoplunnis punctata (Nettastomatidae)	MNHN	MNHN 1965-0649	3	CS:hp2, hp1 Ds:hp3	III
Hoplunnis punctata (Nettastomatidae)	UF	UF 216386	2	Ds:hp4, hp5	III
Conger conger (Congrinae)	UGMD (De Schepper, 2007)	UGMD 53065	1	Dry skeleton	III
Conger conger (Congrinae)	commercial trade (De Schepper, 2007)		1	DS	III
Heteroconger hassi (Heterocongrinae)	UGMD (De Schepper, 2007)	UGMD 175374	2	CS:hh1 Ds:hh2	III
Pythonichthys macrurus (Heterenchelyidae)	MNHN	MNHN 1965-0640	5	CS:pm2, pm4 Ds:rest	IV
Anguilla anguilla (Anguillidae)	commercial trade		5	CS:aa1 Ds:rest	IV
Moringua edwardsi (Moringuidae)	MCZ (De Schepper, 2007)	MCZ 44686	2	me1 and 2: Cleared	IV
Pisodonophis boro (Ophichthidae)	commercial trade (De Schepper, 2007)		2	bp1: cleared Ds:bp2	IV
Simenchelys parasiticus (Simenchelyinae)	AMS	I.28736-024 I.20095-031	5	CS:sp3 Ds:rest	V
Ilyophis brunneus (Ilyophinae)	UF	UF 222355 UF 230514 UF 130897	7	CS:ib1 Ds:rest	V
Synaphobranchus brevidorsalis (Synaphobranchinae)	USNM	USNM 273427-115	3	CS:sb2 Ds:rest	V
Gymnothorax prasinus (Muraeninae)	AMS	I.28736-024 I.20095-031	4	CS:gp2 Ds:gp1, gp3	VI
Anarchias allardicei (Uropterygiinae)	AMS	I.17102-063	5	CS:aa1 Ds:rest	VI
Anarchias allardicei (Uropterygiinae)	UF	UF 318044	3	Ds: aa6, aa7	VI
Ariosoma gilberti (Bathymyrinae)	UF	UF 230612 UF 10803	16	CS:ag2 Ds:ag1,ag12	VI
Eurypharynx pelecanoides (Eurypharyngidae)	MNHN	MNHN 1980-1354	3	CS:ep2, Ds:ep1, ep3	VII
Eurypharynx pelecanoides (Eurypharyngidae)	NHMD	P2340411 P2340414 P2340415 P2340416 P2340418	5	CS:ep6 Ds:rest	VII

2.2. Methods

2.2.1. Preparation of specimens

2.2.1.1. Anaesthesia, sacrifice and fixation

Specimens of *Anguilla anguilla* were anaesthetized in a 0.001% water solution MS 222 (ethyl 3-aminobenzoic acid methanesulfonate salt – Sigma Chemical Co) and subsequently killed with an overdose of MS-222 (Procedure occurred in accordance with the Belgian law in the protection of laboratory animals (KB d.d. November 14th, 1993)). Then, specimens were fixed using a 4% buffered formalin solution (at neutral pH). This widely used fixative was additionally injected in the specimens to improve and allow steady fixation of deeper tissue. Using this fixative allowed us to apply clearing and staining method, as explained below.

2.2.2. Morphology

In order to examine the detailed morphology of soft and hard tissue structures, different procedures were applied. For studying the osteology, *in toto* cleared and stained material and data from CT-scanning were examined. Myological as well as osteological features were studied based on dissections. Additional information and details on hard and soft tissues were gathered using histological sections.

2.2.2.1. *In toto* clearing and staining

The specimens were cleared and stained according to the protocol of Hanken and Wassersug (1981) and Taylor and Van Dyke (1985) for studying the osteology (Table 2.2 and 2.3). The protocol of Hanken and Wassersug (1981) was slightly modified as the slowly active trypsine was replaced by the more aggressive potassium hydroxide (KOH), leading to equally good results (Table 2.2). In general, concentrations ranging between 0.5% and 3% were used though in large specimens concentrations up to 5% were applied. Alizarine red S (Sigma) and alcian blue 8GX (Sigma) allowed differential staining of bones and cartilage respectively. As the alcian blue 8GX had to be dissolved in ethanol and glacial acetic acid, decalcification of the bone was induced. Ossifications may be masked by this

Table 2.2. Clearing and staining procedure adapted from Hanken and Wassersug (1981).

Step	Solution/Action	Duration
Washing	tap water	24h
Cartilage Staining	alcian Blue (8GX, Sigma): 10mg in 70ml alcohol (96%) + 30 ml acetic acid	6-8h
Dehydratation	96-100% (two times alcohol renewal)	24h
Maceration	75% alcohol	2h
	50% alcohol	2h
	25% alcohol	2h
	aqua dest (two times water renewal)	4h
Bleaching	3-10% H_2O_2 in 0.5% KOH	1-2h
Washing	tap water	24h
Clearing	trypsine solution: 1-4% KOH/trypsine (0.6g in 400ml30% $NaBO_3$)	24h
	OR KOH solution: 0.5%-4%	24h
Bone staining	alizarine red (Sigma): 0.5% KOH in (0.1% alizarine red S in aqua dest)	12h
Preservation	25% glycerin + 75% 0.5% KOH	24h
	50% glycerin + 50% 0.5% KOH	24h
	75% glycerin + 25% 0.5% KOH	24h
	100% glycerin	storage

decalcification process as alizarine red S actually binds onto the calcified matrix of bone (Vandewalle et al., 1998). For that reason some specimens were stained with alizarine red S alone. The protocol of Taylor and Van Dyke (1985) avoids extensive damage from the acid cartilage stain on the bony structures by the alcohol series and the use of borax, and by using KOH instead of trypsin for the clearing (Table 2.3).

2.2.2.2. Dissections

The head of specimens were dissected for the study of both hard and soft tissue structures. Visualization of muscle fiber arrangement, insertion sites and origin was enhanced by the use of a iodium solution (Bock and Shear, 1972). For the study of cartilaginous and bony elements, dissections were also performed on cleared and stained specimens. This allowed the study of the separate elements and of those regions that were invisible in an overall dorsal, ventral and lateral view. The

specimens were examined using an Olympus SZX7 stereomicroscope, equipped with a camera lucida. Digital images were taken using an Olympus SZX9 stereomicroscope, equipped with a ColorView 8 digital camera driven by AnalySIS 5.0 software (Olympus).

2.2.2.3. Histological sections

In order to study the detailed anatomy of the head of *Simenchelys parasiticus* (Simenchelyinae), serial histological cross sections were prepared according to Taylor and Van Dyke (1985) (Table 2.4). Five µm thick sections were made using a Reichert-Jung Polycut microtome. After this, these sections were mounted onto glass slides, stained with toluidin blue (Table 2.5) and covered using DPX.

Table 2.3. Clearing and staining procedure adapted from Taylor and Van Dyke (1985).

Step	Solution/Action	Duration
Dehydratation	50% alcohol	12h
	75% alcohol	12h
	96-100% alcohol	12h
	96-100% alcohol	12h
Cartilage staining	9-30 mg Alcian Blue 8GX in 100 ml of a solution of 40% glacial acetic acid and 60% absolute ethyl alcohol	8-24h
Neutralisation	saturated borax solution ($Na_2B_4O_7.10H_2O$)	48h
Bleaching	10% H_2O_2 in 0.5% KOH	0.5h-...
Clearing	enzyme buffer solution (0.45g in 400 ml of 30% saturated borax solution)	12h-...
Bone staining	alizarin red (Sigma): 0.5% KOH in 0.1% alizarin red, until color switches from deep red to purple (stir)	24h
Further clearing	0.5-3% KOH	12h...
Preservation	25% glycerin + 75% 0.5% KOH	12h
	50% glycerin + 50% 0.5% KOH	12h
	75% glycerin + 25% 0.5% KOH	12h
	100% glycerin	storage

Examination and digital imaging of these sections was done on a Reichert-Jung Polyvar light microscope, also mounted with a ColorView 8 camera driven by AnalySIS 5.0 software (Olympus). This procedure may induce some imperfections as result of shrinking of external tissue (skin) during preparation or embedding; also minor distortion can occur in the whole section by imperfect stretching.

Table 2.4. Technovit 7100 embedding procedure.

Step	Solution/Action	Duration
Vacuum fixation	4% buffered formalin	days to weeks
Washing	tap water	8h
Decalcification	decalc (Histolab)	36h
Washing	tap water	5h
Dehydration	30% alcohol	12h
	50% alcohol	12h
	70% alcohol	12h
	96% alcohol (two times alcohol renewal)	12h
Embedding	technovit 7100 solution A	min. 24h
	technovit 7100 sulution A renewal	min. 48h
	add Technovit 7100 Harder II	12h
	place in deepfreeze	12h
Polymerization	place at room temperature (check progress)	approx. 2h
	Place in oven	1h

Table 2.5. Toluidin blue staining protocol

Step	Solution/Action	Duration
Staining	2g borax in 100 ml Aqua dest, 100 ml Aqua dest and 1g toluidin blue powder (pH = 9)	30 Sec
Rinsing	running tap water	3 min
Dring	on heating plate	3 min
Mounting	covering slide with mounting medium	
Drying	at room temperature	2 h

Table 2.6. Improved trichome staining protocol

Solution/Action	Duration
Parasolve 37°C	10 min
Parasolve room temp	2 min
Alcohol 96%	2 min
Alcohol 96%	2 min
Alcohol 70%	2 min
Alcohol 70%	2 min
Aqua dest	2 min
Aqua dest	2 min
Aqua dest	2 min
Haematoxyline	3 min
2g Haematoxylin, 100ml ethanol 96, 100ml Glycerin, 4g Potasium-aluminium sulfate ($Kal(SO_4)_2 12H2O$), 0.3 g Na-iodide (Boiling together, cooling down and adding 10 ml acetic acid)	
Running tap water	10 min
Acid fuchsine – ponceau de xylidine – orange G	10 sec. (Move)
(a) acid fuchsin: 0.5g acid fuchsin, 1ml acetic acid and 100ml Aqua dest (b) ponceau de xylidine: 0.5g ponceau de xyl, 1ml picric acid and 100ml Aqua dest (c) orange G: 0.5g orange G, 1ml acetic acid and 100ml Aqua dest Mixing 1 part (a), 2 pats (b) and 1 part (c) and making a 50% solution with Aqua dest	
Aqua dest	1 min
Aqua dest	1 min
Aqua dest	1 min
Tungstophosphoric acid hydrate	few seconds
Tungstophosphoric acid hydrate	few seconds
Aqua dest	1 min
Aqua dest	1 min
Anilineblauw – orange G – acetic acid	1 min
100 ml Aqua dest, 2.2 g Orange G, 0.5 g Aniline blue and 8 ml Acetic acid Using 1 part staining solution and 3 parts Aqua dest	
Aqua dest	1 min
Aqua dest	1 min
Acetic acid 1%	2 min
Alcohol 80%	even
Alcohol 96%	even
Alcohol 96%	even
Xylene	

To examine the histological nature of two orobranchial tongue-like appendages of *Pythonichthys macrurus*, these structures were embedded in paraffin. A series of histological sections (5 µm) was cut, stained with an improved trichrome staining protocol and mounted with DPX (Table 2.6). Images of the sections were captured using a digital camera (Colorview 8, Soft Imaging System, Munster, Germany). Also, to study the structure of the suspensorium bone

and skin around the mouth of *Eurypharynx pelecanoides*, small pieces from the hyomandibula, and buccal cavity's skin were embedded in paraffin and cut into 6 µm sections. The sections were stained with hematoxylin-eosin based on Carson and Hladik (2009).

2.2.2.4. Shape analysis

For visualization purpose, the overall shape differences between the three species; *Hoplunnis punctata, Conger conger* and *Heteroconger hassi*, was presented as deformation grids using tpsSpline (version 1.16; Rohlf, 2004a). The purpose of tpsSpline is to facilitate the comparisons of pairs of 2D configurations of landmarks. For this, 11 landmarks (Table 2.7) were digitized on one specimen of each species using tpsDig (version 2.08; Rohlf, 2005). The package tpsUtil (version 1.26; Rohlf, 2004b) was used to generate the required tps file.

Table 2.7: Definition of landmarks used for the shape analysis on the skull

Number	Definition of landmark
1	The anteriormost end of the rostral region
2	The anterior end of the maxillary
3	The anteriormost end of the interorbital space
4	The anterodorsal end of the basisphenoid which contacts the frontal in the posterior wall of the
5	The anterior end of the pterotic bone
6	The contact point of the frontal to the anterior end of the contact line of two parietals
7	The posterodorsal end of the neurocranium
8	The anterior suspensorial articulation
9	Operculo-hyomandibular articulation
10	Quadrato-mandibular joint
11	The posterior end of the maxillary

2.2.2.5. Visualization

Camera lucida: Drawings of the osteology, based on cleared and stained specimens, and myology, based on dissected specimens, were made using a stereoscopic microscope (Olympus SZX7), equipped with a camera lucida.

CT-scanning: To visualize the osteological structures of the head of *Simenchelys parasiticus* and *Eurypharynx pelecanoides,* the specimens were scanned at the modular micro-CT setup of Ghent University (Masschaele et al. 2007; http://www.ugct.ugent.be) using the directional tube head, at 80 kV tube voltage.

2.2.3. Terminology

In order to avoid misinterpretations, the terminology applied throughout this dissertation is defined below. The chosen terminologies are based on the experiences of De Schepper (2007) and comments of D.G. Smith, (Smithsonian, USA: Anguilliform Specialist) (personal communication).

Terminology of cranial skeletal elements follows that of Böhlke (1989c), Rojo (1991), De Schepper et al. (2005) and De Schepper (2007).

- Terminology used to define sutures and articulations follows Hildebrand (1995).
- The terminology for the anterior and posterior ceratohyal bones follows De Schepper et al. (2005). The frequently used terminology ceratohyal bone and epihyal bone, respectively, is not used because it suggests incorrect homologies (De Schepper et al., 2005).
- The epiotic of teleosts is considered to be an ossification of the occipital arch that has invaded the otic region and so this bone is termed "epioccipital" (Patterson, 1975).
- The angular complex is the result of a fusion of the articular with the retro-articulo-angular complex (Robins, 1989). In adult eels neither a separate angular nor a retroarticular is discernable. They generally fuse to form a single bony element. The angular with the retroarticular are observed to fuse first and later during ontogeny this complex fuses with the articular (Tesch, 2003).

- The Hyomandibula is considered as composed of a fused hyomandibula and metapterygoid (Belouze, 2001), strongly connected or even fused with the quadrate. As the homology of suspensorial elements in Anguilliformes is still ambiguous, the terminology of Belouze (2001) is followed, in which the palatopterygoid bone according to Belouze (2001), may represent the ectopterygoid of teleosts (Tesch, 2003).
- Terminology of the circumorbital bones of the cephalic lateral line system follows Böhlke (1989c), Rojo (1991) and Adriaens et al. (1997).
- Terminology of the cephalic lateral line system follows of Böhlke (1989c).
- Terminology of the chondrocranial development follows Adriaens and Verraes (1997) and Geerinckx et al. (2005).

Muscle terminology followed Winterbottom (1974) and De Schepper et al. (2005). The branchial muscles terminology followed Nelson (1967), Winterbottom (1974) and Mehta and Wainwright (2007).

Chapter 3

Head Morphology of the Duckbill Eel, *Hoplunnis punctata*

Chapter three

Head Morphology of the Duckbill Eel, *Hoplunnis punctata* (Regan, 1915; Nettastomatidae: Anguilliformes) in Relation to Jaw Elongation

Modified from:

Soheil Eagderi, Natalie De Schepper and **Dominique Adriaens** (2007).
Head morphology of a duckbill eel, *Hoplunnis punctata* (Nettostomatidae: Anguilliformes).
Journal of Morphology 268(12): 1069-1070.

Soheil Eagderi and **Dominique Adriaens** (2010).
Head morphology of the duckbill eel, *Hoplunnis punctata* (Regan, 1915; Nettastomatidae: Anguilliformes) in relation to jaw elongation.
Zoology 113(3): 148-157.

3.1. Abstract

Hoplunnis punctata, a member of the anguilliformes, is a long-snouted eel that lives in benthic habitats of the continental shelf of tropical waters of world. The purpose of this study was to examine the skull morphology of this little known nettastomatid and to understand the changes associated with jaw elongation as well as the implications of jaw elongation on the feeding apparatus. We present a detailed description of the cranial osteology and myology of *H. punctata* and how these characters differ from *Conger conger* (Congrinae: Congridae), a representative with moderate jaw length; and *Heteroconger hassi* (Heterocongrinae: Congridae), a representative with a short jaw. Shape comparison shows a caudal displacement of the hyomandibula bone, quadrate-mandibular articulation and opercle-hyomandibular joint; decrease in the depth of the neurocranium and increase in the distance between the anterior suspensorial facet and the posterior end of orbit in *H. punctata* as a result of the elongation of the preorbital region. These characteristics along with its immobile, long maxilla and well-developed adductor mandibulae complex, suggest that food may be obtained by powerful biting. Jaw elongation potentially affects the functioning of the feeding apparatus in *H. punctata* by providing more space for the olfactory rosette; increasing bite speed and reducing drag during prey capture.

3.2. Introduction

The evolution of the feeding system in fishes has been the subject of many functional morphology studies (Lauder, 1982; Ferry-Graham and Lauder, 2001a; Wilga, 2005; Westneat, 2004; Wainwright, *et al*, 2007). Difference in feeding mode may be reflected in different morphological specializations of the head, in relation to different functional demands (Wainwright and Bellwood, 2002). A morphological comparative analysis of the cephalic region in its proper phylogenetic context, can then allow a better understanding of the morphological changes, leading to extensive morphological specialization. This may then also allow a better understanding of the implication on the performance as changes occur. One aspect related to this is the elongation of the rostral region and jaw length, which originated as the result of a convergent evolution among many teleost lineages (Westneat, 2004). The anguilliform fishes have adapted to diverse life styles, which may be linked to the wide range of cranial morphologies. This cranial variation, with associated muscles, can be expected to largely reflect evolutionary patterns of feeding specialization in the Anguilliformes. We use an evolutionary perspective to compare the feeding apparatus of three species of the anguilliforms to better understand the changes involved with elongating the jaws.

The Nettastomatidae or duckbill eels are a group of long-snouted eels, mainly found on the outer continental shelf and continental slope of the tropics. Little is known about their biology, except for their benthic habits. They are non-burrowing or crevice-dwelling eels, feeding on a variety of small fishes and invertebrates (Smith, 1989b).

This study was conducted to understand the morphological peculiarities of the skull associated with jaw elongation and the resulting implications for the feeding apparatus in the duckbill eel, *Hoplunnis punctata*. We provide a detailed description of the cranial osteology and myology of *H. punctata* and its differences with that of representatives of two closely related anguilliform subfamilies: *Conger conger* (Congrinae: Congridae), with a moderate jaw length; and *Heteroconger hassi* (Heterocongrinae: Congridae), with a short jaw length. The Nettastomatidae together with the Congrinae, Muraenesocidae, Heterocongrinae and Derichthyidae

form a monophyletic group and the Notacanthiformes, a closely-related elopomorph taxon with a short jaw, is considered as outgroup (Wang et al., 2003; Fig. 3.1).

3.3. Material and methods

For anatomical descriptions, five alcohol-preserved specimens of *Hoplunnis punctata* obtained from the Musée National d'Histoire Naturel of Paris and Florida Museum of Natural History (MNHN 1965-0649 and UF 216386) were examined. The specimens were of the following size range (Standard Length (SL), distance from the tip of the snout to the end of the caudal peduncle) HP1: SL= 365 mm; HP2: SL= 314 mm; HP3: SL= 311 mm; HP4: SL= 598 mm and HP5: SL= 531 mm. Two specimens were cleared and stained according to the protocol of Hanken and Wassersug (1981) for studying the osteology. For the dissections, muscle fibers were stained according to Bock and Shear (1972). Specimens were studied using a stereoscopic microscope (Olympus SZX-7) equipped with a camera lucida. Strictly, for visualization purpose, the overall shape differences observed between the three species is presented as deformation grids using tpsSpline (version 1.16; Rohlf, 2004a) (see chapter 2: Table 2.7). The specimens used were from the Zoological Museum of the Ghent University (*Conger conger*; UGMD 53065) and 3D Pictures of *Heteroconger hassi* provided by De Schepper (2007).

The terminology of cranial bones follows Böhlke (1989c). The terminology for the anterior and posterior ceratohyal bones follows De Schepper et al. (2005). The frequently used terminology ceratohyal bone and epihyal bone, respectively, is not used because it suggests incorrect homologies. Musculature terminology follows Winterbottom (1974) and De Schepper et al. (2005). The cranial osteology and myology of *Heteroconger hassi* and *Conger conger* have already been described by De Schepper, et al. (2007) and De Schepper (2007), respectively.

3.4. RESULTS

3.4.1. Cranial Osteology of *Hoplunnis punctata*

The neurocranium is elongated with a forward prolongation of the premaxillo-ethmovomeral complex, which consists of the premaxilla, ethmoid and pars vomeralis (Fig. 3.2a, b). The olfactory organ of *H. punctata* fills the long olfactory

fossa, which is spread almost over the entire preorbital region. The pars vomeralis of the premaxillo-ethmovomeral complex laterally forms a crest to which the anterodorsal edge of the palatopterygoid is connected. The pars vomeralis of the premaxillo-ethmovomeral complex bears one row of enlarged, strongly pointed piercing teeth (Figs. 3.2b and 3.3a).

The orbital region is comprised of the frontals, basisphenoid, pterosphenoids and parasphenoid. The frontals expand laterally creating shelves over the orbits. The anterolateral corners of these shelves are pointed forward and each bear two pores for the supraorbital canal (Fig. 3.2a). The frontals enclose the opening of the supraorbital canal at the level of the anterodorsal margin of the orbits (Fig. 3.2a). The frontals have fused and bear a ridge at the midline (Fig. 3.2a). The unpaired basisphenoid has a process that barely extends into the orbit (Fig. 3.3a). The well-developed optic foramen is present between the basisphenoid and frontal bones (Fig. 3.2b). The pterosphenoids form the lateroposterior part of the postorbital region. The pterosphenoid is attached to the basisphenoid, parasphenoid, sphenotic, pterotic and frontal. The olfactory foramen is present between the pterosphenoid and basisphenoid (Fig. 3.2b). The parasphenoid, which is connected to the basisphenoid, is a long shaft of bone that extends from the toothed pars vomeralis bone of the premaxillo-ethmovomeral complex up to the basioccipital. It forms the ventral surface of the neurocranium and is narrow under the orbits.

The otic region comprises of the pterotics, sphenotics, parietals, prootics and epiotics. The pterotics form the major lateral longitudal brace of the skull and comprises of two parts. The superficial portion is tubular, and is anteriorly connected to the opening of the supraorbital canal that is formed by the frontal. The tubular portion of the pterotic forms a canal enclosing the cephalic lateral line system. The deeper part, forming the basis for the tubular portion, slightly overlaps with the surrounding bones. Posteriorly the pterotic bears the posterior suspensorial articulatory facet. The posterior border of the pterotic passes slightly the posterior margin of the supraoccipital. The sphenotic is directed ventroanteriorly and bears an extensive sphenotic process (Fig. 3.2a, b). Medially the sphenotic process bears the lateral part of the anterior suspensorial articulatory facet. The large parietal bones are fused and are situated posteriorly against the frontals. The frontal ridge

is continuous with a parietal ridge in the midline. This ridge is the origin for the A2βp and A2βa subsections of the adductor mandibulae muscle complex, which pass laterally over the parietal and hyomandibula. The prootic forms the anterior part of the otic bulla. The posterior end of the prootic is attached to the basioccipital and laterally attaches to the pterotic (Fig. 3.2b). The posterior rim of the pterophenoid is covered by the anterior rims of two prootic bones and these two bones meet each other in the midline above the parasphenoid bone (Fig. 3.2b). The suture between the basioccipital and prootic is interdigitating (Fig. 3.2b). The jugular foramen is present on the anterior part of the prootic (Fig. 3.2b). The trigemino-facial foramen is posterior to the jugular foramen (Fig. 3.2b). The epiotics form the posterodorsal face of the cranium and medially contact the supraoccipital (Fig. 3.2a).

The occipital region is comprised of the supraoccipital, exoccipitals and basioccipital. These three bones form the posterior wall of the neurocranium. The supraoccipital is surrounded by the epiotics, parietals and exoccipitals and bears a small median crest (Fig. 3.2a). Caudally, the exoccipitals are domed and dorsally border the foramen magnum. Also, the exoccipitals ventrally connects to the basioccipital. The big occipital condyle of the basioccipital forms the posterior end of the neurocranium. It forms the ventral margin of the foramen magnum. The basioccipital bone extends anteriorly to the posterior border of the prootics and forms the posterior part of the otic bullae.

The nasal, a long bone, possesses a broad wing at the rear of its tip (Fig. 3.4a). It encloses the anterior part of the supraorbital canal. The single infraorbital is a long, tube-shaped bone. The infraorbito-premaxillo-ethmovomeral ligament connects the anterior end of the infraorbital bone to the premaxillo-ethmovomeral complex. Furthermore the maxillo-premaxillo-ethmovomero-infraorbital ligament connects the posterior end of the infraorbital to the posterodorsal side of the maxillary. The infraorbital encloses the body of the infraorbital canal and its posterior part curves dorsally (Fig. 3.4b).

The maxillary is ankylosed anteromedialy to the premaxillo-ethmovomeral complex (Fig. 3.3a). The primordial ligament connects the posterior edge of the maxillary to the posterolateral face of the mandibular (Fig. 3.5a). The maxillo-premaxillo-

ethmovomero-infraorbital ligament connects the posterodorsal face of the maxillary to the posterior part of the infraorbital and the posterior part of the ventral crest of the premaxillo-ethmovomeral bony complex (Fig. 3.5a). The maxillary bears a row of small, pointed teeth on its anterior half and a double row of smaller teeth on its posterior half (Fig. 3.6a). The lower jaw is slightly shorter than the upper jaw (Fig. 3.3a). The dentary complex is elongated and its coronoid process is connected to the angular complex. The mandibular teeth are arranged in two rows, with the medial row comprising caniniform teeth that are larger than the ones in the lateral row (Fig. 3.6b). The angular complex consists of the fused angular and articular, bearing a small retroarticular process. The angular complex possesses a posterior process behind the meckelian fossa (Fig. 3.6b). The retroarticular process is directed caudomedially.

The suspensorium is comprised of five elements: the hyomandibula, quadrate, palatopterygoid, preopercle and a cartilaginous element where the symplectic bone would be found (Fig. 3.3b). The preopercle is described as part of the opercular series (see below). The cartilaginous element of the suspensorium is situated ventral to the hyomandibula (Fig. 3.3b). The hyomandibula and quadrate are closely connected and form a solid structure. The hyomandibula articulates dorsally with the neurocranium via two articular condyles. The anterior one fits into a socket formed by the sphenotic and pterotic, whereas the posterior one fits into a facet on the pterotic. The lateral face of the suspensorium has an elevated ridge for the origin of the A2αv and A3 subsections of the adductor mandibulae muscle complex and insertion of the levator arcus palatine muscle. The opercle articulates with a condyle on the posterior edge of the hyomandibula (Fig. 3.3b). The palatopterygoid is attached to the anterior edge of the quadrate by connective tissue, and it is firmly connected to the lateral face of the premaxillo-ethmovomeral complex, at the caudal face of the maxillo-ethmovomeral articulation facet. The palatopterygoid ligament also connects the suspensorium to the palatopterygoid (Fig. 3.3b).

The opercular series is comprised of four bones: the preopercle, interopercle, subopercle and opercle (Fig.3.7a). The distal margins of the opercular bones were lightly stained in the specimens studied. The medial face of the anterior process of the preopercle is connected to the lower jaw through the angulo-preopercular

ligament. The two preopercular pores are present on the dorsal rim and anterior process of the preopercle, respectively. The interopercle is triangular in shape and is covered laterally by the posterior portion of the preopercle. The interopercle is connected to the angular complex via the angulo-interopercular ligament. The subopercle abuts against the caudal edge of the interopercle and curves along the entire posterior margin of the opercle. The subopercle is attached to the opercle by connective tissue. The fan-shaped opercle articulates with the opercular condyle of the hyomandibula through its anterior process (Fig. 3.3b). The operculo-interopercular ligament connects the medial face of the anterior process of the opercle to the dorsomedial face of the interopercle (Fig. 3.3b).

The hyoid complex consists of the unpaired, long cylindrical basihyal, spatulate urohyal, paired anterior ceratohyals and paired posterior ceratohyals (Fig. 3.7b, c). The posterior part of the urohyal expands vertically and is blade-like in its lateral aspect. The anterior ceratohyals are the largest elements of the hyoid arch, which articulate with the urohyal. The anterior ceratohyal is interdigitated posteriorly with the posterior ceratohyal. Two of seven branchiostegal rays are connected to the anterior ceratohyal and the others to the posterior ceratohyal. The branchiostegal rays curve dorsally along the ventral border of interopercle. They reach up to the caudal border of the subopercle. The posterior ceratohyals are connected to the suspensorium and angular complex by two ceratohyalo-hyomandibular and ceratohyalo-angular ligaments, respectively (Fig. 3.7c).

3.4.2. Cephalic lateral line system

The cephalic lateral line system is comprised of the supraorbital canal, adnasal canal, infraorbital canal, temporal canal, preoperculo-mandibular canal and supratemporal commissure. The supraorbital canal extends from the tip of the snout to the interorbital region, and bears fourteen pores. The adnasal canal, a short ascending branch of the infraorbital canal, starts at the rear of the anterior nostril. The infraorbital canal curves dorsally into the postorbital region. This canal bears four pores exiting from infraorbital and five pores on the postorbital region. The preoperculo-mandibular canal starts almost from the rostral tip of the dentary and its anterior part runs in an inferior crest of the dentary complex. This canal

curves dorsally into the postorbital region and enters into the posterior end of the temporal canal (Fig.3. 4b). The supratemporal commissure connects the right and left cephalic lateral line system. The ethmoid canals were not observed.

3.4.3. Cranial myology of *Hoplunnis punctata*

The large adductor mandibulae muscle complex is comprised of the sections A2 and A3. Despite a small and indirect connection between tendon A2αv and the maxillary via the primordial ligament (which could suggest a homology with A1), this subsection was termed A2αv based on the terminology of Winterbottom (1974) and due to its main insertion being onto the posteromedial face of the lower jaw (Fig. 3.5a). The section A2 can be subdivided into four subsections: A2β anterior, A2β posterior, A2α dorsalis and A2α ventralis (Fig. 3.5a). The subsection A2βp is the largest portion of the adductor mandibulae muscle complex and originates musculously from the supraoccipital, epiotic, parietal and frontal. It inserts tendinously onto the dorsomedial edge of the coronoid process and the anterior portion of the meckelian fossa. The subsection A2βa originates musculously from the frontal and parietal, and inserts tendinously onto the medial face of the coronoid process. The posterior portion of the subsection A2βa lies medial to the anterior portion of the subsection A2βp. The subsections A2βa and A2βp are attached laterally to a single tendon of A2β. The subsection A2αd originates musculously from the posterolateral face of the hyomandibula and the posteroventral face of the pterotic. It inserts tendinously onto the dorsomedial edge of the angular complex. The superficial portion of the subsection A2αv originates musculously from the anterolateral face of the preopercle, with its medial fibers attaching musculously to the hyomandibula and quadrate. The subsection A2αv inserts through a tendon onto the posteromedial face of the angular process and musculously on the medial face of this process. A section Aω was not observed.

The section A3 is situated medial to the subsection A2β and covers the dorsolateral face of the levator arcus palatini muscle and the posterior portion of the adductor arcus palatini muscle (Fig. 3.5b). This section originates musculously from the lateral ridge of the hyomandibula, the ventral face of the sphenotic, the anteroventral face of the pterotic, the dorsolateral side of the pterosphenoid and

the posteroventral face of the frontal's lateral expansion. It inserts tendinously into the meckelian fossa. The section A3 slightly bulges laterally at the level of its vertical midline.

The levator arcus palatini muscle originates musculously and tendinously from the ventral face of the sphenotic process and the dorsolateral faces of the prootic (Fig. 3.5c). This muscle bulges slightly in the midline. It inserts musculously on the anterior face of the lateral ridge and the ventrolateral face of the hyomandibula.

The adductor arcus palatini muscle originates from the ventrolateral face of the parasphenoid, the ventrolateral face of the basisphenoid, the ventral face of pterosphenoid and the anterolateral face of the prootic (Fig. 3.5c). It fills the posterior part of the fissura infraorbitalis and inserts musculously on the caudomedial surface of the palatopterygoid and the medial face of the hyomandibula. A thick posterior portion of the adductor arcus palatini muscle could be discriminated based on a discrete change in thickness from an anterior thin part, but two parts still forming a continuous muscle sheet. The thicker portion of the adductor arcus palatini muscle runs up to the medial face of the hyomandibula. The fibers of the posterior part of the adductor arcus palatini muscle take up the position where the adductor hyomandibulae muscle would be found.

The levator operculi muscle originates tendinously from the caudal margin of the pterotic. Its fibers are directed caudoventrally and diverge, inserting musculously on the dorsal part of the lateral face of the opercle (Fig. 3.5a, b).

The adductor operculi muscle originates musculously from both the posterior part of the pterotic and the exoccipital. Proximally, its fibers run continuously with the fibers of the levator operculi but insert on the dorsomedial surface of the opercle (Fig. 3.5c).

The dilatator operculi muscle is situated posterior to the levator arcus palatine muscle and the section A3. The dilator operculi muscle is a triangular muscle, with the apex pointing caudoventraly (Fig. 3.5b). This muscle originates musculously from the posteroventral face of the sphenotic and the posterolateral face of the pterotic. The dilatator operculi muscle inserts tendinously on the small process, which is situated on the dorsal side of the anterior process of the opercle (Figs. 3.5c and 3.7a).

Two separate halves (right and left) of the protractor hyoidei muscle connect the lower jaw to the hyoid arch. Each of these portions originates tendinously from the medial face of the dentary at the rear of the dentary symphysis and inserts by means of a tendon on the dorsal surface of the posterior ceratohyal (Fig. 3.5d).
The sternohyoideus muscle originates musculously from the lateral surface and tendinously from the antroventral face of the cleithrum bone, with some of its fibers merging with those of the hypaxial muscle. The sternohyoideus is a bipinnate muscle and the posterior fibers of the left and right halves attach via a central tendon on the posterior end and ventral face of the urohyal. The anterior fibers of left and right halves of the sternohyoideus muscle attach musculously on the lateral sides of the posterior part of the urohyal (Fig. 3.5d).
The hyohyoideus muscle complex in teleosts generally includes three components: the hyohyoideus inferioris, hyohyoideus abductor and hyohyoidei adductors. However, in *H. punctata* these muscles are undifferentiated and merged as a thin sac-like muscle sheet meeting its counterparts at the ventral midline. The ventral fibers of the hyohyoideus muscle complex attach to the dorsal face of the branchiostegal rays. This sac-like muscle connects to the medial face of the opercle and reaches dorsally up to the horizontal septum.
The epaxial musculature attaches to the exoccipitals, pterotics and supraoccipital. The hypaxial musculature attaches to the basioccipital.

3.4.4. Shape analysis

The deformation grids in Figure 3.8 clearly show a distinct elongation of the preorbital region, including the snout, lower jaw and maxillary bone going from *Conger conger* and *Heteroconger hassi* to *Hoplunnis punctata* (Fig. 3.8). This elongation then results in the quadrate-mandibular articulation being positioned well to the back in *H. punctata* and *C. conger*, up to the posterior region of the orbit, whereas this joint is situated at the midpoint of the orbit in *H. hassi.* The deformation grids also indicate a more dorsal position of this articulation, reflecting a relative decrease in depth of the suspensorium in *H. punctata* compared to the other two. The same decrease in depth is also observed in neurocranium.

The distance between the anterior suspensorial facet and the posterior end of the orbit is larger in *H. punctata,* this in relation to a reduction of the orbit size and a backward displacement of the hyomandibula.

The anterior end of the pterotic is extended substantially in *C. conger* and forms a small shelf over the posterior part of the orbit, but in *H. punctata* and *H. hassi* it is situated in the postorbital region. Such a shelf is absent in *H. hassi* and is formed rather by the lateral expansion of the frontal in *H. punctata*. The opercle-hyomandibular joint is also positioned caudal to the posterior edge of the neurocranium in *H. punctata* (Fig. 3.8).

3.5. Discussion

3.5.1. Morphological changes towards jaw elongation:

Hoplunnis punctata and *Conger conger* are active predators, whereas *Heteroconger hassi* lives in burrows and projects the front portion of the body from the burrow to feed on zooplankton (Casimir and Fricke, 1971; Smith 1989a). *Conger conger* is a nocturnal predator feeding on fishes, crustaceans and cephalopods (Bauchot and Saldanha, 1986). *Heteroconger hassi* feeds on the plankton-loaded currents by snapping and picking small zooplanktonic particles (Smith, 1989a; Vigliola et al., 1996; Castle and Randall, 1999; De Schepper et al., 2007), whereas *Hoplunnis punctata* is a benthic fish and feeds on small fishes and invertebrates (Smith, 1989b).

Comparison of morphological structures with different configurations, particularly in a phylogenetic context may help the proper understanding of morphological evolutionary changes within functional units. Hence, the morphological differences on the head of the representatives with long (*H. punctata*), moderate (*C. conger*) and short (*H. hassi*) jaw lengths, used in this study, may allow a better understanding of the morphological changes toward the elongation of the rostral region and jaws.

3.5.1.1. Osteology: The long preorbital region of *H. punctata* and moderate one in *C. conger* differs in shape from that in *H. hassi*, which possess a particularly short one (Fig. 3.8). The frontals of *H. punctata*, *C. conger* and *H. hassi* are fused into a

single unit, just as in the Derichthyidae (Robins, 1989) and Muraenesocidae (Smith, 1989c), which is considered a derived character in Anguilliformes (Belouze, 2001). There is no frontal shelf over the eyes and frontal ridge in *H. hassi* and *C. conger*, unlike in *H. punctata*. The parietals have not fused in *C. conger* and *H. hassi*, but a fusion is observed in *H. punctata*. The fusion of parietals is a unique character state in Anguilliformes (Belouze, 2001). The conical mandibular and vomeral teeth of *H. punctata* are large and sharp, whereas those of *H. hassi* are small. The teeth of upper and lower jaws in *C. conger* are arranged in a double row, with big incisiform outer teeth and small inner ones. The posterior edge of the supraoccipital crest does not reach the posterior edge of the skull in *H. punctata* while that of *C. conger* reaches beyond the posterior edge of the skull. This crest is absent in *H. hassi*. Absence of the supraoccipital crest is a plesiomorphic condition which is seen in fossil Anguilliformes (Belouze, 2001).

The quadrate and hyomandibula of *H. punctata* and *C. conger* are strongly connected and form a solid structure. These two bones seem slightly mobile in *H. hassi* with respect to each other, since they move somewhat when are pressed by forceps. There is no symplectic in *C. conger*, but a cartilaginous element is present posterior to the quadrate in *H. hassi* and ventral to the hyomandibula in *H. punctata*. A posterocaudal process of the subopercle is connected to the caudal border of the opercle in *H. punctata* and *C. conger*, while in *H. hassi* this process is lacking.

3.5.1.2. Myology: The adductor mandibulae muscle complex of *H. punctata* and *C. conger* is greatly enlarged compared to that of *H. hassi*. De Schepper et al. (2007) mentioned that the expansion of the adductor mandibulae muscle of *H. hassi* may have been restricted by its large eyes. The adductor mandibulae muscle complex comprises sections A2 (with one subsection), A3 and Aω in *H. hassi*. In *C. conger*, a medial subsection A2β and lateral subsection A2α are found, as well as two subsections of A3 that insert on the medial face of the mandibular by a single tendon (Fig. 3.9). The Aω section of the adductor mandibulae muscle, which is found in most major osteichthyan groups (Diogo et al., 2008), is not present in some species in all groups within the Teleostei (Nakae and Sasaki, 2004; Hertwig,

2008). Hence, the presence of section Aω in *H. hassi* may be a retained plesiomorphic character, but in the current absence of additional myological data of other anguilliform taxa, this needs to be confirmed. The presence of an intermandibularis muscle and differentiated hyohyoideus inferioris muscle are two features in *H. hassi* that are not found in *H. punctata* and *C. conger*. The shape comparison of the skull of the three species studied shows a relatively longitudinal and latitudinal stretching of the suspensorium and postorbital region in *H. hassi*. In relation to this elongation, the adductor arcus palatini muscle in *H. hassi* is prolonged rostrally up to the anterior portion of the orbit.

The adductor hyomandibulae muscle is present as a separate muscle in *H. hassi*. This muscle has been reported in *C. conger* by De Schepper (2007), lying medial to the adductor arcus palatine muscle. It has been described as "difficult to distinguish" (De Schepper, 2007). It seems that this muscle has a configuration similar to the one described here for *H. punctata*. It is, therefore, morphologically an adductor hyomandibulae. In generalized, lower teleosts the adductor arcus palatini muscle connects the prootic to the dorsomedial face of the hyomandibula (Winterbottom, 1974). Based on Winterbottom (1974), the term adductor arcus palatini is applied to a muscle that has expanded anteriorly along the floor of the orbit, as is seen in *H. punctata* and *C. conger* and an adductor hyomandibulae muscle is only distinguished by the presence of separate anterior adductor arcus palatine muscle.

3.5.1.3. Jaw elongation: Substantial differences in the length of the rostral region and jaw length can be observed between representatives of the monophyletic group comprising the Heterocongrinae-Derichthyidae clade (clade A) and the Congrinae-Muraenesocidae-Nettastomatidae clade (clade B) (Fig. 3.1). The members of clade A possess a short to moderate preorbital region and those of clade B a moderate to long one, as seen in *H. punctata*. In clade B, especially Muraenesocidae and Nettastomatidae possess a substantially elongated preorbital region (Smith, 1989c).

Regarding the plesiomorphic condition of Anguilliformes for having a short rostral region (Belouze, 2001), as is seen in many Anguilliformes, and considering the

phylogenetic relationship of the Congrinae, Muraenesocidae and Nettastomatidae (Robins, 1989; Smith, 1989b; Wang et al., 2003; Obermiller and Pfeiler, 2003; Lopez et al., 2007), the elongation of jaws in the clade B should be considered as a derived character.

Presence of a separate premaxillary (median unit) in *Derichthys serpentinus* (Derichthyidae), a member of clade A, is a unique attribute among the Anguilliformes (Robins, 1989). Robins (1989) mentioned the trend in Derichthyidae towards a fusion of the premaxillaries with the ethmoid to form the premaxillo-ethmovomeral complex. Some derichthyid species such as *Nessorhamphus ingolfianus* bear a moderate snout with the premaxillaries fused to the ethmoid (Robins, 1989). Furthermore, *H. hassi* possesses a very short rostral region, which does include a premaxillo-ethmovomeral complex. Differences in the preorbital elements of clade A and B indicate that the formation of a premaxillo-ethmovomeral complex in clade A should not be considered as reflecting the ancestral condition leading towards snout elongation in clade B. Hence, based on parsimony criterion, it would be easy to conceive an evolutionary trend toward a separation of the premaxillary from a premaxillo-ethmovomeral complex in *D. serpentinus*.

3.5.2. Functional considerations of snout elongation

The observed differences in the feeding apparatus of these anguilliforms, especially those related to jaw elongation, can be considered having a potential influence on the functionality of this apparatus. However, this would require performance testing to empirically support this hypothesis (Arnold, 1983).

The maxillary in *Hoplunnis punctata* is connected firmly to the premaxillo-ethmovomeral complex along most of its length, while in *Heteroconger hassi* only the anterior portion of the maxillary is resting on this bony complex. This configuration of the maxillary in *H. hassi*, combined with the forward position of the quadrate-mandibula joint, result in a small and more oblique mouth border, which has been regarded as a specialization for snapping planktonic prey (Rosenblatt, 1967). This specialization in *H. hassi* may then compensate for the lacking of upper

jaw protrusion due to the immobility of the premaxillary (being fused to the ethmoid and vomer).

The posterior position of the quadrate-mandibular joint in *H. punctata* results in a large mouth with a longer lower jaw that may allow a rapid mouth closing (see below). The relatively narrow and low skull in *H. punctata* implies a shallow orobranchial chamber, which along with its immobile, long maxillaries suggests that food may be obtained by biting rather than by filtering or engulfing through suction feeding (Schaeffer and Rosen, 1961). Fishes that rely on high-velocity lunges followed by biting, rather than suction, exhibit longer strike times (Porter and Motta, 2004; Mehta and Wainwright, 2007b), and the kinematics of benthic biters appear to be typically slower than for suction feeding (Alfaro et al., 2001; Rice and Westneat, 2005; Konow and Bellwood, 2005). Biting may represent an important behavioural adaptation enabling predators to subdue large prey (Mehta and Wainwright, 2007b). It is thus not surprising to find a wide range of morphologically diverse biters (Westneat 2004; De Schepper et al., 2008; Grubich et al., 2008; Mehta, 2009).

The strongly developed adductor mandibulae muscle complex of *H. punctata* and *C. conger*, compared to a rather small one in *H. hassi*, also suggests their prey capturing mode occurs using biting. Enlarged adductor mandibulae muscles may allow a powerful bite force by increasing the mechanical load on skeletal elements such as dentary complex, suspensorium and neurocranium (Herrel et al., 2002; Van Wassenbergh et al., 2004). A predatory life style is considered the plesiomorphic condition for the Anguilliformes (Gosline, 1971; Smith, 1989a), with hypertrophied jaw muscles being common (Böhlke et al., 1989).

The maxillaries of the Anguilliformes are tightly joined to the cranium and are immobile or can move very little (Eaton, 1935). Hence, the lower jaw is considered as the sole contribution of jaw rotation, with the quadrate-mandibular joint working as a fulcrum (Alexander, 1967; Westneat, 2004). Based on the velocity advantage (small input/output lever ratio), a long lower jaw may result in a faster mouth closing (biting speed), which would be an advantage for a predator feeding on elusive prey. Simultaneously, this low ratio also implies a lower mechanical advantage. Hence, having a high input force generated by hypertrophied adductor

mandibulae muscles, as seen in *H. punctata* and *C. conger*, can compensate this deficiency and produce sufficiently high biting forces during snapping bite movements.

Elongation of the rostral region that comprise a deep lateral fossa as olfactory chambers, provide more space for the olfactory rosette in benthic *H. punctata*, which is also substantially long and large. Related to this, an improved olfaction would benefit their predatory life style to detect prey. The size of the rosette is proportional to the fish's ability to smell, and the broadly spaced nares provide a significantly greater separation between the olfactory rosettes, which could lead to an enhanced ability to resolve odor gradients (Kajiura et al., 2005).

Elongation of the jaws along with the reduction of the suspensorium and neurocranium depths i.e. reduction of the head diameter such as in *H. punctata* may also provide a hydrodynamic advantage for drag reduction during feeding strikes and swimming. Fish (1998) pointed out that departure from a smoothly rounded head in a number of aquatic animals that have anterior projecting beaks, bills, and rostrums, may be related to a better function of their feeding morphology requiring grasping jaws. The alternating concave and convex profile of the anterior part of the body, which is seen in aquatic animals with projecting anterior structures, may induce a stepwise, gradual drag pressure change that can reduce skin friction in animals during swimming (Bandyopadhyay, 1989; Bannasch, 1995; Bandyopadhyay and Ahmed, 1993). The relatively small surface area of the anterior projection can also decrease drag in conjunction with a reduced pressure gradient during swimming (Kramer, 1960; Videler, 1995).

The cranial anatomy of *H. punctata* shows a number of different features compared to the studied short snouted species, which may be related to the observed elongation of the snout. Also, some features may reflect differences in prey capturing behavior, such as large and sharp piercing teeth on the pars vomeralis and mandibular bones, depth and anteriorly reduction of the suspensorium, enlarged adductor mandibulae muscle complex, reduction of neurocranial depth and posterior position of the quadrate-mandibular joint. The jaw elongation can assemble some advantages such as providing more space for the olfactory rosette,

increasing velocity advantage (biting speed) and drag reduction to promote the prey capture kinematics as a benthic biter predator.

Acknowledgments:

We thank D.G. Smith, (Smithsonian, USA) and R Mehta (UcDavis, USA) for their valuable comments. We thank P. Pruvost (Paris Natural History Museum, MNHN), R. H. Robins and A. Lopez (Florida Museum of Natural History) for making museum specimens available and N. De Schepper (UGent, Belgium) for providing 3D pictures of *Heteroconger hassi*.

Chapter 4

Cephalic Morphology of *Pythonichthys macrurus*

Chapter four

Cephalic Morphology of *Pythonichthys macrurus* (Heterenchelyidae: Anguilliformes): Specializations for Head-First Burrowing

Modified from:

Soheil Eagderi and **Dominique Adriaens (2010).**

Cephalic morphology of *Pythonichthys macrurus* (Heterenchelyidae: Anguilliformes): specializations for head-first burrowing.

Journal of Morphology 271(9): 1053-1065.

4.1. Abstract

The Heterenchelyidae, a family of Anguilliformes, are highly specialized fossorial eels. This study was conducted to evaluate the cranial specialization in relation to head-first burrowing behavior in the heterenchelyid *Pythonichthys macrurus*. Detailed descriptions are provided of the cranial myology and osteology of *P. macrurus* and its differences with those of representatives of three families: the Moringuidae (*Moringua edwardsi*), a head-first burrower; the Anguillidae (*Anguilla anguilla*), a non-burrowing representative, and the Ophichthidae (*Pisodonophis boro*), a head and tail-first burrower. This comparison may help to get a better understanding of the cranial specialization of head-first burrowers in heterenchelyids and moringuids. We recognize as morphological adaptations to burrowing: reduced eye size, a caudoventral orientation of the anteromedial section of the adductor mandibulae muscle complex, the posterior position of the quadrate-mandibular joint, a solid conical skull, large insertion sites of epaxial and hypaxial muscles on the neurocranium, widened cephalic lateral line canals extending into the dermal cavities, and a ventral position of the gill openings.

4.2. Introduction

Anguilliform fishes, a large group of elongated, cosmopolitan teleosts (Nelson, 2006), are adapted for wedging through small openings or crevices (Gosline, 1971; Smith, 1989c). They have evolved to a range of different life styles from pelagic to burrowing, the latter from head-first (Heterenchelyidae, Moringuidae) to tail-first (Ophichthidae). The head-first burrowers have been shown to have specific cephalic

features (McCosker et al., 1989; Smith 1989a, d, e; De Schepper et al., 2005, 2007b), but an interesting question is whether head-first burrowing eels converge on a similar morphology or whether there are different ways to be a headfirst burrower. De Schepper et al. (2005, 2007b) considered some features such as eye reduction, modifications of the cranial lateral line system, jaw adductor hypertrophy, hyperossification, and tapering of the skull as cephalic adaptations for headfirst burrowing behavior in Ophichthidae and Moringuidae.

The mud eels or heterenchelyids, one of the 15 families of the Anguilliformes, are a highly specialized family of burrower eels. They comprise two genera (*Pythonichthys* and *Panturichthys*) with eight species and are considered well adapted to their burrowing habits (Smith, 1989a). The members of this family are found in the tropical zone of the Atlantic, Mediterranean, and eastern Pacific and virtually nothing is known about their behavior, except for their burrowing habits (Smith, 1989a). Blache (1968) described that they live on sandy or silty bottoms and feed on small worms, crustaceans, and molluscs. In contrast to tail-first burrowing taxa, such as Ophichthidae, the heterenchelyids are headfirst burrowers, thereby resembling the habit of the Moringuidae (Smith and Castle, 1972; Smith, 1989e).

The aim of this study was to describe the cranial morphology and recognize possible specializations for head-first burrowing behavior in *Pythonichthys macrurus*, a member of the Heterenchelyidae. Hence, a comparison of the cephalic characteristics of this heterenchelyid species with those of another group of head-first burrowing eels, the Moringuidae, is conducted. Also, a comparison of the cranial morphology of head-first burrower eels with that of a non-burrowing, closely related anguilliform family will allow to recognize structural changes that are adaptive for a head-first burrowing lifestyle. Hence, *P. macrurus* will be compared with representatives of three families: the Moringuidae (*Moringua edwardsi*), a head-first burrower; the Anguillidae (*Anguilla anguilla*), a non-burrowing representative; and the Ophichthidae (*Pisodonophis boro*), a head- and tail-first burrower.

Böhlke (1989b) considered the Heterenchelyidae, Anguillidae, and Moringuidae to form a monophyletic clade based on morphological data (see Fig. 4.1). However,

Smith (1989e) mentioned that the relationship of the Heterenchelyidae and Moringuidae is a matter of conjecture and resemblances between them are based on plesiomorphic characters or characters related to their fossorial habits. Smith (1989e) also pointed out that it is difficult to find synapomorphies that are not based on reduction or losses of characters in Heterenchelyidae and Moringuidae. Because earlier studies have based the relationship of Heterenchelyidae and Moringuidae on the analysis of external morphology and osteological data, we hope to add valuable data to the cladistic analysis by studying their cranial myology. It seems that these head-first burrowers have undergone a strong selection for protecting the head during burrowing. By analyzing character state transformations of the myological components involved, the evolution of these adaptations for head-first burrowing may become evident in an explicit phylogenetic context. In particular, the study of Belouze (2001) did not support the monophyly of Heterenchelyidae and Moringuidae. Also, the phylogenetic tree based on mitochondrial ribosomal DNA sequences did not support the monophyly of the Anguillidae and Moringuidae (Obermiller and Pfeiler, 2003). Although Anguillidae and Moringuidae are more closely related to each other than to heterenchelyids, we predict that the heterenchelyid, *P. macrurus* will exhibit more morphological features in common with *M. edwarsi*, but with different pattern being related to synapomorphies of the Moringuidae and Anguillidae. Also, the presence of the convergent features observed in strictly head-first burrowers is predicted in the non-strictly head-first burrower, *P. boro*, but to a lesser degree.

4.3. Materials and methods

Five alcohol-preserved specimens of *Pythonichthys macrurus*, obtained from the Musée National d'Histoire Naturel of Paris (MNHN 1965-0640), were examined. The specimens were the following sizes in Standard Length (SL): PM1: SL = 288.9 mm, PM2: SL = 229.6 mm, PM3: SL = 442.5 mm, PM4: SL = 245mm, and PM5: SL = 189.3 mm). Five commercially obtained specimens of *Anguilla anguilla* (AA1: SL = 503 mm, AA2: SL = 484 mm, AA3: SL = 548 mm, AA4: SL = 518 mm, and AA5: SL = 491 mm) were examined. Two specimens (PM2 and PM4) of *P. macrurus* were cleared and stained with alizarin red S and alcian blue according to the protocol of

Hanken and Wassersug (1981). Muscle fibers of the dissected specimens were stained according to Bock and Shear (1972). The specimens were studied using a stereoscopic microscope (Olympus SZX-7), equipped with a camera lucida. To examine the histological nature of two orobranchial tongue-like appendages of *P. macrurus*, a series of histological sections (5 µm) was cut, stained with an improved trichrome staining protocol and mounted with DPX (based on PM1). Images of the sections were captured using a digital camera (Colorview 8, Soft Imaging System, Munster, Germany).

Muscle terminology follows Winterbottom (1974) and De Schepper et al. (2005). Terminology of cranial skeletal elements follows Böhlke (1989c) and Rojo (1991). The epiotic of teleosts is considered to be an ossification of the occipital arch that has invaded the otic region and so this bone is termed "epioccipital" (Patterson, 1975). The cranial osteology of *Moringua edwardsi*, *Pisodonophis boro*, and *Anguila anguilla* has been described in detail by De Schepper et al. (2005), Tilak and Kanji (1969), and Tesch (2003), respectively. The head myology of *M. edwardsi*, *P. boro*, and *A. anguilla* have already been described in detail by De Schepper et al. (2005), De Schepper et al. (2007b), and De Schepper (2007), respectively.

4.4. Results

4.4.1. Cranial osteology of *Pythonichthys macrurus*

The neurocranium of *Pythonichthys macrurus* forms one solid unit and tapers from the otic region toward the tip of the snout (see Fig. 4.2). The ethmoid region is comprised of the premaxillo-ethmoid complex, vomeral bone and nasal bones. The latter are described with respect to the lateral line system (see below). The vomeral bone forms the anterior base of the skull and is situated ventral to the parasphenoid (Figs. 4.2b and 4.3a). The vomerine teeth are arranged in one to two rows with teeth of various lengths. The olfactory fossa is relatively small and lies between the pars ethmoid of the premaxillo-ethmoid complex and the anterior border of the lateral expansion of the frontal bone (Fig. 4.3a). A pore is present on the olfactory fossa (Fig. 4.3a).

Anteriorly, a small median ridge is present where the two frontal bones meet. Each frontal bone bears two arches on its dorsal surface, which support the posterior part

of the supraorbital canal and the frontal commissure (Figs. 4.3a and 4.4a). These two frontal arches are in a perpendicular position to each other, with the lateral expansions of the frontal bones forming the base of these arches (Fig. 4.2a). The small eye of *P. macrurus* is situated under the lateral expansion of the frontal bone. Anteriorly, the frontal bones border the premaxillo-ethmoid complex. The entire frontal arches and the arch-like infraorbital bones are covered with thick connective tissue. The basisphenoid forms the posterior border of a small orbit and is situated dorsal to the parasphenoid. It bears two dorsal wings that are surrounded by the frontal bones, pterosphenoids, and parasphenoids (Fig. 4.2b). The foramen opticum is present between the two wings of the basisphenoid that bears a tube-like structure on its anteroventral portion. The parasphenoid runs from the orbits posteriorly, with its middle ridge continuing below the prootic and basioccipital bones (Fig. 4.2b). The parasphenoid is bifurcated at its posterior end with a basioccipital process wedged in-between (Fig. 4.2b). Together with the prootic bone, the pterosphenoid borders the foramen for the trigemino-facial nerve complex (Fig. 4.2b). The lacrimal and infraorbital bones are described with respect to the cranial lateral line system (see below).

The otic region comprises the sphenotic, pterotic, prootic, epioccipital, and parietal bones. The sphenotic bone bears a rostroventrally directed process and forms the anterior wall of the anterior articulatory facet of the hyomandibula (Fig. 4.2b). The process bears a small pore on its ventral face, whereas the rest of the ventral surface is pitted. The pterotic bone overlaps with the frontal, parietal, and prootic bones. The pterotic bone anteriorly bears a tubular structure in which the temporal canal enters and which opens at its posterior end. The posterior facet of the hyomandibula and the posterior portion of the anterior articulatory facet are enclosed by the pterotic bone. The prootic bones form the anterior portion of the large otic bullae, which are also enclosed by the exoccipital bones and basioccipital bone. The epioccipital bones form the medial margin of the posterior opening of the pterotic tubular structure. The parietal bones show a serrated suture at the midline (Fig. 4.2a). They bear an anterolateral process that overlaps with the frontal bones.

The occipital region comprises the exoccipital bones, basioccipital bone, and supraoccipital bone. The supraoccipital bone is surrounded by the epioccipital and

parietal bones and bears a small crest at the midline (Fig. 4.2a). The exoccipital bones are domed and bear pitted borders with the foramen magnum. Two ring-like extrascapular bones are present posterior to the occipital region. They are covered with a thick layer of connective tissue and also support the supratemporal commissure.

The maxillary bone is ankylosed anteromedialy to the neurocranium. Anteriorly, it bears a dorsal ascending process that medially possesses a maxillary condyle (Fig. 4.3a). The posterior end of the maxillary bone is connected to the dorsolateral face of the lower jaw via the primordial ligament. The conical maxillary teeth lie in two rows (Fig. 4.5a, b). The anterior tip of the lower jaw is positioned slightly anterior to the upper jaw and its teeth run up to the coronoid process (Fig. 4.5c). The coronomeckelian is a small element on the anteroventral side of the Meckelian fossa, enclosed by the dentary bone (Fig. 4.5c). The dentary bone forms the coronoid process that is connected to the angular bony complex. The mandibular teeth are arranged in two rows with a medial row and a longer lateral row (Fig. 4.5c). The angular bony complex consists of the fused retroarticular, angular, and articular bones. The mandibular articulation facet is dorsal to the angular bony complex (Fig. 4.5c). The retroarticular process is directed caudally. The preopercle-angular and interopercle-angular ligaments connect the retroarticular to the medial faces of the preopercle and interopercle bones, respectively.

The suspensorium consists of four bones, i.e., the hyomandibula, quadrate, palatopterygoid, and preopercle. The preopercle is described as part of the opercular series (see below). The symplectic bone is fused to the posterior portion of the quadrate. The hyomandibula bears a distinct ridge on its lateral surface. The hyomandibula articulates dorsally with the neurocranium via two articular condyles, the anterior one situated on its anterodorsal corner (Fig. 4.3b). The long, posterior suspensorial articular condyle is formed by a caudally extended posterodorsal process of the hyomandibula (Fig. 4.3b). The opercular bone articulates with a ventrocaudally directed condyle, at the posterior edge of the hyomandibula. The hyomandibula-quadrate axis is directed vertically, thus positioning the quadrate-mandibular articulation posterior to the orbit. The palatopterygoid is a broad bone and only its posterior end is connected to the quadrate by connective tissue (Fig.

4.3b). The hyomandibular-palatopterygoid ligament connects the dorsal margin of the palatopterygoid to the hyomandibular ridge.

The opercular series comprises five elements (opercle, preopercle, interopercle, subopercle, and supra-preopercle). The preopercle bears a tubular, arch-like structure with an anterodorsal projection on its anterolateral face (Fig. 4.3b). This arch-like structure, which is covered by thick connective tissue, encloses a part of the preoperculo-mandibular canal (Figs. 4.3b and 4.4a). The posterior portion of the preopercle overlaps and is connected to the anteriorhalf of the interopercle. The preopercleangular ligament connects the anteromedial rim of the preopercle to the angular bony complex. The interopercle is a relatively large rectangular bone. The interopercle-angular ligament is attached to the anteromedial face of the interopercle and continues posteriorly to the posterior end of the posterior ceratohyal bone. The subopercle is situated ventral to the opercle, to which it is firmly attached. Connective tissue also attaches it to the interopercle. A small ventral process is present on the rostroventral end of the opercle and acts as the attachment point for the dilatator operculi muscle. The supra-preopercular bone, which encloses part of the preoperculo-mandibular canal, lies above the anterior portion of the opercle (Fig. 4.3b).

The hyoid complex consists of the unpaired median basihyal and urohyal bones and paired anterior and posterior ceratohyal bones (see Fig. 4.6).This expansion, comprising the urohyal articular facets, lies ventrally against the anterior end of the ceratohyal bones, and the basihyo-ceratohyal ligaments connects the lateroventral faces of the basihyal bone to the ventral face of the anterior ceratohyal bones (Fig. 4.7a). The urohyal bone is expanded anteriorly and is connected to the anterior end of the anterior ceratohyal bones via small urohyo-ceratohyal ligaments (Fig. 4.7a). The basihyal bone is a cylindrical bone, which is expanded posteriorly (Fig. 4.6a). No separate hypohyal bone could be distinguished. The anterior ceratohyal bone is connected to the suspensorium by means of the ceratohyo-hyomandibular ligament (Fig. 4.7a). A total of nine branchiostegal rays are supported by the anterior and posterior ceratohyal bone (Fig. 4.6b). All of them articulate with the posterior ceratohyal bone, with the exception of one. The branchiostegal rays curve dorsally

along the ventral border of the interopercle and reach up to the caudal border of the opercle.

The cranial lateral line system comprises the supraorbital, infraorbital, temporal and preoperculo-mandibular canals, and the frontal and supratemporal commissures. The ethmoid and adnasal canals are absent. The cranial lateral line canals are widened due to the arched bony elements that enclose them. The nasal bone lies on the anterodorsal face of the olfactory organ and supports the anterior portion of the supraorbital canal. The main body of the nasal bone is tube-like, bearing a ventrolaterally positioned wing (Fig. 4.4b). The frontal- nasal ligament connects the nasal bone to the anteroventral corner of the lateral expansion of the frontal bone (Fig. 4.7b). The posterior part of the supraorbital canal is supported by the anterior frontal arch, which is expanded laterally (Fig. 4.4a). The frontal commissure is enclosed by the posterior frontal arches (Fig. 4.4a). Four infraorbital bones seem merely to be lying in an arched position (Fig. 4.4b). The lacrimal and four infraorbital bones support the infraorbital canal. The anterior part of the infraorbital canal is enclosed by the lacrimal bone. The tubular lacrimal bone bears an anteriorly flattened part superimposing the maxillary dorsal process. Dorsally, this flattened part of the lacrimal bone bears a more narrow tubular structure (Fig. 4.4b). The primordial ligament continues anteriorly and connects to the posterior part of the lacrimal bone. The supra- and infraorbital infraorbital canal anastomose in the front of the pterotic opening and continue into the temporal canal. The preoperculo-mandibular canal begins in the ventroanterior tip of the dentary bone. It runs inside the mandibula, which bears six pores (Fig. 4.4b). The preoperculo-mandibular canal is curved caudodorsally after exiting the mandibula and is enclosed by the arch-like structure of the preopercle (Fig. 4.4b). A supra-preopercular bone encloses the posterior portion of the preoperculo-mandibular canal before anastomosing with the temporal canal. The supratemporal commissure is enclosed by two ring-like extrascapular bones (Fig. 4.7b). Despite existing pores on some bony elements that enclose the lateral line system, such as those of the lower jaw, the cephalic lateral line system bears few tiny pores on the preoperculo-mandibular canal. These are visible under high magnification, implying reduced head pores.

4.4.2. Cranial myology of *Pythonichthys macrurus*

4.4.2.1. Muscles of the cheek

The adductor mandibulae complex, the most conspicuous muscle of the cheek, is subdivided into the sections A2, A3, and Aω. The section A2 is subdivided into two subsections: A2a and A2b. The A2a is the ventral element of the adductor mandibulae muscle complex and has a fleshy origin at the lateral face of the hyomandibula, quadrate, and the anterior rim of the preopercle; it has an additional origin as a tendon from the posterolateral face of the hyomandibula. This tendon is also connected to the thick connective tissue, which covers the arch-like structure of the preopercle. The A2a inserts as a tendon on the medial face of the coronoid process and as a muscle on the posteromedial face of the angular bony complex. The lateral face of the A2-tendon connects to the posterior edge of the primordial ligament and inserts on the posteromedial face of the mandibula (Fig. 4.7b). The subsection A2b is the largest and most posterodorsal element of the adductor mandibulae muscle complex. It has a muscular origin on the frontal, parietal and supraoccipital bones and inserts as a muscle and with tendons on the dorsomedial face of the Meckelian fossa. A posterior portion of the subsection A2b that is situated lateral to the levator arcus palatini muscle, bulges posteriorly. The A3-section of the adductor mandibulae muscle complex has a fleshy origin from the ventral face of the lateral expansion of the frontal bone, the anterolateral face of the sphenotic process and the pterosphenoid bone, and inserts as a tendon onto the Meckelian fossa. The posterior fibers of the section A3 are directed ventrally whereas its anterior fibers are directed more caudoventrally (Fig. 4.7c). The section Ax arises as a tendon from the anteroventral fibers of the subsection A2b. It inserts into the Meckelian fossa along with the ventral fibers of the subsection A2b.

The levator arcus palatini muscle originates as a tendon from the dorsal portion of the hyomandibular ridge. Its fibers are spread radially and insert on the parietal bone, the supraoccipital bone, the posterior region of the pterotic bone, and the posterodorsal process of the hyomandibular bone (Fig. 4.7c).

The adductor arcus palatini is a rectangular muscle with its fibers originating from the posteroventral side of the pterosphenoid and the ventrolateral face of the

sphenotic bone. It inserts with fibers on both the lateral and medial face of the anterodorsal part of the hyomandibular bone. There is no insertion on the palatopterygoid. Its dorsal fibers are covered by the anterior portion of the dilatator operculi muscle (Fig. 4.7d).

The adductor hyomandibulae muscle connects with fibers to the basioccipital, prootic, and parasphenoid bones and runs to the dorsomedial face of the hyomandibular bone. Its anterior margin is situated at the level of the anterior margin of the hyomandibular bone.

The undifferentiated levator operculi and adductor operculi muscles, which can be considered as a single levator/adductor opercula muscle, direct caudoventrally (Fig. 4.7b). Based on different origins of muscle parts, the levator/adductor operculi muscle can be divided into an anterior, mesial, and posterior bundle. The anterior bundle has a fleshy origin from the ventral edge of the posterodorsal process of the hyomandibular bone. Its lateral fibers insert on the dorsolateral face of the opercle, whereas the medial fibers insert on the dorsomedial face of the opercle. The mesial bundle originates as a tendon from the posterior end of the posterodorsal process of the hyomandibular bone and inserts with fibers on the dorsolateral face of the opercle (Fig. 4.7b). The posterior bundle originates as a tendon from the posterior process of the pterotic bone and its lateral and medial fibers insert on the dorsolateral and dorsomedial faces of the opercle, respectively (Fig. 4.7d).

The dilatator operculi is triangular in shape (Fig. 4.7d). It originates with muscle fibers from the posterolateral face of the sphenotic bone and ventrolateral face of the pterotic bone. It inserts as a tendon on the rostroventral process of the opercle.

4.4.2.2. Ventral muscles of the head

Left and right halves of the protractor hyoidei muscle merge at the midline of their length, but remain separated at their ends. Each halves of this muscle originate as a tendon from the medial face of the dentary bone, just at the rear of the dental symphysis. They insert with muscle fibers on the ventral faces of the anterior and posterior ceratohyal bones (Fig. 4.7a).

Left and right bundles of the sternohyoideus muscle merge in the midline after originating with fibers from the entire anterior and the anterolateral margin of left

and right cleithra. They insert on the posterior end of the urohyal bone via the sternohyoideus tendon (Fig. 4.7a).

The hyohyoideus muscle complex in teleosts generally includes three components (the hyohyoideus inferioris, hyohyoideus abductor, and hyohyoidei adductores). However, in *P. macrurus* they are undifferentiated, merging anteriorly as a thin saclike muscle sheet meeting their counterparts at the ventral midline. Posteriorly, both muscle halves remain separate at the end of the orobranchial cavity. This sac-like muscle interconnects the medial faces of the branchiostegal rays, opercle, and subopercle and reaches dorsally up to the horizontal septum between the epaxial and hypaxial muscles.

4.4.2.3. Body muscles

The epaxial muscles insert directly on the epioccipital bones, dorsal rim of the exoccipital bone, and as an aponeurosis on the supraoccipital bone. The dorsal fibers of the epaxial muscles connect to the fascia of the adductor mandibulae muscle complex and thick connective tissue, which covers the ring-like extrascapular bones. The hypaxial muscles insert as an aponeurosis on the ventrocaudal border of the basioccipital and exoccipital bones.

Two tongue-like appendages are present in the roof of the orobranchial mucosa (see Fig. 4.8). Each appendage contains a cavity with few, short muscle fibers inserting on its internal base. This may resemble a morphology similar to that of the palatal organ of cypriniform fishes, and hence a similar function in assisting the transport of food could be speculated (Sibbing et al., 1986, Hernandez et al., 2007). However, further research is required to elucidate the true nature of this organ.

4.5. Discussion

4.5.1. Cranial specializations related to head-first burrowing

Burrowing behavior is considered useful to use the substratum for protection, crypsis, and feeding purposes (Subramanian, 1984; Bozzano, 2003), and is observed to occur in various degrees in anguilliform fishes. *Pythonichthys macrurus* appears to remain buried in the substratum except, perhaps, for brief excursions in

search of food (Smith, 1989a). *Moringua edwardsi* spends all its time burrowed in the sand when it is immature (Gordon, 1954; Gosline, 1965), whereas adults of this species limit their fossorial behavior to when they leave their burrows during the night (Smith, 1989b). *Pisodonophis boro* penetrates the substrate tail-first but it is able to burrow head-first as well (Tilak and Kanji, 1969; Subramanian, 1984; Atkinson and Taylor, 1991). It is known to burrow for shelter and to find food (Subramanian, 1984). Anguilla anguilla is a non-burrowing species (Tesch, 2003).

4.5.1.1. Eye reduction: *Pythonichthys macrurus* shares several cranial features with two non-heterenchelyid burrowing anguilliforms. One of these characters is eye reduction. Eye reduction in ophichthids and moringuids are considered to be adaptations to head-first burrowing (De Schepper et al., 2005, 2007b). Eye reduction is observed in many other fossorial elongated fishes such as Clariidae (Devaere et al., 2001, 2004), Mastacembelidae (Poll, 1973), and Anguilliformes (De Schepper et al., 2004, 2005, 2007b; Aoyama et al., 2005). The reduced eye of the Ophichthidae and Moringuidae has been reported to be adaptations for head-first burrowing (McCosker et al., 1989; Smith 1989a, d; De Schepper et al., 2005, 2007b). The smaller eye size, particularly in relation to the macrophthalmic ancestral state of Anguilliformes (Böhlke, 1989a), can have a substantial effect on the spatial design of head (Boel, 1985). Eye reduction allows a caudoventral orientation of the anteromedial section of the adductor mandibulae muscle complex in *P. boro* and *M. edwardsi* (De Schepper et al., 2005, 2007b), and the reduction of the circumorbital bones to small tubular bones in *M. edwardsi*, clariids and ophichthids (Tilak and Kanji, 1969; McCosker et al., 1989; Bozzano, 2003; Devaere et al., 2004; De Schepper et al., 2007b). Eye reduction also has been linked to the hypertrophy of the jaw muscle in anguilliform clariids (Devaere et al., 2001). Hence, the reduction of the eye in *P. macrurus* may be linked to the caudoventral orientation of the anteromedial section of the adductor mandibulae muscles complex (the section A3) and tubular circumorbital bones. Furthermore, the opaque skin of the eye in *P. macrurus* may also be adaptive to burrowing. This feature has been reported in *Ophichthus rufus* (Ophichthidae) as an adaptation to protect from mechanical injury when this eel routinely enters and leaves a burrow (Bozzano, 2003).

4.5.1.2. Widened cephalic lateral line canals: Because of the associated reduced vision, other sensory systems (such as olfactory, somatosensory, lateral line and auditory systems) may become more important to provide environmental information (Gordon, 1954; Montgomery, 1989). Chemical sensory cues may predominate in burrowing organisms that their vision is considered poorly developed (Pankurst and Lythgoe, 1983). Klages et al. (2002) has pointed out that finding prey for organisms that usually wait for food by resting on the sea floor or inside burrows is based on the detection of the noise (the residual low-level sound) produced by elastic waves at the water-sea floor interface. Unlike *M. edwardsi*, which has its cephalic lateral line canals widened into dermal cavities, *P. macrurus* has widened canals enclosed in the arched bony elements of the skull under the skin. This widened cephalic lateral line canals may function as a kind of sensory pads, which are stimulated mechanically during burrowing when in contact with prey (De Schepper et al., 2005). Most of the widened canals of the cephalic lateral line system of *P. macrurus* lack external pores, except for the tiny pores of the preoperculo-mandibular canal. *Moringua edwardsi* lacks any external pores of the cephalic lateral line system, whereas tail-first burrower, *P. boro*, retains pores in all the canals of the cephalic lateral line system. The lack of head pores has the advantage of avoiding the entering of sediment into the canals during head-first burrowing (De Schepper et al., 2005).

4.5.1.3. Gill opening: The opercle is orientated posteroventrally in *P. macrurus*, *M. edwardsi*, and *P. boro* whereas that one of *A. anguilla* is directed caudally. As a result of this configuration, the gill opening is positioned more ventrally in the burrowing species. This may prevent entering of sediment into gill cavity (Gosline, 1971; Smith, 1989c).

4.5.1.4. Different orientation of the anterior section of the adductor mandibulae muscle complex: The hyomandibulo-quadrate axis of *P. macrurus*, *M. edwardsi*, and *P. boro* is directed dorsoventrally, in contrast to the forwardly inclined one in *A. anguilla*. As a result, the quadrate-mandibular articulation is positioned posterior to the orbit. In addition to the small size of eye, the posterior position of the quadrate-mandibular joint in these species also creates space allowing a caudoventral orientation of the anterior section of the adductor

mandibulae muscle complex. The anterior fibers of the section A3 in *P. macrurus* are directed caudoventrally, whereas its posterior fibers are directed vertically. An opposite orientation of the different section of the adductor mandibulae muscle complex (caudoventrally versus rostroventrally) can thereby help in preventing the dislocation of the mandibular joint, even when large forces are exerted that induce torque forces (De Schepper et al., 2007b). This stabilization of the mandibular joint may especially prevent the dislocation of the lower jaw during initial head-first penetration considered as first stage of burrow construction (James et al., 1995).

Despite of a short and sharp snout, which is considered to be an adaptation to head-first burrowing (McCosker et al., 1989; Smith, 1989b, c), the posterior position of the quadrate-mandibular joint also results in a large mouth gap and a longer lower jaw. A large gape and longer lower jaw combined with large teeth on the upper and lower jaws in *P. macrurus* suggest a potential for rapid mouth closing and dealing with large prey items. Many bentic, lie-in-wait or cryptic predators have particularly large mouths that can be opened and closed rapidly to grasp prey (Helfman et al., 1997; Mehta and Wainwright, 2007; Mehta, 2009; Eagderi and Adriaens, 2010a).

4.5.1.5. Skull shape and large insertion sites of body muscles on the neurocranium: The modification of the skull into a solid conical structure with sharp snout, as seen in *P. macrurus* and two other fossorial species, *M. edwardsi* and *P. boro*, may facilitate burrowing, where power is provided by the cylindrical body (Castle, 1968; Smith, 1989d). Smith (1989d) mentions rapid movements of the body, just beneath the surface, for subterranean hunting and feeding in burrowing Anguilliformes. The large insertion sites of the epaxial and hypaxial muscles on the neurocranium (comprising exoccipital, epioccipital, basioccipital, and supraoccipital bones), which are also connected to the adductor mandibulae muscle complex, in *P. macrurus* can be considered an advantage for transferring forces from the body onto the head. The physical coupling between the jaw muscles and the epaxial muscles has been observed in *M. edwardsi* and *P. boro* (De Schepper et al., 2005, 2007b). Burrowing fishes appear to use two main strategies: mouth excavation or compression and displacement of sediment by body movement

(Atkinson and Taylor, 1991). The head morphology of *P. macrurus* suggests that the second strategy is the burrowing method applied.

4.4.2. Variable degree of head-first burrowing specializations in Anguilliformes

Compared with *Anguilla anguilla*, *Moringua edwarsi*, and *Pisodonophis boro*, *Pythonichthys macrurus* exhibits several unique characters such as presence of the frontal arches, the preopercle with its arch-like structures, the tubular and arch-like circumorbital bones, the arch-like suprapreopercular bone, and two ring-like extrascapular bones, which support portions of the cephalic lateral line canals. These characters are all considered synapomorphies for heterenchelyids (Belouze, 2001).

Only *M. edwarsi* lacks a basisphenoid, and *P. macrurus* was the only anguillid in this study to exhibit a separate vomeral bone. Fusion of premaxillary, ethmoid, and vomeral bones, forming the premaxillo-ethmovomerine complex in *M. edwardsi*, *A. anguilla*, and *P. boro*, is considered synapomorphic for Anguilliformes (Eaton, 1935; Gosline, 1980; Smith, 1989c). The palatopterygoid of *A. anguilla* is connected at both ends to the quadrate bone and the premaxillo-ethmovomerine complex, respectively, whereas the palatopterygoid of *M. edwardsi*, *P. macrurus*, and *P. boro* attaches only to the suspensorium. The pectoral fins are present in both *A. anguilla* and *P. boro* but are weakly developed in *M. edwardsi*. According to Böhlke (1989b), all heterenchelyids lack pectoral fins, whereas moringuids have weakly developed pectoral fins. Body elongation combined with limblessness allows unhindered movement below the substrate surface (Gans, 1975; Pough et al., 1998).

The adductor mandibulae muscle complex of *P. macrurus* shows similar components but a different configuration with that of the other fossorial species studied, except for the lack of the section A1 in *M. edwardsi* and *P. boro*. In basal actinopterygian fishes, the section A1 is defined by its dorsal position in the adductor mandibulae muscle complex and its insertion on the maxillary bone through a long tendon or on the maxillary bone itself (Eaton, 1935; Winterbottom, 1974). The presence of such a section A1 has been reported in *M. edwardsi* and *P. boro* (De Schepper et al., 2005, 2007b). In *A. anguilla* and *P. macrurus*, a small tendinous connection was

found between the ventral subsection of the section A2 and the maxillary bone via the primordial ligament. Based on the terminology of Winterbottom (1974) and regarding its main insertion on the lower jaw, this section in *A. anguilla* and *P. macrurus* was considered as a subsection of A2. Hence, the section A2 of the adductor mandibulae muscle complex of *A. anguilla* consists of four subsections (A2a, A2d, A2v, and A2m; Fig. 4.9a, b, d). The homology of each muscle of the adductor mandibulae complex (variously determined as a subdivision, section, or subsection) is accepted on the basis of sharing an identical insertion pattern onto the jaws, following the traditional nomenclature used for the adductor mandibulae muscles (Vetter, 1878; Winterbottom, 1974; Nakae and Sasaki, 2004). Migrations of the muscle insertions have likely occurred in evolutionary history of the elopomorphs, resulting in the lumping of non-homologous muscles under a single name. Hence, the insertion of the ventral subsection of the A2 in *A. anguilla* and P. *macrurus* may have migrated from the maxillary bone to the lower jaw as a non-homologous subsection of the A2.

Despite external, osteological and musculature similarities among the fossorial species studied, the configuration of their head musculature exhibits more diversity. The anterior part of the section A2 and entire section A3 is directed caudoventrally in *M. edwardsi*, whereas only the section A3 in *P. boro* and anterior fibers of the section A3 in *P. macrurus* are directed caudoventrally. The levator arcus palatini muscle is positioned caudally in *P. macrurus* compared with the one in the other species studied. Also, the levator arcus palatini muscle connects the posterior elements of the neurocranium, such as the parietal, supraoccipital, and pterotic bones to the posterodorsal face of the hyomandibular bone. In the three others, however, this muscle connects the ventrolateral face of the orbitotempral elements of the neurocranium, such as the sphenotic and parasphenoid bones, to the lateral face of the suspensorium. Merging left and right bundles of the sternohyoideus and protractor hyoidei muscles in *P. macrurus* is another difference in the head musculature of the species studied. The cephalic features that are considered specializations for a burrowing mode of life, such as a reduced eye, dorsoventral positioning of the hyomandibula-quadrate axis, caudoventral orientation of the anteromedial section of the adductor mandibulae muscle complex, a widened

cephalic lateral line system that extends into the dermal cavities, ventral positioning of the gill opening, and large insertion sites of epaxial and hypaxial muscles on the neurocranium are absent in non-burrower anguillids (*A. anguilla*). Characteristics that are shared exclusively by *M. edwardsi* and *A. anguilla*, such as the premaxillo-ethmovomerine complex, the pectoral fin and separate protractor hyoidei muscle are considered as synapomorphies for the monophyletic group that comprised the Anguillidae and Moringuidae. The presence of features that are associated with head-first burrowing in *P. boro* suggest convergence with the studied fossorial fishes.

Different patterns of head-first burrowing features for the Heterenchelyidae and Moringuidae reveal that there is more than one way to restructure the skull for head-first burrowing. Alternatively, similar morphological characteristics, resulting from similar environmental pressures related to fossorial habit, may also explain the clustering of heterenchelyids and moringuids in the phylogenetic tree presented by Böhlke (1989c). Including data of the head musculature of the three studied fossorial eels, may provide additional information which we can use to resolve the phylogenetic relationship of anguilliform fishes (Diogo, 2004).

ACKNOWLEDGMENTS

The authors would like to thank P. Pruvost (Paris Natural History Museum, MNHN) for providing museum specimens, N. De Schepper (Ghent University) for offering her examined material, B. De Kegel (Ghent University) for her technical assistance, and D.G. Smith (Smithsonian, USA) for his valuable comments.

Chapter 5

Cephalic Specialization in a Parasitic Eel, *Simenchelys parasiticus*

Chapter five

Cephalic Specialization in an alleged Parasitic Eel, *Simenchelys parasiticus* (Simenchelyinae: Synaphobranchidae)

Soheil Eagderi, Joachim Christiaens, Matthieu Boone, Patric Jacobs and **Dominique Adriaens**

Cephalic Specialization in a Parasitic Eel, *Simenchelys parasiticus* (Simenchelyinae: Synaphobranchidae).

To be submited: Copeia

5.1. Abstract

The pugnose eel, *Simenchelys parasiticus,* is the only member of the Simenchelyinae, occurring worldwide from tropical to temperate latitudes. This deep-water eel has been described as being parasitic. This study, based on head musculoskeletal morphology, tries to provide a characterisation of the specializations of the pugnose eel in relation to this alleged parasitism. Its cranial myology and osteology are compared with the ancestral morphology of non-parasitic representatives of two other subfamilies of the Synaphobranchidae, i.e. *Ilyophis brunneus* (Ilyophinae) and *Synaphobranchus brevidorsalis* (Synaphobranchidae). The cephalic musculoskeletal elements of *S. parasiticus*, compared to the situation in *I. brunneus*, and *S. brevidorsalis* show some morphological modifications, such as the stretchable skin around the small terminal mouth opening, cutting-edge teeth, a stout mouth closing apparatus with large associated muscles, a large tongue-like secretory structure and branchial arches with the capacity to transport food items in the buccal cavity. These may represent modifications in relation to its specialized way of feeding, however not allowing to falsify or support the hypothesis of parasitism (versus scavenging).

5.2. Introduction

Pugnose eel, *Simenchelys parasiticus* is a specialized deep-water eel, occurring worldwide from tropical to temperate lattitudes (Nelson, 2006). *Simenchelys parasiticus* has been described as being parasitic, burrowing into the bodies of halibut and other large fish (Goode and Bean, 1896; Bigelow and Schroeder, 1953), whereas, Castel (1961) concluded that this eel is probably more of a scavenger

than a predator. Robins and Robins (1989) also pointed out that the presumed mode of feeding is to rasp and remove the flesh of dead or dying fishes by twisting movements, gradually excavating a path into a carcass. Two pugnose eels have been found nestled into the heart of a shortfin mako shark displaying its potential to enter into another living organism to which they caused some degree of harm (Caira et al., 1997).

Little is known about the feeding behavior of *S. parasiticus*, except for the above-mentioned observations. If *S. parasiticus* would be parasitic, then the cephalic specialization in which it differs from other members of the family Synaphobranchidae, may reflect structural adaptations to parasitism. These morphological specialisations, especially structures of the feeding apparatus, may help to better understand the actual feeding behaviour of this species. The pugnose eel belonging to the monotypic Simenchelyinae, represents the only known parasitic species within the three subfamilies of Synaphobranchidae (Nelson, 2006). Within synaphobranchids, the maximum parsimony tree based on mitochondrial ribosomal DNA sequences supports the monophyly of the Simenchelyinae, Ilyophinae and Synaphobranchinae (Lopez et al., 2007). As such, a comparison with the ancestral morphology of the non-parasitic condition is performed, where the cephalic features of representatives of two other subfamilies of the Synaphobranchidae, i.e. *Ilyophis brunneus* (Ilyophinae) and *Synaphobranchus brevidorsalis* (Synaphobranchidae), are studied.

5.3. Material and methods

For the anatomical description, five alcohol-preserved specimens of *Simenchelys parasiticus* (I.28736-024 and I.20095-031), seven specimens of *Ilyophis brunneus* (UF 222355, UF 230514 and UF 130897) and three specimens of *Synaphobranchus brevidorsalis* (USNM 273427-115) obtained from the Australian Museum (I), Florida Museum of Natural History (UF) and Smithsonian National Museum of Natural History (USNM) were examined. The specimens were of following size in Total Length, (TL) *S. parasiticus*; SP1: TL: 192 mm; SP2: TL: 218.5 mm; SP3: TL: 199 mm; SP4: TL: 203; SP5: TL: 279 mm; SP6: TL: 353 mm; *I. brunneus*; IB1: TL: 503 mm; IB2: TL: 348 mm; IB3: TL: 273 mm; IB4: TL: 573 mm; IB5: TL: 491

mm; IB6: TL: 496 mm; IB7: TL: 497 mm; *S. brevidorsalis*; SB1: TL: 472 mm; SB2: TL: 357 mm; SB3: TL: 397 mm.

One specimen of each species (SP3, SB2 and IB1) was cleared and stained with alizarin red S and alcian blue according to the protocol of Taylor and Van Dyke (1985) for osteological examinations. Dissections with muscle fiber staining according to Bock and Shear (1972) were performed. To study the detailed internal morphology of the head, serial histological cross sections were generated. One specimen (SP1; I.34900-002) was decalcified using Decalc 25%, dehydrated through an alcohol series, and embedded in Technovit7100. Series of sections (5 µm) were cut using a Leica Polycut SM 2500, stained with Toluidin blue, and mounted with dpx. Another specimen (SP4) was scanned at the modular micro-CT setup of Ghent University (Masschaele et al. 2007; http://www.ugct.ugent.be). The specimen was scanned using the directional tube head, at 80 kV tube voltage. The detector was an a:Si flat panel (Varian Paxscan 2520) with CsI scintillator. The detector was used in binning mode, enlarging the detector pixels to 254^2 µm². The geometric magnification of 7.94 resulted in an effective voxel size of 32^3 µm³. In total 1001 projections were made covering the full 360 degrees. The raw data was processed and reconstructed using the in-house developed CT software Octopus (Vlassenbroeck *et al.* 2007) and rendered with VGStudio Max (Volume Graphics GmbH Heidelberg, Germany) and Amira 4.1.0 software (Mercury Computer Systems GmbH Mérignac, France). The lateral line system was visualised by manually drawing it in Rhino 3D (McNeel).

Muscle terminology follows Nelson (1967), Winterbottom (1974) and De Schepper et al. (2005). Terminology of cranial skeletal elements follows Böhlke (1989a) and Rojo (1991). The epiotic of teleosts is termed "epioccipital", thereby following Patterson (1975). The external morphology of *S. parasiticus* has been described by Regan (1912), Jaquet (1920), Solomon-Raju and Rosenblatt (1971), and Robins and Robins (1989). Also, brief osteological features of *S. parasiticus* were described by Jaquet (1920) and Robins and Robins (1989). The cranial osteology of *Ilyophis brunneus* and *Synaphobranchus* species has been described in detail by Robins (1971).

5.4. Results

5.4.1. Cranial osteology of *Simenchelys parasiticus*

The neurocranium tapers from the otic region towards the snout (Fig. 5.1a). The ethmoid region is comprised of fused premaxillaries and ethmoid bones, forming the premaxillo-ethmoidal complex, and the vomer. The nasal bones cover the olfactory rosettes that locate above the snout (Fig. 5.2c). Anteriorly, the fused premaxillaries spread laterally and form a maxillary articular facet on their posterior face. The anteroventral part of the premaxillo-ethmoidal complex bears two rows of teeth: an anterior one with large teeth with a cutting edge, and a posterior one with two small, blade-like teeth (Fig. 5.1b). The dentition of the vomer is discontinuous with that of the premaxillo-ethmoidal complex and bears five chisel-like teeth on its anteroventral face (Fig. 5.1b). Posteriorly, the vomer wedges into the anteroventral part of the parasphenoid.

The orbital region comprises the nasals, preorbitals, supraorbital, infraorbitals, postorbitals, frontal, basisphenoid, pterosphenoids and parasphenoid. The nasals, preorbitals, supraorbital, infraorbitals and postorbitals are described in relation to the cephalic lateral line system (see below). A single fronta elementl is formed by the fused frontal bones and bears two small pores on the lateral face of its midsection (Fig. 5.1a). The foramen olfactorius is present on the anterolateral face of the frontal (Fig. 5.1a). The frontal bears a groove that lies in the extension of the pterotic process and supports the posterior end of the supraorbital canal before it anastomoses with the infraorbital canal (Figs. 5.2a and 5.3a). The foramen opticum is present between the two anteroventral parts of the frontal and dorsal wings of the basisphenoid (Fig. 5.2a). The basisphenoid forms the posteroventral wall of the orbit and its ventral rim is enclosed by the parasphenoid. The basisphenoid bears two wings that form the ventral part of the large foramen opticum. The pterosphenoid is situated posterior to the basisphenoid and bears a hole at its margin with the prootic (Fig. 5.1b). Anteriorly, the parasphenoid runs dorsal to the vomer and forms the floor of the orbit. It spreads at its midsection and forms two lateral alar processes that overlie the posteromedial face of the pterosphenoids (Fig. 5.1b). Posteriorly, the parasphenoid is bifurcated and bears a small keel on its ventral surface (Fig. 1b).

The otic region comprises the pterotics, sphenotics, parietals, prootics and epioccipitals. The pterotic forms the lateral brace of the neurocranium and its anterior part forms a tubular-like structure that encloses the anterior part of the temporal canal. Posteriorly, this canal opens at the caudal border of the pterotic (Fig. 5.3a). The anterior suspensorial articulatory facet is bordered medially by the pterotic, and laterally by the sphenotic (Fig. 5.1b). The posterior suspensorial articulatory facet comprises a caudodorsally directed groove in the pterotic, with its lateral wall formed by the posterolateral crest of the pterotic (Fig. 5.1b). The ventral surface of the sphenotic is connected to the dorsolateral part of the prootic. The sphenotic process is directed anteroventrally. The parietals posteriorly surround the lateral sides of the supraoccipital and overlie its anterior part. The parietal connects to the posterior rim of the epioccipital that forms the dorsal rim of the posterior wall of the neurocranim, along with the supraoccipital. The epioccipital also forms the posterodorsal face of the neurocranium. The prootics form the ventrolateral midsection of the neurocranial floor and laterally bear L-shaped depressions where the levator interni and externi muscles of the branchial arches originate. The trigemino-facial foramen is present anterior to the posterior margin of the otic bulla on the prootic (Fig. 5.1b).

The occipital region comprises the supraoccipital, exoccipitals and basioccipital. These bones, together with epioccipitals, form the posterior wall of the neurocranium. Anteriorly, the supraoccipital bears a process that wedges into the interparietal suture (Fig. 5.1a). Posteriorly, it bears a posterior wing-like process directed caudally with a crest on its ventral face. In addition to the foramen magnum, a relatively large opening is present ventral to the supraoccipital on the posterior wall of the neurocranium that is bordered by supra-, exo and epioccipitals. The foramen magnum is bordered dorsally and laterally by the exoccipitals, and ventrally by the basioccipital. The exoccipitals are domed towards the foramen magnum from its epioccipital margin. The exoccipital is extended ventrally to contribute to the ventral surface of the neurocranium and is situated between the basioccipital and posterior part of the pterotic (Fig. 5.1b). The anterolateral faces of the basioccipital, together with the anteromedial part of the exoccipitals and posterior part of the prootics form two relatively small otic bullae (Fig. 5.1b). The

posterior end of the parasphenoid covers the anterior midline of the basioccipital that wedges into the posterior incisure of the parasphenoid (Fig. 5.1b).

The lower jaw is deep and stout. The dento-spleno-mentomeckelian complex i.e. the dentary complex bears one row of the teeth with cutting edges that reaches up to the coronoid process on the posterior part of the dentary (Fig. 5.4a). Also, three small, blade-like teeth could be observed medial to this row (Fig. 5.4a). Ventrally, the dentary bone bears five large pores of the preoperculo-mandibular canal, which is extended into the lateroventral groove of the angular complex (Fig. 5.3b). In addition, the dentary complex bears five small nerve pores on its laterodorsal face (Fig. 5.2a). The coronomeckelian bone is situated at the rear of the posteromedial margin of the dentary complex inside the Meckelian fossa. The angular complex consists of the fused angular, articular and retroarticular bones. The angular complex bears the mandibular articular facet immediately above the retroarticular, and is directed caudodorsally. With the lower jaw, two ligaments are associated: interoperculo-angular and ceratohyalo-angular ligaments that attach on the posterior face of the retroarticular (Fig. 5.4a). The primordial ligament connects the laterodorsal face of the angular complex to the posterodorsal margin of the maxillary (Fig.5.2a). The lower jaw is slightly protruding.

The maxillary is a stout bone, with its ascending process medially possessing a premaxillo-ethmoidal articular condyle. The maxillary bears a depression on the lateral face of its anterior ascending process in which the anterior part of the olfactory rosette is fitted (Fig. 5.2a). The maxillo-premaxillo-ethmoidal ligament connects the anterior margin of the maxillary to the lateral expansion of the anterior tip of the premaxillo-ethmoidal complex. Thick fleshy lips surround the jaws (Fig. 5.2c). Also, the entire olfactory capsule and the posterior three fourth along the length of the jaws are covered by thick connective tissue of the dermis (Fig. 5.5b). The maxillary also bears a laterodorsal depression on its midsection in which the posterior part of the infraorbital bone fits. The maxillary bears a single row of twelve teeth with cutting edges (Fig. 5.4b).

The suspensorium comprises four elements: the hyomandibula, quadrate, palatopterygoid and preopercle (Fig. 5.2b). The preopercle is described as part of the opercular series (see below). The hyomandibula, quadrate and palatopterygoid

are tightly connected. The hyomandibula dorsally articulates with the neurocranium through the anterior and posterior condyles (Fig. 5.2b). The hyomandibula bears a posterodorsal process that the posterior condyle is situated anterior to this process on the dorsal edge of the hyomandibula (Fig. 5.2b). The suspensorial fossa is formed by the anterior parts of the hyomandibula and quadrate, and a posterior, broadened part of the palatopterygoid and a ridge is present posterior to this fossa. The hyomandibula also bears a pore on the midsection of its ridge and a lateral process on the dorsal end of this ridge (Fig. 5.2b). The hyomandibula-quadrate axis is inclined anteriorly, thus positioning the quadrate-mandibular joint at the level of the posterior part of the orbit (Fig. 5.2a). The opercular condyle of the hyomandibula is situated on the posteromedial face and is directed caudoventrally (Fig. 5.2b). The palatopterygoid is connected posteriorly to the anterodorsal edge of the hyomandibula and anteriorly to the lateroventral face of the midsection of the vomer (Fig. 5.2a).

The opercular series is comprised of four bones: the preopercle, interopercle, subopercle and opercle (Fig. 5.6a). The preopercle forms a groove to enclose the preoperculo-mandibular canal. Anteriorly, it bears a wing that connects to the posteroventral edge and medial face of the hyomandibula by connective tissue (Fig. 5.6a). The interopercle is connected to both the opercle and mandibula by a ligament: the interoperculo-angular and operculo-interopercular ligaments (Fig. 5.6a). The interopercle covers the ventral part of the preopercle. The subopercle connects to the posterior edge of the opercle by connective tissue. The subopercle anteriorly bears two posterior processes forming its anterior incisure (Fig. 5.6a). The opercle is a brace-like bone that curves posteriorly. The opercular series are also covered by a thick layer of connective tissue. The small gill slits are positioned well posterior to the caudal border of the gill cover and are even located on the ventral side of the body, at the level of the posterior edge of the cleithra.

The hyoid complex consists of a median, short basihyal and urohyal, dorsal and ventral hypohyals, and anterior and posterior ceratohyals (Fig. 5.6b). The basihyal is a cylindrical bone with expanded posterior condyle that articulates with the hypohyals (Fig. 5.6b). A thick layer of glandular tissue covers the basihyal. The tongue-like structure contains many secretory unites with large secretory cells that

opens on its dorsal surface through the ducts (Fig. 5.5b, c). The urohyal is small and bears two dorsal hypohyal condyles and a posterior process to which attaches the sternohyoideus muscle. The ventral and dorsal hypohyals posteriorly interdigitates with the anterior ceratohyal. The ventral hypohyal bears a socket on its ventral face in which the urohyal condyle articulates. Dorsally, the dorsal hypohyal bears the basihyal facet. The anterior ceratohyal is tightly connected to the posterior ceratohyal. The nine branchiostegal rays are connected to the posterior ceratohyal and are curved caudally along the ventral and caudal border of the interopercle, reaching up to the posterior and dorsal region of the opercle. The ceratohyalo-angular ligament connects the dorsolateral face of the posterior ceratohyal to the angular complex (Fig. 5.6b).

The cephalic lateral line system comprises the supraorbital, infraorbital, temporal, and preoperculo-mandibular canals, and the frontal and supratemporal commissures (Fig. 5.3a). The supraorbital canal starts at the anterior end of the nasal bone and is extended towards the anterior groove of the frontal (Fig. 5.3a). The nasal bone is a plate-like bone with an irregular margin and dorsally forms a tubular structure that supports the anterior part of the supraorbital canal (Fig. 5.3b). The largest part of the nasal was only lightly stained in the specimen studied. The supraorbital bone is a small ossicle that surrounds the supraorbital canal, just anterior to the anastomosis with the infraorbital canal. The infraorbital canal starts at the anterior end of the small preorbital bone that is situated at the level of the anterior margin of the olfactory rosette (Fig. 5.3). Then, the tubular infraorbital bone, which is located on the dorsal face of the maxillary, encloses the infraorbital canal (Fig. 5.3). There are four small, tube-like postorbital elements that enclose the infraorbital canal at the postorbital region (only the ventral element of these bones was stained in specimens studied) (Fig. 5.3b). The temporal canal runs inside the anterior groove of the frontal and the bony canal of the pterotic. The preoperculo-mandibular canal starts at the rostral tip of the dentary bone and runs posteriorly inside the mandibular canal. Then it continues into the sensory groove of the preopercle before anastomosing with the posterior end of the temporal canal, as the latter exits the skull (Fig. 5.3a). The preoperculo-mandibular canal bears six small, external pores. The frontal commissure lies on the posterior

part of the premaxillo-ethmoidal complex. The supratemporal commissure runs under the posterior part of the adductor mandibulae muscle complex at the level of the second vertebra (Fig. 5.3a).

The gill arches are comprised of the following bones: two basibranchial bones (Bb I and II) (and two unossified basibranchials; Bb III and Bb IV), three pairs of hypobranchials (Hb I-III), five pairs of ceratobranchials (Cb I-V), one pair of upper pharyngeal tooth plates (UP), four pairs of epibranchials (Eb I-IV), three pairs of infrapharyngobranchials (Ib II-IV) and one pair of lower pharyngeal tooth plates (LP) (Fig. 5.7a).

5.4.2. Cranial myology of *Simenchelys parasiticus*

The large adductor mandibulae muscle complex comprises the sections A2 and A3. The section A2 is subdivided into a dorsal A2β and a ventral A2α (Fig. 5.8a). The subsection A2β is the largest element of the adductor mandibulae muscle complex (Fig. 5.8a). Its anterior part bulges and has the same direction as the posterior part. The bulged part of the A2β is attached to the posterodorsal part of the tendon A2β, which inserts on the medial face of the dentary (anterior to the Meckelian fossa) and its coronoid process. The tendon A2β also forms a tendinous sheet between the lateral and medial fibers A2β (Fig. 5.5a). The posterior fibers of A2β are also attached to the ventral part of this tendon. The posterior part of the large A2β covers the anterior part of the epaxial muscles and connects tightly to their dorsal faces by connective tissue (Fig. 5.8a). The subsection A2β is also connected to its counterpart and dorsally originates musculously from the supraoccipital, epioccipital, parietal, frontal and pterotic bones.

The subsection A2α is the ventral element of the adductor mandibulae muscle complex that originates musculously from the anterior face of the preopercle, posterodorsal process of the hyomandibula, posterior parts of the hyomandibula and quadrate, anterior face of the suspensorial fossa and ventral face of the lateral process of the hyomandibula (Fig. 5.8a). Its lateral fibers insert tendinously on the dorsoposterior edges of the dentary and angular bones. The medial fibers of A2α insert musculously onto the posterior part of the Meckelian fossa. There is also a tendon A2α, which runs ventral to the lateral fibers of the A2α and inserts onto the

posteroventral part of the Meckelian fossa. The dorsomedial fibers of the subsection A2α are merged with the ventromedial ones of A2β. The section A3 originates musculously from the ventral part of the frontal, anterior part of the pterotic, dorsal face of the pterosphenoid and anterodorsal face of the sphenotic process (Fig. 5.8b). This muscle inserts musculously onto the ventral part of the Meckelian fossa.

The large levator arcus palatini comprises two subsections (Fig. 5.8b). The anterior subsection has its lateral fibers originating musculously from the lateroventral face of the sphenotic process, whereas its medial fibers originate tendinously ventral to that (Fig. 5.8b, c). This subsection diverges ventrally and inserts musculously on the anterior part of the quadrate and hyomandibula at the level of the suspensorial fossa. The posterior subsection of the levator arcus palatini originates musculously from the pterotic, parietal, anterior part of the epioccipital and posterior part of the frontal. Its lateral fibers insert tendinously on the lateral margin of the lateral process of the hyomandibula and the medial fibers insert musculously on the medial face of the lateral process of the hyomandibula (Fig. 5.8b).

The large adductor arcus palatini starts at the level of the posterior part of the orbit and originates musculously from the anteroventral face of the parasphenoid, prootic and pterosphenoid (Fig. 5.8c). This muscle is extended caudally to the medial face of the posterior process of the hyomandibula and inserts musculously on the dorsolateral margin of the palatopterygoid, anteromedial face and medial face of the midsection of the hyomandibula, and medial face of the quadrate.

The adductor hyomandibula is a small muscle that lies lateral to the adductor arcus palatini. It originates musculously from the ventrolateral depression of the prootic and inserts on the medial face of the hyomandibula, dorsal to its opercular condyle.

The dilatator operculi originates musculously from the posteroventral face of the sphenotic and pterotic and, inserts tendinously on the anterolateral face of the opercle (Fig. 5.8c).

The levator operculi originates musculously from the posteromedial face of the posterior process of the hyomandibula, but its posterior fibers are connected tightly to the lateroventral face of the epaxials by connective tissue. This muscle inserts musculously on the dorsal edge and lateral face of the opercle (Fig. 5.8b).

The adductor operculi originates musculously from the ventrolateral part of the pterotic. It is directed caudoventrally and inserts musculously on the dorsomedial margin the opercle (Fig. 5.8c).

The thick protractor hyoidei originates musculously from the medial face of the dentary at the rear of the dental symphysis (Fig. 5.8d). This muscle inserts musculously on the lateral face of the posterior ceratohyal, below the origin of the hyohyoideus inferioris muscle.

The sternohyoideus muscle inserts musculously on the lateral sides of the urohyal, and through a tendinous sheet that separates the left and right halves. The muscle originates musculously from the ventrolateral face of the cleithrum (Fig. 5.8d).

The hyohyoideus inferioris muscle originates musculously from the dorsal face of the posterior ceratohyal. Both muscle halves continue ventrally to connect to a median raphe, lying at the anterior to the hyohyoideus superior muscle complex (Fig. 5.8d).

The hyohyoideus superior muscle complex forms a sheet of fibers that interconnects the successive branchiostegal rays, where anterodorsally its fibers attach to the medial faces of the opercle and subopercle, ventromedial face of the hyomandibular posterior process and the medial face of the adductor operculi muscle (Fig. 5.8a). Both muscle halves meet their counterpart ventrally at a hyohyoidal fascia but remain separate at the end of the orobranchial cavity. This muscle attaches dorsally to the horizontal septum between the epaxial and hypaxial muscles.

The levator externi muscles originate musculously from the prootic, posterior to the anterior suspensorial articulatory facet. Posteriorly, these muscles are subdivided into three bundles inserting on the posterodorsal faces of the epibranchials I-III (Fig. 5.7b).

The levator interni muscles originate similar to the levator externi muscles and are subdivided into two bundles inserting on the dorsal faces of the infrapharyngobranchials II-IV and the anterodorsal face of the upper pharyngeal tooth plate (Fig. 5.7b).

The large subpharyngealis has longitudinal fibers running on the dorsal sides of the ventral parts of the gill arches, including the basibranchials I-III, hypobranchials I-

II and anterior part of the ceratobranchials I-IV. This muscle originates musculously from the anterodorsal face of the anterior ceratohyals, with counterparts being merged caudally. Their medial fibers insert on the anterior face of the ventral parts of the gill arches and posteriorly are merged with fibers that originate from the dorsal and posterior faces of the ventral parts of the gill arches. It musculously inserts on the anterolateral face of the fourth ceratobranchials above the transversus ventralis muscle (Fig. 5.7b).

The transversus ventralis muscle spans the midline between the anteroventral faces of the fourth pair of ceratobranchials (Fig. 5.7b).

The pharyngocleithralis muscle originates musculously from the lateroventral face of the cleithrum and inserts musculously on the posteroventral and posteromedial faces of the fourth ceratobranchial and the medial faces of the fifth ceratobranchial (Fig. 5.8d).

The pharyngeal tooth plate adductor muscle connects the posterodorsal face of the fourth ceratobranchial bone to the ventral face of the hypobranchial bone of the same arch. The fourth ceratobranchial and fourth hypobranchial are tightly connected to the lower and upper pharyngeal tooth plates, respectively by connective tissue. Contraction of this muscle can bring upper and lower pharyngeal tooth plates together (Fig. 5.7b). Other branchial muscles were not observed.

The epaxial muscles insert musculously on the supraoccipital, epioccipitals, pterotics, exoccipitals and basioccipital. The hypaxial muscles insert tendinously on the posterior part of the otic bullae that are formed by the exoccipitals and basioccipital.

5.4.3. Cranial myology of *Ilyophis brunneus*

The adductor mandibulae muscle complex is also comprised of the sections A2 and A3. The section A2 is subdivided into a dorsal subsection A2β and a ventral subsection A2α (Fig. 5.9a). The subsection A2β, the largest element of the adductor mandibulae muscle complex, inserts through a tendon on the medial face of the coronoid process. The anterior fibers of A2β originate from a common fascia with its counterpart and its posterior fibers originate musculously from the supraoccipital, epioccipital, parietal and posterolateral margin of the pterotic (Fig. 5.9a). The

subsection A2α originates musculously from the posterolateral face of the hyomandibula, anterodorsal face of the preopercle, posterior edge of the suspensorial fossa and dorsal face of the quadrate. The lateral fibers of this subsection insert tendinously on the dorsal edge of the angular bone, posterior edge of the coronoid process and its medial fibers insert musculously onto the Meckelian fossa. The maxillary bone is connected to the dorsolateral face of the angular complex by the primordial ligament that is located ventral to A2α (Fig. 5.9a). The section A3 originates musculously from the anteroventral face of the pterotic, dorsal face of the pterosphenoid, dorsal face of the basisphenoid and anterolateral face of the sphenotic. This muscle inserts musculously on the posteromedial face of the lower jaw from the anterior level of the coronoid process to the anterior edge of the mandibular articulation facet. Both the interoperculo-angular and ceratohyalo-angular ligaments are present (Fig. 5.9b).

The adductor arcus palatini muscle originates musculously from the lateral face of a small ventral keel on the parasphenoid and inserts on the medial face of the quadrate and posteromedial face of the hyomandibula. This muscle starts at the posterior level of the basisphenoid and runs caudally up to the posterior level of the sphenotic. A thin, slender-like pterygoid bone, which is situated under the adductor arcus palatini muscle, connects to the premaxillo-ethmoidal complex and the anterodorsal corner of the quadrate by the pterygideo-premaxillo-ethmoidal and pterygoideo-quadrate ligaments, respectively.

The levator arcus palatini muscle originates musculously from the ventral face of the sphenotic process with its fibers directed caudoventrally (Fig. 5.9b). This muscle inserts musculously on the posterolateral face of the suspensorial fossa that is formed by the anterior parts of the hyomandibula and quadrate.

The dilatator operculi muscle originates musculously from the posteroventral face of the sphenotic and lateroventral face of the pterotic and inserts musculously on the anterolateral face of the opercle (Fig. 5.9b).

The undifferentiated levator and adductor operculi muscle complex is directed caudoventrally (Fig. 5.9a), and originates from the posterodorsal edge of the hyomandibula and ventrolateral face of the exoccipital. The lateral and medial fibers

of the levator/adductor operculi muscle insert musculously on the dorsolateral and dorsomedial faces of the opercle, respectively (Fig. 5.9a, b).

The protractor hyoidei originates tendinously from the medial face of the dentary, posterior to the dental symphysis (Fig. 5.9c). The lateral fibers of this muscle insert musculously on the anterodorsal face of the anterior ceratohyal and its few medial fibers connect to a posterior protractor hyoidei tendon that is attached to the urohyalo-basihyal ligament and anteromedial face of the interopercle (Fig. 5.9c).

The sternohyoideus muscle originates muscoulously from the ventromedial face of the cleithrum, with left and right halves merging before inserting tendinously on the posterior end of the urohyal (Fig. 5.9c).

The hyohyoideus muscle complex of *I. brunneus* forms a sheet of fibers that interconnects the medial faces of the branchiostegal rays, opercle and subopercle and reaches dorsally up to the horizontal septum between the epaxial and hypaxial muscles. Both muscle halves extend ventrally to meet their antimeres to forms a sac-like muscle that covers the branchial chamber (Fig. 5.9a).

The levator externi muscles originate musculously from a depression situated posterior to the anterior suspensorial articulatory facet on the prootic. Posteriorly these muscles are subdivided into three bundles inserting on the posterodorsal faces of the epibranchials III-IV.

The levator interni muscles originate similar as the levator externi muscles and are subdivided into two bundles inserting on the anterodorsal face of the infrapharyngobranchial and dorsal face of the upper pharyngeal tooth plate.

Left and right halves of the subpharyngealis run on the dorsal sides of the ventral parts of the gill arches, including the basibranchials I-III, hypobranchials I-II and anterodorsal faces of the ceratobranchials III-IV. Each half of this muscle originates musculously from the anteromedial face of the anterior ceratohyal and inserts on the anterior part of the fourth ceratobranchial.

The pharyngocleithralis muscles originate musculously from the lateroventral face of the cleithra and insert musculously on the posteroventral face of the last basibranchials and anteroventral face of the lower pharyngeal tooth plates.

The pharyngeal tooth plate adductor muscle connects the posterodorsal face of the fourth ceratobranchial bone to the ventral face of the fourth hypobranchial bone.

The transversus ventralis muscle spans the midline between the anteroventral faces of the fourth pair of ceratobranchials.
The obliquus dorsalis muscle interconnects the posterodorsal face of the fourth epibranchial to the anterodorsal face of the infrapharyngobranchial I.
The ventral retractor muscle connects the posteroventral face of the lower pharyngeal tooth plate to the dorsolateral face of the cleithrum.
The epaxial muscles insert musculously on the supraoccipital, exoccipitals and pterotics, epioccipitals. The hypaxial muscles insert musculously and tendinously on the exoccipitals and basioccipital.

5.4.4. Cranial myology of *Synaphobranchus brevidorsalis*

The adductor mandibulae muscle complex is also comprised of the sections A2 and A3. The section A2 is subdivided into a dorsal subsection A2β and a ventral subsection A2α (Fig. 5.10a). The subsection A2β originates musculously from the supraoccipital, parietal, posterior part of the frontal and anterior part of the pterotic. The subsection A2β inserts tendinously on the dorsal edge of the short coronoid process and musculously at the anterior level of the long Meckelian fossa. The lateral fibers of A2α originate musculously from the posterior part of the hyomandibula and anterodorsal face of the tube-like preopercle (Fig. 5.10a). They insert musculously at the posterior level of the Meckelian fossa, whereas the medial fibers originate musculously from the posterior face of the suspensorial fossa that is formed by the anterior parts of the hyomandibula and quadrate. The medial fibers of A2α are inserted musculously on the posteroventral margin of the Meckelian fossa and posterodorsal face of the coronomeckelian bone. The section A3 is a strip-like muscle that originates musculously from the anteroventral face of the sphenotic process (Fig. 5.10b). It is directed caudoventrally and inserts musculously on the posterior face of the coronomeckelian bone.
The adductor arcus palatini muscle starts at the level of the lateral expansion of the parasphenoid with fibers directed caudoventrally. This muscle originates musculously from the lateral face of the midsection of the parasphenoid (Fig. 5.10a). The anterior fibers of the adductor arcus palatini inserts on the posterior part of the pterygoid that is connected to the anterodorsal end of the quadrate

process by the pterygoideo-quadrate ligament. The posterior fibers of this muscle insert musculously on the anterodorsal edges of the anterior process of the quadrate.

The adductor hyomandibulae muscle originates musculously from the posterior part of the sphenotic and ventromedial face of the prootic and inserts muscoulously on the anteromedial face of the hyomandibula.

The levator arcus palatini muscle originates both tendinously and musculously from the lateroventral and ventral faces of the sphenotic process (Fig. 5.10b). It is directed caudoventrally and inserts musculously on the anterolateral faces of the hyomandibula and quadrate (Fig. 5.10b).

The dilatator operculi is a strip-like muscle that originates musculously from the posteroventral face of the sphenotic process and runs caudoventrally (Fig. 5.10b). It is connected to the dilatator operculi tendon after entering the posterior groove of the hyomandibula and inserts on a lateral process of the opercle situated on its anterolateral face (Fig. 5.10b).

The levator operculi muscle originates musculously from the medial face of the posterodorsal margin of the hyomandibula and ventral face of the posterior process of the pterotic. It is directed caudoventrally and inserts musculously on the laterodorsal face of the opercle (Fig. 5.10a).

The adductor operculi muscle originates musculously from the ventroposterior face of the exoccipital and ventromedial face of the pterotic. It inserts on the dorsomedial margin of the opercle (Fig. 5.10b).

The protractor hyoidei originates tendinously from the medial face of the dentary, at the rear of the dental symphysis (Fig. 5.10c). The medial fibers of the protractor hyoidei insert musculously on the anterodorsal face of the anterior ceratohyal, whereas a small bundle of its lateral fibers extends caudally and inserts musculously on the posterolateral face of the posterior ceratohyal (Fig. 5.10c).

The sternohyoideus is similar to that of *I. brunneus* but its left and right halves originate from the ventrolateral faces of the cleithra (Fig. 5.10c).

The hyohyoideus muscle complex is connected to its counterpart at its median raphe to form a thin sac-like sheet of fibers that cover the branchial chamber. Its fibers interconnect the successive branchiostegal rays and dorsally attach to the

ventral rim of the epaxial fascia and the horizontal septum between the epaxial and hypaxial muscles.

The levator externi muscles originate musculously from a pterotic depression situated posterior to the anterior suspensorial articulatory facet. Posteriorly these muscles are subdivided into four bundles inserting on the posterodorsal faces of the epibranchials I-IV.

The levator internus muscle originates from the pterotic depression, medial to the levator externi muscles. This muscle inserts on the dorsal face of the upper pharyngeal tooth plate.

The subpharyngealis runs on the dorsal side of the ventral parts of the gill arches, including the basibranchials I-IV, hypobranchials I-II and anterodorsal faces of the ceratobranchials III-IV. Both halves of this muscle originate tendinously from the basibranchialo-hypohyal ligament and insert on the anterior part of the fourth ceratobranchial.

Origin and insertion of the pharyngocleithralis, tooth plates adductor and ventral retractor muscles in *S. brevidorsalis* are similar with those of *I. brunneus.*

The epaxial muscles insert musculously on those parts of the epioccipitals, pterotics, exoccipitals and basioccipital that contribute to form the posterior wall of the neurocranium. The hypaxial muscles insert tendinously on the left and right sides of the otic bullae formed by the anteroventral part of the basioccipital.

5.5. Discussion

5.5.1. Variation in cranial morphology of Synaphobranchidae

Diversity in feeding habits can be considered as being reflected in those structural elements associated with feeding, in relation to different functional demands (Wainwright and Bellwood, 2002, Konow and Sanford, 2008). *Ilyophis brunneus*, the muddy arrowtooth eel, feeds on annelids and crustaceans (Smith et al., 1999; Heemstra et al., 2006). *Synaphobranchus brevidorsalis*, the shortdorsal cutthroat eel, is assumed to feed on decapods, amphipods, cephalopods and fishes, just like other *Synaphobranchus* species (Houston and Haedrich, 1986; Saldanha and Bauchot, 1986). In contrast to this more generalised way of feeding, *Simenchelys parasiticus* has been described as being parasitic or a scavenger, burrowing into the

bodies of other fishes (Bigelow and Schroeder, 1953; Castel, 1961; Robins and Robins, 1989; Goode and Bean, 1896; Caira et al., 1997). Hence, comparison of the head musculoskeletal morphology of *I. brunneus*, *S. brevidorsalis* with that of *S. parasiticus*, representatives of the three subfamilies of Synaphobranchidae that show different feeding habits, may help to better understand the nature of the morphological specializations of the feeding apparatus in *S. parasiticus*. This provides an indirect tool to test the hypothesis that it would be specialized for this parasitic way of feeding.

5.5.1.1. Osteology: The characters of *S. parasiticus* are a combination of primitive features and uniquely derived characters. *Simenchelys parasiticus* resembles the synaphobranchids in many features of its osteology, with some exceptions that may be related to an adaptation to its feeding behavior.

The preorbital region of *I. brunneus* is relatively long, that of *S. brevidorsalis* is moderate, whereas *S. parasiticus* bears a short snout. The palatopterygoid of *S. parasiticus* is firmly connected to the suspensorium (hyomandibula and quadrate) and neurocranium, whereas only a slender pterygoid is presents in *I. brunneus* and *S. brevidorsalis*. The pterygoid of *I. brunneus* and *S. brevidorsalis* is connected to the suspensorium and neurocranium via a ligament.

The hyomandibula-quadrate axis is slightly inclined posteriorly in *S. brevidorsalis*, unlike a vertical one in *I. brunnensis*. This axis is inclined forward in *S. parasiticus* and hence the quadrate-mandibular articulation is positioned at the level of the posterior part of the orbit. A posterior position of the quadrate-mandibular articulation, caudal to the posterior end of the neurocranium, is coupled to an elongation of the lower jaw, resulting in a large, non-circular mouth gape in *I. brunneus* and *S. brevidorsalis* with slender jaws. A phenomenon also observed in other long-jawed Anguilliformes (Eagderi and Adriaens, 2010 a, b). In contrast, *S. parasiticus* has short, deep and stout upper and lower jaws.

The hypohyal and urohyal of *S. parasiticus* are completely modified compared to those in *I. brunnensis* and *S. brevidorsalis*. The urohyal of *S. parasiticus* is short and large unlike the long, slender-like one of *I. brunnensis* and *S. brevidorsalis*. The urohyal of the *S. parasiticus* provides a large insertion area for the sternohyoideus

muscle, and has two dorsal condyles that articulate with the ventral hypohyals, whereas it articulates with the anterior ceratohyals in *I. brunnensis* and *S. brevidorsalis*. The dorsal and ventral hypohyals of *S. parasiticus* are firmly connected to the anterior ceratohyals, whereas only a small shaft-like hypohyal is present in *I. brunnensis* and *S. brevidorsalis*.

Externally *S. parasiticus* differs from other anguilliform species in having uniserial cutting edged teeth, a small terminal narrow mouth opening and a very large tongue-like structure (Regan, 1912). The presence of the small, simple teeth on the maxillary, dentary and vomer (very numerous in the first two) in *I. brunnensis* and *S. brevidorsalis* is a primitive characteristic of the Synaphobranchidae (Robins and Robins, 1989). The cutting edge teeth of the maxillary and lower jaw in *S. parasiticus* are uniserial and aligned with their cutting edges situated laterally, forming a scissor-like structure. The chisel-like teeth on the premaxillo-ethmoidal complex, vomer, maxillary and lower jaw of *S. parasiticus* can be considered beneficial when removing big chunks of flesh from prey.

The mouth opening of *S. parasiticus* is covered by a multilayer epithelial tissue similar to a transitional epithelium that is specialised for dealing with extensive stretching (Swanson, 1996; Genten et al., 2009). This multilayered epithelium of the oral mucosa shows the presence of numerous goblet cells (Fig. 5.5). Also, the dermis around its mouth opening is thick and bears a thick stratum compactum, consisting of a dense connective tissue giving the skin strength and elasticity (Swanson, 1996) (Fig. 5.5). Hence, the anterior tip of the bony snout in *S. parasiticus* is positioned some distance away from the anterior tip of the fleshy snout (Fig. 5.2c). The tongue-like structure of *S. parasiticus* fills the ventral part of the buccal cavity and, considering its histological nature seems to be a secretory organ with large secretory cells organised in many secretory units (Fig. 5.5).

5.5.1.2. Myology: The cephalic myology of *S. parasiticus* shows remarkable differences in both size and shape of the muscles, compared to the condition in *Ilyophis brunneus* and *Synaphobranchus brevidorsalis,* particularly in the muscles of the ventral surface of the head. Also, the adductor mandibulae muscle complex of

S. parasiticus is greatly enlarged compared to that of *I. brunneus* and *S. brevidorsalis*.

Simenchelys parasiticus bears an enlarged levator arcus palatini with an anterior and a posterior subsection, and with its origin extended almost to the posterior part of the neurocranium. In *I. brunneus* and *S. brevidorsalis*, the muscle originates only from the ventral part of the sphenotic process and is not subdivided. Also, *S. parasiticus* bears a large adductor arcus palatini muscle and smaller adductor hyomandibulae. A distinct adductor hyomandibulae is absent in *I. brunneus*.

The muscles of the ventral surface of the head in *S. parasiticus* are large and show more specializations compared to those of *I. brunneus* and *S. brevidorsalis*. The hyohyoideus inferioris muscle is a differentiated part in the hyoideus muscle complex in *S. parasiticus*, but not in *I. brunneus* and *S. brevidorsalis*. In addition, the protractor hyoidei and sternohyoideus of *S. parasiticus* are larger in comparison to the other two species studied.

The levator externus, levator internus, subpharyngealis, pharyngocleithralis and pharyngeal tooth plate adductor muscles are gill arch muscles present in all three species and seem to be synapomorphic in the synaphobranchids but shared with other Anguilliformes such as muraenids. However, the levator externus, levator internus, subpharyngealis and pharyngocleithralis muscles are well-developed in *S. parasiticus* compared to the two other species studied.

5.5.2. Cranial specializations in relation to parasitism

Parasitism by marine fishes is not a common strategy, but it does occur in a number of different species (Hutchins et al., 2003). *Simenchelys parasiticus* has been found burrowed into the flesh of various bottom-dwelling fishes, but has also been recorded from the heart of a mako shark (Caira et al., 1997). The modified cephalic musculoskeletal elements of *S. parasiticus*, compared to those of *Ilyophis brunneus* and *Synaphobranchus brevidorsalis*, may reflect the specialized way of feeding in this pugnose eel.

The small terminal mouth opening of *S. parasiticus* surrounded by a thick and stretchable skin and its gape reaches posterior to the nostrils, halfway of its short blunt snout. *Simenchelys parasiticus* may utilize this specialized terminal mouth in

order to attach to its host, forming a seal with its lips. In contrast, *I. brunneus* and *S. brevidorsalis* bear a large, noncircular mouth gape due to the posterior position of the quadrate-mandibular articulation. An aquatic predator with a large, non-circular mouth gape as in muraenids is able to move jaws into a biting position without pushing potential prey away from the opened mouth, and hence consume large preys (Porter and Motta, 2004; Mehta and Wainwright, 2007b, 2008, 2009).

The cutting edge and blade-like teeth of *S. parasiticus* on the premaxillo-ethmoidal complex, upper and lower jaws, along with the enlarged adductor mandibulae muscle complex can be employed to shear and remove a chunk of flesh from its prey, just like scissors. The biting mechanism of *S. parasiticus* may show some similarities with that of the cookie-cutter shark, *Isistius brasiliensis*. This small shark attaches to the prey by forming a seal with its fleshy lips. The upper jaw of *I. brasiliensis* is reduced in size and is composed of two pieces: an anterior section that can pivot dorsally, and a posterior section. Presumably, its upper jaw pivots at this junction when the shark is attached to its prey with its upper jaw, allowing the shark to pivot dorsally about this joint and sink its lower jaw teeth into the prey (Jones, 1971; LeBoeuf et al., 1987; Shirai and Nakaya, 1992).

The tight connection of the large palatopterygoid of *S. parasiticus* to the suspensorium and neurocranium may be linked to its ability for a powerful bite. Grubich et al. (2008) pointed out that a large palatoquadrate can function as a shock absorber to protect the eye orbit from high impact forces during the strike and subsequent bites in the great barracuda.

The stout mouth closing apparatus, as observed in the jaws in *S. parasiticus* may reflect the presence of large mechanical loads from muscle forces during biting (Duellman and Trueb, 1986; Hildebrand, 1995, Summers et al., 1998; Devaere et al., 2001), which can be expected to be large considering the hypertrophied jaw adductor muscles. Enlarged adductor mandibulae muscles of *S. parasiticus* with a perpendicular insertion of the tendon A2β and the fibers of A3 onto the lower jaw, suggest an adaptation to powerful biting due to an efficient force transfer during mouth closure (Devaere et al., 2001; Herrel et al., 2002). Also, the insertion surface of the adductor mandibulae muscles is along two thirds of the length of the lower jaw in *S. parasiticus*. This, together with the short jaws, implies a bigger

mechanical advantage (larger input/output lever ratio), but a reduced biting velocity, all which are linked to a large biting force. In contrast, *I. brunneus* and *S. brevidorsalis* bear long jaws with the length equal or longer than the neurocranium, which indicates that these predators rely on a high-velocity jaw closure for capturing prey (Norton and Brainerd, 1993; Ferry-Graham et al., 2001b, 2001c; Porter and Motta, 2004; Kammerer et al., 2005; De Schepper et al., 2008; Eagderi and Adriaens, 2010a). Also, the adductor mandibulae muscles of *S. parasiticus* are attached to the epaxial muscles. The coupling between the jaw muscles and the epaxial muscles could be considered an advantage for transferring forces from the body onto the head during feeding (Liem and Osse, 1975; Caroll, 2004; De Schepper et al., 2005).

The large protractor hyoidei and sternohyoideus of *S. parasiticus* suggests the ability to ventrally expand the buccal cavity and produce suction forces (Lauder, 1985; De Visser and Barel, 1998; Carroll, 2004; Sanford and Wainwright, 2002; Mehta and Wainwright, 2007b; Konow and Sanford, 2008). Also, *S. parasiticus* bears a heavily ossified urohyal-ceratohyal system to support these two large muscles. We speculate that these specializations of *S. parasiticus* may be beneficial for creating higher suction force to attach to its prey, thereby assisted using its fleshy lips.

The bony elements of the branchial arches in the three studied synaphobranchids do not show an extreme reduction like those of muraenids do but they bear many similar corresponding musculature attachments to those of the muraenids that enable them to transport relatively large prey into the esophagous using their pharyngeal jaws (Mehta and Wainwright, 2007a). In these species, the levator externi, levator interni, subpharyngealis, pharyngeal tooth plate adductor and pharyngocleithralis muscles of the synaphobranchids could play a role in protracting and retracting the branchial arches for transferring food in the buccal cavity. The levator externi and levator interni muscles could then lift the dorsal parts of the branchial arches and shift them forward at the same time (Vandewalle et al., 2000; Mehta and Wainwright, 2007a). The subpharyngealis and protractor hyoidei muscles can then pull the ventral parts of the branchial arches forward. The pharyngeal tooth plate adductor muscles could then bring the lower and upper

tooth plates together to grasp the food items. The pharyngocleithralis muscles and extended sternohyoideus muscle may then draw the branchial arches back and downward to its resting position (Vandewalle et al., 2000; Mehta and Wainwright, 2007a). It is suggested that this synapomorphic feature of Synaphobranchids i.e. the potential for mechanical transport system, would be still advantagous for specialised way of feeding in *S. parasiticus* to transport chunks of removed flesh from a prey into the esophagus, while it is attached to it. After having bitten of a chunk of flesh and during manipulation of food in the buccal cavity, the food may be continmated with the secretions of the large tongue-like structure, before being transferred into the esophagous.

In addition, Bigelow and Schroeder (1953) pointed out that the body of *S. parasiticus* is covered by a sheet of mucus when drawn out of the water. Such a slimy body of *S. parasiticus* may be advantageous during excavating a path into the body of the prey.

The cephalic musculoskeletal system of the pugnose eel, *S. parasiticus*, at least shows that it has the structural modifications needed to remove chunks of flesh from a food item and excavating into it. In this process, *S. parasiticus* can use its stretchable skin around a small terminal mouth opening, cutting edge teeth, short and stout jaws and associated muscles, and transferring the removed flesh into the esophagus using branchial arches, while being attached to its prey. However, this does not rule out any of the two strategies, whether it is a scavenger or a true parasitic eel.

ACKNOWLEDGMENTS

The authors would like to thanks **M. McGrouther** (Australian Museum), **R.H Robins and J.A Lopez** (Florida Museum of Natural History) and **D. Johnson** (National Museum of Natural History-Smithsonian Institution) for providing museum specimens, **N. De Schepper** (Ghent University) for her assistance and **D.G. Smith** (Smithsonian, USA) for his valuable comments.

Chapter 6

Cephalic Specializations in Relation to a Second Set of Jaws in Muraenids

Chapter six

Cephalic Specializations in Relation to a Second Set of Jaws in Muraenids

6.1. Abstract

The Muraenidae, one of the largest clades within the anguilliform fishes, exhibit an innovative feeding mechanism that allows them to transport large prey items from the oral jaw all the way back towards the esophagus using the pharyngeal jaws (Mehta and Wainwright, 2007a). The current study was conducted to show the degree to what trade-offs in muraenids may have arisen in the oral feeding apparatus, in relation to this pharyngeal transport system. Hence, the head musculoskeletal features of *Anarchias allardicei* (Uropterygiinae: Muraenidae) and *Gymnothorax prasinus* (Muraeninae: Muraenidae) were compared with that of a closely-related outgroup with a hydraulic-based prey transport, *Ariosoma gilberti* (Bathymyrinae: Congridae) and a detailed description of their cranial osteology and myology is provided. The results showed that this innovative feeding mechanism may be linked to many cephalic modifications such as, the stout and robust neurocranial elements, an elongated lower jaw as the result of the posterior position of the quadrato-mandibular articulation, enlarged teeth of oral jaws and premaxillo-ethmovomeral complex, reduction in the movable cranial bones and their muscular connections, hypertrophied adductor mandibulae muscle complex, presence of the quadrato-maxillary and preoperculo-angular ligaments, connection of the quadrate to the A2 tendon of the adductor mandibulae complex, caudoventral orientation of the fibers of the large A3 section of the adductor mandibulae complex.

6.2. Introduction

The eels of the Anguilloidei are a suborder comprising fifteen families, thereby forming the richest suborder within the Elopomorpha. The Muraenidae, one of the largest clades within the anguilliforms and known as morays, include about 200 species within more than fifteen genera (Böhlke et al., 1989; Nelson, 2006). Two monophyletic subgroups are recognized, i.e. Uropterygiinae and Muraeninae (Obermiller and Pfeiler, 2003; Wang et al., 2003; Lopez et al., 2007). Typically morays are shallow-water reef and crevice-dwelling eels. They are carnivores and

their abundance and biomass within shallow water reef in general is much greater than casually perceived (Böhlke et al., 1989; Santos and Castro, 2003). The muraenids bear an innovative feeding mechanism, which may explain their evolutionary success. Using their pharyngeal jaws, muraenids are capable to transport large captured prey items from the oral jaw all the way back towards the esophagus (Mehta and Wainwright, 2007a) (Fig. 6.1).

In contrast to the morays, most ray-finned fishes use a suction-induced flow of water to move prey from the oral jaws to the pharyngeal jaws (Gillis and Lauder, 1995; Mehta and Wainwright, 2007a, 2008). Therefore, the presence of the specialized mechanical transport system in morays provides an opportunity to better understand morphological changes on the head musculoskeletal system in relation to a novel feeding behavior and this within a proper phylogenetic framework. Hence, by comparing the cephalic morphology of representatives of both lineage within morays, uropterygiines and muraenines, as well as representative of a closely-related anguilliform family that still possesses the plesiomorphic hydraulic-based prey transport system, the cephalic morphological changes in relation to this specialization may be better understood.

This study was aimed to better understand the morphological changes of the head that have occurred during evolution, associated with the mechanical transport system in moray eels. Hence, we provide a detailed description of the cranial myology and osteology of *Anarchias allardicei* (Uropterygiinae: Muraenidae), *Gymnothorax prasinus* (Muraeninae: Muraenidae) and representative of a closely-related anguilliform family with a hydraulic based prey transport, *Ariosoma gilberti* (Bathymyrinae: Congridae) and compare their head musculoskeletal features to reveal the implications of the mechanical transport system on the head morphology of morays. The choice for this outgroup is based on the single most parsimonious tree of elopomorph fishes, using the combined data of mitochondrial 12S ribosomal RNA sequences, which supports the monophyly of the clade comprising Muraenidae and Bathymyrinae (Congridae) (Obermiller and Pfeiler, 2003).

6.3. Material and methods

For the anatomical description, four alcohol-preserved specimens of *Gymnothorax prasinus* (I.28736-024 and I.20095-031), eight specimens of *Anarchias allardicei* (I.17102-063 and UF 318044) and sixteen specimens of *Ariosoma gilberti* (UF 230612 and UF 10803) obtained from the Australian Museum and Florida Museum of Natural History were examined. The specimens were of following size in Total Length, (TL) *G. prasinus* (GP)1: TL: 437 mm; GP2: TL: 385.5 mm; GP3: TL: 497mm; GP4: TL: 447.2; *A. allardicei* (AA)1: TL: 99 mm; AA2: TL: 101 mm; AA3: TL: 108 mm; AA4: TL: 107 mm; AA5: TL: 110 mm; AA6: TL: 146 mm; AA7: TL: 129 mm; AA8: TL: 136 mm; *A. gilberti* (AG)1: TL: 133 mm; AG2: TL: 182 mm; AG3: TL: 134 mm; AG4: TL: 143 mm; AG5: TL: 162 mm;, AG6: TL: 149 mm; AG7: TL: 132 mm; AG8: TL: 152 mm; AG9: TL: 132 mm; TL: 145.5 mm; AG10: TL: 156.5 mm; AG11: TL: 129 mm; AG12: TL: 198 mm; AG13: TL: 157 mm; AG14: TL: 151 mm; AG15: TL: 123.5 mm; AG16: TL: 133 mm. One specimens of each species (GP2, AA1 and AG2) was cleared and stained with Alizarin red S and Alcian blue according to the protocol of Hanken and Wassersug (1981) for osteological examinations. Dissections with muscle fiber staining according to Bock and Shear (1972) were performed. Specimens were studied using a stereoscopic microscope (Olympus SZX-7) equipped with a camera lucida.

The musculature terminology follows Winterbottom (1974), De Schepper et al. (2005) and Mehta and Wainwright (2007a). The circumorbital bones of the cephalic lateral line system follow Adriaens et al. (1997). Terminology of cranial skeletal elements follows Nelson (1966), Böhlke (1989c) and Rojo (1991). The epiotic of teleosts is termed "epioccipital", thereby following Patterson (1975). The terminology of scarf joint follows Hildebrand (1995).

6.4. Results

6.4.1. Cranial osteology: *Ariosoma gilberti* (Bathymyrinae: Congridae)

The neurocranium forms one unit, tapering from the otic region towards the anterior end of the frontal bone and then continuing as a narrow bar towards the spatulate-like snout (Fig. 6.2a). The ethmoid region is comprised of the fused premaxillaries, ethmoid and vomeral bones, as the premaxillo-ethmovomeral

complex, as well as the nasals. The nasal bone is described with respect to the lateral line system (see below). The premaxillo-ethmovomeral complex bears a lateral process, which is directed anteroventrally with a small horizontal process at its end (Figs. 6.2 and 6.3a) and the olfactory rosette is located anterior to this process. The anteroventral face of the premaxillo-ethmovomeral complex is dentigerous with anterior, longer and recurved caniniform teeth (Fig. 6.2b).

The orbital region comprises the two small lacrimal bones, four infraorbital bones, frontal bones, parasphenoid, basisphenoids and pterosphenoids. Posteriorly, the frontal bones are connected with the parietal bones by an extensive scarf joint (Fig. 6.2a). Also, left and right frontal bones show a minor scarf joint (Fig. 6.2a). The ventroposterior rim of the frontal bone encloses the anterior portion of the temporal canal, which enters this bony canal at the connection between the frontal and pterosphenoid (Fig. 6.3a). The frontal forms the posterodorsal wall of the large orbit, and the foramen opticum lies between the ventral portions of the frontal bones. Anteriorly, the frontal bears a small lateral process over the orbit with a pore on its posterior part. The basisphenoid forms the posteroventral wall of the orbit and bears a small fossa on its anteroventral face. The dorsal part of this bone runs into the optic foramen and overlaps ventrally with the parasphenoid. The pterosphenoid is surrounded by the frontal, basisphenoid, parasphenoid, sphenotic and prootic bones. The pterosphenoid possesses a pore on its lateral face (Fig. 6.3a). The parasphenoid is bifurcated at its two ends and forms the ventral element of the orbit. At the midpoint, the parasphenoid bone bears distinct alar processes as well as a ventral keel (Fig. 6.2b).

The otic region is comprised of the sphenotics, pterotic, prootics, parietals and epioccipitals. The sphenotic is connected to the prootic bone by a bony strut of the prootic. The sphenotic contributes to form the anterior suspensorial articulatory facet, together with the prootic bone (Figs. 6.2b and 6.3a). The sphenotic bone bears a lateral process directing vertically. The pterotic bone braces the neurocranium laterally and encloses the posterior portion of the temporal canal, which opens at the posterodorsal face of the pterotic (Figs. 6.4a). Posteriorly, this bone connects to the exoccipital bone and contributes to form the posterior wall of the neurocranium. The posterior articulatory facet for the hyomandibula is formed

by the pterotic bone (Fig. 6.2b). The large prootic forms the anterior part of the otic bullae, with the foramen trigemino-facialis at the anterior edge of the bulla and two pores anterior to this foramen (Fig. 6.2b). The prootic possesses a long dorsal projection on its anterodorsal corner that runs under the posterior portion of the frontal. The anterior part of the parietal is covered by the frontal bone forming a relatively extended scarf joint.

The occipital region consists of the exoccipital and basioccipital bones. A surpraoccipital is absent. Both exoccipital bones are interconnected posterodorsally. The exoccipital bones ventrally form a depression on the posteroventral face of the neurocranium (Fig. 6.2b). The foramen magnum is bordered dorsally and laterally by the exoccipitals and ventrally by the condyle of the basioccipital. The basioccipital forms the posterior portion of the large otic bullae and wedges into the long posterior incisure of the parasphenoid.

The lower jaw ventrally forms a long groove, enclosed deep internal wall and shorter external wall, which supports the anterior part of the preoperculo-mandibular canal (Figs. 6.3a and 6.4a). The anterior portion of the lower jaw represents the dento-spleno-mentomeckelian complex, here referred to as the dentary complex. The dentary complex posterodorsally bears the coronoid process with a small coronomeckelian bone ventral to the process and bearing an apophysis on its medial face (Fig. 6.5b). The anterior portion of the coronomeckelian is enclosed by the dentary complex. A small Meckelian fossa is present at the rear of the coronomeckelian (Fig. 6.5b). Anteriorly, the dentary teeth are arranged in three rows and posteriorly in two rows of teeth with their tips pointing medially. The angular complex consists of the fused angular and articular bones, bearing a small retroarticular process (Fig. 6.5b). This complex wedges into the dentary complex. The retroarticular process is directed caudally and bears a pore. The opening of a canal is present anterior to the retroarticular process and anteriorly this canal opens into the posterior part of the Meckelian fossa (Fig. 6.5b). Also, there is a small pore on the medial face of this canal. The angular complex bears the caudodorsally directed mandibular articular facet. In the upper jaw, the maxillary bone is attached anteromedially to the premaxillo-ethmovomeral complex via an ascending articular process that is situated at the rear of its anterior end (Figs. 6.3a and 6.5a).

Anteriorly, the maxillary bone bears a patch of pointed teeth and posteriorly a double row of curved and pointed ones with a few posterior teeth that are arranged in a single row. The posterior end of the maxillary bone descends ventrally and is connected to the angular complex via the primordial ligament.

The suspensorium is comprised of four bones: the hyomandibula, quadrate, palatopterygoid and preopercle. The preopercle is described as part of the opercular series (see below). The suspensorium is longer than deep and bears an anterior fossa that is formed by the anterior portions of the hyomandibula and quadrate (Fig. 6.3b). The palatopterygoid anteriorly connects to the anterior part of the parasphenoid (Fig. 6.3a). There is a large synchondrosis at the connection of the palatopterygoid to the suspensorium. The hyomandibula is firmly connected to the quadrate with an interdigitated suture. The axis of the hyomandibula-quadrate inclines forwardly, placing the quadrate-mandibular joint at the level of the posterior part of the orbit (Fig. 6.3a). The hyomandibula bears three articular condyles: an anterior one articulating with the sphenotic and prootic; a posterior one articulating with the pterotic; and the opercular condyle situated at the posterodorsal margin of the hyomandibular bone (Fig. 6.3b). A distinct symplectic was not observed.

The opercular series consists of four bones: the preopercle, interopercle, subopercle and opercle (Fig. 6.6a). The distal margins of the opercular and subopercle bones were lightly stained in the specimen studied. The ventromedial face of the preopercle is connected to the posteroventral rim of the suspensorium. The entire anterolateral face of the preopercle forms a tubular structure that encloses the posterior portion of the preopercular-mandibular canal (Figs. 6.4a and 6.6a). The posterior rim of the preopercle covers the anterior margin of the interopercle. The ventral face of the interopercle curves medially and its anteromedial edge is connected to the angular bony complex by the interoperculo-angular ligament. The subopercle lies curved against the entire posterior margin of the opercle. The fan-shaped opercle articulates through its rostral process to the hyomandibular bone. Two ridges are present on the lateral face of the opercle, anteriorly forming an apophysis at the anterolateral face of the opercular rostrum.

The hyoid complex is comprised of the unpaired basihyal and urohyal, paired anterior and posterior ceratohyals (Fig. 6.6b). The rod-like basihyal bone bears a ventral crest that is connected to the lateral face of the anterior ceratohyal bone by the basihyalo-ceratohyal ligament. Anteriorly, the urohyal bone bears a deep and thick portion with a cross-like ridge on its dorsal face that forms the left and right ceatohyal articular facets. Posteriorly, the urohyal forms a brace-like part that bears two long processes (Fig. 6.6b). The anterior ceratohyal is firmly connected to the posterior one. The anterior ceratohyal ventromedially bears the urohyal articular condyle and dorsomedially the basihyal articular condyle. The posterior part of the posterior ceratohyal curves dorsally and is connected to the posteroventral corner of the angular complex by the ceratohyalo-angular ligament. Four of the eleven branchiostegal rays are connected to the anterior ceratohyal, the others to the posterior ceratohyal. The branchiostegal rays curve dorsally along the ventral border of the interopercle and reach up to the caudal border of the subopercle.

The cephalic lateral line system is comprised of the supraorbital, infraorbital, temporal and preoperculo-mandibular canals, and supratemporal commissure. The ethmoid canal, adnasal canal and frontal commissure were not observed. The supraorbital canal extends over the olfactory rosette to the postorbital region and possesses a single external pore. The anterior openings of the left and right supraorbital canals abut (Fig. 6.4a). The nasal bone is a rectangular bone with a ventral process at its midpoint (Fig. 6.4b). Dorsally, it bears a tubular structure that supports the anterior portion of the supraorbital canal (Fig. 6.4b). This bone was also slightly stained. The infraorbital canal starts at the rear of the snout tip. This canal extends posteriorly and curves dorsally into the postorbital region and anastomoses with the supraorbital canal in front of the entrance of the temporal canal into the skull (Fig. 6.4a). Two lacrimal bones support the anterior part of the infraorbital canal and its posterior part is enclosed by four infraorbital bones before anastomosing with the supraorbital canal (Fig. 6.4b). The infraorbital canal bears five external pores. The temporal canal runs inside the frontal and pterotic bones. The preoperculo-mandibular canal starts from the tip of the dentary complex and runs in the ventral groove of the mandibula. This canal continues into the tubular

part of the preopercle and anastomoses with the posterior end of the temporal canal (Fig. 6.4a). The preoperculo-mandibular canal bears nine external pores.
Almost all ventral elements of the branchial arches are present (Fig. 6.7): Four basibranchial bones (Bb I-VI), two pairs of hypobranchial bones (Hb I-II) (the third pair is smaller and unossified), five pairs of ceratobranchial bones (Cb I-V) (fifth pair is reduced, located ventrally to the pharyngocleithralis muscle), and one pair of lower pharyngeal tooth plates (LP). The dorsal elements of the gill arches present are: Four pairs of epibranchial bones (Eb I-IV), two pairs of the infrapharyngobranchial bones and one pair of the upper pharyngeal tooth plates (UP) (Fig. 6.7). The upper and lower tooth plates bear small teeth, pointing caudally.

6.4.2. Cranial Myology: *Arisoma gilberti*

The adductor mandibulae muscle complex comprises the sections A2 and A3. The section A2 can be subdivided into three subsections: A2α, A2β anterior (A2βa) and A2β posterior (A2βp) (Fig. 6.8a). The lateral fibers of the subsection A2βa originate musculously from the epioccipital, pterotic, parietal and posterior part of the frontal, its medial fibers originating musculously from the anterior part of the sphenotic process. This subsection inserts as a tendon onto the anteromedial face of the coronoid process. The posterodorsal fibers of A2βp are attached to their counterpart and fascially to the epaxial, and originate musculously from the epioccipital, pterotic and parietal. The lateral fibers, together with the lateral fibers of the subsection A2α, are connected to the tendon A2 that inserts on the posteromedial face of the coronoid process. The medial fibers of A2βp also insert musculously on the posteromedial edge of the coronoid process. The lateral fibers of the A2α originate musculously from the preopercle, hyomandibula and quadrate bones. Its medial fibers originate musculously from the lateroposterior face of the hyomandibula and the ventroposterior edge of the suspensorial fossa. They insert musculously on the posteromedial face of the mandibula from the Meckelian fossa to the anterior edge of the retroarticular process.
The section A3 originates musculously from the ventral part of the frontal, pterosphenoid and anterior part of the prootic, and tendinously from the

anteroventral face of the sphenotic process (Fig. 6.8b). The anterior fibers of this muscle insert tendinously on the ventromedial face of the coronoid process, at the rear of the insertion point of the tendon A2β. Its posterior fibers insert onto the dorsal face of the Meckelian fossa.

The adductor arcus palatini is a thin muscle that originates musculously from the ventral keel of the parasphenoid (Fig. 6.8b). This muscle inserts musculously on the laterodorsal face of the palatopterygoid and anteromedial face of the hyomandibula. Its posterior fibers merge with the anteromedial fibers of the adductor hyomandibulae.

The adductor hyomandibulae is distinguished from the adductor arcus palatini due to its thicker diameter. This muscle originates musculously from the anterior part of the basioccipital, pterotic and prootic and inserts musculously on the ventromedial face of the hyomandibula and quadrate.

The levator arcus palatini is situated posterior to the section A3 of the adductor mandibulae muscle complex (Fig. 6.8b). It originates musculously from ventral face of the sphenotic process, lateral face of the prootic and posterior face of the parasphenoid alae and inserts musculously on the lateroventral face of the suspensorial fossa and the laterodorsal face of the hyomandibular body.

The levator operculi comprises a ventral and a dorsal bundle (Fig. 6.8a). The ventral bundle originates tendinously from the posterodorsal depression of the hyomandibula that is situated dorsal to the opercle articular condyle and inserts musculously on the ventrolateral face of the opercle. The dorsal bundle originates tendinously from the lateroventral face of the exoccipital and inserts musculously on the dorsolateral face of the opercle (Fig. 6.8a).

The adductor operculi muscle originates musculously from a ventral depression on the exoccipital and the posterolateral face of the basioccipital. It inserts on the dorsomedial rim of the opercle. The lateral fibers of this muscle merge with the medial fibers of the dorsal bundle of the levator operculi (Fig. 6.8b).

The dilatator operculi is a triangular muscle that is situated posterior to the levator arcus palatini (Fig. 6.8b). It originates musculously from the lateral face of the prootic and ventral face of the pterotic and inserts tendinously onto an apophysis on the anterolateral face of the rostral opercular process (Fig. 6.8b).

The protractor hyoidei muscle connects the posterior ceratohyal to the lower jaw. Each half (right and left) of this muscle originates tendinously from the medial face of the dentary bone at the rear of its symphysis and inserts tendinously on the lateral face of the posterior ceratohyal (Fig. 6.8c).

The sternohyoideus muscle inserts as a tendon on the anterior thicker part of the urohyal and musculously on the medial faces of two posterior processes of the urohyal (Fig. 6.8c). The ventral fibers of the sternohyoideus, which insert on the anteromedial faces of the posterior processes of the urohyal, merge with the ventral extended fibers of the hypaxials. The dorsal fibers of the sternohyoideus, which insert on the entire medial faces of the posterior processes of the urohyal, are divided posteriorly into two bundles and originate from the lateral face of two cleithra.

The hyohyoideus superior muscle connects the posteromedial edge of the posterior ceratohyal to the medial margin of the rostral opercular process (Fig. 6.8c).

The hyohyoideus muscle complex (presumably an undifferentiated complex of the hyohyoideus inferioris and hyohyoidei adductors) is a muscle sheet that lies between the medial faces of the branchiostegal rays and forms a thin sac-like muscle meeting its counterpart at the ventral midline (Fig. 6.8a). The anterodorsal fibers of this muscle attach on the medial face of the opercle and posterodorsally on the horizontal septum between the epaxial and hypaxial muscles, by connective tissue.

The muscles serving the ventral parts of the branchial arches consist of the pharyngocleithralis (PHC), three pairs of the obliqui ventrales (Ob.v I-III), rectus communis (RC) and transversus ventralis of the lower tooth plates (Trans.v). The pharyngocleithralis muscle connects the lower tooth plate to the cleithrum (Fig. 6.7). The obliquus ventralis spans the ceratobranchial-hypobranchial joint of the first three branchial arches. The rectus communis connects the posterodorsal face of the second hypobranchial to the fourth ceratobranchial. The transversus ventralis tendinously connects the pharyngeal lower tooth plates to the posterior end of the fourth basibranchial (Fig. 6.7). The rectus dorsalis I-II (RD I: connects the first and second epibranchial; RD II: connects the second and third epibranchial), medial rectus dorsalis (RD.m; interconnects first and second epibranchial), obliquus

dorsalis I-II (Ob.d I: connects the epibranchial I and infrapharyngobranchial I; Ob.d II: connects epibranchial II and infrapharyngobranchial II) and medial obliquus dorsalis muscle (Ob.d.m: connects the infrapharyngobranchials) are muscles that serve the dorsal part of the branchial arches (Fig. 6.7).

6.4.3. Cranial osteology: *Gymnothorax prasinus* and *Anarchias allardicei* (Muraeninae and Uropterygiinae: Muraenidae)

The general configuration of the skull of *G. prasinus* and *A. allardicei* are very similar. For detailed description of the cranial osteology of *Gymnothorax prasinus* and *Anarchias allardicei*, here is provided only those elements that show differences with respect to *Ariosoma gilberti* to avoid repetition of the elements with same conditions.

The neurocranium of *G. prasinus* and *A. allardicei* is stout and tapers from the otic region towards the posterior part of the premaxillo-ethmovomeral complex. Their ethmoid region comprises the premaxillo-ethmovomeral complex and nasals (Figs. 6.9a and 6.10a). In both species, the olfactory rosette is located dorsal to the rostrum and is separated from the olfactory rosette of other side by a vertical wall of the premaxillo-ethmovomeral complex (Figs. 6.9a and 6.10a). In *G. prasinus* the two left and right inlet tubes of the olfactory system are connected to the premaxillo-ethmovomeral complex canal that are posteriorly opened into the olfactory rosettes. The snout of *G. prasinus* and *A. allardicei* are relatively short and shovel-like in a ventral view (Figs. 6.11b and 6.12b). Posterodorsally, the shovel-like snout of *G. prasinus* bears caudally directed struts on its left and right sides (Fig. 6.11), whereas that of *A. allardicei* possesses the two small processes i.e. the maxillary articular facets (Fig. 6.12). In both species, the dentition of the posterior part of the premaxillo-ethmovomeral complex is separated by a space from the anterior ones (Figs. 6.11b and 6.12b). The dentition of the anterior part of the premaxillo-ethmovomeral complex in *G. prasinus* comprises three rows of large, curved teeth with small teeth between the two lateral rows (Fig. 6.11b). Its teeth of the posterior part are arranged in one row with shorter teeth than those of the anterior ones. The anterior part of the premaxillo-ethmovomeral complex in *A. allardicei* contains of few, pointed teeth on its ventral face with a row of smaller

teeth on its rim (Fig. 6.12b). In addition, some small teeth are scattered among its large teeth (Fig. 6.12b). Its teeth of the posterior part are arranged in one row similar to *G. prasinus* but with three pointed teeth (Fig. 6.12b).

The orbital region of *G. prasinus* consists of the adnasal, lacrimal, infraorbitals, supraorbitals, frontal, basisphenoid, parasphenoid and pterosphenoid bones, whereas that of *A. allardicei* lacks the supraorbital and adnasal bones. In *G. prasinus* the frontal bears an anterodorsal process with a dorsal and a lateral opening (Fig. 6.9a). Also, a small frontal fontanel is present (Fig. 6.11a). In *A. allardicei* the frontal anteriorly bears a T-like groove, anterior to entrance of the temporal canal (Fig. 6.10a). Also, there is a small canal ventral to this frontal groove that posteriorly is connected to the temporal canal (Fig. 6.10a). The frontals of *A. allardicei* overlie the anterior half of the parietals (Fig. 6.12a). The basisphenoid forms the posterior wall of the small orbit in *G. prasinus* and *A. allardicei* (Figs. 6.9a and 6.10a). In both muraenids the basisphenoid bears the optic foramen on its lateral face (Figs. 6.9a and 6.10a). The olfactory foramen of *G. prasinus* is present on the posteroventral face of the basisphenoid (Fig. 6.9), whereas the pterosphenoid of *A. allardicei* bears a canal on its ventral part that encloses the olfactory nerve and this canal is opened on the anterior face of the pterosphenoid as olfactory foramen (Fig. 6.10). The parasphenoid of both muraenids is thick, long bone that forms the floor of the orbit (Figs. 6.9a, 6.10a, 6.11b and 6.12b). Laterally, it expands in the midsection and narrows posteriorly to a narrow point to wedge into the basisphenoid (Figs. 6.11b and 6.12b). Their pterosphenoid is enlarged compared to *A. gilberti*.

The otic region of *G. prasinus* and *A. allardicei* comprises the sphenotics, pterotics, prootics, epioccipitals and parietals. The sphenotic of *G. prasinus* bears a lateral process directing ventrally, whereas that of *A. allardicei* is directed anteroventrally (Fig. 6.10a). In both muraenids the pterotic forms the posterolateral element of the neurocranium and also the long posterior suspensorial articulatory facet (Figs. 6.11b and 6.12b). The prootic of *G. prasinus* is fenestrated with numerous foramia, including the trigemino-facial foramen on its anterolateral face (Fig. 6.11b). Its posterior end also bears an apophysis to which attaches the levator internus muscle of the upper pharyngeal jaw (Fig. 6.13d). The lateroventral part of the prootic in *A.*

allardicei bears a depression with three pores that the levator internus muscle inserts on the center of this depression (Fig. 6.12b). The trigemino-facial foramen of *A. allardicei* present on the anterior rim of the prootic bone (Fig. 6.12b). The parietals of *G. prasinus* are irregularly interdigitated anteriorly with the frontal and posteriorly are bordered by the epioccipital and supraoccipital bones, whereas those of *A. allardicei* show overlapping with the frontals and epioccipitals. A fontanel present at the triple suture point between the supraoccipital and parietals in *G. prasinus* (Fig. 6.11a). In both muraenids the posterior rim of the epioccipital is curved ventrally forming the dorsal rim of the posterior wall of the neurocranium.

The occipital region of *G. prasinus* and *A. allardicei* comprises the supraoccipital, exoccipitals and basioccipitals. Their supraoccipital is situated at the posterodorsal midline of the neurocranium and bears a well-developed crest directing caudally (Figs. 6.9a, 6.10a, 6.11a and 6.12a). Their paired exoccipitals border the foramen magnum with exception of the ventral part, which is bordered by the basioccipital. In both the exoccipital is domed towards the foramen magnum. The basioccipital of *G. prasinus* bears two apophyses on the left and right sides of the wedged posterior end of the parasphenoid that the levator externus muscle of the upper pharyngeal jaws insert on them. The posterior portion of the basioccipital in *G. prasinus* contributes to form a nipple-shaped, short otic bulla together with the exoccipital and prootic (Fig. 6.11b) and posteriorly, it bears four pores. In *A. allardicei* the basioccipital situates between two ventral parts of the exoccipitals and contributes to form the posterior part of the low otic bullae along with the exoccipital and prootic (Fig. 6.12b).

The maxillary of *G. prasinus* is attached to the strut of the posterodorsal process of the premaxillo-ethmovomeral complex. It bears two rows of the caniniform teeth on the anterior half with longer lateral ones, and the teeth on the posterior half are arranged in a single row (Fig. 6.14a). The maxillary in *A. allardicei* is longer than that of *G. prasinus* and is firmly attached to the maxillary articular facet of the premaxillo-ethmovomeral complex (Fig. 6.10a). In *A. allardicei*, the anterior part of the maxillary bears an ascending process that medially possesses two large teeth and a single row of pointed teeth on its anteromedial fossa (Fig. 6.15a). The quadrato-maxillary ligament in *G. prasinus* connects the posterolateral face of the

articulatory condyle of the quadrate to the posterodorsal face of the maxillary (Fig. 6.13a), whereas that of *A. allardicei* runs medial to the suspensorium and attaches to the medial face of the articulatory condyle of the quadrate. In both muraenids the large coronoid process is formed by the dentary complex. Anteriorly, the dentary complex of *G. prasinus* bears two rows of the caniniform teeth with three larger medial ones that continue in a single row of caudally pointed teeth running up to the coronoid process (Fig. 6.14b). The dentary in *A. allardicei* bears two rows of caniniform teeth with a longer median row that is extended to the midpoint of the lateral one (Fig. 6.15b). Also, few small, recurved teeth are present medial to the longer ones (Fig. 6.15b). Laterally, the dentary complex of *G. prasinus* bears six pores of the preoperculo-mandibular canal and one on its anteromedial face (Figs. 6.9a and 6.14b), whereas that of *A. allardicei* bears only five pores (Fig. 6.10a). The coronomeckelian bone in *G. prasinus* is situated between the dentary and angular complexes, ventral to the Meckelian fossa and anteriorly covered by the dentary (Fig. 6.14b) and that of *A. allardicei* is attached to the posteromedial face of the dentary and ventromedial face of the angular complex (Fig. 6.15b).

In both muraenids the angular complex consists of the fused angular, articular and retroarticular bones. Their mandibular articulation facet is positioned at the posterior end of the angular complex directing caudodorsally (Figs. 6.14b and 6.15b). The preoperculo-mandibular canal in both muraenids is opened on the posterior side of the short, caudally directed retroarticular bone. In both muraenids the anterolateral portion of the angular complex overlies the posterior part of the dentary complex. In *G. prasinus* and *A. allardicei*, a short preoperculo-angular ligament connects the posteromedial face of the angular complex to the ventromedial face of the preopercle.

In both muraenids the suspensorium comprises four bones; the hyomandibula, quadrate, palatopterygoid and preopercle (Figs. 6.9b and 6.10b). Anteriorly, the hyomandibula bears a fossa with a pore on its dorsal half (Figs. 6.9b and 6.10b). Medially, the hyomandibula bears a canal that is opened on its dorsomedial face. The posterior articular condyle of the hyomandibula is long with serrated edges on its dorsal midsection. The hyomandibula bears a opercular articular condyle medioventrally directing caudoventrally (Figs. 6.9b and 6.10b). The quadrate bears

a posterior process directing caudally that runs under the peropercle. The hyomandibula-quadrate axis is directed vertically, thus positioning the quadrate-mandibular joint at the occipital level of the neurocranium. Hence, the lower jaw is about equal in length to the neurocranium. The quadrate bears a posterior process on its medial face running caudally under the preopercle. The palatopterygoid is reduced as a thin slender bone attaching to the anteroventral edge of the hyomandibula by connective tissue and ligamentously on the anterior end of the quadrate.

In *G. prasinus* the four elements of the opercular series are reduced in size (Fig. 6.9b). The preopercle is a small, tube-like bone and connected to the quadrate. The preopercle encloses the midsection of the preoperculo-mandibular canal. The opercle bears an anterolateral tuberosity on its articulatory process (Fig. 6.9b). Also, there is a small process on the medial face of the opercular rostral prominence. The small rectangular subopercle and interopercle position anterior to the opercle (Fig. 6.9b). The opercular series of *A. allardicei* shows similar configuration and components with *G. prasinus*, except for lacking a midpoint pore on the lateral face of the preopercle (Fig. 6.10b).

The hyoid complex of *G. prasinus* is extremely reduced and consists of the paired anterior and posterior ceratohyals (Fig. 6.13c). The posterior ceratohyal is connected to the midpoint of the slender anterior ceratohyal by a cartilaginous strut at its anterior end. Also, the posterior ceratohyal is a slender bone that is connected to all eight branchiostegal rays anteriorly and to the medial face of a posterior process of the quadrate by connective tissue. The hyoid complex of *A. allardicei* is also extremely reduced and like *G. prasinus* consists of the paired anterior and posterior ceratohyals with a similar configuration (Fig. 6.16c).

The cephalic lateral line system of *G. prasinus* comprises the ethmoid and adnasal canals in addition to those of *A. gilberti* (Fig. 6.17b). The ethmoid canal is a short descending branch of the supraorbital canal and starts at the anterior edge of the olfactory cavity. It bears a single external pore. The supraorbital canal is caudally extended to the dorsal pore of the anterolateral process of the frontal. Anteriorly, it is enclosed by a tube-like nasal bone and posteriorly by two supraorbital bones (Fig. 6.17a). The supraorbital canal bears one external pore. The infraorbital canal

is curved dorsally into the postorbital region after exiting the first infraorbital bone positioned ventral to the orbit (Fig. 6.17a). This canal anstomoses with the supraorbital canal inside the anterolateral process of the frontal. The infraorbital canal bears four exteral pores. Aneriorly, the infraorbital canal is supported by the lacrimal and first infraorbital bones and posteriorly, by the three infraorbital bones (Fig. 6.17a). The adnasal canal is an ascending branch of the infraorbital canal exited from the medial face of the ventral infraorbital bone at its midpoint. This canal is supported at its midpoint by the adnasal bone. All circumorbital bones are tubular (Fig. 6.17a). The preoperculo-mandibular canal runs inside the mandibula (Fig. 6.17b).

In comparison to *G. prasinus*, the cephalic lateral line system of *A. allardicei* lacks the ethmoid and adnasal canals and possesses a frontal commissure (Fig. 6.18b). The posterior part of the supraorbital canal in *A. allardicei* is entered to the anterior part of the T-like groove of the frontal. The nasal bone was not stained completely. The supraorbital canal bears three external pores. The frontal commissure runs inside the dorsal part of the frontal groove (Fig. 6.18b). The infraorbital canal anstomoses with the supraorbital canal in the front of the T-like groove of the frontal. This canal bears five external pores. Two lacrimal and six infraorbital bones support the infraorbital canal (Fig. 6.18a). The preoperculo-mandibular canal bears six external pores.

In *G. prasinus* the ventral elements of the reduced gill arches are the following: four pairs of ceratobranchials (Cb I-IV) and one pair of lower pharyngeal tooth plates (LP) (Fig. 6.19b). Its dorsal elements of the gill arches are comprised of the four pairs of epibranchials (Eb I-IV) and one pair of upper pharyngeal tooth plates (UP) (Fig. 6.19a). The gill arches *A. allardicei* bear two pairs of infrapharyngobranchials (Ib II-III) in addition to those of *G. prasinus* (Fig. 6.20).

6.4.4. Cranial Myology: *Gymnothorax prasinus* and *Anarchias allardicei*

The configuration of the hypertrophied adductor mandibulae muscle complex of *Gymnothorax prasinus* and *Anarchias allardicei* are very similar. Their adductor mandibulae complex comprises the sections A2 and A3. The section A2 in *G. prasinus* is subdivided into two subsections: a hypertrophied A2 lateral (A2αl) and

strip-like A2 medial (A2γ) (Fig. 6.13a, b). The hypertrophied A2αl of *G. prasinus* is the largest element of the adductor mandibulae complex and its fibers originate from the frontal, parietal, pterotic, supraoccipital, hyomandibula and quadrate bones. The lateroanterior fibers of the A2αl insert as a tendon on the medial face of the dentary at the rear of the coronoid process, whereas its lateroposterior fibers are attached as a tendon on the mediodorsal edge of the coronoid process and medial margin of the angular bone. Also, the later tendon is connectd to the lateral face of the articulatory condyle of the quadrate by a tendon. The medial fibers of the A2αl in *G. prasinus* insert musculously into the Meckelian fossa (Fig. 6.13c). The A2γ of *G. prasinus* is positioned posterior to the levator arcus palatini muscle and runs medial to the dilatator operculi muscle (Fig. 6.13b). The fibers of A2γ originate from the posterodorsal face of the hyomandibula bone and insert by a tendon on the angular complex at the ventral rim of the Meckelian fossa (Fig. 6.13b).

The A2 section of *A. allardicei* can also be subdivided into two subsections; A2 dorsal (A2β) and A2 ventral (A2α) (Fig. 6.16a). The A2β is the largest component and its fibers originate from the frontal, parietal, pterotic, epioccipital and supraoccipital bones. This muscle inserts as a tendon on the ventromedial face of the coronoid process and musculously on the medial rim of the dentary and angular, posterior to the coronoid process. The tendon A2β is connected on the posterolateral face of the maxillary by a tendon. The A2α of *A. allardicei* is the ventral element and has a muscle origin at the posterior part of the hyomandibula and quadrate bones (Fig. 6.16a). The medial fibers of the A2α insert musculously into the Meckelian fossa, and its lateral fibers attach both tendinously and musculously on the posteromedial face of the angular complex. In both muraenids the lateroposterior fibers of the left and right A2 subsection (A2αl in *G. prasinus* and A2β in *A. allardicei*) merge with their counterparts fibers and are also connected tendinously to the epaxial muscles and a fascia seperating them from the levator operculi muscle (Figs. 6.13a and 6.16a).

The A3 section of the adductor mandibulae muscle complex in *A. allardicei* and *G. prasinus* is a large muscle with its anterior fibers directing caudoventrally (Figs. 6.13b and 6.16b). In *G. prasinus*, it originates musculously from the frontal, pterosphenoid, pterotic, posterior part of the basisphenoid, parasphenoid and

anterolateral face of the sphenotic bones (Fig. 6.13b). The anterior fibers of A3 of *G. prasinus* are connected to the ventromedial face of the angular complex as a tendon and its posterior fibers attach musculously to its posteromedial face. The A3 of *A. allardicei* originates musculously from the frontal, pterosphenoid, posterior part of the basisphenoid and anterolateral face of the sphenotic bones (Fig. 6.16b). The anterior fibers of this section insert as a tendon into the posterior part of the Meckelian fossa and its posterior fibers attach musculously on the posterodorsal margin of the medial face of the angular complex.

The adductor arcus palatini of *G. prasinus* and *A. allardicei* originate musculously from the depression of the prootic at the rear of the trigemino-facial foramen and inserts on the anteromedial face of the hyomandibula and dorsomedial face of the quadrate (Fig. 6.13d).

The levator arcus palatini in *G. prasinus* and *A. allardicei* is positioned posterior to the A3 section of the adductor mandibulae complex that also covers its anterodorsal part (Figs. 6.13b and 16b). Its fibers originate from the ventral and medial faces of the sphenotic process and lateroventral face of the pterotic. This muscle inserts on the posterior face of the suspensorial fossa, posterior face of the hyomandibula and anterodorsal margin of the quadrate (Figs. 6.13b and 6.16b).

The adductor hyomandibulae muscle connects the posteroventral margin of the medial face of the hyomandibula to a depression on the posterolateral face of the exoccipital in *G. prasinus* and *A. allardicei* (Fig. 6.13d).

The dilatator operculi is a strip-like muscle in both *G. prasinus* and *A. allardicei*, directed caudoventrally (Figs. 6.13b and 6.16b). In *A. allardicei* the dilatator operculi originates musculously from the lateral face of the sphenotic process and inserts as a tendon onto the anteromedial face of the opercular rostral prominence (Fig. 6.16b). In *G. prasinus* it originates musculously from the lateral face of the sphenotic process and ventrolateral face of the pterotic and inserts on the process of the medial face of the opercular rostral prominence (Figs. 6.13b and 6.16b).

The levator operculi of *A. allardicei* originates as a tendon from the posterodorsal edge of the hyomandibula (Fig. 6.16b), whereas in *G. prasinus* this is only the case for anterior fibers. In the latter species, the posterior fibers originate from a tendon that attaches to the epaxial muscles and anterior part of the horizontal septum

between the epaxial and hypaxial muscles (Fig. 6.13d). The levator operculi inserts on the lateral faces of the opercle, subopercle and interopercle in both *G. prasinus* and *A. allardicei* (Figs. 6.13b and 6.16b).

The adductor operculi muscle originates in both *G. prasinus* and *A. allardicei* as a tendon from the dorsomedial corner of the hyomandibula and inserts on the medial faces of the opercle, subopercle and interopercle (Fig. 6.13d). In *G. prasinus*, the adductor operculi tendon is also connected to the tendon of the epaxial muscles.

The protractor hyoidei muscle connects the long, thin and flexible anterior ceratohyal bone to the lower jaw in both *G. prasinus* and *A. allardicei*. It originates tendinously from the medial face of the dentary bone, close to the symphysis, and inserts musculously on the anterior face of the anterior ceratohyal (Figs. 6.13c and 6.16c).

The sternohyoideus in *G. prasinus* and *A. allardicei* originates anteriorly from the anterior half of the anterior ceratohyal, in the extensions of the hypaxial muscles. Its lateral fibers originate from the posterior half of the anterior ceratohyal, forms the rectus communis to protract the lower pharyngeal jaw (Figs. 6.13c and 6.16c).

The small hyohyoideus superior in *G. prasinus* connects the posterior end of the posterior ceratohyal to a small process on the medial face of opercular rostral prominence (Fig. 6.13d). This muscle is absent in *A. allardicei*.

The hyohyoideus muscle complex in *G. prasinus* and *A. allardicei* is a muscle sheet that lies between the medial faces of the branchiostegal rays and forms a thin sac-like muscle meeting its counterpart at the ventral midline (Figs. 6.13a and 6.16a). The dorsal fibers of this muscle complex attach to the horizontal septum between the epaxial and hypaxial muscles.

The epaxial muscles in *G. prasinus* and *A. allardicei* insert musculously on the epioccipital, supraoccipital, exoccipital and basioccipital bones. The hypaxial muscles merge with the sternohyoideus muscle.

In both muraenids the rectus communis muscle attaches to the fourth ceratobranchial bone (Figs. 6.13c and 6.16c). The fibers of the levator externus and levator internus in *G. prasinus* insert on the basioccipital and prootic bones, respectively. Those of *A. allardicei* are attached to the exoccipital and the prootic,

respectively. Other muscles serving the branchial arches of *G. prasinus* and *A. allardicei* are similar to those described in Mehta and Wainwright (2007a).

6.5. Discussion:

Ariosoma gilberti (Ogilby, 1898) lives in burrows on the flat sandy bottom of the continental shelf and feeds on mobile crustaceans, cephalopods and fishes. They are tail-first burrowers and emerge from their burrow at night to forage (Rosenblatt, 1958; Asano, 1962; Smith, 1989a). The immobile maxillary equipped with large pointed teeth, the caniniform and backwardly curved teeth of the mandibula, the large, pointed teeth of the anterior tip of the premaxillo-ethmovomeral complex and an anterior moderate mouth gape of *A. gilberti* suggest grasping and impaling of elusive prey upon capture (Lauder, 1980b; Alfaro et al., 2001; Porter and Motta, 2004). Combined with the large jaw closing muscles, they will assist in preventing escape during subsequent transport. Also, the large lateral and ventral bony elements of the skull and associated muscles linked to the buccal cavity expansion and large opercular series in which is provided more room for the orobranchial cavity, suggest the presence of a hydraulic, suction-based mechanism as subsequent transport behavior in *A. gilberti*. In this mechanism, fishes transmit the piece or whole of the prey into the esophagus by hydraulic suction that is produced by depressing the mandible (Grubich et al., 2008).

Morays on the other hand, are carnivores and shallow-water reef, crevice-dwelling eels that are found in all tropical and subtropical oceans and seas, with a few species occurring in temperate waters (Böhlke et al., 1989; Santos and Castro, 2003; Young and Winn, 2003). Morays like many animals such as snakes and gulper fishes, swallow their large prey as a whole (Yukihira et al., 1994; Santos and Castro, 2003; Westneat, 2007). It is quite evident that morays have a different head architecture than snakes, and even the more closely related gulper eels, to perform this function. Morays have evolved an alternative to this hydraulics-based prey transport to move large prey from the oral jaws to the pharyngeal jaws (Mehta and Wainwright, 2007a). Modification of the branchial arches in relation to the pharyngeal jaw functionality in muraenids has been described by Mehta and Wainwright (2008). In comparison to other Anguilliformes, including the closely-

related *A. gilberti* that still perform the hydraulic-based prey transport, some cephalic features of muraenids can be considerd as specializations to seize and devoure large prey in relation to the presence of this second set of jaws.

The neurocranial elements of muraenids, such as premaxillo-ethmovomeral complex and parasphenoid are stout and robust, compared to that of *A. gilberti*. The reinforcements of neurocranial elements may help in resisting high impact forces during biting and prey grabbing.

The posterior position of the quadrato-mandibular articulation, being approximately at the level of the posterior margin of the neurocranium, is associated with the elongation of the lower jaw and a large, noncircular mouth gape in muraenids. A pattern of jaw elongation as in muraenids is also found in Synaphobanchidae that also posses a similar gill arch musculature, suggesting the capacity to transport food in their buccal cavity. However, synaphobranchids do possess an almost complete set of branchial arches (see chapter 5). An aquatic predator with a large, noncircular mouth gape, as seen in muraenids, can allow to move the jaws into a biting position (without pushing potential prey away from the opened mouth), as well as consuming large preys (Castle, 1968; Porter and Motta, 2004; Mehta and Wainwright, 2007a, 2008, 2009). Furthermore, the presence of long lower jaws facilitates fast mouth closure, effective for capturing mobile and elusive prey, is beneficial in these predators that are known to rely on high-velocity jaw closure for capturing prey (Lauder, 1979; Norton and Brainerd, 1993; Westneat, 2004; Porter and Motta, 2004; Eagderi and Adriaens, 2010a). For instance, mechanical advantage for opening and closing of the lower jaw in *Gymnothorax javanicus* is low, i.e. this fish can bite fast (Westneat, 2004). In contrast to muraenids, in other Anguilliformes with elongated jaws such as the Nemichthyidae, Nettastomidae and Serrivomeridae, jaw elongation is rather coupled to the elongation of the rostral region (Smith and Nielsen, 1989; Tighe, 1989; Eagderi and Adriaens, 2010a).

The posterior displacement of the gill arches in anguilliforms is likely related to the reduction of the head diameter (Nelson, 1966), with the gill arches displaced from a position beneath the cranium to one behind it. Hence, a jaw elongation coupled to a backwards shift of the quadrate-mandibular joint in muraenids (instead of elongation of the rostral region) may be beneficial for having a fast bite without

increasing the distance between the impaling point of prey on the mandibula and the pharyngeal jaws.

Moray eels display a considerable enlargement of the teeth of the oral jaws and premaxillo-ethmovomeral complex, compared to *A. gilberti*. Almost the full anterior half of the dentary complex of muraenids is dentigerous with larger anterior teeth, and those teeth of the maxillary and premaxillo-ethmovomeral complex are extended caudally up to its ventroposterior portion. It can be noted that muraenids likely impale large prey by the anterior part of the oral jaw. The teeth in the oral jaws can restrain the prey even if only in contact with a small portion of the prey by sinking a few teeth into the prey (Mehta and Wainwright, 2007b).

Species with enlarged jaw adductors appear "adapted" to grab the prey item at posterior part of the jaws (Gans and De Vree, 1987), whereas this probably is not the case in muraenids. Morays are well suited for closing the tips of the jaws at high velocities but they have a mechanical disadvantage at their tips in terms of force production (Porter and Motta, 2004). Maximization of force and velocity transfer in mouth closing systems, as trade-offs, have been suggested before in fish species (Westneat, 1994, 2004; Turingan et al., 1995; Collar et al., 2005; Kammerer et al., 2005; Van Wassenbergh et al., 2005; De Schepper et al., 2008). Morays, therefore, with their hypertrophied jaw-closing muscles, long lower jaw and large, sharp teeth can be expected to generate relatively large forces to bite and impale the prey by their teeth. Then, the pharyngeal jaws can protract to deliver a second bite (Mehta and Wainwright, 2007b).

Muraenids show a reduction in the movable cranial elements and a thin slender palatopterygoid. Also the opercular bones of muraenids are reduced in size and the hyoid apparatus is restricted to two slender anterior and posterior ceratohyal bones. Furthermore, muraenids show a reduction in the number and size of the bones of the branchial arches such as the basibranchial and hypobranchial bones. Mehta and Wainwright (2008) pointed out that the reduction or loss of the ventral elements of the branchial arches, hyoid apparatus and their muscular connections in muraenids may be linked to the absence of the hydraulic transport system, and hence the need for another mechanical transport system. In doing so, these

reductions did provide more room in the orobranchial cavity facilitating the mobility of the pharyngeal jaws.

Speed alone is not the sole characteristic of morays that is related to feeding on large prey. The adductor mandibulae muscle complex in *A. allardicei* and *G. prasinus* is larger than that of *A. gilberti*. The powerful bite to impale prey is another requirement to overtake the large prey in muraenids. The hypertrophied adductor mandibulae muscle complex of moray eels, which is almost restricted to the external most jaw adductor, suggests this powerful bite (Devaere et al., 2001; Herrel et al., 2002; Van Wassenbergh et al., 2004). Muraenids with hypertrophied jaw muscles bear a large and elevated supraoccipital crest, to increase the insertion site area for the jaw muscles (De Schepper, 2007). However, *A. gilberti* with smaller jaw muscle even lacks the supraoccipital bone.

Grabbing large prey items and dragging them into the pharynx using the second set of grasping jaws can induce dislocating forces onto the quadrate-mandibular joint in muraenids. Some specializations of muraenids, including (1) the presence of the quadrato-maxillary and preoperculo-angular ligaments, (2) the connection of the quadrate to the A2 tendon of adductor mandibulae complex, and (3) the caudoventral orientation of the fibers of large A3 can help preventing a dislocation of the mandibular joint. The caudoventrally muscle oriention can pull the mandibula up- and forward, thereby counteracting the impact force onto the joint generated by mouth closing muscle. The presence of caudoventrally orientated fibers of the A3 also is advantageous in head-first burrowers in preventing such a dislocation (De Schepper et al., 2007b; Eagderi and Adriaens, 2010b). The fibers of the large A3 section run caudoventrally in muraenids, in contrast to anteroventral direction in *A. gilberti*. In addition, the reduction of the anterior part of the suspensorium along with the lengthening of the pterosphenoid in both morays (compared to *A. gilberti*), provides additional space for the large A3 section.

The posterior position of the adductor arcus palatini and adductor hyomandibulae muscles in muraenids could be related to the posterior position of the suspensorium and the lengthening of the pterosphenoid, and hence may not necessarily be an adaptive change. This is also reflected in the fact that the lateral motion of the suspensorium, a key component of buccal expansion in most teleosts (Lauder,

1985) and observed in morays during respiration, appeared to be too slow to result in sufficient suction flow velocities to move prey items (Mehta and Wainwright, 2007a).

An innovative pharyngeal jaw apparatus, as present in morays, enabled the use of a mechanical transport system rather than a hydraulic one to pull prey into the esophagus (Mehta and Wainwright, 2007a). The current study shows that this innovative feeding mechanism may be linked to many cephalic modifications in addition to those of branchial arches, which have been described by Mehta and Wainwright (2007a). These marked moifications such as the stout and robust neurocranial elements, an elongated lower jaw as the result of the posterior position of the quadrato-mandibular articulation, enlarged teeth of oral jaws and the premaxillo-ethmovomeral complex, reduction in the movable cranial bones and their muscular connections, hypertrophied adductor mandibulae muscle complex, presence of the quadrato-maxillary and preoperculo-angular ligaments, connection of the quadrate to the A2 tendon of adductor mandibulae complex, caudoventral orientation of the fibers of the large A3 section of adductor mandibulae complex, are more than subtle modifications in existing systems that was already proposed by Mehta and Wainwright (2007a), in order to allow an optimal performance of the cranial musculo-skeletal system.

ACKNOWLEDGMENTS

The authors would like to thanks **M. McGrouther** (Australian Museum), **R. H Robins and J. A Lopez** (Florida Museum of Natural History) for providing museum specimens, **N. De Schepper** (Ghent University) for her assistances, **D. G. Smith** (Smithsonian, USA) and **R. S. Mehta** for their valuable comments.

Chapter 7

Head Morphology of the Pelican Eel, *Eurypharynx pelecanoides*

Chapter seven

Head Morphology of the Pelican Eel, *Eurypharynx pelecanoides* (Saccopharyngoidei: Eurypharyngidae)

7.1. Abstract

Eurypharynx pelecanoides, as only member of the Eurypharyngidae, is found in the bathyal zone of the tropical and temperate areas of all oceans. It is characterized by the reduction and loss of many structural elements of the head and by an extreme modification of many of the remaining elements. The study was aimed to understand to what degree the ancestral anguilliform cranial musculoskeletal system has become modified into this highly specialized 'gulping' feeding system in *E. pelecanoides*. Hence, a detailed description is added to the current knowledge, as well as the description of the cranial osteology to those already known and a complete head musculature. In relation to these extensive modifications, possible implications for the functioning of the feeding apparatus were described based on its cephalic musculoskeletal system and a broadcasted short footage (sixty-five seconds) of a feeding pelican eel in the BBC documentary series (Blue planet: Eposide2 - The Deep, 2001). The results revealed that many extreme modifications of head structures of *E. pelecanoides* are to be seen in relation to functional shifts compared to those of other Anguilliformes. Also, it shows two novel cephalic muscles that have no equivalent in other fishes, as far as we know.

7.2. Introduction

The Saccopharyngoidei or gulper eels are well-known deep-sea fishes that occur at bathypelagic depths throughout the world's oceans (Bertelsen et al., 1989). The family of the Eurypharyngidae, together with the Saccopharyngidae, Monognathidae and Cyematidae, belong to this suborder. The Saccopharyngoidei generally have been considered to be close relatives of the true eels (suborder Anguilloidei), because they show a similar leptocephalus larval stage (Greenwood et al., 1966; Inoue et al., 2001). Phylogenetic analysis using the mitogenomic data of the Eurypharyngidae and Saccopharyngidae have demonstrated not only these gulper eels form a sister-group relationship with a high probability (100%), but also they

are deeply nested within the Anguilliformes (true eels), strongly suggesting that they have been derived from an eel-like ancestor (Inoue et al., 2003; 2010) (Fig. 1.7). Wang et al. (2003), Obermiller and Pfeiler (2003) and Inoue et al. (2010) also confirmed the monophyly of the Anguilloidei and Saccopharyngoidei clade within the anguilliforme fishes inferred from mitochondrial ribosomal RNA sequences.

Eurypharynx pelecanoides is the only member of the family Eurypharyngidae (McCosker, 1998) and is found in the bathyal zone of the tropical and temperate areas of all oceans (Böhlke, 1966). It is characterized by the reduction and loss of many structural elements of the head and by an extreme modification of many of the remaining elements (Bertin, 1934; Tchernavian, 1947; Bertelsen et al., 1989). Compared to the Anguilloidei, *E. pelecanoides* shows the loss of many bony elements such as premaxillaries, palatopterygoids, symplectics, pterosphenoids, supraoccipital, hyoid arches, opercular series, branchiostegal rays, and pectoral fin and girdle (Bertin, 1934; Tchernavian, 1947; Bertelsen et al., 1989).

Eurypharynx pelecanoides, or pelican eel, is actively searching for food during swimming by its whip-like tail (Nielsen et al., 1989). Also, *E. pelecanoides* bears a complex organ with numerous tentacles at the end of its tail, which is presumably a lure to attract the prey (Nielsen and Bertelsen, 1985). It feeds on wide range of prey such as fishes, crustaceans, cephalopods, sargassum weeds, chaetognathans, urochordataes, scyphozoaens and nemertines (Nielsen et al., 1989).

Since the description of *E. pelecanoides* by Vaillant (1882), its bizarre appearance due to the extremely enlarged jaws and suspensorium resulting in a huge gape at the tip of the eel-like body, has attracted much attention from many researchers (Gill and Ryder, 1883; Nusbaum-Hilarowicz, 1923; Bertin, 1934; Tchernavian. 1947; Bertelsen et al., 1989; Nielsen et al., 1989). Its external morphology and anatomical description, such as osteological features, caudal organ, lateral line system have been described by Vaillant (1882), Gill and Ryder (1883), Nusbaum-Hilarowicz (1923), Bertin (1934) and Tchernavian (1947) and stomach content and assumed feeding strategy by Nielsen et al., (1989). Despite these works, it is still poorly known and little detailed osteological information is available. Also, the hypothesized feeding strategy of this gulper eel, deduced from its head morphology by Nielsen et al. (1989) does not correspond to the broadcasted short footage of a

feeding gulper eel in the BBC documentary series (Blue planet: Eposide2 - The Deep, 2001; http://www.youtube.com/watch?v=INJ5Tk7Nbi4).

This study provides a detailed description of the cranial osteology to those already known and a complete description of the head musculature. This can help to understand to what degree the ancestral anguilliform cranial musculoskeletal system has become modified into this highly specialized 'gulping' feeding system in *E. pelecanoides*. In relation to these extensive modifications, possible implications for the functioning of the feeding apparatus are described. Because of the great depth of the habitat of *E. pelecanoides*, aspects of its behavior are largely the subject of conjecture. Hence, a functional morphological interpretation of the bizarre cephalic characters of *E. pelecanoides* provides an insight to better understand its feeding behavior, since most morphological characters are generally correlated with functional demands (Liem, 1967).

7.3. Material and methods

For the anatomical description, eight alcohol-preserved specimens of *Eurypharynx pelecanoides* (1980-1354, P2340411, P2340414, P2340415, P2340416 and P2340418), obtained from the Musée National d'Histoire Naturel of Paris and Natural History Museum of Denmark, were examined. Due to a damaged tail in two of the specimens of *E. pelecanoides* (EP4 and 8), their total length was estimated based on the preanal length. The specimens were of the following size range in Total Length (TL): EP1: TL= 515 mm; EP2: TL= 446 mm; EP3: TL= 491 mm; EP4: TL= 502; EP5: TL= 506 mm; EP6: TL= 120 mm; EP7: TL= 376 mm; EP8: TL= 445 mm. Two specimens (EP2 and EP6) were cleared and stained with alizarin red S and alcian blue according to the protocol of Taylor and Van Dyke (1985), for osteological examinations. Dissections with muscle fiber staining according to Bock and Shear (1972) were performed.

To study the structure of the suspensorium bones and skin, small pieces from the hyomandibula and buccal skin of EP3 were embedded in paraffin and cut into 6 µm sections. The sections were stained with hematoxylin-eosin, following Carson and Hladik (2009).

Another specimen (EP7) was scanned at the modular micro-CT setup of Ghent University (Masschaele et al., 2007; http://www.ugct.ugent.be) using the directional tube head, at 80 kV tube voltage. The detector was an a:Si flat panel (Varian Paxscan 2520) with CsI scintillator. The specimen was imaged at the full detector resolution of 1496x1880 pixels of 127^2 µm². Due to the elongated shape of the sample, a smaller geometric magnification of 2.2 was used, resulting in an effective voxel size of 58^3 µm³. In total 1001 projections of 1496x1880 pixels were made covering the full 360 degrees. The raw data was processed and reconstructed using the in-house developed CT software Octopus (Vlassenbroeck *et al.* 2007) and rendered with VGStudio Max (Volume Graphics GmbH Heidelberg, Germany) and Amira 4.1.0 software (Mercury Computer Systems GmbH Mérignac, France).
Muscle terminology follows Winterbottom (1974). Terminology of cranial skeletal elements follows Böhlke (1989a) and Rojo (1991). The epiotic of teleosts is termed "epioccipital", thereby following Patterson (1975). Terminology of the chondrocranium follows Adriaens and Verraes (1997) and Geerinckx et al. (2005).

7.4. Results

7.4.1. Cranial osteology

The bony neurocranium is comprised of only perichondral bones that are connected synchondrously. The neurocranium is flattened ventrodorsally. Strikingly, the anterior portion of the skull (ethmoid and orbital regions) is completely unossified, except for a rod-like vomeral bone that ventrally supports this cartilaginous rostrum. This cartilaginous element seems to comprise the ethmoid plate, trabecula cranii and anterior portion of the taenia marginalis (orbital cartillages). Laterally, it forms the orbits that are only bordered dorsally and caudally by bone i.e. frontal and sphenotic, respectively (Figs. 7.1a and 7.2). The vomer is positioned at the midline of the ventral face of the cartilaginous rostrum and is extended caudally where it is connected to the anterodorsal face of the parasphenoid (Fig. 7.2b).
The orbital region comprises the nasals, frontals, and parasphenoid. The nasal bones are two small bones on the dorsal face of the cartilaginous snout. The olfactory rosette is positioned on the anterodorsal corners of the cartilaginous rostrum. The frontal bones are situated posterior to the cartilaginous rostrum (Fig.

7.2a). Laterally, the frontal connects to the sphenotic and posteriorly, to the parietal (Fig. 7.2a). The parasphenoid is a strip-like bone possessing a midline ridge on its ventral face (Fig. 7.2b). It forms the posterior base of the neurocranium and runs caudally, ventral to the prootics and basioccipital (Figs. 7.1a and 7.2b).

The otic region comprises the sphenotics, pterotics, parietals, prootics and epioccipitals. Dorsally, the sphenotic forms the anterolateral portion of the bony neurocranium ventrally bearing two tube-like swellings that are directed ventrocaudally (Fig. 7.1a). The anteroventral margin of the sphenotic is attached to the posteroventral face of the rostrum by thick connective tissue. The sphenotic along with prootic and pterotic bones border the large suspensorial articular facet (Fig. 7.2b). The pterotic forms the lateral brace of the neurocranium and its anterior part, i.e. the dermo-pterotic, is fused to the anteroventral edge of its posterior part, i.e. the auto-pterotic. Lateroventrally, it bears a ventrally directed process (Fig. 7.2b).

The epioccipitals form the roof of the skull along with parietals (Fig. 7.2a). The posterior parts of epioccipitals are curved ventrally and contribute to form the spherically shaped posterior wall of the neurocanium (Figs. 7.1a and 7.2a). The posteromedial corners of these bones are positioned between the two exoccipitals bones. The prootics form the ventral midsection of the neurocranial floor and laterally are connected to the pterotic and sphenotic. A foramen is present on the lateral margin of the prootic (Fig. 7.2b).

The occipital region comprises the exoccipitals and basioccipital. This region is not excavated for muscle insertion as Anguilloidei. The foramen magnum is bordered dorsally and laterally by the exoccipitals and epioccipitals, and ventrally by the basioccipital (Fig. 7.2a). The exoccipitals are domed towards the foramen magnum. The exoccipitals are extended ventrally to contribute to the ventral surface of the neurocranium and is situated between the basioccipital and posterior portion of the pterotics (Fig. 7.2b). It bears a large foramen on its ventral face. The basioccipital posteriorly forms the occipital condyle (Fig. 7.2b).

The maxillary is a thin but extremely elongated bone, connected posteriorly to the posterior depression of the mandibula through the maxillo-mandibular ligament (Fig. 7.1b). The anterior ends of the maxillaries are interconnected at the midline,

and lie ventral to the neurocranium. They are connected to the anteroventral margin of the cartilaginous rostrum by a broad ligamentous sheet that also laterally attaches to the anterodorsal edges of the maxillaries and the lateral tendon of the levator arcus palatini muscle (Fig. 7.3a). The configuration of the maxillaries as well as their connections to each other and to the neurocranium is unique, even for Anguilliformes. The maxillary bears numerous small teeth on its ventral and anterodorsal faces. The elongated mandibula consists of the fused dentary, angular, articular and retroarticular. It bears a depression on its anteromedial face with numerous small teeth on its dorsomedial rim (Fig. 7.1).

The suspensorium is directed caudoventrally and consists of an extremely elongated hyomandibula and quadrate bones (Fig. 7.1a). The suspensorial bones are elongated cartilagnous rods covered with a thin layer of perichondral bone. The hyomandibula bears a ridge at the midline of its medial face and a ridge on its dorsolateral face (Fig. 7.1a). Anterolaterally, it bears a depression that serve as the insertion face of the lateral fibers of the levator arcus palatini. The hyomandibula articulates with the neurocranium via a single articular condyle (Fig. 7.1a). Its dorsomedial face is connected to the ventral face of the pterotic by the pterotic-hyomandibular ligament. The quadrate is a tube-like bone, connected to the hyomandibula by a synchondrosis. Thick connective tissue surrounds this joint. Posteriorly, it bears the lateral and medial condyles which fits into the mandibular facet of the mandibula (Fig. 7.1). The lateral face of the lateral condyle bears a small process onto which the lateral mandibulo-quadrate ligament inserts (Fig. 7.3a). A similar medial mandibulo-quadrate ligament then connects the medial face of the medial condyle to the posterior depression of the mandibula (Fig. 7.1b). The hyomandibula and quadrate are perichondral ossifications retaining a hyaline cartilaginous core. The chondrocyte cells of this cartilage are scattered in its dense matrix (Fig. 7.4b).

A thick, black skin encloses the buccal cavity and contains both dermal and epidermal melanophores. Distribution of the melanophors is dense in the epidermis, whereas dermal melanophors are more scattered among collagen fibers (Fig. 7.4a). The internal dermis contains a thick layer of connective tissue. The striated muscle

fibers are present between the external and internal dermis of skin, running transversally (Fig. 7.4a).

7.4.2. Cranial myology:

The adductor mandibulae muscle complex of *E. pelecanoides* shows extreme modifications. It originates musculously from the anterior face of the quadrate and inserts through a transverse tendon on the anteromedial face of the mandibula (Figs. 7.1b and 7.3a). This muscle is unipennate. No subdivisions could be recognized.

The adductor arcus palatini originates musculously from the ventromedial face of the prootic and inserts musculously on the anterodorsal rim of the medial face of the hyomandibula (Fig. 7.3a).

The levator arcus palatini is the largest muscle of the head. It originates tendinously and musculously from the anterolateral margin of the sphenotic, and as lateral tendon from the orbito-ethmoid cartilage (Fig. 7.3a). The lateral fibers of this muscle insert on the dorsolateral depression and lateral ridge of the hyomandibula, and musculously and tendinously on the dorsolateral margin of the quadrate, ventral to the anterior portion of the adductor mandibulae muscle (Fig. 7.3a). The medial fibers of the levator arcus palatini insert musculously on the anteromedial face of the hyomandibula.

The adductor hyomandibulae connects musculously the posterior face of the pterotic to the dorsoposterior edge and dorsolateral rim of the medial face of the hyomandibula (Fig. 7.3b). The laterl fibers form a separate bundle which attaches tendinously to the dorsal tendon of the anterior depressor mandibulae muscle (Fig. 7.3a).

Eurypharynx pelecanoides also bears two novel cephalic muscles that have no equivalent in other fishes, as far as we know. Based on their insertions, they are considered as an anterior and posterior depressor mandibulae muscle (Fig. 7.3a). The anterior depressor mandibulae muscle originates tendinously from the ventromedial face of the pterotic and inserts on the anterior edge of the mandibula, via a slender but long, sesamoid bone (Fig. 7.3a). Anteriorly, this sesamoid bone is connected musculously and tendinously to the anterior depressor mandibulae

muscles and posteriorly, to a strip-like ligament that distally runs over the articulatory head of the quadrate before inserting on the anteriormost edge of the mandibula. As such, the quadrate head functions as a pulley for this anterior depressor muscle. The posterior depressor mandibulae muscle is a small and short bundle that originates tendinously from the lateroventral face of the sphenotic and inserts as a tendon on the anterior portion of the above mentioned sesamoid bone (Fig. 7.3a). The tendon of the posterior depressor mandibulae muscle runs inside the muscle bundle and attaches to the anterior part of the sesamoid bone.

Laterally, the epaxial muscles are covered with a muscle sheet with its anterior fibers inserting tendinously on the lateroventral process of the pterotic (Fig. 7.3). The rest of the epaxial muscles insert tendinously on the posterior margin of the parietals and musculously on the entire face of the epioccipitals. The hypaxial muscles insert tendinously on the anteroventral face of the basioccipital (Fig. 7.3).

7.5. Discussion:

Nelson (2006) considered the Saccopharyngoidei as comprising "perhaps the most anatomically modified of all vertebrate species". In contrast to other anguilliforms, the monotypic Eurypharyngidae bear a greatly enlarged mouth resulting from an extensive elongation of the suspensorium and jaws (Bertin, 1934; Tchernavian, 1947). The loosely-hinged mouth is covered by a thick, black skin that can withstand an extensive distending of the buccal cavity. The skull of *E. pelecanoides* reflects some paedomorphis features, such as the unossified orbito-ethmoid cartilage and the superficially ossified skull roof bones. This condition is similar to that found in the Saccopharyngidae and Monognathidae (Nielsen and Bertelsen, 1985; Bertelsen and Nielsen, 1987). The unossified rostrum of *E. pelecanoides* possesses a unique shape resembling that of the Early Devonian actinopterygian, *Dialipina* (Schultze and Cumbaa, 2001).

The hyomandibula of *E. pelecanoides* articulates with the neurocranium via a single articular condyle that provides its freedom for forward and backward movements. The quadrate is probably fused to the symplectic because dorsally it is connected to the hyomandibula by a synchondrosis and not through an interdigitating suture as in other anguilliform species. The primitive teleost condition of the hyomandibula is

to be connected only with the symplectic through a simple synchondrosis (Forey et al., 1996).

In contrast to the general condition in Anguilliformes, the suspensorium and the attached muscles, such as the levator arcus palatini and adductor hyomandibulae muscles, contribute to closing and opening of the jaws (rather than only add-and abducting of the suspensorium). Such a situation can show that constructions have the potential to serve purposes other than the function for which they are designed (Dullemeijer, 1991; Gould and Vrba, 1982). Hence, these elements can be called upon to serve a new purpose.

It is difficult to homologize some cranial elements of *E. pelecanoides* with those of Anguilliformes. The homology of the anterior and posterior depressor mandibulae muscles is the subject of conjecture. Their configuration and function are unique compared to those of other anguilliforms, hence they probably are novel cephalic muscles. On the other hand, based on the traditional naming system of the adductor mandibulae muscles (Vetter, 1878; Winterbottom, 1974; Nakae and Sasaki, 2004), they may be homologues with one of the A2 sections or subsections of the adductor mandibulae muscle complex but with the insertion site having migrated to the anterolateral face of the mandibula.

Because of the great depths at which *E. pelecanoides* lives, aspects of its behavior are largely the subject of speculation. However, its head musculoskeletal system strongly suggests the capacity to engulf prey by its enormous mouth (Nielsen et al., 1989). Nielsen et al. (1989) rejected swiming with a open mouth towards a prey item in *E. Pelecanoides* because of its narrow gill opening. Instead, Nielsen et al. (1989) proposed that *E. Pelecanoides* would open its huge mouth at a short distance from the prey, less than its jaw length, after a forward trust with the closed jaws. Based on Nielsen et al. (1989), *E. Pelecanoides* opens its mouth by slackening the adductor mandibulae and further by the pressure of the water caused by the forward movement of the head like a parachute. In this assumed way of feeding, the jaw muscles close the mouth slowly by bringing a triangular lid formed by the bones of the lower jaw and the elastic skin streched between them (Fig, 7.5).

Based on the cephalic musculoskeletal system and a broadcasted short footage of a feeding pelican eel in the BBC documentary series (Blue planet: Eposide2 - The Deep, 2001), the skin of *E. pelecanoides* appears to be a loose flap when the mouth is still closed. After detecting the prey, *E. pelecanoides* opens its mouth, which can be realized by the contraction of the anterior and posterior depressor mandibulae muscles, until the mandibula lies at a horizontal level. The lateral bundle of the adductor hyomandibulae could also contribute to depress the mandibula because of its attachment to the anterior depressor mandibulae muscles. At the same time, the levator arcus palatini may protract the long suspensorium to almost forty five degrees. In addition, the contraction of the lateral fibers of the levator arcus palatini muscle can abduct the suspensorium to distend the buccal cavity.

Then the anterior and posterior depressor mandibulae and levator arcus palatini muscles can continue to open the huge mouth and synchronously, the epaxial muscles elevate the head. In this stage, the mouth opening is restricted mainly to a depression of the lower jaw, where *E. pelecanoides* opens its mouth until it makes nearly a right angle with the suspensorial axis. Meanwhile, all loose skin around the mouth becomes stretched and participates to form an expanded buccal cavity.

After that, *E. pelecanoides* thrusts its head towards the prey with the mouth opened. In this way the prey and the water surrounding it maw be enclosed in the buccal cavity by the forward movement of the head. The lateral fibers of the epaxial muscles that insert as a tendon on the ventrolateral process of the pterotic may play a role to fix the position of its small head at a horizontal position during opening of the large mouth or moving towards the prey with opened mouth.

After engulfing of the prey, the adductor mandibulae muscle may elevate the lower jaw to close the mouth. The configuration of the adductor mandibulae muscle, being unipennate and with short fibers connecting to a long tendon, probably provides an advantage for forceful closing of an extreme long lower jaw and avoiding the engulfed prey from escaping. A unipennate muscle with a large pennation angle and shorter muscle fibers has the positive effect of allowing more muscle fibers to attach along the tendon plate, thereby exerting greater contractile forces (Narici and Magnaris, 2006).

After closing the large mouth, the adductor hyomandibula muscle may bring the suspensorium back to its starting position and the adductor arcus palatini muscle adducts the suspensorium medially. Returning the long suspensorium to its starting position may also bring the mandibula backward. Most probably, mouth closure is slow because of the highly force inefficient lever system of the elongated jaw. During slow mouth closure, little engulfed water would then be expelled. The volume of the buccal cavity then is gradually reduced sieving out through the narrow gill opening by closing the long suspensorium and jaws and by contraction of the elastic skin around the mouth. The latter is possible when the muscle fibers inside the skin around the buccal cavity contract and return skin to its resting state (Fig. 7.4a).

Nielsen et al. (1989) pointed out that food items stay in the ventral pouch of the buccal cavity for a while before entering the stomach as seen in the BBC documentary series (Blue planet: Eposid2 - The Deep, 2001) (Fig, 7.6). The prey then probably is covered with a secretion of the glandular (with acidophilic proteinaceous granules) and mucous goblet cells that cover a pale area on the ventral side of hypaxial muscles that run from the mouth opening to the esophagus (Nielsen et al., 1989).

The trapped prey will be transported to the heavily folded esophagus, that has a columnar epithelium on the top of the ridges and numerous unicellular glands (Nielsen et al., 1989), and subsequently to an expandable stomach (Nubaum-Hilarowics, 1923; Nielsen et al., 1989). The contraction of the skin around the mouth using the muscle fibers of the thick skin after mouth closure will help to conduct the prey to the esophagus and subsequently to the stomach (Nubaum-Hilarowics, 1923).

This study based on head morphology of *E. pelecanoides* and an observation of the live animal revealed that those previously assumed feeding strategies based on solely morphological data, does not correspond with those we proposed except for keeping food items in the ventral pouch of mouth, contraction process of the elastic skin around the mouth and transporting food to the heavily folded esophagus. However, this study cannot reject the possibility of the assumed feeding strategy of *E. pelecanoides*.

ACKNOWLEDGMENTS

The authors would like to thanks **P. Pruvost** (Musée National d'Histoire Naturel of Paris) and **P. R. Møller** (Natural History Museum of Denmark, Copenhagen University) for providing museum specimens, **J. G.** Nielsen (Natural History Museum of Denmark, Copenhagen University) for providing valuable references, **T. Geerinckx** (Ghent University) for his valuable comments.

Chapter 8

General Discussion

Chapter eight

General Discussion

The major feature of life's history is a legacy of perpetual change. Despite an apparent permanence of the natural world, change characterizes all things on earth and produces various forms of life. Understanding the diversity of life as the result of evolution can help to understand the historical processes that generate and maintain species diversity and adaptations through evolutionary history. The evolution of the cranial musculoskeletal system in animals is an excellent case study of the way form changes in relation to change in functional demands within a context of a changing environment. It reflects the plasticity of evolutionary processes, in how structures that are used in a certain way can be remodeled to meet changing functional requirements. The feeding apparatus in association with the hyoid arches, suspensorium and gill arches and their associated muscles is to be expected to be strongly involved in these changes.

8.1. Evolutionary pattern of structural changes in the head musculoskeletal system

The goal of this study is to explore the structural diversity of the cranial musculoskeletal system in Anguilliformes. By integrating the obtained data with data from literature can also unravel evolutionary patterns that explain the observed changes in the head musculoskeletal system. Structural changes, as an adaptation to a changing function or environment, could be constrained by ancestral condition. Hence, knowing the ancestral or primitive condition of the head morphology is especially important to explore evolutionary changes from there on with the resulting diversity in the Anguilliformes.

Regan (1909, 1912) recognized the Anguilloides (Apoda) as distinct from other eel-like fishes based on the absence of separate premaxillaries, which are united with the vomer and the ethmoid into a premaxillo-ethmovomeral complex. However, in

some cases the vomer is present as a separate bone (Marshall, 1962) such as in the Heterenchelyidae and Synaphobranchidae. Some researchers consider this separate vomer in some anguilliform families as an autogenous vomeral tooth plate, whereas the (toothless) vomeral bone itself is then included within the complex (D. Johnson, Smithsonian museum: personal communications). However, this needs further investigations. This premaxillo-ethmovomeral complex limits the mobility of the upper jaw elements, and in many anguilliform lineages is associated with a considerably enlarged jaw adductor musculature. Hence, an adaptation to a predatory way of life has been assumed (Gegory, 1933; Gosline, 1971). Fusion of the ethmoid bone into a premaxillo-ethmovomeral complex is also a synapomorphy of recent Anguilliformes (Belouze, 2001). However, the lateral process of the premaxillo-ethmovomeral complex in Bathymyrinae and Muraenesocidae has been interpreted as fused lateral ethmoids (Belouze, 2001).

Jaw elongation:

The short rostral (antero-orbital) region is the plesiomorphic state of Anguilliformes, as seen in Heterocongrinae and Colocongridae (Belouze, 2001). However, different evolutionary patterns have resulted in jaw elongation in Anguilliformes. A first pattern involves the elongation of the premaxillo-ethmovomeral complex, as seen in the Cyematidae, Nemichthyidae, Serrivomeridae and Nettastomatidae. These rapacious feeders display considerable enlargement of the teeth and jaws (Castle, 1968). For instance, the dentigerous areas are enlarged by the forward prolongation of the snout (premaxillo-ethmovomeral complex), as seen in the nettastomatid *Hoplunnis punctata*. This can be linked to some advantages, such as providing more space for the olfactory rosette, but also increasing velocity advantage (biting speed) and reducing drag (see chapter 3). These adaptations can improve the prey capture kinematics of this benthopelagic, biter predator. Also, the larger adductor mandibulae muscle complex of *H. punctata* (Nettastomatidae), compared to that of *Serrivomer sp.* (Serrivomeridae) and *Nemichthys scolopaceus* (Nemichthyidae), indicates that forceful biting at the posterior part of the jaws

(biting of fairly larger prey) might be favored, a benefit for *H. punctata* that feeds on larger benthic preys (Smith, 1989b).

As a second pattern of jaw elongation in Anguilliformes, the mouth has become enlarged by a backward elongation of the mandibula coupled to a posterior position of the quadrate-mandibula joint, tilting the suspensorial axis into a backwardly-oblique angle as seen in *Anarchias allardicei* and *Gymnothorax prasinus* (Muraenidae), *Ilyophis brunneus* and *Synaphobranchus brevidorsalis* (Synaphobranchidae), *Kaupichthys hyoproroides* (Chlopsidae) and *Myrophis vafer* (Ophichthidae). This modification is associated with a large, noncircular mouth gape that enables very large prey to be seized and devoured. This pattern of jaw elongation can provides a fast bite, without increasing the distance between the pharyngeal jaws and the tip of oral jaws. The gill arch morphology of these species with such a jaw elongation shows the potential to transport food items in the buccal cavity (see below). Hence, this pattern of jaw elongation in Anguilliformes is probably linked to the presence of a highly specialized mechanical transport system but needs further investigations.

A third pattern of jaw elongation is seen in *Eurypharynx pelecanoides* (Eurypharyngidae), resulting from an extensive elongation of the suspensorium and the jaws (Bertin, 1934; Tchernavian, 1947). The hyomandibula of *E. pelecanoides* articulates with the neurocranium via a single articular condyle that provides its freedom for forward and backward movements, whereas the hyomandibula of other Anguilliformes dorsally bears two articular condyles, as in most teleosts. As a result, the movement of the suspensorium is restricted to medio-lateral rotations only. Still, even in those cases, some structural variation exists at the level of these articulations, as for example the posterior articular condyle in *Anarchias allardicei* and *Gymnothorax prasinus* (Muraenidae), *Ilyophis brunneus* and *Synaphobranchus brevidorsalis* (Synaphobranchidae), is longer compared to the one in other anguilliforms (see chapters 5 and 6).

Suspensorial modifications:

With respect to the suspensorium, the long quadrate of *E. pelecanoides* probably is dorsally connected to the hyomandibula by a synchondrosis and not through an interdigitating suture as in other anguilliform species. The primitive teleost condition is for the hyomandibula to be connected only with the symplectic through a simple synchondrosis (Forey et al., 1996). In most eels the symplectic is not present as a separate bone, whereas only a distinct cartilaginous processus symplecticus on the hyomandibula can be observed in eel larvae (Norman, 1926; Tesch, 2003). Consequently, it has already been suggested that a symplectic bone in Anguilliformes has become fused with the hyomandibula or the quadrate (Leiby, 1981). The symplectic could be found as a fused bony portion at the posterior part of the quadrate in *Pythonichthys macrurus* (Nettastomatidae) or as a small cartilaginous part in *Hoplunnis punctata* (Heterenchelyidae). Also, a cartilaginous symplectic has been described posterior to the quadrate in *Heteroconger hassi* (Congridae) (De Schepper, 2007).

With respect to the suspensorial musculature, and in relation to the elongated jaws in *E. pelecanoides* (Eurypharyngidae), the suspensorial muscles contribute to a closing and opening of the jaws (rather than only ad- and abducting of the suspensorium), in contrast to the general condition in Aguilliformes. Such a situation in *E. pelecanoides* can show that such a feature has the potential to serve purposes other than the ancestral function, for which it is adapted (Dullemeijer, 1991). These elements can then be called upon to serve a new purpose (Gould and Vrba, 1982). Also, in *E. pelecanoides*, it is difficult to homologize some other cranial elements with those of other anguilliforms. The very distinct cranial morphology of *E. pelecanoides* is already distinct from the leptochalus larval stage, with an oblique mouth gape, a long lower jaw, and very long patch of thin teeth extending forward from the top of the upper jaw (Miller, 2009) (Fig. 8.1).

Dentition patterns:

Tooth morphology of Anguilliformes may reflect differences in prey capturing behavior. For instance, teeth can be large, sharp and piercing like those of *H.*

punctata (Nettastomatidae), or chisel-like as in *Simenchelys parasiticus* (Simenchelyinae). The long and sharp teeth on the anterior part of the neurocranium in most anguilliform families may be used to impale prey and are useful for prey holding. *S. parasiticus* differs from other anguilliform species in having chisel-like teeth. The cutting edge and blade-like teeth of *S. parasiticus* on the premaxillo-ethmoidal complex, maxillary and lower jaw, along with the enlarged adductor mandibulae muscle complex may be employed to shear and remove a chunk of flesh from larger prey, just like using scissors (see chapter 5). *Eurypharynx pelecanoides* (Eurypharyngidae) and *N. scolopaceus* (Nemichthyidae) bear numerous small teeth on their jaw tooth bands. In species with long jaws, such as *H. punctata* (Nettastomatidae), *Serrivomer* sp. (Serrivomeridae) and *N. scolopaceus* (Nemichthyidae), the tooth rows of the jaws extend further posteriorly, thus increasing the functional capacity of the jaw system for grabbing prey. Biting with the posterior teeth is also advantageous because higher bite forces are produced (Herrel et al., 2002).

Suction feeding versus biting:

Simenchelys parasiticus and *Heteroconger hassi* are two examples of anguilliforms that may rely on suction forces during feeding. In these two species with short jaw, the hyomandibula-quadrate axis is tilted forwardly and the anterior part of the suspensorium is extended forward. In addition, they bear a well-developed palatopterygoid connected at its ends to the neurocranium and the quadrate. Such a configuration may be related to their ability to produce suction by providing more room for the oral cavity (however, kinematic studies to support the hypotheses of suction feeding still need to confirm this) (see chapter 3 and 5). These two species also bear well-developed ventral muscles of the head, which may confirm the importance of producing suction. Large ventral muscles in *S. parasiticus*, including the protractor hyoidei and sternohyoideus, suggest the ability to ventrally expand the buccal cavity more, hence producing suction forces (Lauder, 1985; De Visser and Barel, 1998; Carroll, 2004; Sanford and Wainwright, 2002; Mehta and Wainwright, 2007b; Konow and Sanford, 2008). I speculate that these

specializations of *S. parasiticus* may be beneficial for creating higher suction forces to attach to its prey, thereby assisted by its fleshy lips (see chapter 5).

The adductor mandibulae muscle complex of Anguilliformes shows variation in size, components and insertion sites. Some Anguilliformes possess small jaw muscles (e.g., *Heteroconger hassi*), whereas others have substantially enlarged ones (e.g., *Hoplunnis punctata*, *Conger conger*, *Simenchelys parasiticus* and *Gymnothorax prasinus*). Enlarged adductor mandibulae muscles may allow a powerful bite by increasing the mechanical load on skeletal elements such as mandibula, suspensoria and neurocranium (Herrel et al., 2002; Van Wassenbergh et al., 2004). A predatory life style is considered the plesiomorphic condition for the Anguilliformes (Gosline, 1971; Smith, 1989a), with hypertrophied jaw muscles being common (Böhlke et al., 1989) and this suggest a derived condition of *H. hassi*.

Jaw musculature:

The A2 and A3 sections of the adductor mandibulae muscle complex are oriented caudoventrally in some anguilliform families, such as muraenids, moringuids and synaphobranchids. A caudoventrally oriented muscle can pull the mandibula upward and forward and redistribute forces, i.e. little resultant force impacts the joint. An opposite orientation of the different sections of the adductor mandibulae muscle complex (caudoventrally versus anteroventrally) can also help in preventing the dislocation of the mandibular joint, even when large forces are exerted that induce torque forces (De Schepper et al., 2007a) (Fig. 8.2).

The insertion site of the jaw muscles differ based on the lower jaw configurations. In nettastomids with long jaws, the muscles insert on the posterior portion of the mandibula, whereas in muraenids these muscles' insertion sites are enormously expanded on the posterior half of the mandibula.

Anarchias allardicei and *Gymnothorax prasinus* (Muraenidae) show an adductor mandibulae muscle complex where muscle mass is hypertrophied. The hypertrophied adductor mandibulae muscle complex can be expected to be very efficient for biting and impaling the prey. These muraenids also bear a large and

elevated supraoccipital crest, to increase the insertion area for the jaw muscles (De Schepper, 2007). However, *Ariosoma gilberti* (Bathymyrinae), with smaller jaw muscles, even lacks the supraoccipital bone. Along with the hypertrophied adductor mandibulae muscle of muraenids, neurocranial elements, such as the premaxillo-ethmovomeral complex and parasphenoid, are deep and robust. This may help in resisting the generated higher impact forces during prey grabbing and biting (see chapter 6).

Based on the terminology of Winterbottom (1974) and the traditional nomenclature used for the adductor mandibulae muscles (Vetter, 1878; Winterbottom, 1974; Nakae and Sasaki, 2004), all in this study examined species only have the A2 and A3 sections of the adductor mandibulae muscle complex. The absence of the A1 is to be expected, because Anguilliformes lack a mobile upper jaw. A section A1 has been reported in *Moringua edwardsi* and *Pisodonophis boro* (De Schepper et al., 2005, 2007a).

Epaxial musculature:

The epaxial muscles also show quite some variation in their insertion to the neurocranium, even with a direct attachment onto the jaw muscles in anguilliforms. In primitive teleosts the epaxial muscles insert laterally within the roofed and unroofed posttemporal fossa and medially on the rear of the neurocranial wall (Forey et al., 1996). In Anguiliformes they also insert on the posterior wall, but in eels with large jaw muscles, such as the Muraenidae and Heterenchelyidae, the epaxial muscles also attach tendinously or fascially to the jaw muscles. The large insertion sites of the epaxial muscles and its functional coupling to jaw muscle contraction are considered an advantage for transferring forces from the body onto the head during head-first burrowing or during rotational feeding (Helfman and Clark, 1986). Furthermore, the epaxial muscles probably contribute to elevate the neurocranium during mouth opening in some Anguilliformes. In Eurypharyngidae the epaxial muscles laterally bear a muscle sheet that with its anterior fibers inserts tendinously on the lateroventral process of the pterotic bone. This novel, lateral

fibers of the epaxial muscles may play a role in stabilizing the position of its small head during opening of the large mouth (see chapter 7).

Opercular series:

The opercular series is well-developed in some families such as the Congridae and Anguillidae. This series also possesses various shapes and sizes in Anguilliformes. The opercular series is reduced in the Muraenidae, the sub- and interopercle are lost in *Nemichthys* (Nemichthyidae), whereas Eurypharyngidae lack the opercular series as a whole. Like in other Teleostei, the opercular series of studied species also contributes to the feeding system by their connection to the mandibula due to having the interoperculo-angular ligaments that triggering one of the biomechanical systems to depress the mandibula (Westneat, 1990). The preopercular bone in many anguilliform families supports the preoperculo-mandibular canal of the cephalic lateral line system. This bone also is an insertion site of the jaw adductor, as observed in many anguilliform families. The opercle and subopercle has not increased in length as the gill apparatus became elongated.

Gill arch morphology:

Synapomorphic for Anguilliformes are gill arches that are displaced posteriorly so that the bony connection with the neurocranium no longer exists. This is likely related to the reduction of the head diameter (Nelson, 1966). Losses of an interconnection between the gill skeleton and the cranium may also be related to the expansibility of the pharynx, which is obvious in eels. The posterior displacement of gill arches is slight in *Conger conger* (Congridae) and extreme in *Gymnothorax prasinus* (Muraenidae) and *Moringua edwardsi* (Moringuidae), whereas in *Simenchelys parasiticus* (Simenchelyinae), they are positioned beneath the neurocranium (see chapter 5).

Respiration of eels is carried out by a very characteristic and strong pump-like action of the branchial chamber, the water being forced over the gills. The development of a long, narrow branchial chamber may facilitate the respiratory process in Anguilliformes (Tesch, 2003). The well-developed levator operculi, adductor operculi and dilatator operculi muscles, as well as the sheet-like

hyohyoideus muscle complex are the main muscles that probably serve to expand and contract this long, narrow branchial chamber of the Anguilliformes. The position of the gill opening may differ from a ventral one in fossorial species (*e.g., Pythonichthys macrurus*) to a lateral one in pelagic species like *Serrivomer* sp. (Serrivomeridae).

The gill arches of the Anguilliformes bear a series of small tooth plates associated with the fifth ceratobranchials that are opposed to the dorsal tooth plates. The numerous teeth of these plates are pointed and long in some anguilliforms, such as *G. prasinus*, *A. allardicei* (Muraenidae) and *Kaupichthys hyoproroides* (Chlopsidae). Nelson (1966) mentioned that on the basis of the nature of the teeth and the branchial musculature of some Anguilliformes, such as Muraenidae, these tooth plates apparently function in moving food from the jaws to the esophagus. They have developed in relation to mechanical problems involved in moving relatively large food items through a secondarily elongate pharynx (Nelson, 1966). Mehta and Wainwright (2007a) described the pharyngeal jaws of morays, where they actually demonstrated that these jaws are indeed capable of transporting large prey items from the oral jaw toward the esophagus. The presence of this mechanical prey transport system shows that despite a backward displacement of gill arches, they still keep their role in manipulating prey.

Our study showed that in *Ilyophis brunneus* and *Synaphobranchus brevidorsalis* (Synaphobranchidae), many similar corresponding muscle attachments are present, just as those found in muraenids (see Chapter 5). In *I. brunneus* and *S. brevidorsalis* it is claimed that the capacity to transport food in the buccal cavity is possible, despite having a complete gill skeleton compared to a highly reduced one in muraenids (see Chapter 5). I examined the gill arches of *Kaupichthys hyoproroides* (Chlopsidae) and *Serrivomer* sp. (Serrivomeridae) and observed structures that could be associated with such a transport system. Hence, it should be noted that an investigation of the gill arches of Anguilliformes, like the comparative study of Nelson (1966), but also including the musculature

attachments, can help to better understand the feeding behavior and possible evolutionary changes of this mechanical prey transport system.

Cephalic lateral line system:

Many eels show a sedentary life style, showing many morphological adaptations for their burrowing behavior (see Chapter 4). Examples like smaller eye size, solid conical skull, widened cephalic lateral line canals extending into the dermal cavities, and ventral position of the gill openings, as observed in *Pythonichthys macrurus* (Heterenchelyidae) and *Moringua edwardsi* (Moringuidae), are considered to be specializations for head-first burrowing (Chapter 4). Also, different patterns in head-first burrowing features in Heterenchelyidae and Moringuidae reveal that there is more than one way to restructure the skull in relation to head-first burrowing. For instance, *Pythonichthys macrurus* (Heterenchelyidae) bears arch-like structures, which support the widened preopercular-mandibular canal, where as that of *Moringua edwardsi* (Moringuidae) lacks these bony structures. Also, as an alternative hypothesis, the widened cephalic lateral line canals can be used to detect hidden prey items in the sea bed as seen in cichlids and deep sea fishes (Webb, 2002).

The cephalic lateral line system of the examined Anguilliformes is generally well-developed. It frequently is cavernous and porous and is supported by many bones of the skull that have different shapes within anguilliforms. For instance, the preoperculo-mandibular canal in some Anguilliformes runs inside the mandibula, with some pores connecting to the exterior (e.g., *Pythonichthys macrurus*) whereas in others the mandibula only bears a groove on its lateral or ventral faces that supports this canal (e.g., *Hoplunnis punctata*) (see chapter 3).

8.2. Adaptive versus non-adaptive morphological evolution

Internal constraints in a vertebrate skull reflect various structural and spatial interactions between components (Liem, 1980; Lauder, 1981b; Barel, 1985). Changes in one component of the head generally occur in relation to changes in other components that may be considered as non-adaptive morphological change.

For example jaw elongation as a result of the elongation of the premaxillo-ethmovomeral complex as seen in *Hoplunnis punctata* (Nettastomatidae) can be coupled to an increased distance between the anterior suspensorial facet and the posterior edge of the orbit (see chapter 3).

Another change in this regard is observed in *Heteroconger hassi* (Congridae), a representative with short jaws, where orbit size, and hence eye size, is enlarged. In general, eye size is an important parameter for vision efficiency (Barel, 1985; Barel et al., 1989). Hence, all features of the eye may be considered adaptations to meet visual requirements associated with a particular lifestyle. The short rostral region of *H. hassi* brings the eyes to the snout tip, allowing close up binocular vision for this plankton feeder (De Schepper et al, 2007a). On the other hand as a non-adaptive morphological change, the expansion of the adductor mandibule muscles of *H. hassi* has been restricted by the large eyes (De Schepper et al., 2007a).

Eye reduction in *Pisodonophis boro* (Ophichthidae), *Moringua edwardsi* (Moringuidae) and *Pythonichthys macrurus* (Heterenchelyidae) is considered to be an adaptation to head-first burrowing, i.e. to dark and muddy envoronment (chapter 4). Relatively small orbits leave more room for the bony elements and the jaw adductor muscles. Consequently, the hard biting anguilliforms, such as *Simenchelys parasiticus* (Simenchelyinae) and *P. macrurus* (Heterenchelyidae), which have small eyes, possess large jaw adductor mandibulae muscles (Chapter 5).

The circumorbital bones have different shapes and sizes in Anguilliformes and support the cephalic lateral line system. The arched, large circumorbital bones of heterenchelyids provide more space for the widened cephalic lateral line canals that is considered as an adaptive feature for this head-first burrower (chapter 4). On the other hand, a variety in shape and size of circumorbital bones probably is related to their compromising for space with other head structures such as jaw closing muscles, eye, etc. The reduction of the bony skull elements may occur in favor of the sensory organs (Haken, 1983; wake, 1986).

The presence of the large olfactory rosette in other anguilliforms may be related to other factors rather than having predatory life style as seen in *Hoplunnis punctata* (Nettastomatidae). The olfactory organs are of great biological importance as they help in detection of food and prey (Parker, 1922) and in other behaviors like parental care, recognition of sexes (Nordeny, 1971), orientation etc. In *Serrivomer sp.* (Serrivomeridae) and *Nemichthys scolopaceus* (Nemichthyidae), the elongated premaxillo-ethmovomeral complex is not as deep as in *H. punctata* (Nettastomatidae) to provide large olfactory chambers; hence their olfactory rosette is confined to a smaller space anterior to the eye. Also, the examined Serrivomeridae and Nemichtyidae have larger eyes, which is likely to be related to being pelagic predators. Hence, size and shape of the olfactory organs of some anguilliformes may reflect spatial interactions between head components rather than representing a truly adaptive characteristic.

A caudoventrally oriented jaw muscle may be an adaptive morphological change in both head-first burrowers and in fishes that feed on large prey items, such as muraenids in preventing the dislocation of the mandibular joint (see chapters 4 and 6). On the other hand, in many anguilliform families, the palatopterygoid is reduced and has lost its connection at one or both ends. The reduction of the anterior part of the suspensorium, along with the elongation of the elements of the otic region in some species (e.g., *Anarchias allardicei* and *Gymnothorax prasinus*: Muraenidae), may provide more space for jaw muscles, particularly those directing caudoventrally. This may be linked to the observation of the well-developed adductor hyomandibulae muscle being present in anguilliform families such as muraenids (see chapter 6).

8.3. Some concluding remarks

What this dissertation reveals about the various aspects of the pattern of evolutionary changes and diversity of head musculoskeletal system in Anguilliformes seems fragmentary within this specious order. In addition to this comparative anatomical study on the structural diversity of the cranial

musculoskeletal system, this study is in line with many evolutionary biology studies attempted to contemplate on structural variation. However, deducing functional correlates of such variation has proven to be a challenging task (Russell and Bauer, 2005). Still, in lack of live specimens for a biomechanical study, this approach, which depends upon the assumption of a close match between structure and function (Lauder, 1995), can still provide an insight into possible functions of structures as most morphological characters are generally correlated with functional demands (Bock and Von Wahlert, 1965; Liem, 1967). An example of this approach is the study of Nelson (1966) that suggested a mechanical prey transport system in muraenids by their pharyngeal jaws. Forty years later this suggested function was confirmed by Mehta and Wainwright (2007a) using high speed and radiography filming.

Adaptations are characteristics that enhance the survival or reproduction as a result of natural selection, and that have brought into existence creatures that are in many respects marvelously well-designed. As a pattern, the chisel-like teeth in the alleged parasite *Simenchelys parasiticus* (Simenchelyinae), along with the fleshy lips, small terminal mouth opening, large ventral head muscles and jaw muscles, and a large tongue-like structure, suggest a well-fitted cranial architecture for its special mode of life (see chapter 5). This comparative study of the anatomy, as a method of studying adaptation, thus revealed these features of which the adaptive nature (in relation to this mode of life) could be tested against the basal morphology of non-parasitic representatives of the Synaphobranchidae.

8.4. Insights for further research

This study can also provide insights for future investigations about which structure should be carefully considered. For instance, many studies in Anguilliformes have been accomplished solely based on osteology, hence the myology of those is poorly known. Some authors explain which muscular characters are particularly 'highly corroborative' i.e. non-homoplasic and reliable characters reflecting the true pattern of an evolutionary relationship (Diogo, 2005). This study shows the importance of

the muscular features of the head that clearly reflect different strategies in evolutionary changes in the anguilliforms. Data on head musculature can also be considered as valuable data to be included in a phylogenetic analysis although understanding the homology of those may be difficult (Diogo, 2005).

The Anguilliformes apparently show a reductive trend within the skeleton. Many features of the head of eels are highly simplified, but whether this is because of loss, fusion, or primitive absence still needs to be further examined based on ontogenetic or more elaborate comparative and phylogenetic studies.

Summary

Summary

The general goal of this dissertation is to document the structural patterns and evolutionary changes in the head musculoskeletal system of several Anguilliform taxa in relation to different trends of specializations, such as (1) jaw elongation (*Hoplunnis punctata*: Nettastomatidae), (2) head-first burrowing (*Pythonichthys macrurus:* Heterenchelyidae), (3) parasitic feeding (*Simenchelys parasiticus* :Simenchelyinae; Synaphobranchidae), (4) a pharyngeal system for mechanical transport of captured prey in muraenids, and (5) extraordinarly modified cephalic system in *Eurypharynx pelecanoides* (Eurypharyngidae).

- The head musculoskeletal system of *H. punctata*, a representative of Anguilliformes with a long jaw, was compared with that of *Conger conger* (Congridae), a representative with moderate jaw length; and *Heteroconger hassi* (Congridae), a representative with a short jaw. A shape comparison showed that some structural changes in the head of *H. punctata* are as a result of the elongation of the preorbital region. Also, the results showed that jaw elongation potentially affects the functioning of the feeding apparatus in *H. punctata* by increasing biting speed and reducing drag during prey capture.
- The head musculoskeletal features of *P. macrurus* were compared with those of the Moringuidae (*Moringua edwardsi*), a head-first burrower; the Anguillidae (*Anguilla anguilla*), a non-burrowing representative and the Ophichthidae (*Pisodonophis boro*), a head and tail-first burrower. The result of this comprative study showed some cranial features of *P. macrurus* as morphological adaptations for its burrowing behavior. Different patterns of head-first burrowing features for the Heterenchelyidae and Moringuidae revealed that there is more than one way to restructure the skull for head-first burrowing.
- The cranial osteology and myology *Simenchelys parasiticus,* an alleged parasitic eel were compared to those of non-parasitic representatives of two other subfamilies of the Synaphobranchidae, i.e. *Ilyophis brunneus* (Ilyophinae) and *Synaphobranchus brevidorsalis* (Synaphobranchinae). The cephalic musculoskeletal elements of *S. parasiticus*, compared to the situation in *I. brunneus*, and *S. brevidorsalis* show some morphological modifications, such as the stretchable skin

around the small terminal mouth opening, cutting-edge teeth, stout mouth closing apparatus with its large associated muscles, large tongue-like secretory structure and branchial arches with the capacity to transport food items in the buccal cavity.

• The head musculoskeletal features of *Anarchias allardicei* (Uropterygiinae: Muraenidae) and *Gymnothorax prasinus* (Muraeninae: Muraenidae) were compared with that of a closely-related out-group with a hydraulic based prey transport, *Ariosoma gilberti* (Bathymyrinae: Congridae). The result showed that this innovative feeding mechanism is probably linked to many cephalic modifications such as, stout and robust neurocranial elements, elongated lower jaw the as result of the posterior position of the quadrato-mandibular articulation, enlarged teeth of the oral jaws and premaxillo-ethmovomeral complex, reduction in the moable cranial bones and their muscular connections, hypertrophied adductor mandibulae muscle complex, presence of the quadrato-maxillary and preoperclo-angular ligaments, connection of the quadrate to the A2 tendon of the adductor mandibulae complex, caudoventral orientation of the fibers of large A3 section of the adductor mandibulae complex.

• A detailed description of the cranial osteology and myology of *E. pelecanoides* was provided. In relation to its extensive modifications, possible implications for the functioning of feeding apparatus were described based on its cephalic musculoskeletal system and a broadcasted short footage (sixty-five seconds) of this gulper eel in the BBC documentary series (Blue planet: Eposide2 - The Deep, 2001). The result revealed that many extreme modifications of head structures of *E. pelecanoides* are to be seen in relation to functional shifts compared to those of other Anguilliformes.

The present dissertation may lead to a better understanding of relations between morphological modifications and components that may change with or are coupled to other modifications in the head of Anguilliformes. As main conclusion it should be said that potential cephalic features are linked to each other and may be indirectly related to other morphological or physiological structural elements, i.e. they form a close network. In addition such a comparative anatomy study may reveal crucial information of spatial and functional interactions between the specific components.

Literature Cited

LITRATURE CITED

Aarestrup K, Okland F, Hansen MM, Righton D, Gargan P, Castonguay M, Bernatchez L, Howey P, Sparholt H, Pedersen MI, McKinley RS. 2009. Oceanic spawning migration of the european eel (*Anguilla anguilla*). Science 325: 1660-1660.

Adriaens D, Verraes W. 1997. The ontogeny of the chondrocranium in *Clarias gariepinus*: trends in siluroids. Journal of Fish Biology 50: 1221-1257.

Adriaens D, Verraes W, Taverne L. 1997. The cranial lateral-line system in *Clarias gariepinus* (Burchell, 1822) (Siluroidei: Clariidae): morphology and development of canal related bones. European Journal of Morphology. 35(3): 181-208.

Adriaens D, Devaere S, Teugels GG, Dekegel B, Verraes W. 2002. Intraspecific variation in limblessness in vertebrates: a unique example of microevolution. Biological Journal of the Linnean Society 75:367-377.

Alexander R McN. 1967. The functions and mechanisms of the protrusible upper jaws of some acanthopterygian fish. Journal of Zoology, London 151: 43-64.

Alfaro ME, Janovetz J, Westneat MW. 2001. Motor control across trophic strategies: muscle activity of biting and suction feeding fishes. American Zoologist 41: 1266-1279.

Arnold SJ. 1983. Morphology, performance and fitness. American Zoologist 23: 347-361.

Aoyama J, Shinoda A, Sasai S, Miller MJ, Tsukamoto K. 2005. First observations of the burrows of *Anguilla japonica*. Journal of Fish Biology 67: 1534-1543.

Asano H. 1962. Studies on the congrid eels of Japan. Bulletin of the Misaki Marine Biology Institute of Kyoto University I: 1-143.

Atkinson RJ, Taylor AC. 1991. Burrows and burrowing behaviour of fish. In: Meadows PS, Meadows A, editors. The Environmental Impact of Burrowing Animals and Animal Burrows. Oxford: Clarendon Press. pp. 133-155.

Bandyopadhyay PR. 1989. Viscous drag reduction of a nose body. AIAA Journal 27: 274-282.

Bandyopadhyay PR, Ahmed A. 1993. Turbulent boundary layers subjected to multiple curvatures and pressure gradients. Journal of Fluid Mechanics 246: 503-527.

Bannasch R. 1995. Hydrodynamics of penguins – an experimental approach. In: Dann, P. Norman, I. Reilly, P. (Eds.), The penguins: Ecology and management. Norton, NSW: Surrey Beatty and Sons, pp. 141-176.

Barel CDN. 1985. A matter of space*:* constructional morphology of cichlid fishes. Thesis, Univ Leiden.

Barel CDN, Anker GCh, Witte F, Hoogerhoud RJC, Goldschmidt T. 1989. Constructional constraints and its ecomorphological implications. Acta morphologica Neerlando-Scandinavica 27: 83-109.

Bauchot M-L, Saldanha L. 1986. Congridae (including Heterocongridae). In: Whitehead P.J.P. Bauchot, M-L. Hureau, J-C. Nielsen, J. Tortonese, E. (Eds.), Fishes of the north-eastern Atlantic and the Mediterranean. Vol 2. Paris: UNESCO, pp. 567-574.

BBC Documentary series. 2001. Blue planet: Eposid2 - The Deep.

Belouze A. 2001. Compréhension morphologique et phylogénétique des taxons actuels et fossils rapports aux Anguilliformes (Poissons, Téléostéens). Thèse de doctorat paléoenvironment et palèobiosphère l'Université Claude Bernard Lyon I, 407 p.

Bertelsen E, Nielsen JG. 1987. The deep sea eel family Monognathidae (Pisces, Anguilliformes). Steenstrupia 13(4): 141-198.

Bertelsen E, Nielsen JG, Smith DG. 1989. Suborder Saccopharyngoidei: families Saccopharyngidae, Eurypharyngidae, and Monognathidae. In: Böhlke EB. (Ed.), Fishes of the Western North Atlantic. Sears Foundation for Marine Research, New Haven, pp. 636-655.

Bertin L. 1934. Les poissons apodes appartenant au sous-ordre des Lyoméres. Dana Rep 3: 1-56

Bigelow HB, Schroeder WC. 1953. Fishes of the gulf of Maine. Fishery Bulletin Fish & Wildlife Service 53, U.S. Printing Service, Washington, D.C. 577 p.

Blache J. 1968. Contribution a la Connaissance de Poisons Anguilliformes de la Cote Occidentate d'Afrique (Neuvieme Note/les Heterenchelyidae). Bulletien de l'I.F.N.T. XXX, ser, A, no 4.

Bock WJ, Von Wahlert G. 1965. Adaptation and the form-function complex. Evolution 19: 269-299.

Bock WJ, Shear RC. 1972. A staining method for gross dissection of vertebrate muscles. Anatomischer Anzeiger Bd 130: 222–227.

Boel CDN. 1985. A Matter of Space [Dissertation]. The Netherlands: Leiden University.

Böhlke JE. 1966. Order Iniomi and Lyomeri. In: Fishes of the western north Atlantic Mem. Memoir Sears Foundation for Marine Research. pp. 603-628.

Böhlke EB. 1989a. In: Fishes of the Western North Atlantic. Part 9. New Haven, CT: Sears Foundation for Marine Research. 1055 p.

Böhlke EB. 1989c. Methods and terminology**.** In: Böhlke EB. (Ed), Fishes of the Western North Atlantic. New Haven: Sears Foundation for Marine Research, p. 1-8.

Böhlke EB, McCosker JE, Böhlke JE. 1989. Family Muraenidae. In: Böhlke E.B. (Ed), fishes of the Western North Atlantic. New Haven: Sears Foundation for Marine Research, pp. 104-206.

Bozzano A. 2003. Vision in the rufus snake eel. *Ophichthus rufus*: adaptive mechanisms for a burrowing life-style. Marine Biology 143: 167-174.

Brock JP. 2000. The Evolution of adaptive systems. Academic Press. 642 p.

Caira JN, Benz GW, Borucinska J, Kohler NE. 1997. Pugnose eels, *Simenchelys parasiticus* (Synaphobranchidae) from the heart of a shortfin mako, *Isurus oxyrinchus* (Lamnidae). Environmental Biology of Fishes 49: 139-144.

Caldwell MW. 2003. "Without a leg to stand on": on the evolution and development of axial elongation and limblessness in tetrapods. Canadian Journal of Earth Science 40: 573-588.

Carroll AM. 2004. Muscle activation and strain during suction feeding in the largemouth bass *Micropterus salmoides.* Journal of Experimental Biology 207: 983–991.

Carroll RL. 1997a. Patterns and processes of vertebrate evolution. Cambridge Paleobiology Series. 447 p.

Carroll RL. 1997b. The fossil record of elongation and limb reduction as a model of evolutionary patterns. Journal of Morphology 232: 241.

Carson F, Hladik C. 2009. Histotechnology: a self-instructional text, 3nd edition, ASCP Press, Chicago. pp. 114-115.

Casimir MJ, Fricke HW. 1971. Zur function, morphologie und histochemie der schwanzdrüse bei röhrenaalen (Pisces, Apodes, Heterocongridae). Marin Biology 9: 339-346.

Castle PHJ. 1961. Deep-water eels from Cook Strait, New Zealand. Zool. Pub. Vict. Univ. N.Z. 27: 1-30.

Castle PHJ. 1968. The world of eels. Tuatara: Journal of the Biological Society 16(2): 87-97.

Castle PHJ, Mccosker JE. 1999. A new genus and two new species of *Myrophine* Worm-eels, with Comments on *Muraenichthys* and *Scolecenchelys* (Anguilliformes: Ophichthidae). Records of the Australian Museum 51: 113-122.

Castle PHJ, Randall JE. 1999**.** Revision of Indo-Pacific garden eels (Congridae: Heterocongrinae), with descriptions of five new species. Indo-Pacific Fishes 30: 2-53.

Chen Y-Y, Mok H-K. 2001. A new synophobranchid eel, *Dysomma longirostrum* (Anguilliformes: synophobranchidae), from the northeastern coast of Taiwan. Zoological Studies 40(2): 79-83.

Cohn MJ, Tickle C. 1999. Developmental basis of limblessness and axial patterning in snakes. Nature 399: 474-479.

Collar DC, Near TJ, Wainwright PC. 2005. Comparative analysis of morphological diversity: does disparity accumulate at the same rate in two lineages of centrarchid fishes? Evolution 59: 1783-1794.

Darwin C. 1859. On the Origin of Species by Means of Natural Selection, or Preservation of Favored Races in the Struggle for Life. John Murray. London.

De Schepper N. 2007. Evolutinary morphology of body elongation in teleosts: aspects of convergent evolution [dissertation]. Ghent University.

De Schepper N, Adriaens D, Teugels GG, Devaere S, Verraes W. 2004. Intraspecific variation in the postcranial skeleton morphology in African clariids: A case study of extreme phenotypic plasticity. Zoological Journal of the Linnean Society of London 140: 437-446.

De Schepper N, Adriaens D, De Kegel B. 2005. *Moringua edwardsi* (Moringuidae:Anguilliformes): cranial specialization for head-first burrowing? Journal of Morphology 266: 356–368.

De Schepper N, De Kegel B, Adriaens D. 2007a. Morphological specialization in Heterocongrinae (Anguilliformes: Congridae) related to burrowing and feeding. Journal of Morphology 268: 343–356.

De Schepper N, De Kegel B, Adriaens D. 2007b. *Pisodonophis boro* (Ophichthidae: Anguilliformes): specialization for headfirst and tail-first burrowing? Journal of Morphology 268: 112-126.

De Schepper N, Van Wassenbergh S, Adriaens D. 2008. Morphology of the jaw system in trichiurids: trade-offs between mouth closing and biting performance. Zoological Journal of the Linnean Society 152: 717-736.

Devaere S, Adriaens D, Verraes W, Teugels GG. 2001. Cranial morphology of the anguilliform clariid *Channallabes apus* (Günther, 1873) (Teleostei: Siluriformes): Adaptations related to powerful biting? Journal of Zoology 255: 235-250.

Devaere S, Teugels GG, Adriaens D, Huysentruyt F, Verraes W. 2004. Redescription of *Dolichallabes microphthalmus* (Poll, 1942) (Siluriformes. Clariidae). Copeia 1: 108-115.

De Visser J, Barel CDN. 1998. The expansion apparatus in fish heads, a 3-D kinetic deduction. Netherlands Journal of Zoology 48: 361-395.

Diogo R. 2004. Muscles versus bones: catfishes as a case study for an analysis on the contribution of myological and osteological structures in phylogenetic reconstructions. Animal Biology 54: 373-391.

Diogo R. 2005. Morphological evolution, adaptations, homoplasies, constraints and evolutionary trends: catfishes as a case study on general phylogeny and macroevolution. Science publisher, Inc, NH, USA. 491 p.

Diogo R, Hinits Y, Hughes SN. 2008. Development of mandibular, hyoid and hypobranchial muscles in the zebrafish: homologies and evolution of these muscles within bony fishes and tetrapods. BMC Developmental Biology 8, 24.

Duellman WE, Trueb L. 1986. Musculoskeletal system. In: Biology of Amphibians. Duellman WE and Trueb L, editors. New York: McGraw-Hill. pp. 289–364.

Dullemeijer P. 1974. Concepts and approaches in animal morphology. Van gorcum, Assen.

Dullemeijer P. 1991. Evolution of biological constructions: concessions, limitations, and pathways. In: Schmidt-Kittler N, Vogel K, (Eds). Constructional Morphology and Evolution, Springer, Berlin, pp. 313–329.

Eagderi S, Adriaens D. 2010a. Head morphology of the duckbill Eel, *Hoplunnis punctata* (Regan, 1915; Nettastomatidae: Anguilliformes): a case of jaw elongation. Zoology 113(3): 148-157.

Eagderi S, Adriaens D. 2010b. Cephalic morphology of *Pythonichthys macrurus* (Heterenchelyidae: Anguilliformes): specializations for head-first burrowing. Journal of Morphology 271(9): 1053-1065.

Eagderi S, Adiriaens D. (submitted). Cephalic specialization in a parasitic eel, *Simenchelys parasiticus* (Simenchelyinae: Synaphobranchidae). Copeia.

Eaton, T.H. Jr., 1935. Evolution of the upper jaw mechanism in teleost fishes. Journal of Morphology 58: 157-72.

Felsenstein J. 1985. Phylogenies and the comparative method. American Naturalist 125:1-15.

Ferry-Graham LA, Lauder GV. 2001a. Aquatic prey capture in ray-finned fishes: A century of progress and new directions. Journal of Morphology 248: 99-119.

Ferry-Graham LA, Wainwright PC, Bellwood DR. 2001b. Prey capture in long-jawed butterflyfishes (Chaetodontidae): the functional basis of novel feeding habits. Journal of Experimental Marine Biology and Ecology 256: 167–184.

Ferry-Graham LA, Wainwright PC, Hulsey CD, Bellwood DR. 2001c. Evolution of mechanics of long jaws in Buterflyfishes (Family Chaetodontidae). Journal of Morphology 248: 120–143.

Fish FE. 1998. Imaginative solutions by marine organisms for drag reduction. In: Meng, J.C.S. (Ed.), Proceedings of the International Symposium on Seawater Drag Reduction. Newport, Rhode Island, pp. 443-450.

Fisher RA. 1930. The genetical theory of natural selection. Oxford Univ. Press (Clarendon), Oxford.

Forey PL. 1973. Relationships of elopomorphs. In: Greenwood PH, Miles RS, Patterson C, (Eds). Interrelationships of Fishes. Zoological Journal of the Linnean Society, 53 (Suppl. 1), Academic Press, New York, pp. 351–368.

Forey PL, Littlewood DTJ, Ritchie P, Meyer A. 1996. Interrelationship of Elopomorph fishes. In: Stiassny MLJ, Parenti LR, Johnson GD, (Eds). Interrelationships of Fishes. Academic Press, San Diego, CA. pp. 175–191.

Gans C. 1975. Tetrapod limblessness: evolution and functional corollaries. American Zoologist 15: 455-467.

Gans C, De Vree F. 1987. Functional bases of fiber length and angulation in muscle. Journal of Morphology 192: 63-85.

Geerinckx T, Brunain M, Adiaens D. 2005. Development of the chondrocranium in the suckermouth armored catfish *Ancistrus* cf. *triradiatus* (Loricariidae, Siluriformes). Journal of Morphology 266(3): 331-355.

Genten F,Terwinghe E, Danguy A. 2009. Atlas of fish histology. Enfield (NH): Science Publishers. pp. 64-74.

Gill T, Ryder JA. 1883. On the anatomy and relationship of the Eury*pharyngidae.* Proceedinf United States National Museum 6: 262-273.

Gillis GB, Lauder GV. 1995. Kinematics of feeding in bluegill sunfish: is there a general distinction between aquatic capture and transport behaviors? Journal of Experimental Biology 198: 709–720.

Goode GB, Bean TH. 1896. Oceanic ichthyology. Smithsonian Contribution Knowledge 981:1-553.

Gordon SM. 1954. The eel genus *Stilbiscus*. Copeia 1: 11–15.

Gosline WA. 1961. Some osteological of modern lowe teleostean fishes. Smithson Misc Collns 142(3):1-42.

Gosline WA. 1965. Teleostean phylogeny. Copeia 1: 186–194.

Gosline WA. 1971. Functional morphology and classification of teleostean fishes. University Press of Hawaii, Honolulu. 208 p.

Gosline WA. 1980. The evolution of some structural systems with reference to the interrelationships of modern lower teleostean fish groups. Japanese Journal of Ichthyology 21: 1-24.

Gould SJ, Vrba E. 1982. Exaptation - a missing term in the science of form. Paleobiology 8: 4-15.

Greenwood PH, Rosen DE, Weitzman SH, Myers G. 1966. Phyletic studies of teleostean fishes, with a provisional classification of living forms, Bulletin of the American Museum of Natural History 131: 339-456.

Gregory WK. 1933. Fish skulls: a study of the evolution of natural mechanisms. Transactiosn of the American Philosophical Society 23(2): 75-481.

Grubich J, Rice AN, Westneat MW. 2008. Functional morphology of bite mechanics in the great barracuda (*Sphyraena barracuda*). Zoology 111: 16-29.

Hanken J, Wassersug R. 1981. The visible skeleton. a new double-stain technique reveals the nature of the "hard" tissues. Functional Photography 16: 22-26.

Heemstra PC, Hissmann K, Fricke H, Smale MJ. 2006. Fishes of the deep demersal habitat at Ngazidja (Grand Comoro) Island, Western Indian Ocean. South African Journal of Science 102: 444-460.

Helfman GS, Clark JB. 1986. Rotational feeding: overcoming gape-limited foraging in anguillid eels. Copeia 3: 679-685.

Helfman GS, Collette BB, Facey DE. 1997. The Diversity of fishes. Blackwell Science, Inc. USA, 597 p.

Hernandez LP, Bird NC, Staab KL. 2007. Using zebrafish to investigate cypriniform evolutionary novelties: Functional development and evolutionary diversification of the kinethmoid. Journal of Experimental Zoology 308B: 625-641.

Herrel A, Adriaens D, Verraes W, Aerts P. 2002. Bite performance in clariid fishes with hypertrophied jaw adductors as deduced by bite modelling. Journal of Morphology 253: 196–205.

Hertwig ST. 2008. Phylogeny of the Cyprinodontiformes (Teleostei, Atherinomorpha): the contribution of cranial soft tissue characters. Zoologica Scripta 37(2): 141–174

Hildebrand M. 1995. Analysis of vertebrate structure. Fourth Edition.Wiley, New York.

Houston KA, Haedrich RL. 1986. Food habits and intestinal parasites of deep demersal fishes from the upper continental slope east of Newfoundland, northwest Atlantic Ocean. Marine Biology 92: 563-574.

Hulet WM, Robison RC. 1989. The evolutionary significance of the leptocephalus larva. In: Böhlke EB, (Ed). Fishes of the Western North Atlantic. Part 10, Sears Foundation for Marine Research, New Haven, pp. 669-677.

Hutchins M, Thoney DA, Loiselle PV, Neil Schlager N. 2003. Grzimek's animal life encyclopedia. Second edition. Volumes 4–5, Fishes I–II. Farmington Hills, MI: Gale Group.

Inoue JG, Miya M, Tsukamoto K, Nishida M. 2003. Evolution of the deep-sea gulper eel mitochondrial genomes: large-scale gene rearrangements originated within the eels. Molecular Biology and Evolution 20(11): 1917-1924.

Inoue JG, Miya M. 2001. Phylogeny of the basal teleosts, with special reference to the Elopomorpha. Japanese Journal of Ichthyology 48: 75-91 [in Japanese with English abstract].

Inoue JG, Miya M, Miller MJ, Sado T, Hanel R, Hatooka K, Aoyama J, Mark

Inoue JG, Miya M, Tsukamoto K, Nishida M. 2004. Mitogenomic evidence for the monophyly of elopomorph fishes (Teleostei) and the evolutionary origin of the leptocephalus larva. Molecular Phylogenetics and Evolution 32: 274-286.

Inoue JG, Miya M, Miller MJ, Sado T, Hanel R, Hatooka K, Aoyama J, Minegishi Y, Nishida M, Tsukamoto K. 2010. Deep-ocean origin of the freshwater eels. Biological Letters, doi: 10.1098/rsbl.2009.0989

James R, Atkinson A, Roger S, Pullin V. 1995. Observations on the burrows and burrowing behavior of the red band-fish. *Sepola rubescens* L. Marine Ecology 17(1-3): 23-40.

Jamieson BGM. 1991. Fish evolution and systematics: evidence from spermatozoa. Cambridge university press, Cambridge, UK.

Jaquet M. 1920. Contribution á l'anatomie du *Simenchelys parasiticus* Gill. Rèsultat des Campagnes Scientifiques par Albert I, Prince Souverian de Monaco, 56: 1-77.

Jones EC. 1971. *Isitius brasiliensis*, a squaloid shark, the probable of crater wounds on fishes and cetaceans. U.S. Fishery Bulletin 69: 791-798

Kajiura SM, Forni BJ, Summers AP. 2005. Olfactory morphology of carcharhinid and sphyrnid sharks: does the cephalofoil confer a sensory advantage? Journal of Morphology 264**:** 253-263.

Kammerer CF, Grande L, Westneat MW. 2005. Comparative and developmental functional morphology of the jaws of living and fossil gars (Actinopterygii: Lepisosteidae). Journal of Morphology 267: 1017-1031.

Klages M, Muyakshin S, Soltwedel T, Arntz WE. 2002. Mechanoreception, a possible mechanism for food fall detection in deep-see scavengers. Deep-SEA Res I 49: 143-155.

Konow N, Bellwood DR. 2005. Prey-capture in *Pomacanthus semicirculatus* (Teleostei, Pomacanthidae): functional implications of intramandibular joints in marine angelfishes. Journal of Experimental Biology 208: 1421-1433.

Konow N, Sanford CPJ. 2008. Is a convergently derived muscle-activity pattern driving novel raking behaviours in teleost fishes? Journal of Experimental Biology 211: 989-999

Kramer MO. 1960. Boundary layer stabilization by distributed damping. Journal of American Society of Naval Engineers 72: 25-33.

Lauder GV. 1979. Feeding mechanisms in primitive teleosts and in the halecomorph fish *Amia calva*. Journal of Zoology 187: 543-578.

Lauder GV. 1980a. Hydrodynamics of prey capture by teleost fishes. In: Schneck D. editor. Biofluid Mechanics. vol. 2 New York: Plenum Press. pp. 161-181.

Lauder GV. 1981a. Form and function: structural analysis in evolutionary morphology. Paleobiology 7: 430-442.

Lauder GV. 1981b. Intraspecific functional repertoires in the feeding mechanism of characoid fishes: Lebiasina, Hoplias and Chalceus. Copeia 1981: 154-168.

Lauder GV. 1982. Historical biology and the problem of design. Journal of Theoretical Biology 97: 57-67.

Lauder GV. 1982. Pattern of evolution in the feeding mechanism of actinoptergian fishes. American Zoologist 22: 275-282.

Lauder GV. 1985. Aquatic feeding in lower vertebrates. In: Functional Vertebrate Morphology. Hildebrand M, Bramble DM, Liem KF, Wake DB, editors. Cambridge, MA: Belknap Press. pp. 210-229.

Lauder GV. 1990. Functional morphology and systematics: studying functional patterns in an historical context. Annual Review of Ecology and Systematics 21: 317-340.

Lauder GV. 1995. On the inference of function from structure. In: Morphology in Vertebrate Paleontology (J. Thomason, ed), pp. 1-18. Cambridge, England: Cambridge University Press.

LeBoeuf BJ, McCosker JE, Hewitt J. 1987. Crater wounds on northern elephant seals: the cookiecutter shark strikes again. U.S. Fishery Bulletin 85: 387-392.

Leiby MM. 1981. Larval morphology of the eels *Bascanichthys bascanium*, *B. scuticaris*, *Ophichthus melanoporus* and *O. ophis* (Ophichthidae), with a discussion of larval identification methods. Bulletin of Marine Science 31: 46-71.

Liem K. 1967. Functional morphology of the head of the anabantoid teleost fish *Helostoma temmincki*. Journal of Morphology 121: 135-158.

Liem KF, Osse JWM. 1975. Biological versatility, evolution, and food resources exploitation in African cichlid fishes. American Zoologist 15: 427-454.

Lindell LE. 1994. The evolution of vertebral number and body size in snakes. Functional Ecology 8: 708-719

Lopez JA, Westneat MW, Hanel R. 2007. The phylogenetic affinities of the mysterious anguilliform genera *Coloconger* and *Thalassenchelys* as supported by mtDNA sequences. Copeia 4: 959–966

Marshall NB. 1962. Observation on the Heteromi, an order of teleost fishes. Bulletin of the British Museum Natural History (Zoology) 9: 249-270.

Masschaele BC, Cnudde V, Dierick M, Jacobs P, Van Hoorebeke L, Vlassenbroeck J. 2007. UGCT: New X-ray radiography and tomography facility. Nuclear Instruments and Methods in Physics Research Section A 580: 266-269.

Mayr E. 1983. Darwin intellectual revolutionary. Bendall, DS. (Ed.). Evolution from Molecules to Men. Cambridge University Press, pp. 23-42.

McCosker JE. 1998. Eels and their allies. In: Paxton JR and Eschmeyer WN, (Eds). Encyclopedia of Fishes. San Diego: Academic Press. pp. 85-90.

McCosker JE, Böhlke EB, Böhlke JE. 1989. Family Ophichthidae. In: Böhlke EB, editor. Fishes of the Western North Atlantic. New Haven, CT: Sears Foundation for Marine Research. pp. 254-412.

Mishler B. 2003. Phylogeny. In: Keywords and concepts in evolutionary developmental biology. Hall BK, Olson M, eds. Harvard University Press, London. pp. 297-308.

Mehta RS. 2009. Ecomorphology of the moray bite: relationship between dietary extremes and morphological diversity. Physiological and Biochemical Zoology 82(1): 90-103.

Mehta RS, Wainwright PC. 2007a. Raptorial jaws in the throat help moray eels swallow large prey. Nature 449: 79-83.

Mehta RS, Wainwright PC. 2007b. Biting releases constraints on moray eel feeding kinematics. Journal of Experimental Biology 210: 495-504.

Mehta RS, Wainwright PC. 2008. Functional morphology of the pharyngeal jaw apparatus in moray eels. Journal of Morphology 269: 604-619.

Miller MJ. 2009. Ecology of anguilliform leptocephali: remarkable transparent fish larvae of the ocean surface layer. Aqua-BioScience Monographs (ABSM) 2(4): 1-94.

Montgomery JC. 1989. Lateral line detection of planktonic prey. In: Coombs S, Görner P, Münz H, editors. The Mechanosensory Lateral Line. New York: Springer-Verlag. Chapter 28.

Nakae M, Sasaki K. 2004. Homologies of the adductor mandibulae muscles in Tetraodontiformes as indicated by nerve branching patterns. Ichthyological Research 51: 327–336.

Narici M, Magnaris C. 2006. Muscle architecture and adaptations to functional requirements. In: Bottinelli R, Reggiani C, (Eds). Advances in muscle research: Skeletal muscle plasticity in health and disease. pp. 256-288.

Nelson GJ. 1966. Gill arches of the teleostean fishes of the order Anguilliformes Pacific Scientific 20: 391-408.

Nelson GJ. 1967. Branchial muscles in representatives of live eel families. Pacific Science, 21(3): 348-363.

Nelson GJ. 1973. Relationship of clupeomorphs, with remarks on the structure of the lower jaw in fishes.. In: M.L.J. Stiassny, L.R. Parenti and G.D. Johnson, Editors, Interrelationships of Fishes, Academic Press, San Diego, CA. pp. 333–349.

Nelson JS. 2006. Fishes of the world. Fourth edition. John Wiley & Sons, INC. 600 p.

Nielsen JG, Bertelsen E. 1985. The gulper-eel family Saccopharyngidae (Pisces, Anguilliformes). Steenstrupia 11(6): 157-206.

Nielsen JG, Bertelsen E, Jespersen A. 1989. The biology of *Eurypharynx pelecanoides* (Pisces, Eurypharyngidae). Acta Zoologica 70: 187-197.

Nordeny H. 1971. Is the local orientation of anadromous fishes determined by heromones? Nature (Lond.) 233: 411- 413.

Norman JR. 1926. The Development of the chondrocranium of the eel (*Anguilla vulgaris*), with observations on the comparative morphology and development of the chondrocranium in bony fishes**.** Philosophical Transactions of the Royal Society of London Series B 214: 369-464

Norton SF, Brainerd EL. 1993. Convergence in the feeding mechanics of ecomorphologically similar species in the Centrarchidae and Cichlidae. Journal of Experimental Biology 176: 11–29.

Nusbaum-Hilarowicz J. 1923. Etudes d'anatomie comparee sur les poissons provenant des campagnes scientifiques de S.A.S. le Prince de Monaco. Camp Scient Prince Albert I 15: 1-100.

Obermiller LE, Pfeiler E. 2003. Phylogenetic relationships of elopomorph fishes inferred from mitochondrial ribosomal DNA sequences. Molecular Phylogenetics and Evolution 26: 202–214.

Parker GHO. 1922. Smell, taste and the allied senses in the vertebrates. monographs on Experimental Biology, D.B. Lippincelf, Philadelphia.

Pankurst NW, Lythgoe JN. 1983. Changes in vision and olfaction during sexual maturation in the European eel. Journal of Fish Biology 23: 229-240.

Patterson C. 1975. The braincase of pholidophorid and leptolepid fishes, with a review of the actinopterygian braincase. Philosophical Transactions of the Royal Society of London. Series B, Biological Sciences 269: 275-579.

Patterson C., Rosen DE. 1977. Review of ichthyodectiform and other Mesozoic teleost fishes and the theory and practice of classifying fossils. Bulletin of the American Museum of Natural History 158: 81-172.

Pfeiler E. 1986. Towards an explanation of the developmental strategy in leptocephalus larvae of marine fishes. Environmental Biology of Fishes 15: 3–13.

Pfeiler E. 1997. Effect of Ca2+ on survival and development of metamorphosing bonefish (*Albula* sp.) leptocephali. Marine Biology 127: 571–578.

Pfeiler E. 1999. Developmental physiology of elopomorph leptocephali. Comparative Biochemistry and Physiology A123:113-128.

Pfeiler E, Luna A. 1984. Changes in biochemical composition and energy utilization during metamorphosis of *leptocephalous* larvae of the bonefish (*Albula*). Environmental Biology of Fishes 10: 243-251

Poll M. 1973. Les yeux des poissons aveugles Africains et de Caecomastacembelus brichardi Poll en particulier. Ann du Spéléologie 28: 221-230.

Porter HT, Motta PJ. 2004. A comparison of strike and prey capture kinematics of three species of piscivorous fishes: Florida gar (*Lepisosteus platyrhincus*), redfin needlefish (*Strongylura notata*), and great barracuda (*Sphyraena barracuda*). Marine Biology 145: 989-1000.

Pough HF, Andrews RM, Cadle JE, Crump ML, Savitzky AH, Wells KD. 1998. Body support and locomotion. In: Pough HF, editor. Herpetology. New Jersey: Prentice Hall. Chapter 8.

Regan CT. 1909. The classification of teleostean fishes. Annals and Magazine of Natural History 3: 75-86.

Regan CT. 1912. The osteology and classification of the teleostean fishes of the Order Apoda. Annals and Magazine of Natural History 10: 377-387.

Renous S, Hofling E, Gasc JP. 1998. Respective role of the axial and appendicular systems in relation to the transition to limblessness. Acta Biotheorethica 46: 141-156.

Rice AN, Westneat MW. 2005. Coordination of feeding, locomotor and visual systems in parrotfishes (Teleostei: Labridae). Journal of Experimental Biology 208**:** 3503-3518.

Rieppel OC. 1988. Fundamentals of comparative biology. Basel: Birkhauser.

Ridley M. 2004. Evolution. 3rd ed. Wiley-Blackwell, 751 p.

Robins CH. 1971. The comparative morphology of the synaphobranchid eels of the Straits of Florida. Proceeding of the Academy of Natural Science of Philadelphia. 123(7): 153-205.

Robins CH. 1989. Family Derichthyidae. In: Böhlke, E.B. (Ed.), Fishes of the western North Atlantic. New Haven, CT: Sears Foundation for Marine Research, pp. 420–431.

Robins CH, Robins CR. 1989. Family Synaphobranchidae. In: Fishes of the western North Atlantic. Böhlke EB, editor. New Haven, CT: Sears Foundation for Marine Research. pp. 207-253.

Robinson CR. 1989. The phylogenetic relationships of the anguilliform fishes. In: Böhlke EB, editor. Fishes of the western North Atlantic. New Haven: Conn Search Found Mar Res pp. 9-23.

Rojo AL. 1991. Dictionary of evolutionary of fish osteology. Florida: CRC Press. 273 p.

Rohlf FJ. 2004a. tpsSpline, thin-plate spline, version 1.16. Department of Ecology and Evolution, State University of New York at Stony Brook.

Rohlf FJ. 2004b. tpsUtil, file utility program. version 1.26. Department of Ecology and Evolution, State University of New York at Stony Brook.

Rohlf FJ. 2005. tpsDig, digitize landmarks and outlines, version 2.08. Department of Ecology and Evolution, State University of New York at Stony Brook.

Rosenblatt RH. 1958. The status and synonomy of the eastern Pacific eel *Ariosoma gilberti* (Ogilby). Copeia 1958: 52-54.

Rosenblatt RH. 1967. The osteology of the congrid eel *Gorgasia punctata* and the elationships of the Heterocongrinae. Pacific Scientific 21: 91–97.

Russell AP, Bauer AM. 2005. Variation in structure and its relationship to function: correlation, explanation and extrapolation. Chapter 17, In: Variation: A Central Concept in Biology, B. Hallgrímsson and B.K. Hall (Eds.), Academic Press, New York. pp. 399-434.

Saldanha L, Bauchot M-L. 1986. Synaphobranchidae (including Nettodaridae and Simenchelyidae). In: Fishes of the north-eastern Atlantic and the Mediterranean. Whitehead PJP, Bauchot M-L, Hureau J-C, Nielsen J, Tortonese E, editors. UNESCO, Paris. Vol. 2. pp. 586-592.

Sanford, CPJ, Wainwright PC. 2002. Use of sonomicrometry demonstrates link between prey capture kinematics and suction pressure in largemouth bass. Journal of Experimental Biology 205: 3445-3457.

Santos FB, Castro RMC. 2003. Activity, habitat utilization, feeding behavior, and diet of the sand moray Gymnothorax ocellatus (Anguilliformes, Muraenidae) in the South Western Atlantic. Biota Neatropica 3: 1-7.

Schaeffer B, Rosen DE. 1961. Major adaptive levels in the evolution of the actinopterygian feeding mechanism. American Zoologist 1: 187-204.

Schultze H-P, Cumbaa SL. 2001. *Dialipina* and the characters of basal actinopterygians. *In:* Ahlberg PE (Ed). Major events in vertebrate evolution. London, UK: Taylor & Francis. pp. 315-332.

Shirai S, Nakaya K. 1992. Functional morphology of feeding apparatus of the cookie-cutter shark, *Isistius brasiliensis* (Elasmobranchii, Dalatiinae). Zoological Science 9: 811-821.

Sibbing FA, Osse JWM, Terlouw A. 1986. Food handling in the carp (*Cyprinus carpio*): its movement patterns, mechanisms and limitations. Journal of Zoology, London A 210: 161–203.

Smith DG. 1989a. Family congridae. In: Böhlke, E.B. (Ed.), Fishes of the Western North Atlantic. Sears Foundation for Marine Research, New Haven, pp. 460–612.

Smith DG. 1989b. Family Nettastomatidae. In: Böhlke, E.B. (Ed.), Fishes of the western North Atlantic. New Haven, CT: Sears Foundation for Marine Research, pp. 568–567.

Smith DG. 1989c. Family Muraenesocidae. In: Böhlke, E.B. (Ed.), Fishes of the western North Atlantic. New Haven, CT: Sears Foundation for Marine Research, pp. 432–440.

Smith DG. 1989d. Family Moringuidae. In: Böhlke EB, editor. Fishes of the Western North Atlantic. Anguilliformes and Saccopharyngiformes. New Haven, CT: Sears Foundation for Marine Research. pp. 55-71.

Smith DG. 1989e. Family Heterenchelyidae. In: Böhlke EB, editor. Fishes of the Western North Atlantic. Anguilliformes and Saccopharyngiformes. New Haven, CT: Sears Foundation for Marine Research. pp. 48-54.

Smith DG. 1999. Synaphobranchidae. Cutthroat eels. In: FAO species identification guide for fishery purposes. The living marine resources of the WCP. Vol. 3. Batoid fishes, chimaeras and bony fishes part 1 (Elopidae to Linophrynidae). Carpenter KE, Niem VH, editors. FAO, Rome. pp. 1658-1661.

Smith DG. 2004. A new genus and species of congrid eel (Teleostei: Anguilliformes: Congridae) from Western Australia. Records of the Australian Museum 56(2): 143-146.

Smith DG, Castle PHJ. 1972. The eel genus *Neoconger* Girard: Systematics, osteology, and life history. The Bulletin of Marine Science 22: 196-249.

Smith DG, Karmovskaya ES. 2003. A new genus and two new species of congrid eels (Teleostei: Anguilliformes: Congridae) from the Indo-West Pacific, with a redescription and osteology of *Chiloconger dentatus*. Zootaxa 343: 1-19.

Smith DG, Kanazawa RH. 1977. Eight new species and a new genus of congrid eels form the Western North Atlantic with redescriptions of *Ariosoma analis, Hildebrandia guppyi*, and *Rhechias vicinalis*. Bulletin of Marine Science 27(3): 530-543.

Smith DG, Nielsen JG. 1989. Family nemichthyidae. In: Böhlke EB, editor. Fishes of the western North Atlantic. New Haven, CT: Sears Foundation for Marine Research. pp. 441-459.

Solomon-Raju N, Rosenblatt RH. 1971. New record of the parasitic eel, *Simenchelys parasiticus* from the central north pacific with notes on its metamorphic form. Copeia 2: 312-314.

Solomon EP, Berg LR, Martin DW. 2005. Biology, 7th Ed., Brooks/Cole, Thomson Learning, USA.

Subramanian A. 1984. Burrowing behavior and ecology of the crab-eating Indian snake eel *Pisodonophis boro*. Environmental Biology of Fishes 10: 195-202.

Summers AP, Koob TJ, Brainerd EL. 1998. Stingray jaws strut their stuff. Nature 395(6701): 450-451.

Swanson JR. 1996. Anatomy and histology of normal skin. http://www.meddean.luc.edu/lumen/MedEd/medicine/dermatology/melton/skinlsn/sknlsn.htm

Taylor WR, Van Dyke GC. 1985. Revised procedures for staining and clearing small fishes and other vertebrates for bone and cartilage study. Cybium 9: 107-119.

Tcheranvian VV. 1947. Further notes on the structure of the bony fishes of order Lyomeri (*Eurypharynx*). Journal of the Linnean Society (Zoology) 41: 377-393.

Tesch F-W. 2003. The Eel. Third edition. Oxford: Blackwell Science. 408 p.

Tighe KA, 1989. Family Serrivomeridae. In: Böhlke EB, editor. Fishes of the western North Atlantic. New Haven, CT: Sears Foundation for Marine Research. pp. 613-627.

Tilak R, Kanji SK. 1969. Studies on the osteology of *Pisodonophis boro* (Hamilton). Gegenbaurs morpholo- gisches Jahrbuch 113: 501–523.

Turingan RG, Wainwright PC, Hensley DA. 1995. Interpopulation variation in prey use and feeding biomechanics in Caribean Triggerfishes. Oecologia 102: 296-304.

Tsukamoto Y, Okiyama M. 1997. Metamorphosis of the Pacific tarpon, *Megalops cyprinoides* (Elopiformes, Megalopidae) with remarks on development patterns in the Elomorpha. The Bulletin of Marine Science 60: 23–36

Vandewalle P, Gluckman I, Wagemans F. 1998. A critical assessment of the Alcian blue/Alizarine double staining in fish larvae and fry. Belgian Journal of Zoology 128:93-95.

Vandewalle P, Parmentier E, Chardon M. 2000. The branchial basket in teleost feeding. Cybium 24(4): 319-342.

Van Wassenbergh S, Herrel A, Adriaens D, Aerts P. 2004. Effects of jaw adductor hypertrophy on buccal expansion during feeding of air breathing catfishes (Teleostei, Clariidae). Zoomorphology 123: 81-93.

Van Wassenbergh S, Aerts P, Adriaens D, Herrel A. 2005. A dynamical model of mouth closing movements in clariid catfishes: the role of enlarged jaw adductors. Journal of Theoretical Biology 234: 49-65.

Vetter B. 1878. Untersuchungen zur vergleichende anatomie der kiemen und kiefermuskulatur der fische. II. Jenaische Zeitschrift für Naturwissenschaft 12: 431-550.

Videler JJ. 1995. Body surface adaptations to boundary-layer dynamics. In: Ellington, C.P. Pedley, T.J. (Eds.), Biological Fluid Dynamics. Society for Experimental Biology, pp. 1-20.

Vigliola L, Galzin R, Harmelin-Viven ML, Mazeas F, Salvat B. 1996. Hétérocongerina (Téléostei : Congridae). De la pente externe de Moorea (Il de la société, Polynésie Française): distribution et biologie. Cybium 20: 379-393.

Vaillant L. 1882. Sur un poisson des grandes profondeurs de l'Atlantique, l'*Eurypharynx pelecanoides*. Comptes Rendus Hebdomadaires des séances de l'Académie des sciences 95: 1226-1228.

Vlassenbroeck J, Dierick M, Masschaele B, Cnudde V, Van Hoorebeke L, Jacobs P. 2007. Software tools for quantification of X-ray microtomography at the UGCT. Nuclear Instruments and Methods in Physics Research A 580: 442-445.

Wainwright PC, Bellwood DR. 2002. Ecomorphology of feeding in coral reef fishes. In: Sale, P.F. (Ed.) Coral Reef Fishes: Dynamics and Diversity in a Complex Ecosystem. San Diego: Academic Press, pp. 33-55.

Wainwright P, Carroll AN, Collar DC, Day SW, Higham TE, Holzman RA. 2007. Suction feeding mechanics, performance, and diversity in fishes. Integrative and Comparative Biolog 47: 96-106.

Wake MH. 1986. The morphology of *Idiocranium*-Russeli (Amphibia, Gymnophiona), with comments on miniaturization through heterochrony. Journal of Morphology. 189(1): 1-16.

Wang CH, Kuo CH, Mok HK, Lee SC. 2003. Molecular phylogeny of elopomorph fishes inferred from mitochondrial 12S ribosomal RNA sequences. Zoologica Scripta, 32: 231-241.

Ward AB, Brainerd EL. 2007. Evolution of axial patterning in elongate fishes. Biological journal of the Linnean Society. 90(1): 97-116.

Webb JF. 2002. Functional evolution of the lateral line system: implications for fish bioacoustics. Bioacoustics 12 (2/3): 145-147.

Westneat MW. 1990. "Feeding mechanics of teleost fishes (Labridae; Perciformes): a test of four-bar linkage models." Journal of Morphology 205: 269-295.

Westneat MW. 1994. Transmission of force and velocity in the feeding mechanisms of labrid fishes (Teleostei, Perciformes). Zoomorphology 114:103-118.

Westneat MW. 2004. Evolution of levers and linkages in the feeding mechanisms of fishes. Integrative and Comparative Biolog 44: 378-89.

Westneat MW. 2007. Twice bitten. Nature 449: 33-34

Wilga CD. 2005. Morphology and evolution of the jaw suspension in lamniform sharks. Jornal of Morphology 265: 102-19.

Winterbottom, R., 1974. A descriptive synonymy of the striated muscles of the Teleostei. Proceeding of the Academy of Natural Sciences of Philadelphia 125: 225-317.

Young RF, Winn HE. 2003. Activity patterns, diet, and shelter site use for two species of moray eels. *Gymnothorax moringa* and *Gymnothorax vicinus*, in Belize. Copeia 2003: 44-55.

Yukihira H, Shibuno T, Hashimoto H, Gushima K. 1994. Feeding habits of moray eels (Pisces: Muraenidae) at Kuchierabujima. Journal of the Faculty of Applied Biological Science - Hiroshima University (Japan) 33: 159-166.

PUBLICATION LIST OF SOHEIL EAGDERI

Eagderi S, Mojazi Amiri B, Mirvaghefi A. 2006. A histological study on testis structure and spermatogenesis of Bulatmai barbel (*Barbus capito)* migratory to Sefidrood and Polrood Rivers. Journal of the Iranian Natural Resources 139-150. (In Farsi - English Abstract)

Eagderi S, De Schepper N, Adriaens D. 2007. Head morphology of a duckbill eel, *Hoplunnis punctata* (Nettostomatidae: Anguilliformes). Journal of Morphology 268(12): 1069-1070.

Akbarzadeh A, Karami M, Nezami SA, Eagderi S, Bakhtiyari M, Khara H. 2007. Analysis of population structure of pikeperch (*Sander lucioperca*), in Iranian waters of Caspian Sea and Anzali wetland using truss system. Journal of the Iranian Natural Resources 60(1): 127-139. (In Farsi - English Abstract)

Kamal S, Bakhtiyari M, Abdoli A, Eagderi S, Karami M. 2009. Life-history variations of killifish (*Aphanius sophiae*) populations in two environmentally different habitats in central Iran. Journal of Applied Ichthyology 25(4): 474-478.

Eagderi S, Adriaens D. 2010. Head morphology of the duckbill eel, *Hoplunnis punctata* (Regan, 1915; Nettastomatidae: Anguilliformes) in relation to jaw elongation. Zoology 113(3): 148-157.

Eagderi S, Adriaens D. 2010. Cephalic morphology of *Pythonichthys macrurus* (Heterenchelyidae: Anguilliformes): specializations for head-first burrowing. Journal of Morphology 271(9): 1053-1065.

Eagderi S, Adriaens D, Mojazi Amiri B, Khomeirani R. Description of the ovarian follicle maturation of the migratory adult female Bulatmai Barbel (*Barbus capito* (Güldenstädt 1772)) (Cyprinidae, Cypriniformes) in captivity. Belgian Journal of Zoology. Under Revision.

Eagderi S, Christiaens J, Boone M, Jacobs P, Adriaens D. To be submitted. Cephalic specialization in a parasitic eel, *Simenchelys parasiticus* (Simenchelyinae: Synaphobranchidae). Copeia.

Eagderi S, Mehta RS, Dominique Adriaens D. In prep. Cephalic specializations in relation to second set of jaws in muraenids.

Eagderi S, Dierick M, Van Hoorebeke L, Adriaens D. In prep. Head morphology of a Pelican eel, *Eurypharynx pelecanoides* (Saccopharyngoidei: Eurypharyngidae).

UNIVERSITEIT GENT

FACULTY OF **SCIENCES**

Department of **Biology**

Evolutionary Morphology of Vertebrates

Structural diversity in the cranial musculoskeletal system in Anguilliformes: an evolutionary-morphological study

Part 2 - Figures

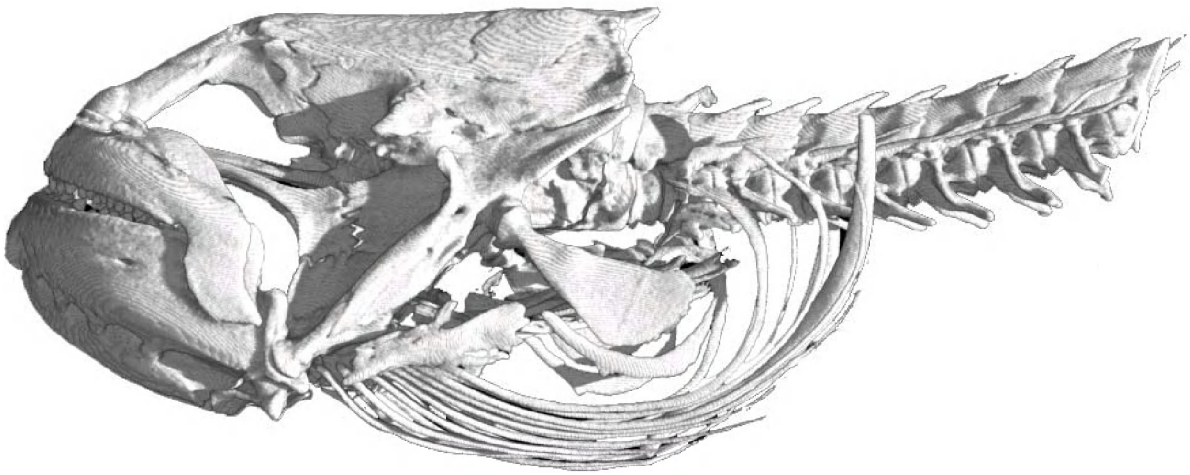

Soheil Eagderi

Thesis submitted to obtain the degree of Doctor in Sciences (Biology)

Academic year 2009-2010
Rector: Prof. Dr. Paul van Cauwenberge
Dean: Prof. Dr. Herwig Dejonghe
Promoter: Prof. Dr. Dominique Adriaens

FACULTY OF SCIENCES

DEPARTMENT OF BIOLOGY

EVOLUTIONARY MORPHOLOGY OF VERTEBRATES

Structural diversity in the cranial musculoskeletal system in Anguilliformes: an evolutionary-morphological study

Part 2 - Figures

Soheil Eagderi

Thesis submitted to obtain the degree of Doctor in Sciences (Biology)

Academic year 2009-2010
Rector: Prof. Dr. Paul van Cauwenberge
Dean: Prof. Dr. Herwig Dejonghe
Promoter: Prof. Dr. Dominique Adriaens

TABLE OF CONTENTS

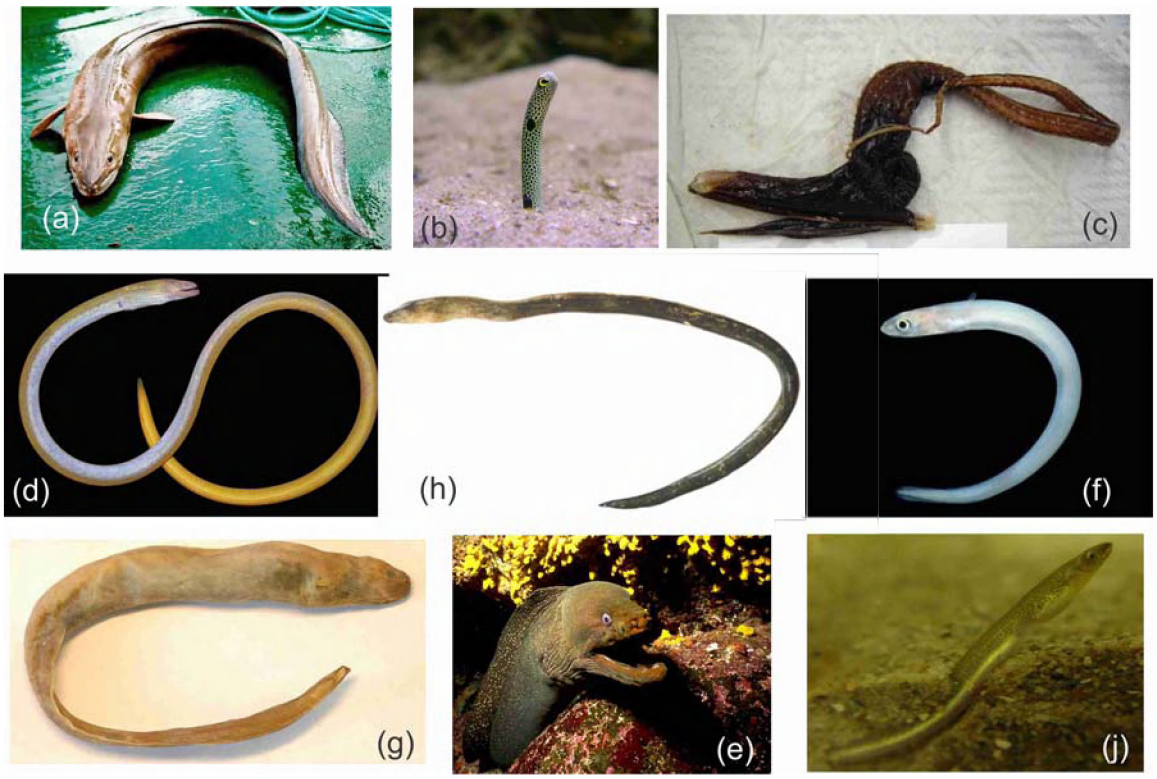

Figure 1.1. Diverse eels. (a) *Conger conger* (Congrinae: Congridae), (b) *Heteroconger hassi* (Heterocongrinae: Congridae), (c) *Eurypharynx pelecanoides* (Eurypharyngidae), (d) *Moringua edwardsi* (Moringuidae), (e) *Strophidon sathete* (Muraeninae: Muraenidae), (f) *Ariosoma gilberti* (Bathymyrinae: Congridae), (g) *Simenchelys parasiticus* (Simenchelyinae: Synaphobranchidae), (h) *Gymnothorax prasinus* (Muraeninae: Muraenidae), (j) *Pisodonophis boro* (Ophichthidae).

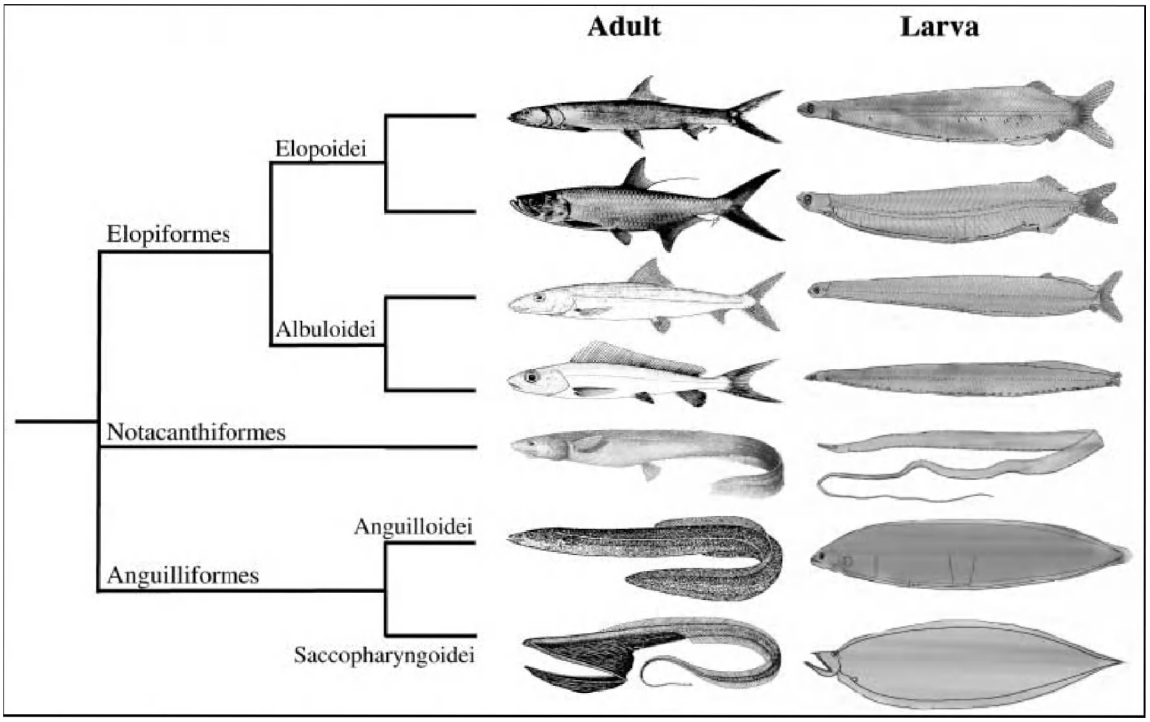

Figure 1.2. Hypothesized interrelationships of the superorder Elopomorpha based on Greenwood et al. (1966), with the leptocephalus larvae of the representative taxa (after Wang et al. 2003).

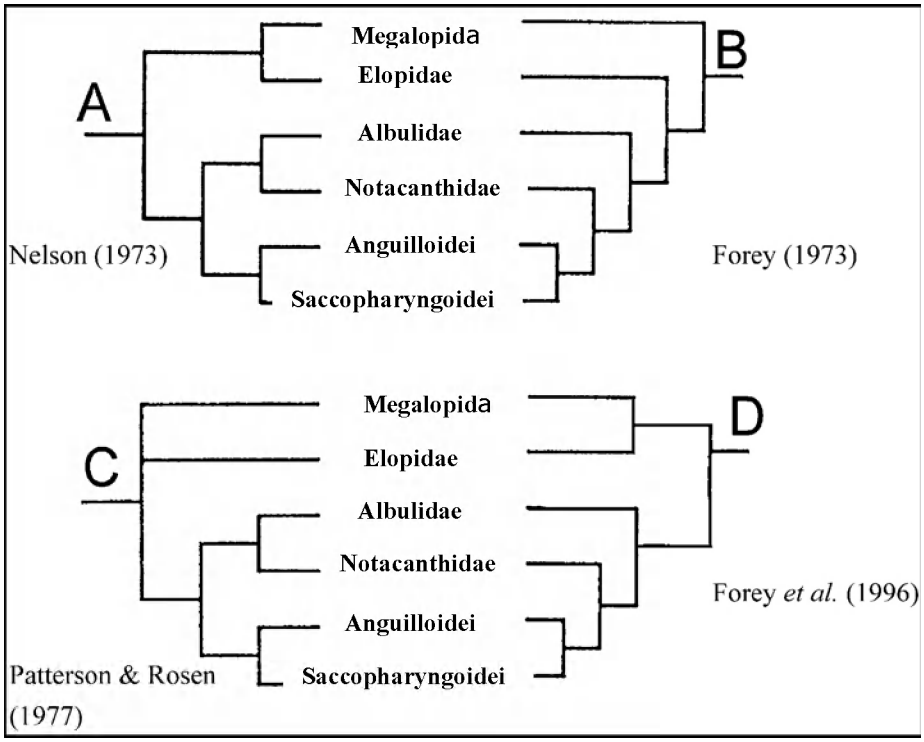

Figure 1.3. A–D. Four hypothetical interrelationships among elopomorph fishes. (A) Nelson (1973), (B) Forey (1973), (C) Patterson and Rosen (1977) and (D) Forey *et al*. (1996) (after Forey et al. 1996).

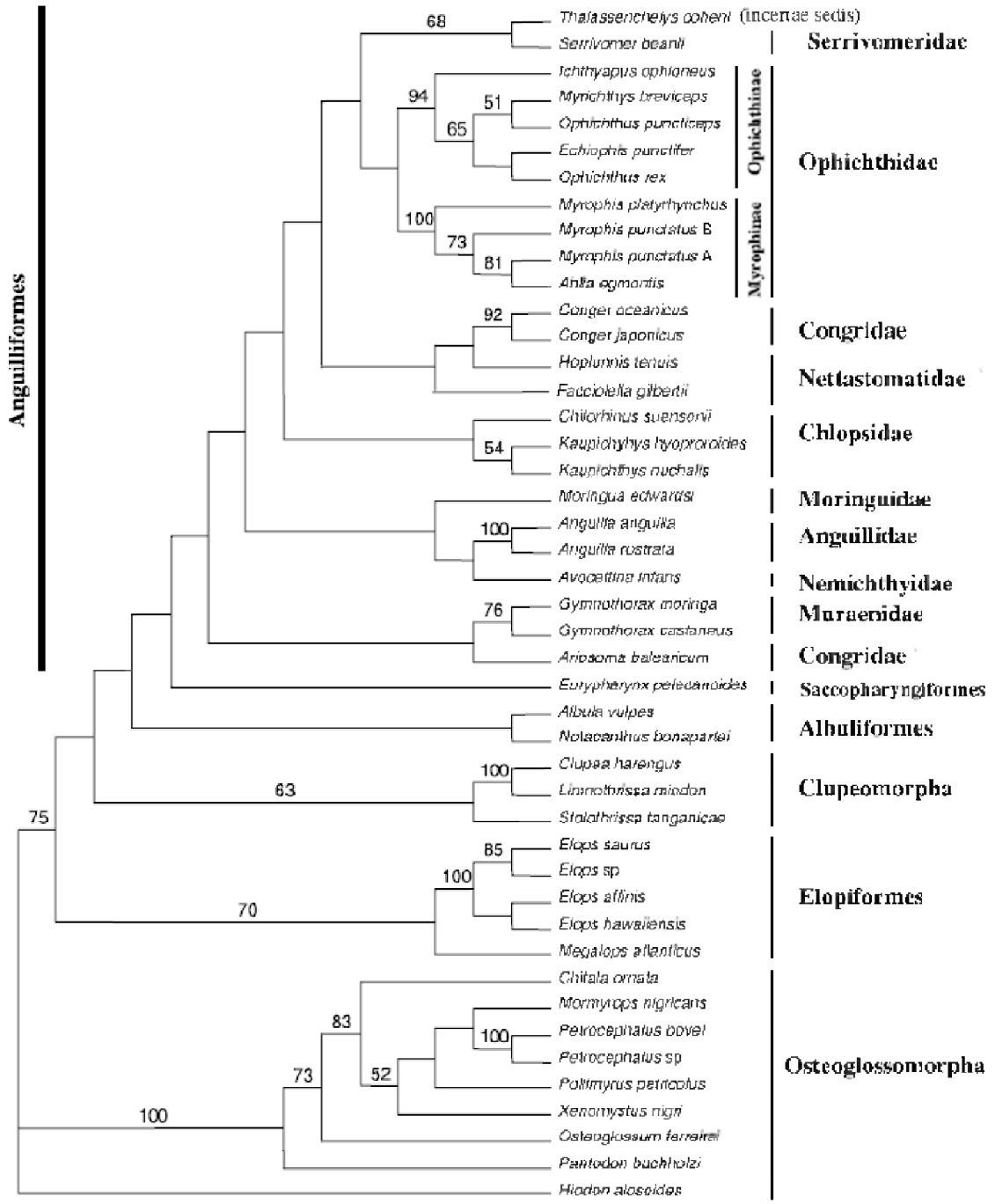

Figure 1.4. Single most parsimonious (MP) tree for the combined 12S and 16S rRNA data set from taxa comprising the superorders Elopomorpha (order Elopiformes, Albuliformes, Saccopharyngiformes, and Anguilliformes), Clupeomorpha, and Osteoglossomorpha (after Obermiller and Pfeiler, 2003)

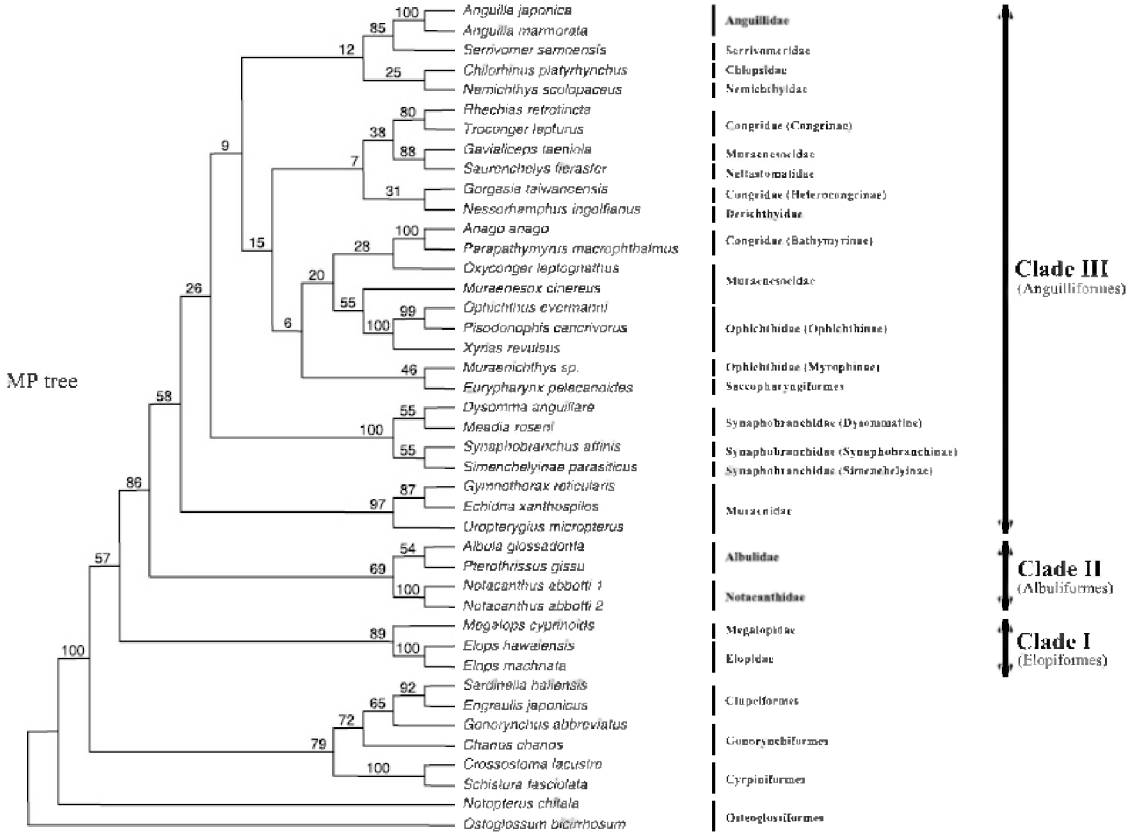

Figure 1.5. Maximum parsimony cladogram inferred from 12S rRNA sequence data. Support for clades with 500 bootstrap values (after Wang et al. 2003).

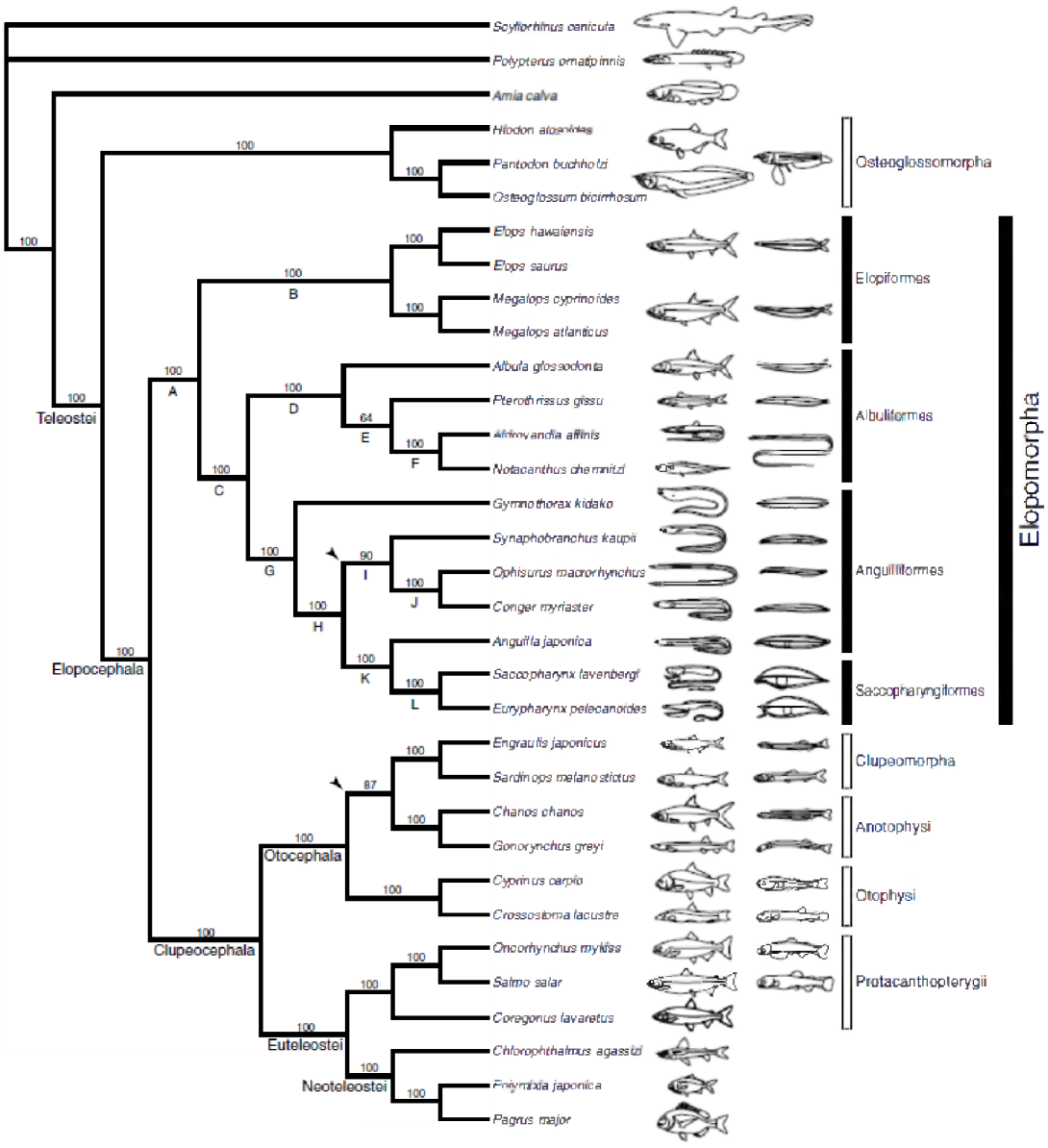

Figure 1.6. The 50% majority rule consensus tree of the 50,000 pooled trees from the two independent Bayesian analyses of mitogenomic data (14,040 bp) from 30 teleosts and three outgroup species using MrBayes 3.0b4 (Huelsenbeck and Ronquist, 2001; Ronquist and Huelsenbeck, 2003) with GTR+I +C model (Yang, 1994) of sequence evolution (after Inoue et al. 2004).

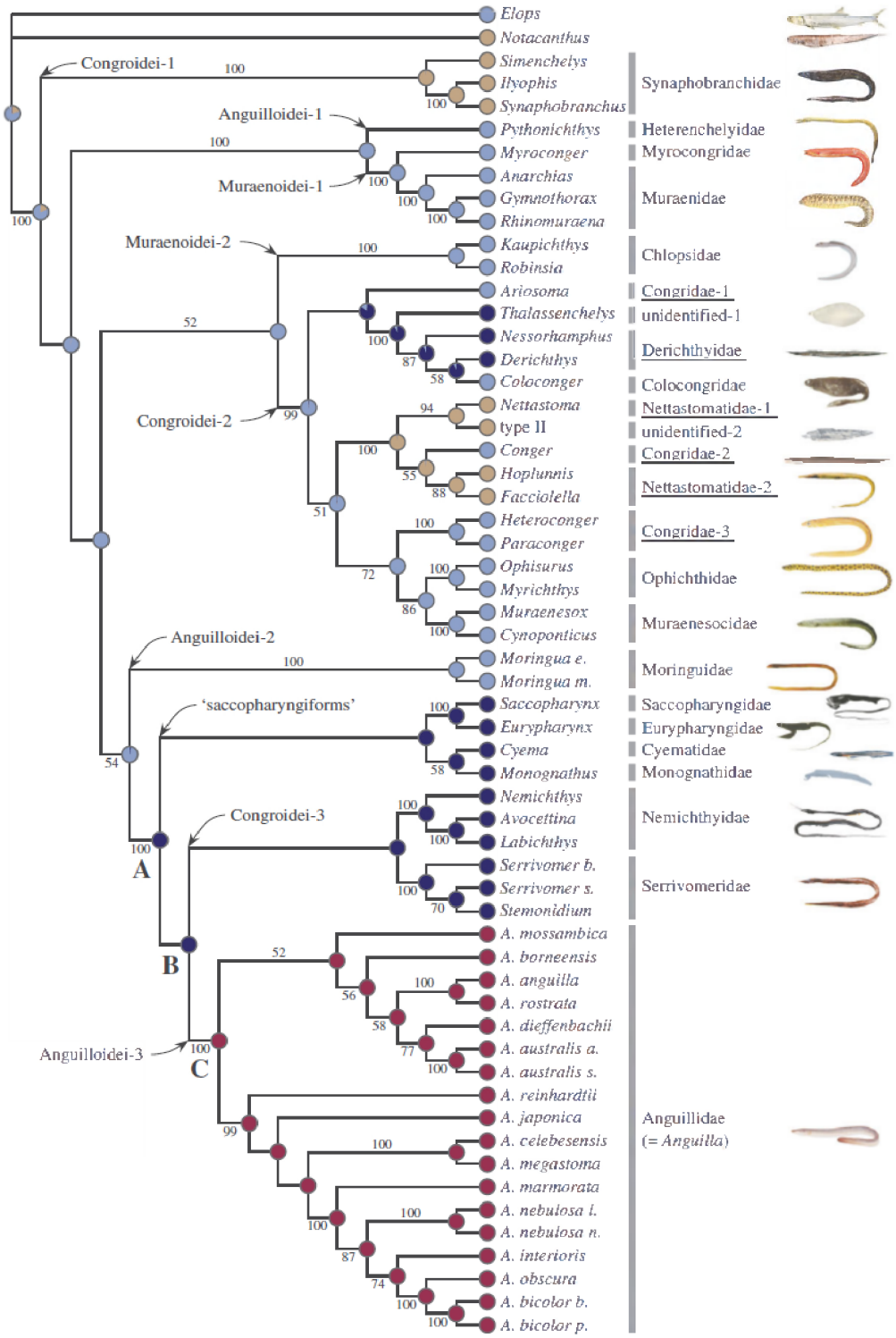

Figure 1.7. The best-scoring maximum likelihood (ML) tree of 58 elopomorph species based on unambiguously aligned whole mitogenome sequences (after Inoue et al. 2010).

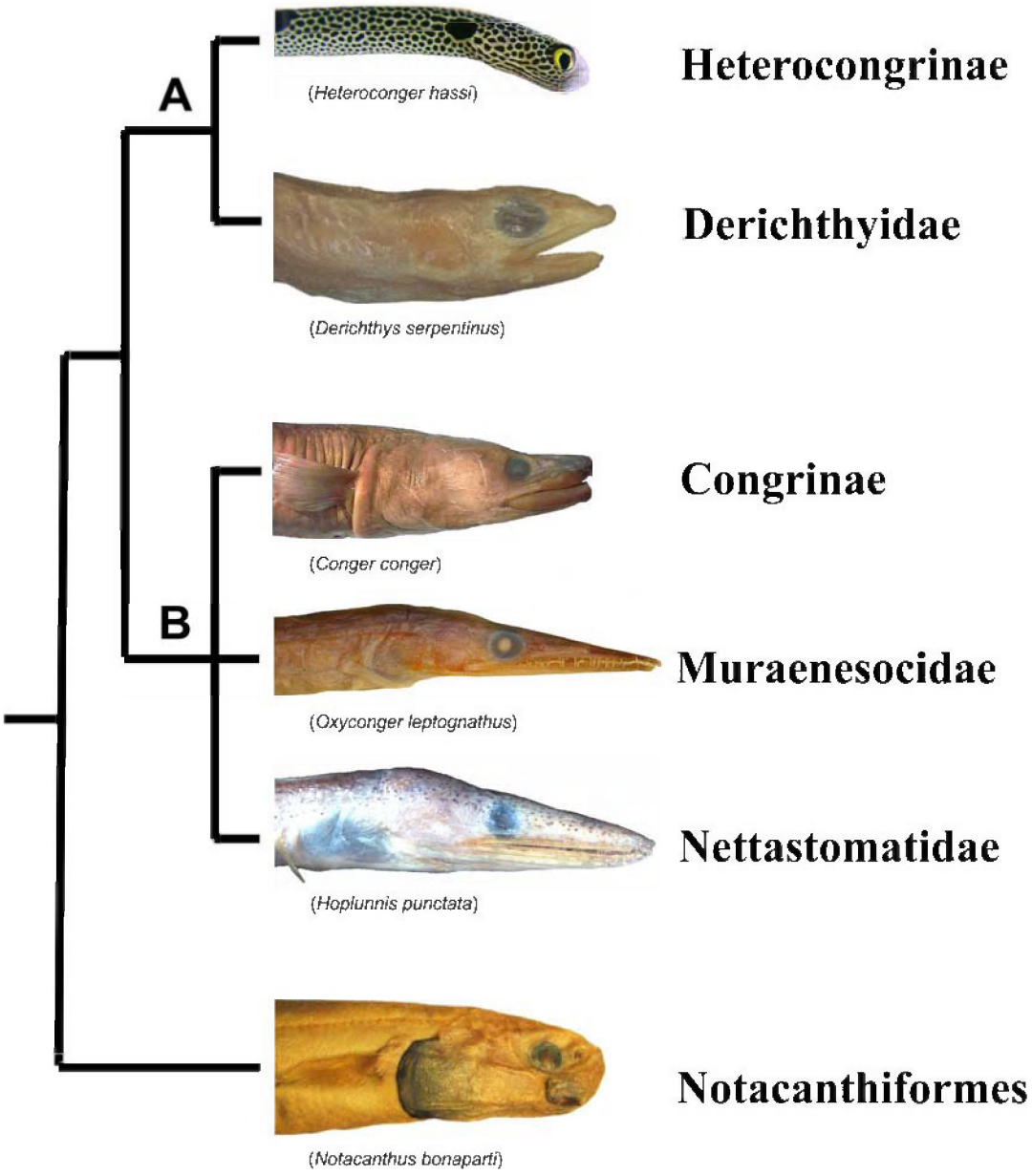

Figure 3.1: Phylogeny of the taxa considered in this study, based on mitochondrial 12S ribosomal RNA and mtDNA sequences (modified after Wang et al., 2002).

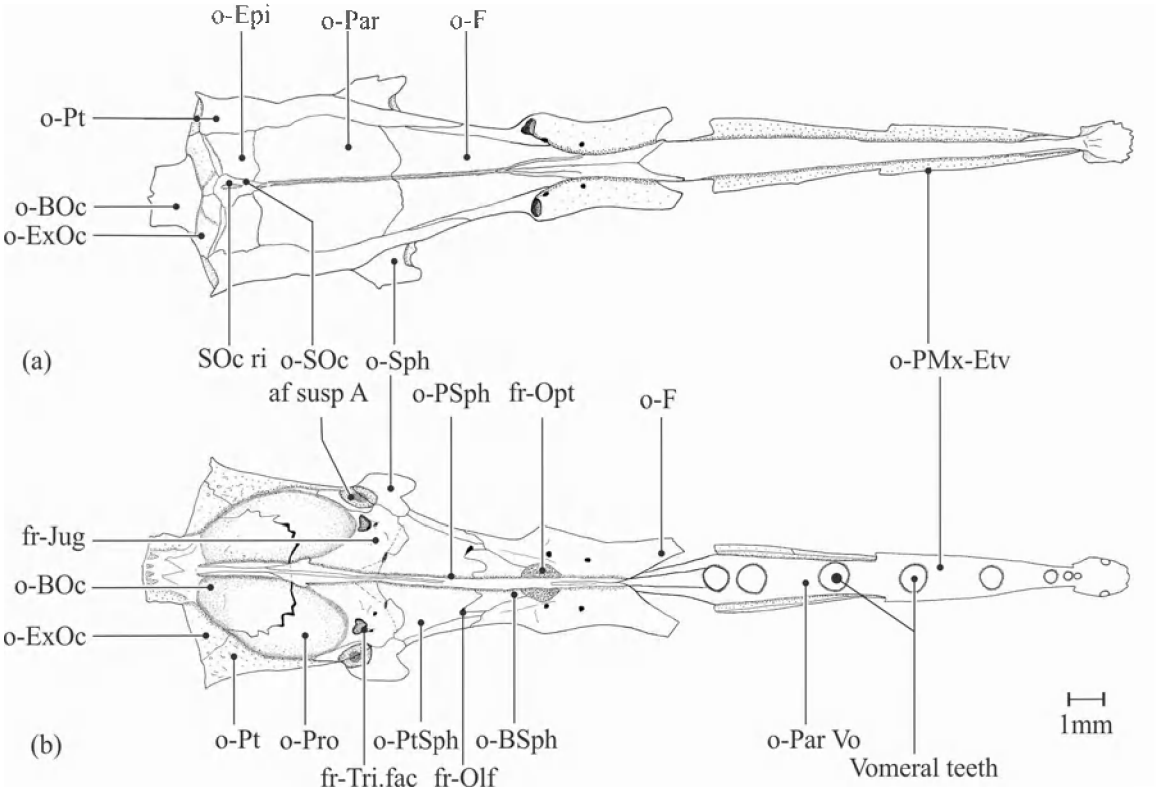

Figure 3.2: Neurocranial bones of *Hoplunnis punctata*. (a) Dorsal view and (b) ventral view. af susp A, anterior suspensorial articulation facet; fr-Jug, foramen jugularis; fr-Opt, foramen opticum; fr-Olf, foramen olfactorius; fr-Tri.fac, foramen trigemino-facialis; o-BOc, basioccipital; o-BSph, basisphenoid; o-Epi, epiotic; o-ExOc, exoccipital; o-F, frontal; o-Par, parietal; o-Par Vo, pars vomeralis of premaxillo-ethmovomeral complex; o-PMx-Etv, premaxillo-ethmovomeral complex; o-Pro, prootic; o-PSph, parasphenoid; o-Pt, pterotic; o-PtSph, pterosphenoid; o-Soc, supraoccipital; o-Sph, sphenotic; SOc ri, supraoccipital ridge.

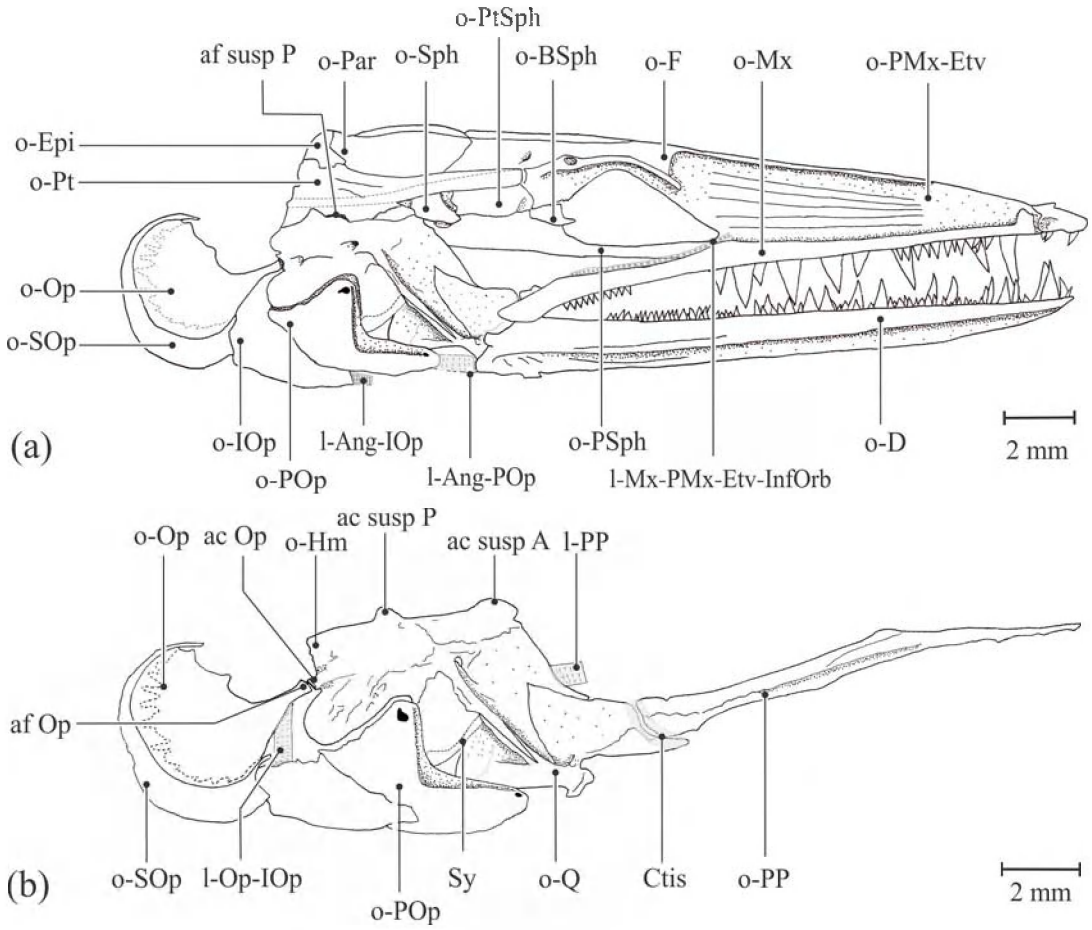

Figure 3.3: Cranial skeleton in *Hoplunnis punctata* (Lateral view). (a) Complete skull (right side) and (b) suspensorium (right side). ac Op, opercular articular condyle; af Op, opercular articular facet ; ac susp A, anterior suspensorial condyle; ac susp P, posterior suspensorial condyle; af susp P, posterior suspensorial articulation facet ; Ctis, connective tissue; l-Ang-Iop, angulo-interopercular ligament; l-Ang-Pop, angulo-preopercular ligament; l-Mx-PMx-Etv-InfOrb, maxillo-premaxillo-ethmovomero-infraorbital ligament; l-Op-IOp, operculo-interopercular ligament; l-PP, palatopterygoidal ligament; o-BSph, basisphenoid; o-D, dentary complex; o-Epi, epiotic; o-F, frontal; o-Hm, hyomandibula; o-Iop, interopercle; o-Mx, maxillary; o-Op, opercle; o-Par, parietal; o-PMx-Etv, premaxillo-ethmovomeral complex; o-POp, preopercle; o-PP, palatopterygoid; o-Pro, prootic; o-PSph, parasphenoid; o-Pt, pterotic; o-PtSph, pterosphenoid; o-Q, quadrate; o-SOp, subopercle; o-Sph, sphenotic; Sy, cartilaginous symplectic.

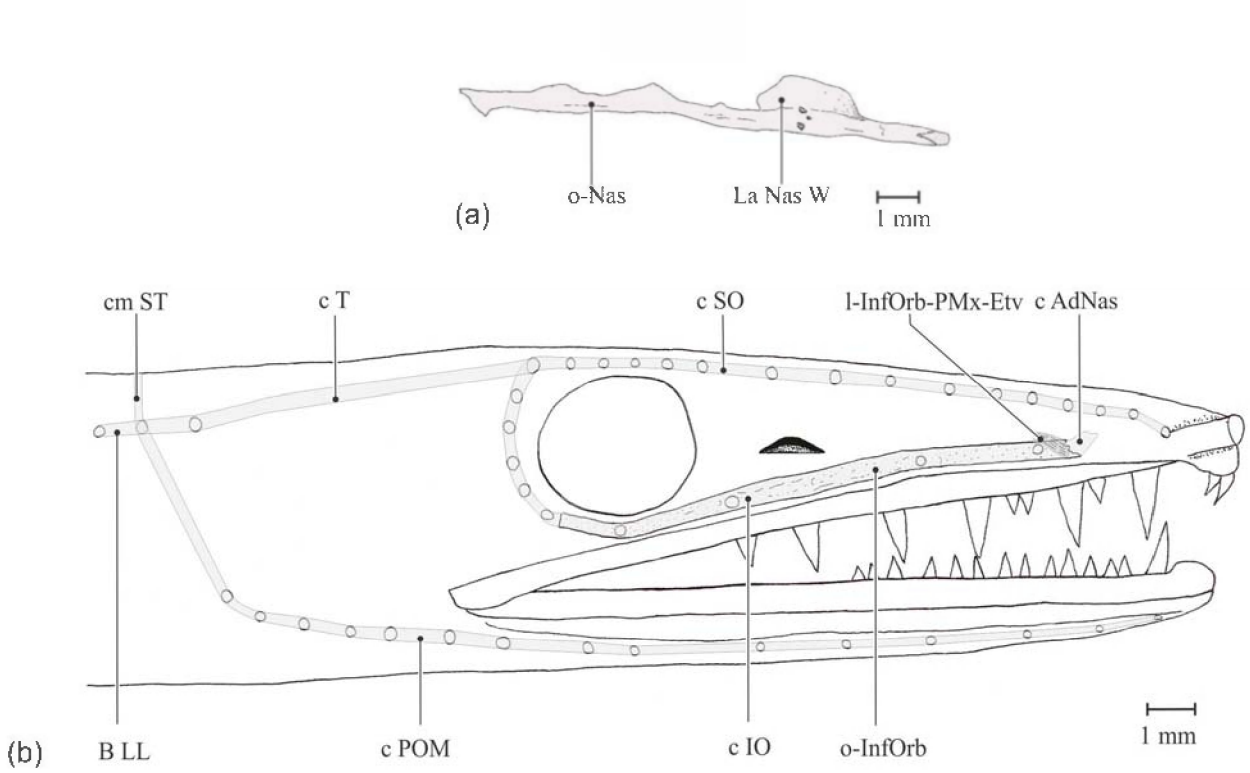

Figure 3.4: The cranial lateral line system of *Hoplunnis punctata*. (a) Dorsal view of the left nasal bone, (b) lateral view of the composing canals (right side). Circles show external sensory pores. B LL, body lateral line system; c AdNas, adnasal canal; c IO, infraorbital canal; c POM, preopercular mandibular canal; c SO, supraorbital canal; c T, temporal canal; cm ST, supratemporal commissure; La Nas W, lateral nasal wings; l-InfOrb-PMx-Etv, infraorbito-premaxillo-ethmovomeral ligament; o-Nas, nasal; o-InfoOrb, infraorbital.

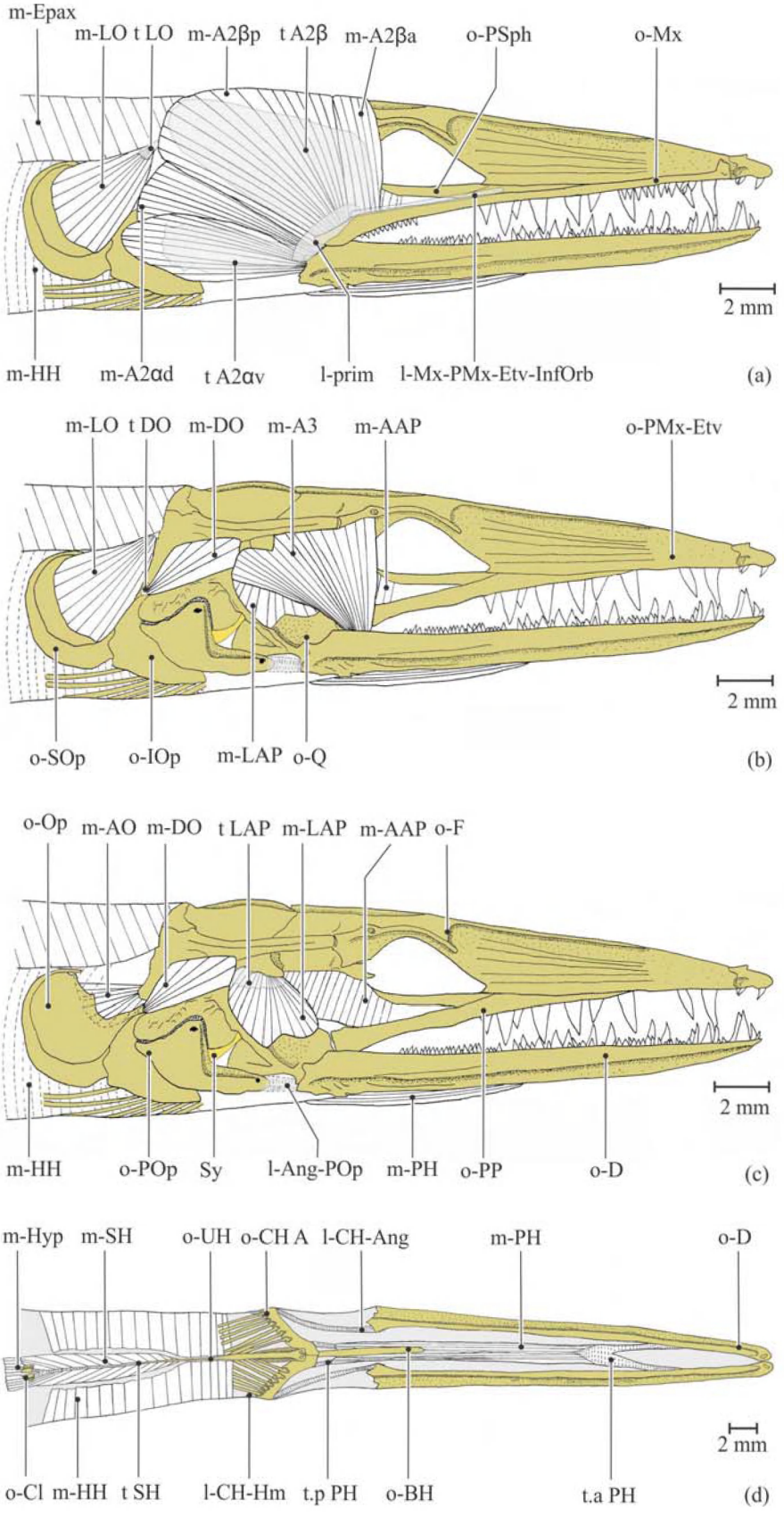
m-Epax
m-LO
t LO
m-A2βp
t A2β
m-A2βa
o-PSph
o-Mx
2 mm
m-HH
m-A2αd
t A2αv
l-prim
l-Mx-PMx-Etv-InfOrb
(a)
m-LO
t DO
m-DO
m-A3
m-AAP
o-PMx-Etv
2 mm
o-SOp
o-IOp
m-LAP
o-Q
(b)
o-Op
m-AO
m-DO
t LAP
m-LAP
m-AAP
o-F
2 mm
m-HH
o-POp
Sy
l-Ang-POp
m-PH
o-PP
o-D
(c)
m-Hyp
m-SH
o-UH
o-CH A
l-CH-Ang
m-PH
o-D
2 mm
o-Cl
m-HH
t SH
l-CH-Hm
t.p PH
o-BH
t.a PH
(d)

Figure 3.5: Lateral view of the cranial muscles of *Hoplunnis punctata*. (a) Skin is removed; (b) maxillary, Primordial ligament and subsections of A2, with exception of A2βd removed; (c) A2βd and A3 are removed; (d) ventral view of the cranial muscles (Skin is removed). l-Ang-Pop, angulo-preopercular ligament; l-CH-Ang, ceratohyalo-angular ligament; l-CH-Hm, ceratohyalo-hyomandibular ligament; l-Mx-PMx-Etv-InfOrb, maxillo-premaxillo-ethmovomero-infraorbital ligament; l-prim, primordial ligament; m-A1, A1 section of the adductor mandibulae muscle complex; m-A2, A2 section of the adductor mandibulae muscle complex; m-A2α, ventral subsection of A2; m-A2αd, dorsal subsection of A2α; m-A2αv, ventral subsection of A2α; m-A2β, dorsal subsection of A2; m-A2βa, anterior subsection of A2β; m-A2βp, posterior subsection of A2β; m-A3, A3 section of the adductor mandibulae muscle complex; m-AAP, adductor arcus palatini muscle; m-AO, adductor operculi muscle; m-DO, dilatator operculi muscle; m-Epax, epaxial muscles; m-HH, hyohyoideus muscle; m-Hyp, hypaxial muscles; m-LAP, levator arcus palatini muscle; m-LO, levator operculi muscle; m-PH, protractor hyoidei muscle; m-SH, sternohyoideus muscle; o-BH, basihyal; o-CH A, anterior ceratohyal; o-Cl, cleithrum; o-D, dentary complex; o-F, frontal; o-Iop, interopercle; o-Mx, maxillary; o-PMx-Etv, premaxillo-ethmovomeral complex; o-Op, opercle; o-POp, preopercle; o-PP, palatopterygoid; o-PSph, parasphenoid; o-Q, quadrate; o-SOp, subopercle; o-UH, urohyal; Sy, cartilaginous symplectic; t A2αv, tendon of A2αv; t A2β, tendon of A2β; t LAP, tendon of levator arcus palatini; t LO, tendon of levator operculi; t.a PH, anterior tendon of protractor hyoidei; t.p PH, posterior tendon of protractor hyoidei; t SH, tendon of sternohyoideus.

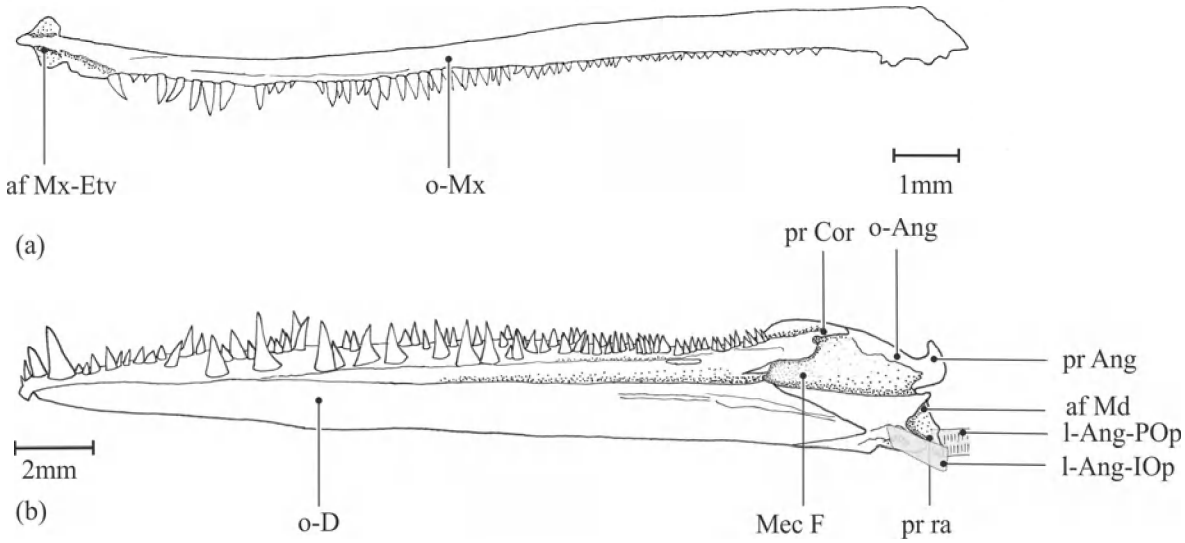

Figure 3.6: Jaw of *Hoplunnis punctata* (right side, medial view). (a) Lower jaw and (b) maxillary. af Md, mandibular articulation facet; af Mx-Etv, maxillo-ethmovomerine articulation facet; l-Ang-Iop, angulo-interopercular ligament; l-Ang-Pop, angulo-preopercular ligament; o-Ang, angular complex ; o-D, dentary complex; o-Mx, maxillary; Mec F, meckelian fossa; pr Ang, angular process; pr Cor, coronoid process; pr ra, process of retroarticular.

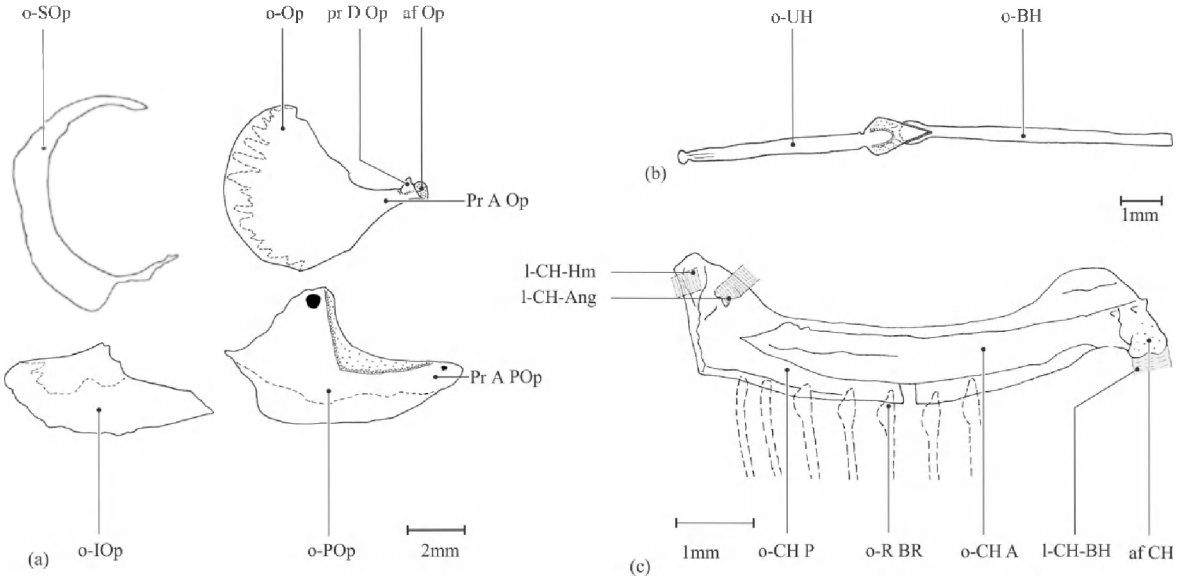

Figure 3.7: Hyoid and opercular series in *Hoplunnis punctata.* (a) Dorsal view of the basihyal and urohyal; (b) the anterior and posterior ceratohyal in a medial view (right side); (c) the opercular series in the lateral view (right side). af CH, ceratohyal articular facet; af Op, opercular articular facet; l-CH-Ang, ceratohyalo-angular ligament; l-CH-BH, ceratohyalo-basihyal ligament; l-CH-Hm, ceratohyalo-hyomandibular ligament; o-BH, basihyal; o-CH A, anterior ceratohyal; o-CH p, posterior ceratohyal; o-Iop, interopercle; o-Op, opercle; o-POp, preopercle; o-SOp, subopercle; o-R Br, branchiostegal rays; o-UH, urohyal; pr A Op, anterior process of opercle; pr A POp, anterior process of preopercle; pr D Op, dorsal process of anterior process of opercle.

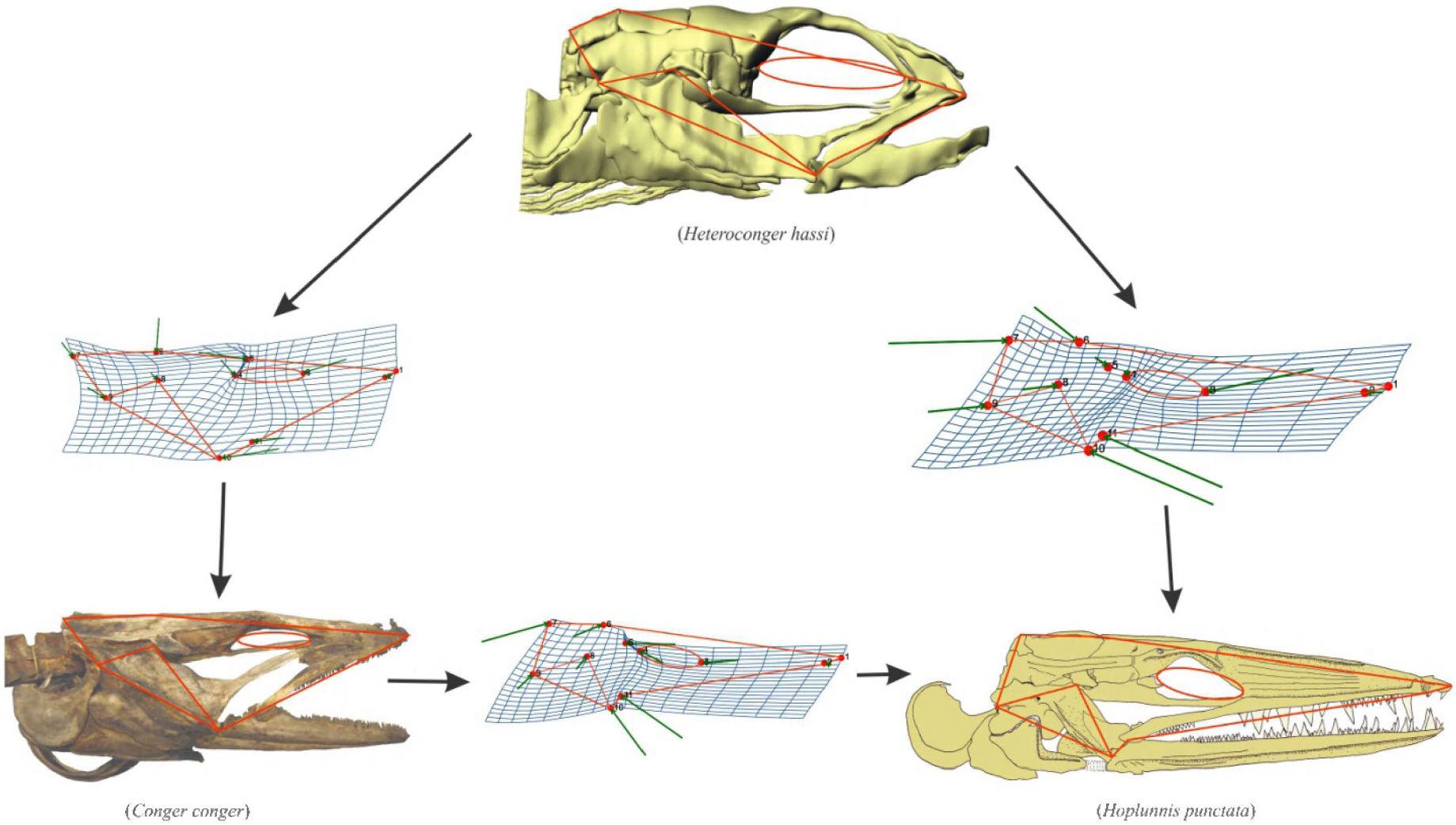
(Heteroconger hassi)
(Conger conger)
(Hoplunnis punctata)

Figure 3.8: Cranial shape differences between *Hoplunnis punctata, Conger conger* and *Heteroconger hassi*: deformation grids show total shape difference going, specially jaw elongation, from species with smaller jaw length toward species with longer one (in a direction as indicated by the big arrows). The lengths of green arrows in the grids represent the shift in homologous landmark (red points) positions among the three studied species. The homologous landmarks were selected to depict an overall shape of the neurocranoim.

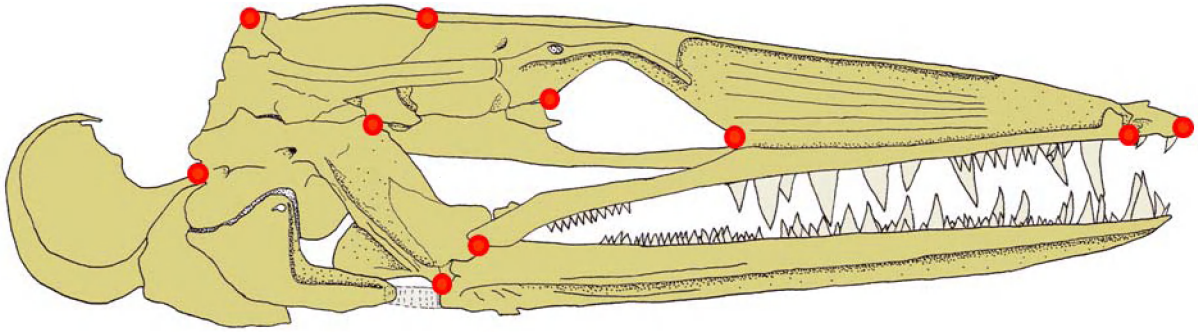

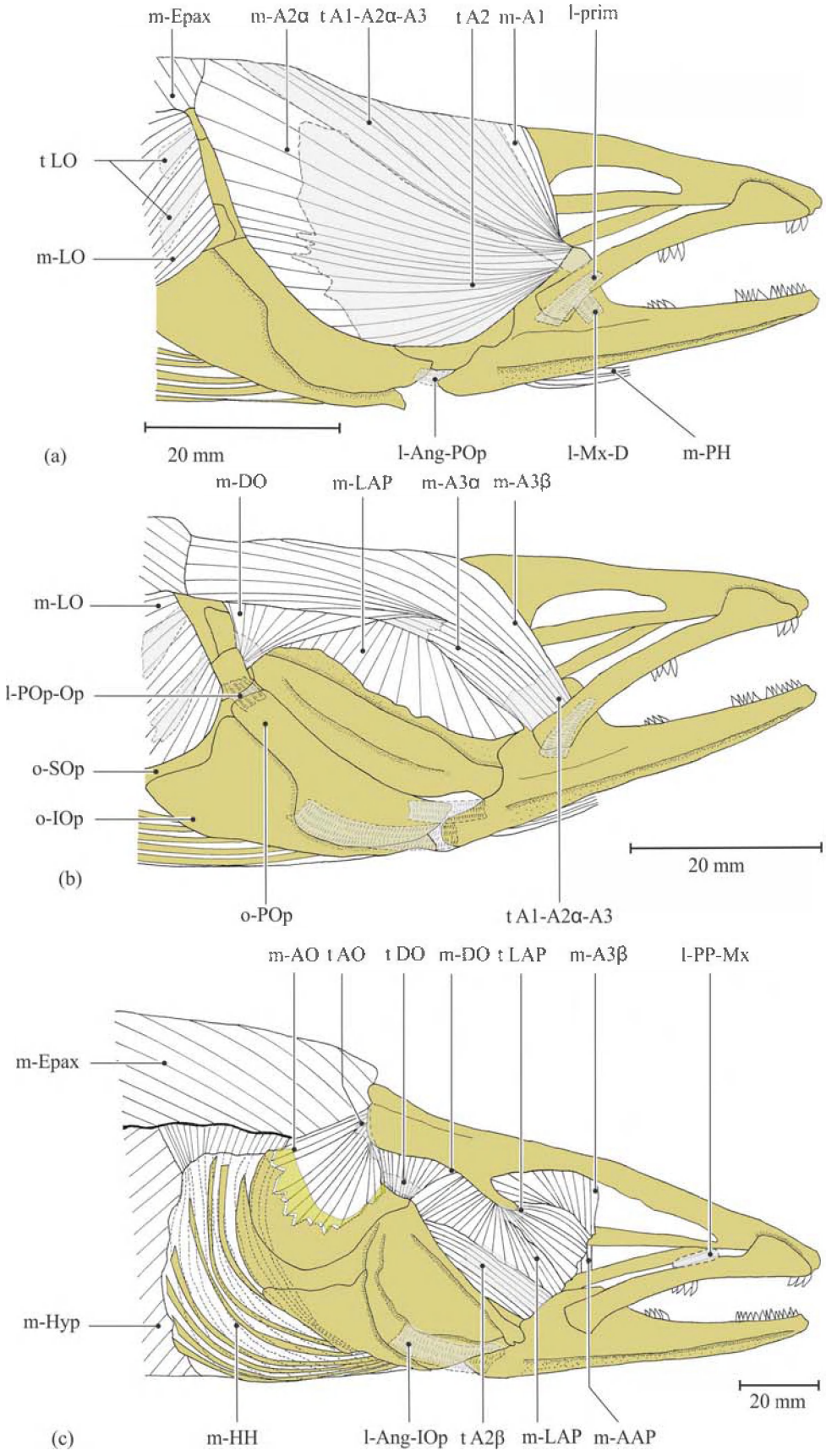
m-Epax
m-A2α
t A1-A2α-A3
t A2
m-A1
l-prim
t LO
m-LO
(a)
20 mm
l-Ang-POp
l-Mx-D
m-PH
m-DO
m-LAP
m-A3α
m-A3β
m-LO
l-POp-Op
o-SOp
o-IOp
(b)
20 mm
o-POp
t A1-A2α-A3
m-AO
t AO
t DO
m-DO
t LAP
m-A3β
l-PP-Mx
m-Epax
m-Hyp
(c)
20 mm
m-HH
l-Ang-IOp
t A2β
m-LAP
m-AAP

Figure 3.9: Lateral view of the cranial muscles of *Conger conger*. (a) Skin is removed; (b) primordial ligament and subsections of A2 exception A2βd are removed; (c) lateral view of the cranial muscles after removing skin, A1, A2 and A3 muscles. (modified after De Schepper, 2007). l-Ang-Pop, angulo-preopercular ligament; l-Ang-Iop, angulo-interopercular ligament; l-Mx-D, maxillo-dentary ligament; l-POp-Op, preoperculo-opercular ligament; l-POp-Op, preoperculo-opercular ligament; l-PP-Mx, palatopterygoideo-maxilla ligament; l-prim, primordial ligament; m-A1, A1 section of the adductor mandibulae muscle complex; m-A2α, ventral subsection of A2; m-A3, A3 section of the adductor mandibulae muscle complex; m-A3α, ventral subsection of A3; m-A3β, dorsal subsection of A3; m-AAP, adductor arcus palatini muscle; m-AO, adductor operculi muscle; m-DO, dilatator operculi muscle; m-Epax, epaxial muscles; m-HH, hyohyoideus muscle; m-Hyp, hypaxial muscles; m-LAP, levator arcus palatini muscle; m-PH, protractor hyoidei muscle; m-LO, levator operculi muscle; o-Iop, interopercle; o-POp, preopercle; o-SOp, subopercle; t A1-A2α-A3, tendon of t A1-A2α-A3; t A2, tendon of A2; t A2β, tendon of A2β; t AO, tendon of adductor operculi; t DO, tendon of dilatator operculi; t LAP, tendon of levator arcus palatini; t LO, tendon of levator operculi.

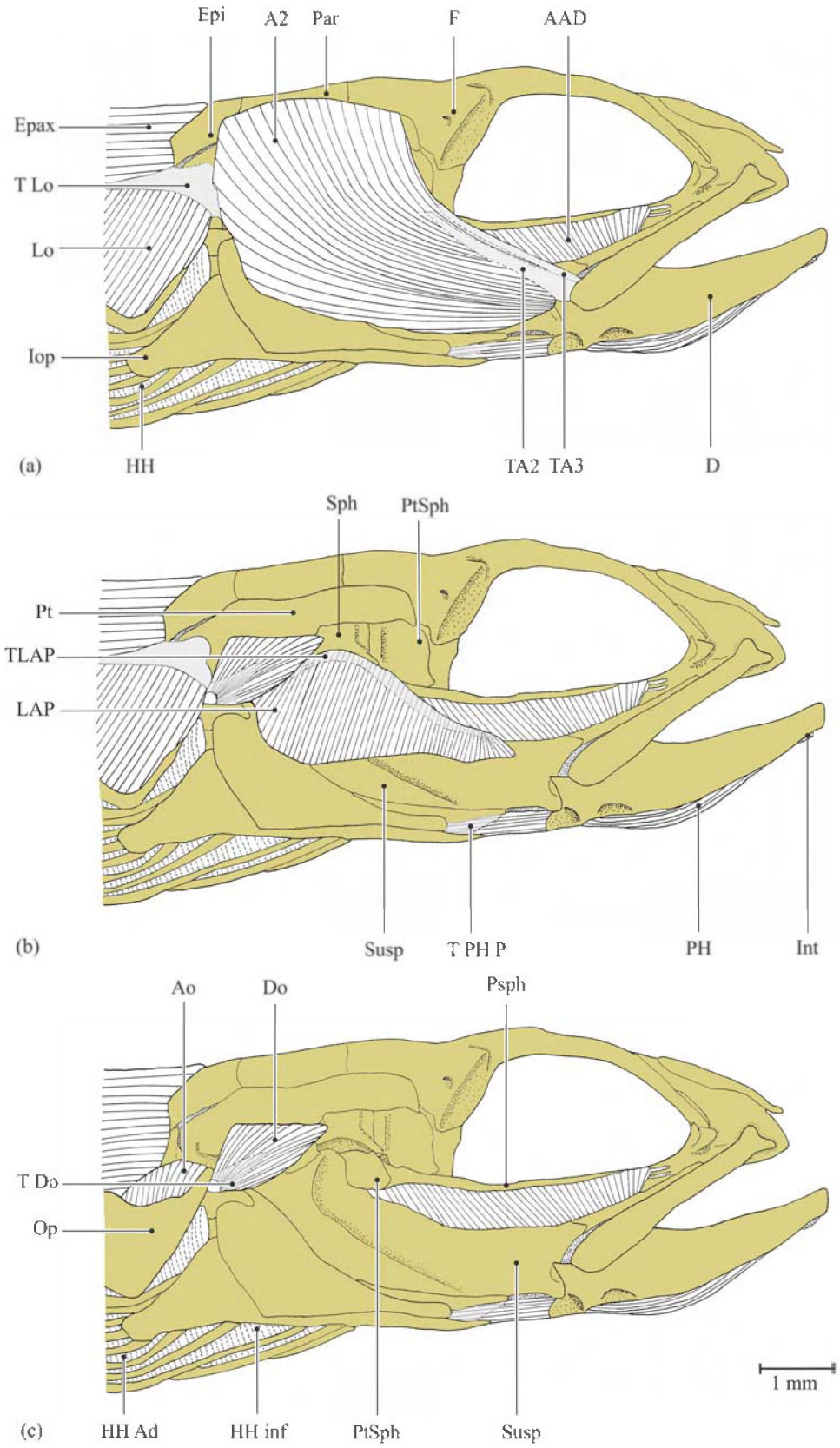
Epi
A2
Par
F
AAD
Epax
T Lo
Lo
Iop
HH
TA2
TA3
D
(a)
Sph
PtSph
Pt
TLAP
LAP
Susp
T PH P
PH
Int
(b)
Ao
Do
Psph
T Do
Op
HH Ad
HH inf
PtSph
Susp
1 mm
(c)

Figure 3.10 (Additional picture): Lateral view of the cranial muscles of *Heteroconger hassi*. (a) Skin is removed, (b) A2 section is removed, and (c) Levator arcus palatini is removed (modified after De Schepper, 2007).

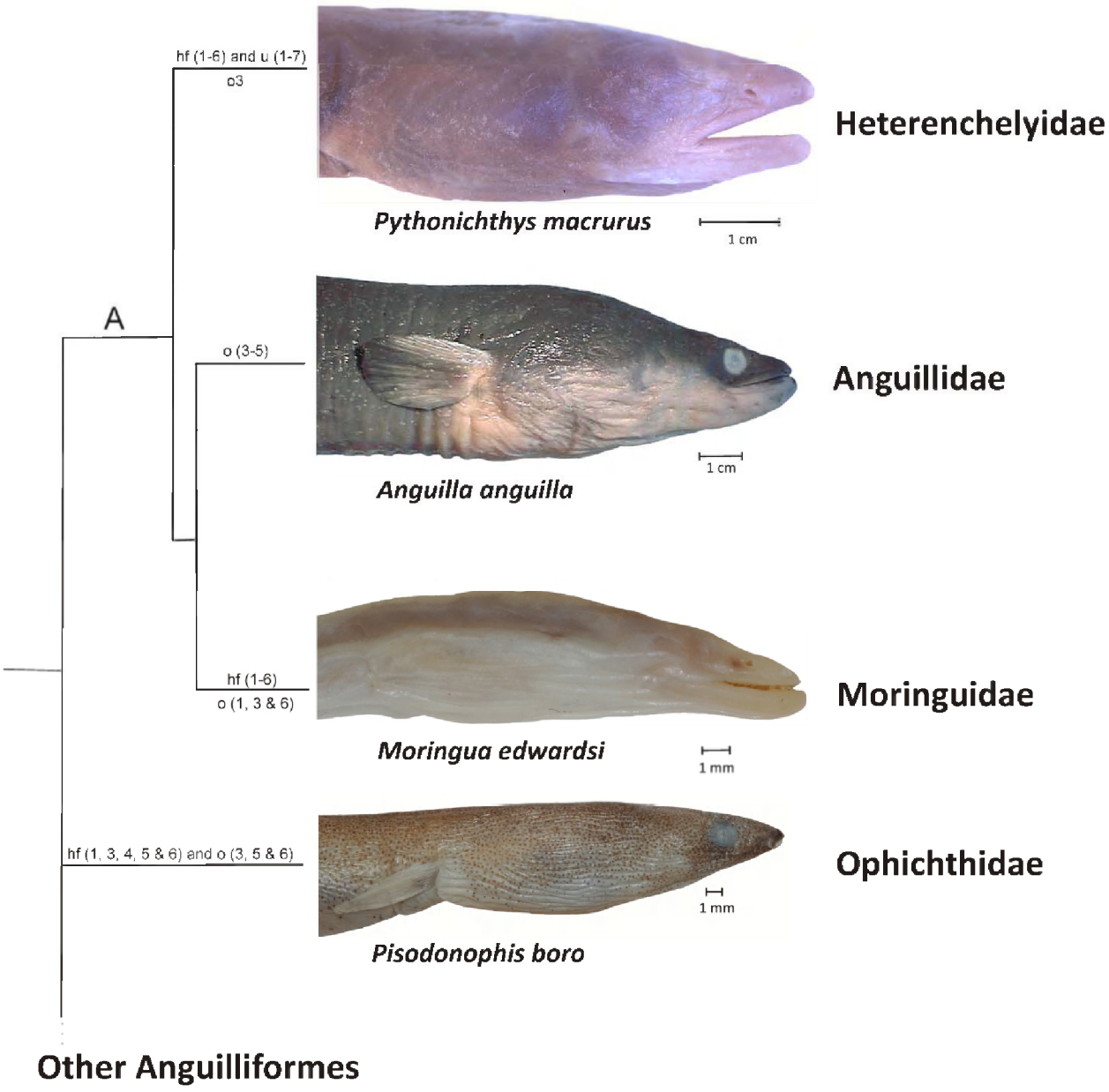
hf (1-6) and u (1-7)
o3
Pythonichthys macrurus
1 cm
Heterenchelyidae
A
o (3-5)
Anguilla anguilla
1 cm
Anguillidae
hf (1-6)
o (1, 3 & 6)
Moringua edwardsi
1 mm
Moringuidae
hf (1, 3, 4, 5 & 6) and o (3, 5 & 6)
Pisodonophis boro
1 mm
Ophichthidae
Other Anguilliformes

Figure 4.1: Cladogram of the taxa examined in this study (modified after Böhlke (1989a). Anguillidae and Moringuidae are monophyletic following Obermiller and Pfeiler (2003). **Features related to head-first burrowing:** Eye reduction (hf1), Widened cephalic lateral line system that extends into the dermal cavities (hf2), Ventral positioning of gill opening (hf3), Caudoventral orientation of the anterior section of the adductor mandibulae muscle complex (hf4), Skull with short and sharp snout (hf5), Large insertion sites of body muscles on the neurocranium (hf6); **Unique characters of *Pythonichthys macrurus*:** Frontal arches (u1), Preopercle with arch-like structures (u2), Tubular and arch-like circumorbital bones (u3), Arch-like suprapreopercular bone (u4), Two ring-like extrascapular bones (u5) and Caudal positioning of the levator arcus palatini muscle (u6), Merging left and right bundles of the sternohyoideus and protractor hyoidei muscles (u7); **Others:** Absence of basisphenoid (o1), Separate vomeronasal bone (o2), Premaxillo-ethmovomerine complex (o3), Connection of the palatopterygoid at its two ends (o4), Well-developed pectoral fins (o5), Absence of A1 section of the adductor mandibulae muscle complex (o6).

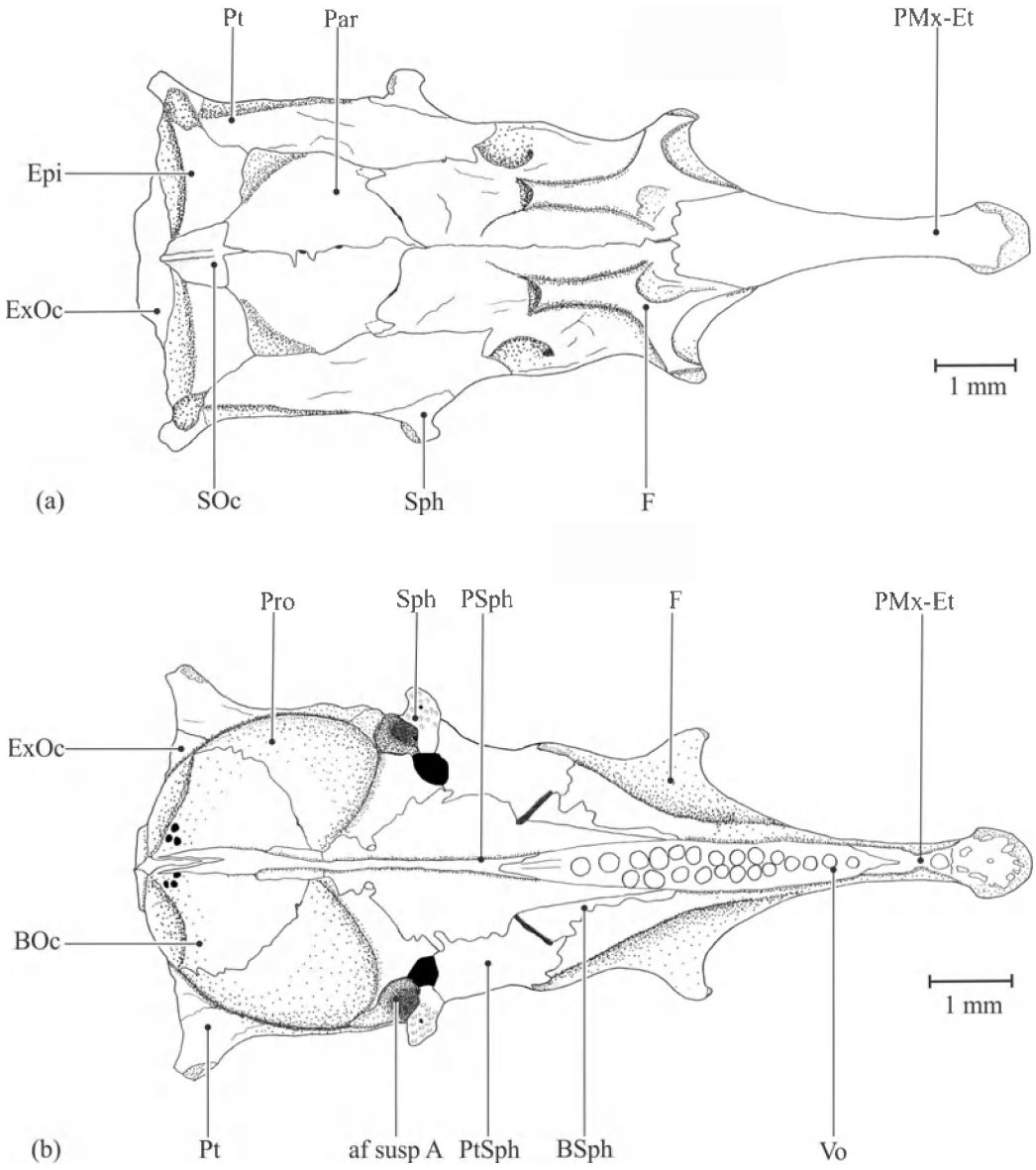

Figure 4.2. Neurocranial bones of *Pythonichthys macrurus*. (a) Dorsal view and (b) ventral view. af susp A, anterior suspensorial articulation facet; af susp p, posterior suspensorial articulation facet; fr-Tri.fac, foramen trigemino-facialis; Lat exp-F, lateral expansion of frontal bone; o-BOc, basioccipital bone; o-BSph, basisphenoid; o-Epi, epioccipital bone; o-ExOc, exoccipital bone; o-F, frontal bone; o-Par, parietal bone; o-PMx-Et, premaxillo-ethmoid complex; o-Pro, prootic bone; o-PSph, parasphenoid; o-Pt, pterotic bone; o-PtSph, pterosphenoid; o-SOc, supraoccipital bone; o-Sph, sphenotic bone; o-Vo, vomeral bone.

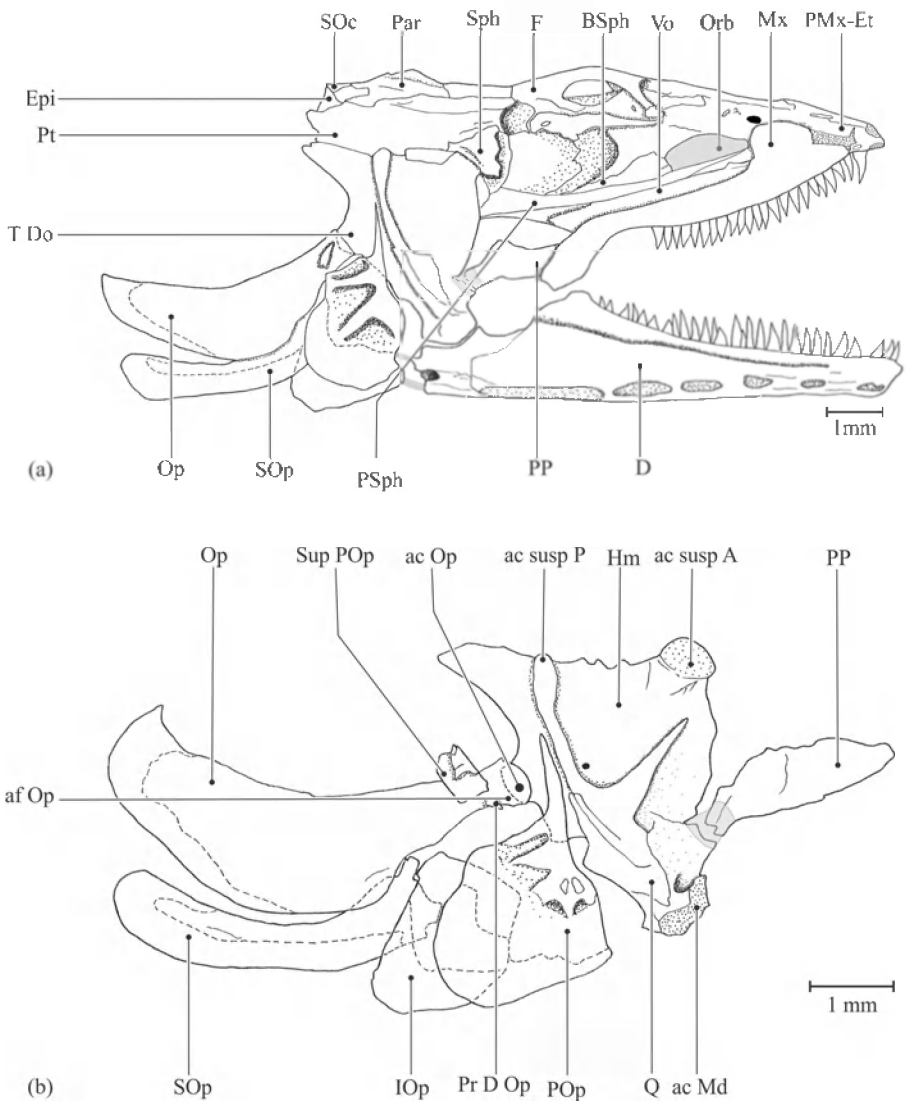

Figure 4.3. Cranial skeleton in *Pythonichthys macrurus* (lateral view). (a) Complete skull (right side) and (b) suspensorium (right side). ac Op, opercular articular condyle; af Op, opercular articular facet ; ac susp A, anterior suspensorial condyle; ac susp P, posterior suspensorial condyle; fs Olf, olfactory fossa; o-BSph, basisphenoid bone; o-D, dentary complex; o-Epi, epioccipital bone; o-F, frontal bone; o-Hm, hyomandibular bone; o-Iop, interopercle; o-Mx, maxillary bone; o-Op, opercle; o-Par, parietal bone; o-PMx-Et, premaxillo-ethmoid complex; o-POp, preopercle; o-PP, palatopterygoid; o-PSph, parasphenoid; o-Pt, pterotic bone; o-PtSph, pterosphenoid bone; o-SOc, supraoccipital bone; o-Q, quadrate; o-SOp, subopercle; o-Sph, sphenotic bone; o-Sup Pop, suprapreoperclar bone; o-Sy, symplectic bone; o-Vo, vomeral bone; Orb, orbit.

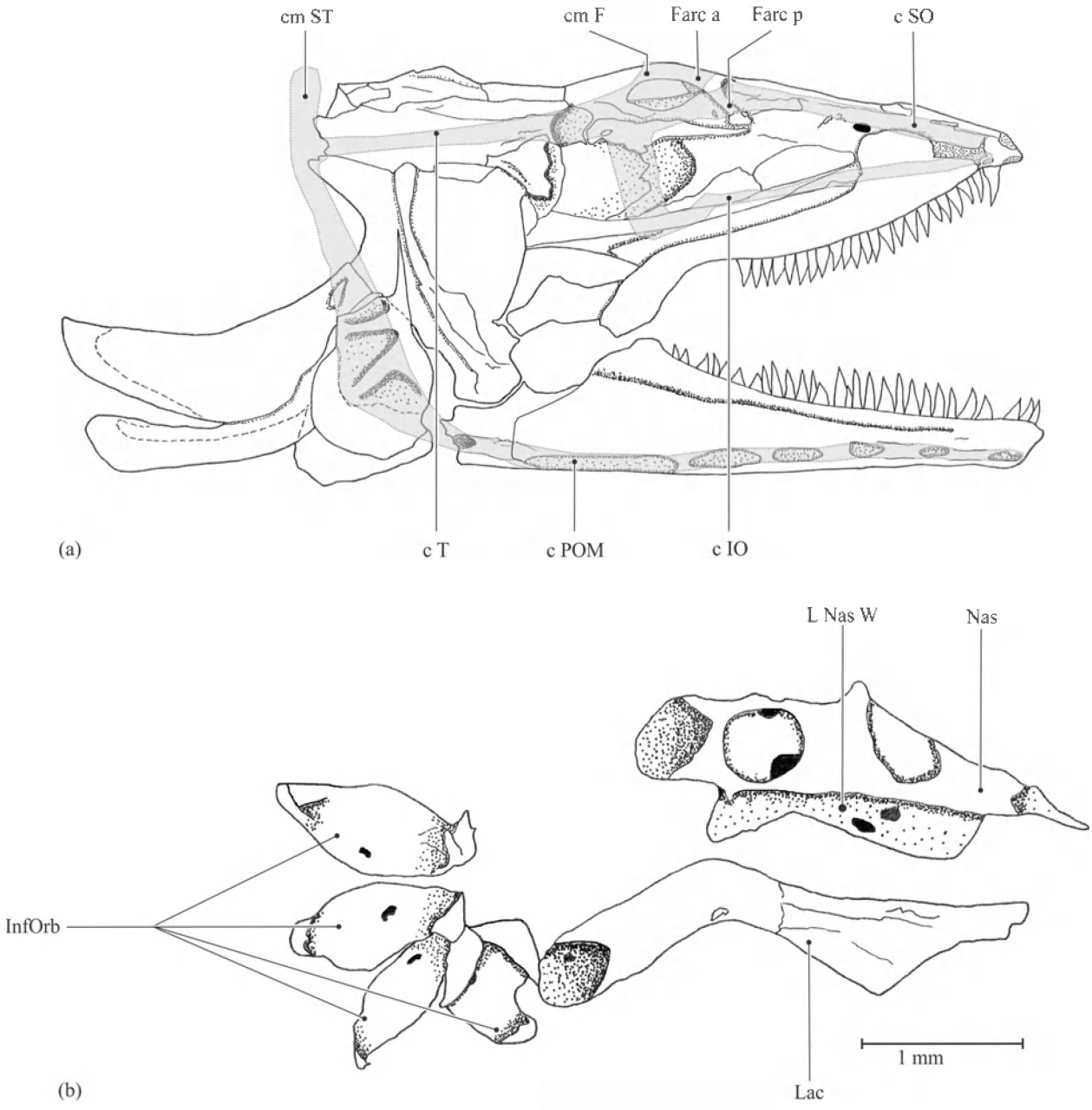
cm ST
cm F
Farc a
Farc p
c SO
(a)
c T
c POM
c IO
L Nas W
Nas
InfOrb
1 mm
(b)
Lac

Figure 4.4. The cranial lateral line system of *Pythonichthys macrurus*. (a) Lateral view of the composing canals (right side). (b) Dorsal view of the left nasal bone, lacrimal bone and infraorbital bones. c IO, infraorbital canal; c POM, preopercular mandibular canal; c SO, supraorbital canal; c T, temporal canal; cm F, Frontal commissure; cm ST, supratemporal commissure; F arc a, anterior frontal arch; F arc p, posterior frontal arch; La Nas W, lateral nasal wings; o-Nas, nasal bone; o-InfoOrb, infraorbital bone ; o-Lac, lacrimal bone.

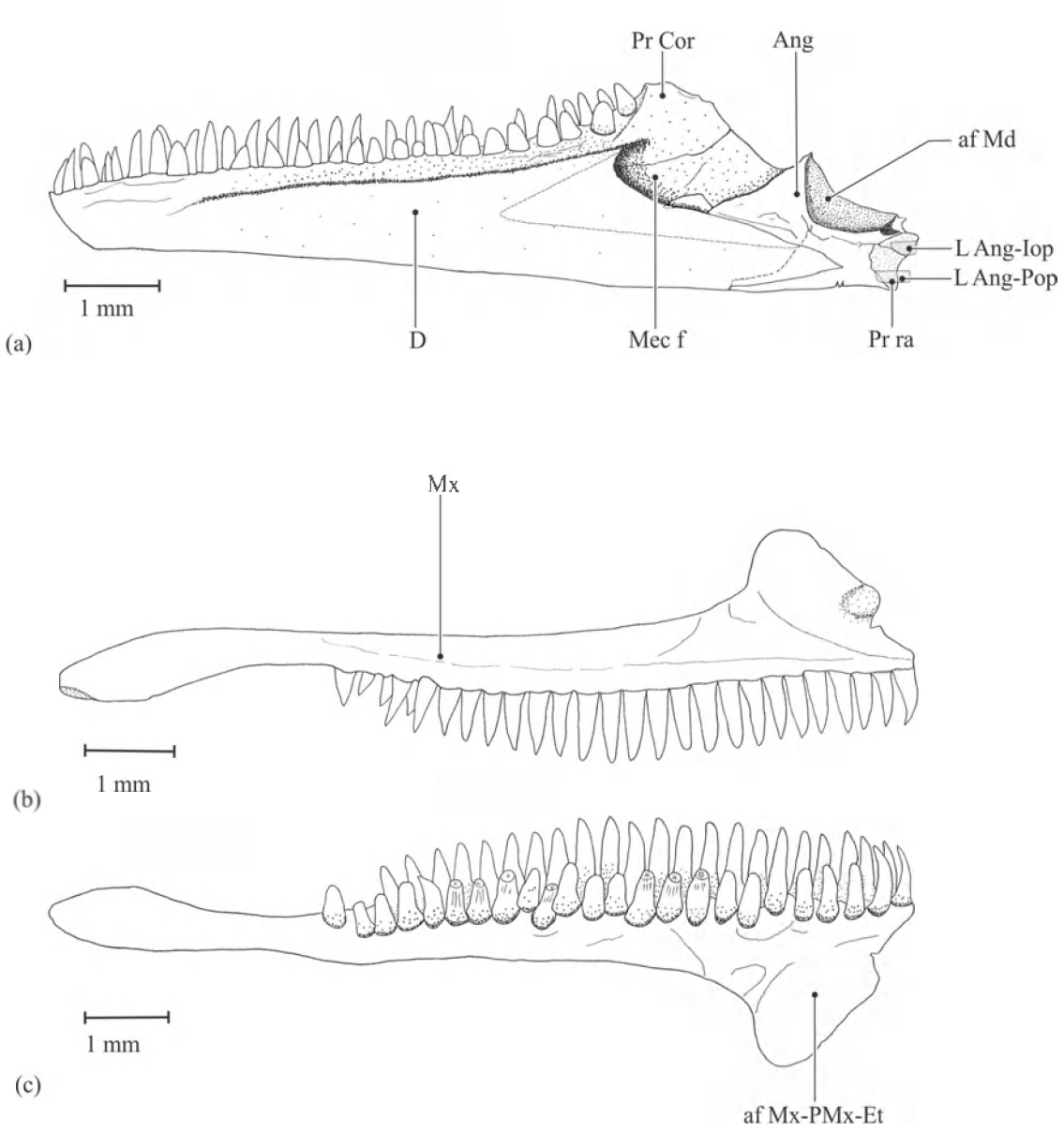

Figure 4.5. Jaw of *Pythonichthys macrurus* (right side) (a-b) maxillary bone; lateral view (a), medial view (b) and (c) lower jaw (medial view). af Md, mandibular articulation facet; ac Mx-Et, maxillo-ethmoidal articulation condyle; ca-CorMec, coronomeckelian cartilage, L Iop-Ang, interoperculo-angular ligament; L Pop-Ang, preoperculo-angular ligament; o-Ang, angular bony complex ; o-D, dentary; o-Mx, maxillary bone; fs Mec, meckelian fossa; pr Cor, coronoid process; pr ra, process of retroarticular bone.

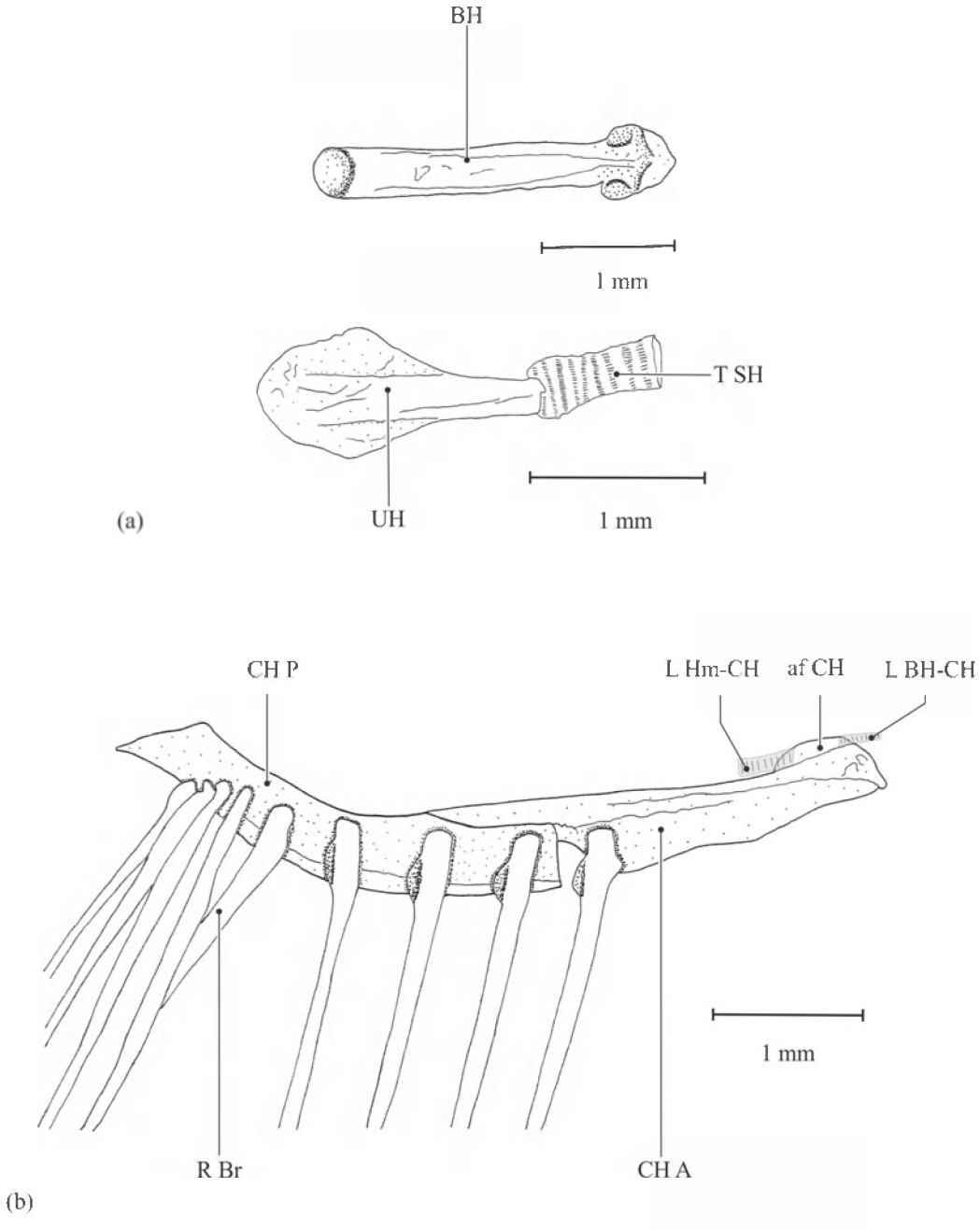

Figure 4.6. Hyoid apparatus of *Pythonichthys macrurus.* (a) Dorsal view of the basihyal and urohyal bones; (b) The anterior and posterior ceratohyal bones in a medial view (right side). af CH, ceratohyal articular facet; L BH-CH, ceratohyalo-basihyal ligament; L CH-Hm, ceratohyalo- hyomandibular ligament; o-BH, basihyal bone; o-CH A, anterior ceratohyal bone; o-CH P, posterior ceratohyal bone; o-R Br, branchiostegal rays; o-UH, urohyal bone.

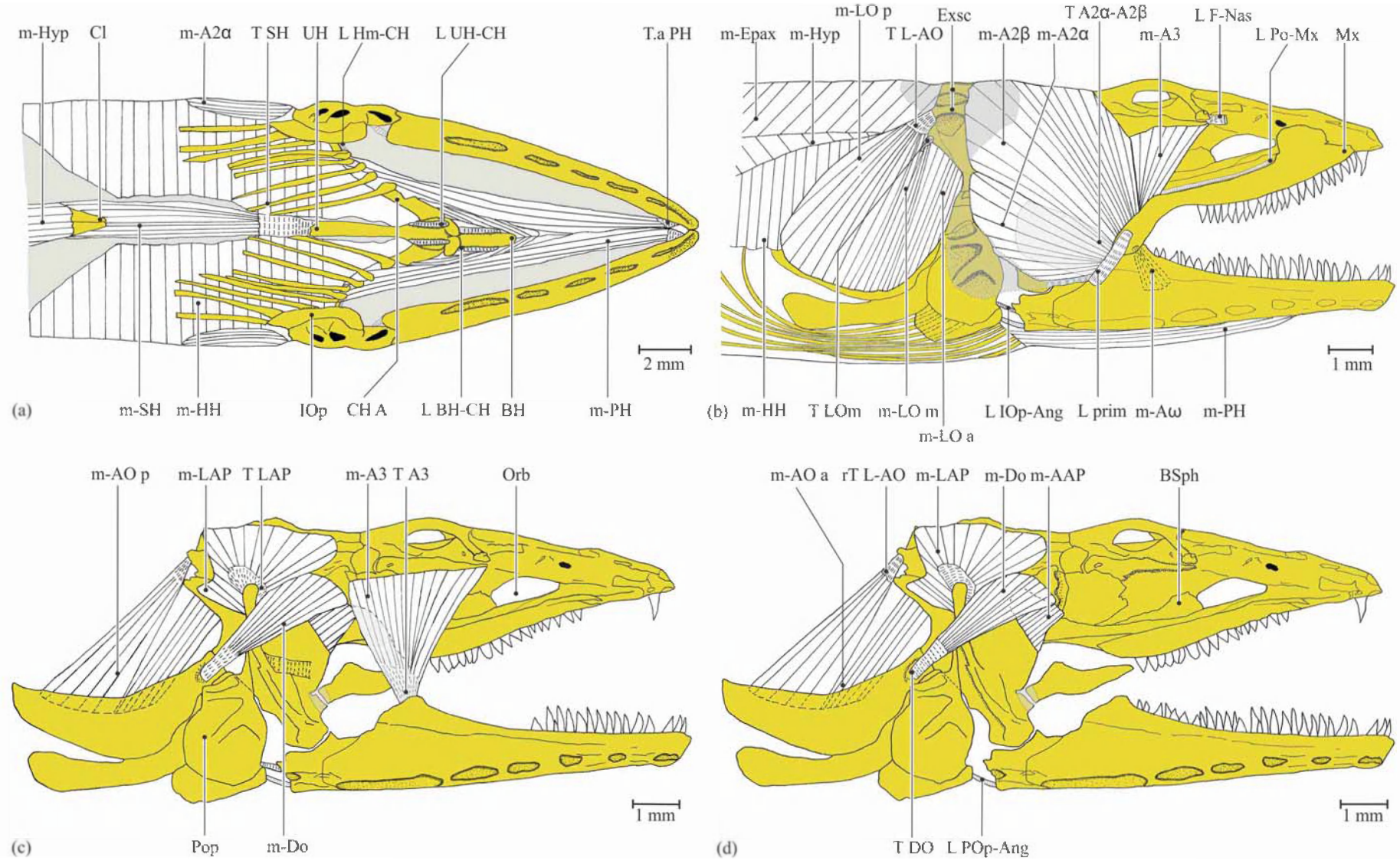
m-Hyp
Cl
m-A2α
T SH
UH
L Hm-CH
L UH-CH
T.a PH
2 mm
(a)
m-SH
m-HH
IOp
CH A
L BH-CH
BH
m-PH
m-LO p
Exsc
T A2α-A2β
L F-Nas
m-Epax
m-Hyp
T L-AO
m-A2β
m-A2α
m-A3
L Po-Mx
Mx
1 mm
(b)
m-HH
T LOm
m-LO m
m-LO a
L IOp-Ang
L prim
m-Aω
m-PH
m-AO p
m-LAP
T LAP
m-A3
T A3
Orb
1 mm
(c)
Pop
m-Do
m-AO a
rT L-AO
m-LAP
m-Do
m-AAP
BSph
1 mm
(d)
T DO
L POp-Ang

Figure 4.7. The cranial muscles of *Pythonichthys macrurus*. (a) Ventral view of the cranial muscles (skin is removed); (b) Skin is removed (lateral view); (c) Maxillary bone, primordial ligament and sections of A2 are removed (lateral view); (d) section A3 are removed (lateral view). L CH-Hm, ceratohyalo-hyomandibular ligament; L F-Nas, frontal-nasal ligament; L Hm-PP, hyomandibula-palatopterygoid ligament; L Iop-Ang, interoperculo-angular ligament; L Po-Mx, preorbital-maxillary ligament; L prim, primordial ligament; L Pop-Ang, preoperculo-angular ligament; m-A2α, ventral subsection of A2; m-A2β, dorsal subsection of A2; m-A3, A3 section of the adductor mandibulae muscle complex; m-AAP, adductor arcus palatini muscle; m-Aω, Aω section of adductor mandibulae muscle complex; m-DO, dilatator operculi muscle; m-Epax, epaxial muscles; m-HH, hyohyoideus muscle; m-Hyp, hypaxial muscles; m-LAP, levator arcus palatini muscle; m-L/AO la, lateroanterior bundle of levator/adductor operculi muscle; m-L/AO m, mesial bundle of levator/adductor operculi muscle; m-L/AO lp, lateroposterior bundle of levator/adductor operculi muscle; m-L/AO mp, medioposterior bundle of levator/adductor arcus palatini muscle; m-L/AO ma, medioanterior bundle of levator/adductor operculi muscle; m-PH, protractor hyoidei muscle; m-SH, sternohyoideus muscle; o-BH, basihyal bone; o-BSph, basisphenoid; o-CH A, anterior ceratohyal bone; o-Cl, cleithrum; o-ExOc, exoccipital bone; o-IOp, interopercle; o-Mx, maxillary bone; o-PMx-Et, premaxillo-ethmoid complex; o-POp, preopercle; o-UH, urohyal bone ; Orb, orbit; r-T L/AO, rest of levator/adductor operculi muscle tendon; T A2, tendon of A2; T A3, tendon of A3; T DO, tendon of dilatator operculi muscle; T LAP, tendon of levator arcus palatini; T L/AO, tendon of levator/adductor operculi; T L/AO m, tendon of mesial bundle of levator/adductor operculi muscle; T.a PH, anterior tendon of protractor hyoidei; T SH, tendon of sternohyoideus.

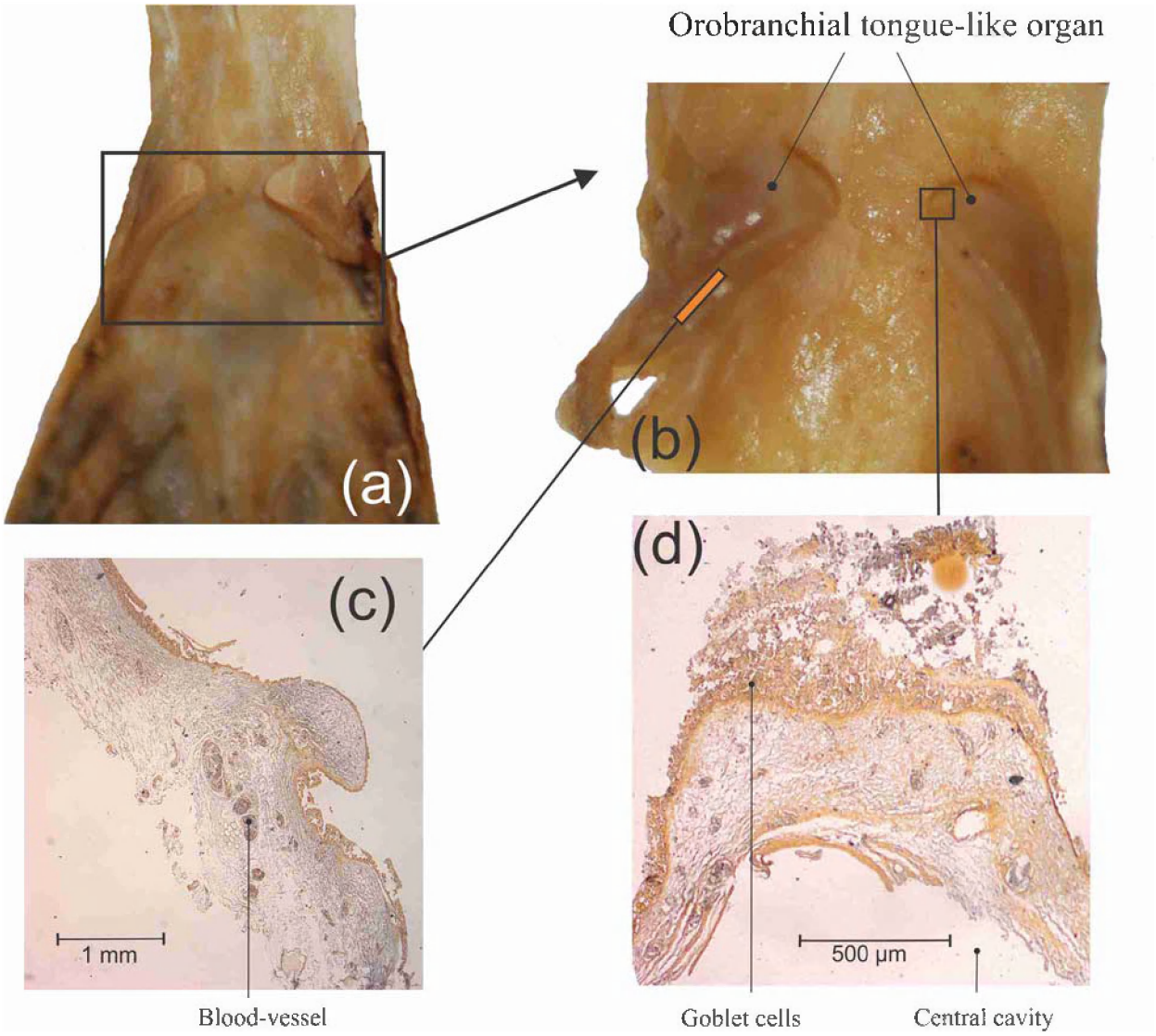
Orobranchial tongue-like organ
(a)
(b)
(c)
(d)
1 mm
500 µm
Blood-vessel
Goblet cells
Central cavity

Figure 4.8. The orobranchial organ of *Pythonichthys macrurus*. (a) Two tongue-like appendages of the orobranchial organ on the roof of the mouth; (b) Closer view of the two tongue-like appendages of the orobranchial organ; (c-d) sagittal section of the orobranchial organ (medial) (c) base region; (d) apex region.

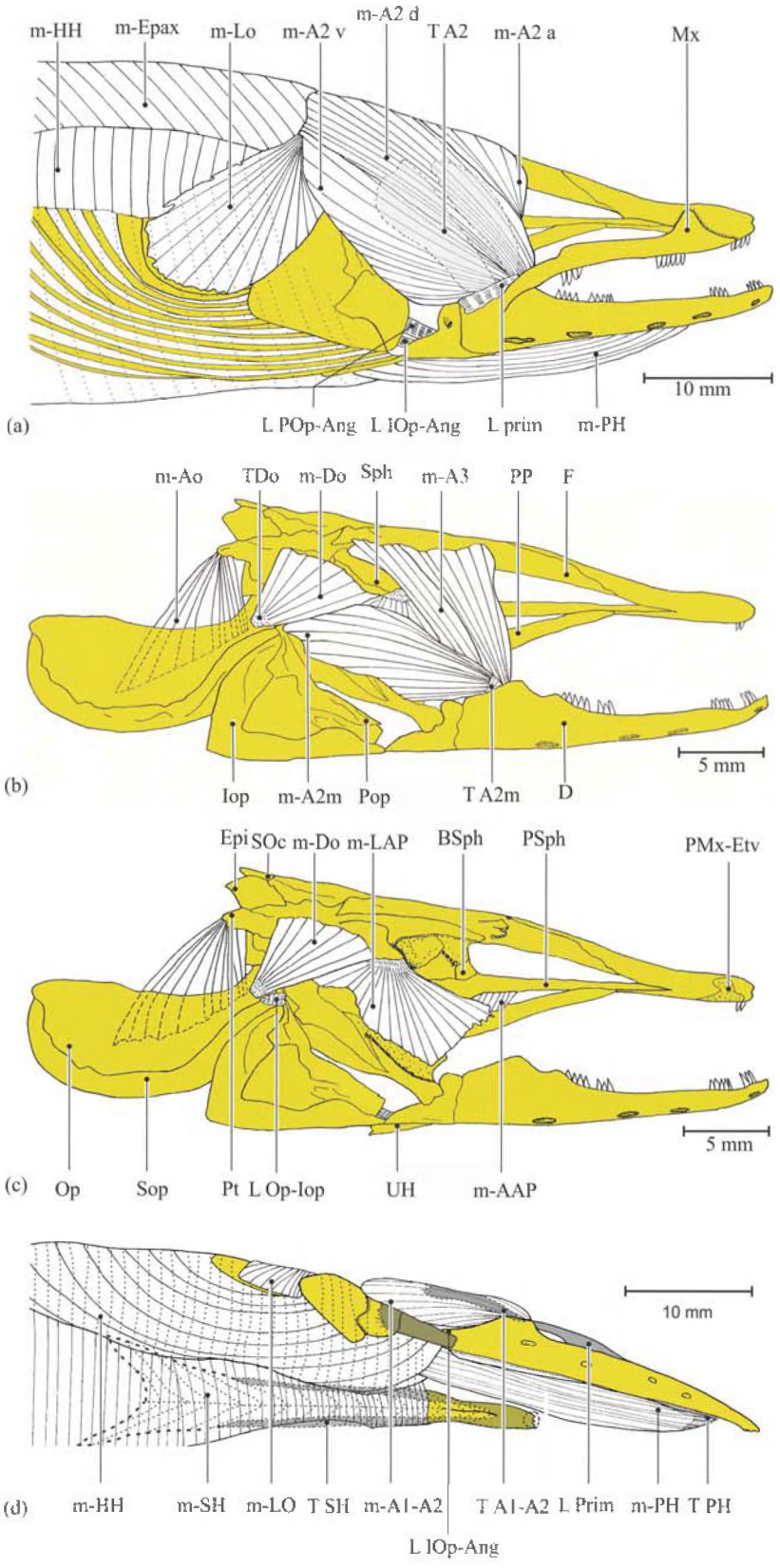
m-HH
m-Epax
m-Lo
m-A2 v
m-A2 d
T A2
m-A2 a
Mx
10 mm
(a)
L POp-Ang
L IOp-Ang
L prim
m-PH
m-Ao
TDo
m-Do
Sph
m-A3
PP
F
5 mm
(b)
Iop
m-A2m
Pop
T A2m
D
Epi
SOc
m-Do
m-LAP
BSph
PSph
PMx-Etv
5 mm
(c)
Op
Sop
Pt
L Op-Iop
UH
m-AAP
10 mm
(d)
m-HH
m-SH
m-LO
T SH
m-A1-A2
T A1-A2
L Prim
m-PH
T PH
L IOp-Ang

Figure 4.9. The cranial muscles of *Anguilla anguilla*. (a) Skin is removed (lateral view); (b) sections A2 except the medial fibers of subsection A2m, hyohyoideus muscle, levator operculi muscle, epaxial muscles, hypaxial muscles, maxillary bone and primordial ligament are removed (lateral view); (c) subsection A2m and subsection A3 are removed (lateral view); (d) ventral view of the right side of the cranial muscles (Skin is removed), (Modified after De Schepper (2007)). L Iop-Ang, interoperculo-angular ligament; L Op-Iop, preoperculo-interopercular ligament; L prim, primordial ligament; L Pop-Ang, preoperculo-angular ligament; m-A2 a, anterior subsection of A2; m-A2 d, dorsal subsection of A2; m-A2 v, ventral subsection of A2; m-A2 m, medial subsection of A2; A3 section of the adductor mandibulae muscle complex; m-AAP, adductor arcus palatini muscle; m-DO, dilatator operculi muscle; m-Epax, epaxial muscles; m-HH, hyohyoideus muscle; m-LAP, levator arcus palatini muscle; m-AO, adductor operculi muscle; m-LO m, levator operculi muscle; m-PH, protractor hyoidei muscle; m-SH, sternohyoideus muscle; o-BSph, basisphenoid; o-D, dentary complex; o-Epi, epioccipital bone; o-F, frontal bone; o-IOp, interopercle; o-Op, opercle; POp, preopercle; o-PP, palatopterygoid; o-PSph, parasphenoid; o-Pt, pterotic bone; o-Mx, maxillary bone; SOc, supraoccipital bone; o-SOp, subopercle; o-Sph, sphenotic bone; o-UH, urohyal bone ; T A2, tendon of A2; T A2 m, tendon of A2 m; T DO, tendon of dilatator operculi muscle; T PH, tendon of protractor hyoidei; T SH, tendon of sternohyoideus.

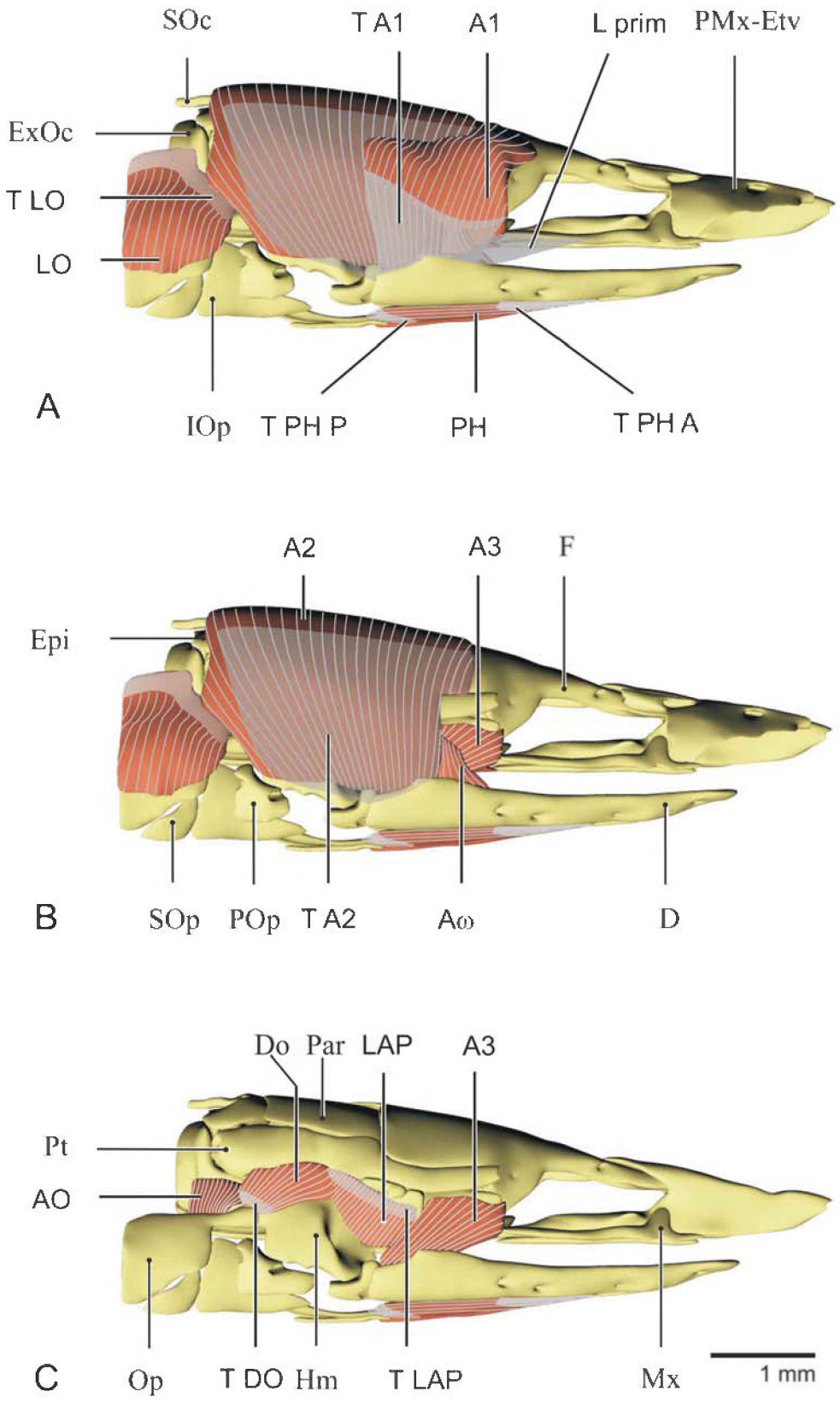
SOc
T A1
A1
L prim
PMx-Etv
ExOc
T LO
LO
A
IOp
T PH P
PH
T PH A
A2
A3
F
Epi
B
SOp
POp
T A2
Aω
D
Do
Par
LAP
A3
Pt
AO
C
Op
T DO
Hm
T LAP
Mx
1 mm

Figure 4.10 (Additional picture): 3D reconstruction of the cranial muscles of *Pisodonophis boro*. The nasal is indicated by an arrow. A: The skin is removed, B: the A1 of the adductor mandibulae complex is removed, C: A2 and Aω of the adductor mandibulae complex and LO are removed (after De Schepper., 2007).

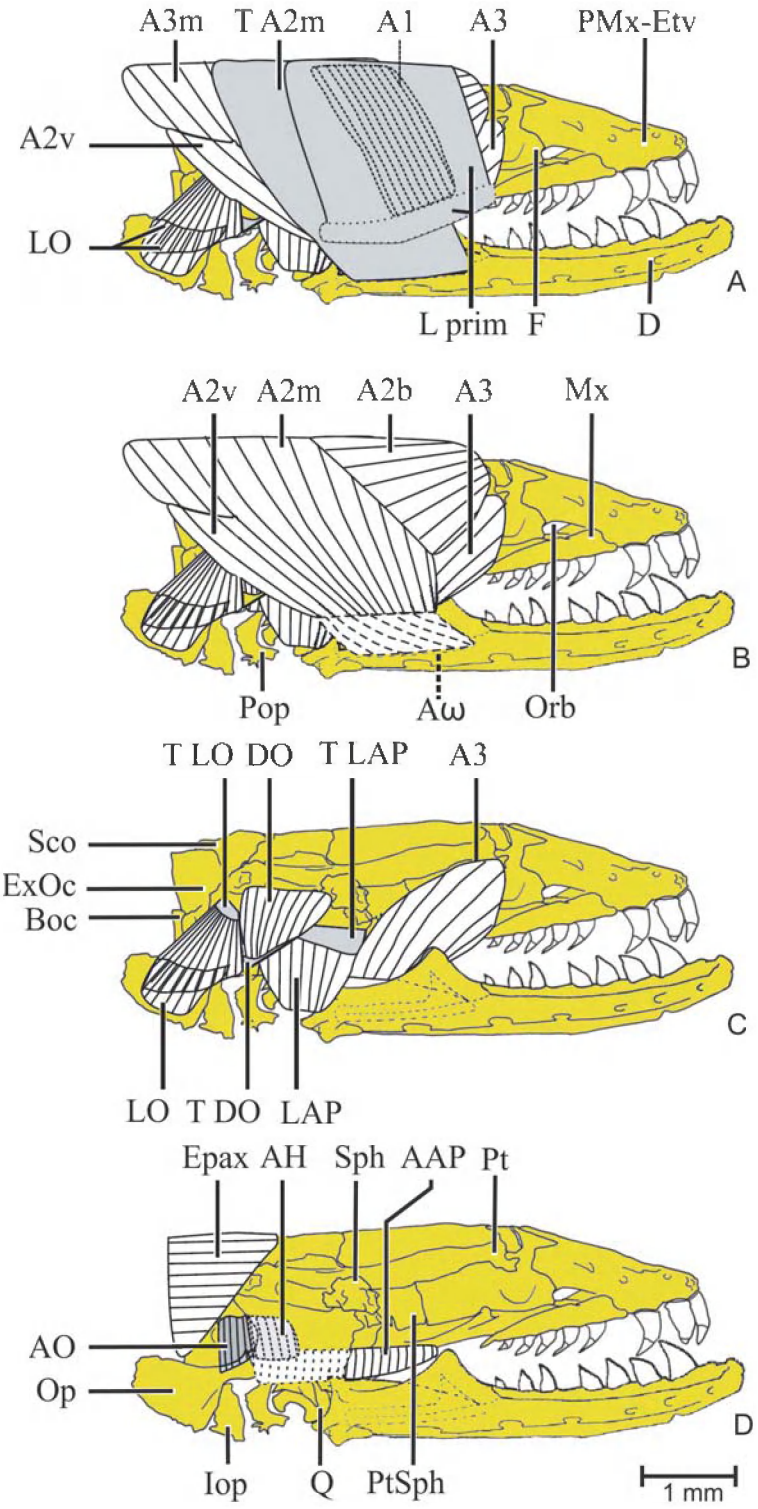
A3m
T A2m
A1
A3
PMx-Etv
A2v
LO
L prim
F
D
A
A2v
A2m
A2b
A3
Mx
Pop
Aω
Orb
B
T LO
DO
T LAP
A3
Sco
ExOc
Boc
LO
T DO
LAP
C
Epax
AH
Sph
AAP
Pt
AO
Op
Iop
Q
PtSph
D
1 mm

Figure 4.11 (Additional picture): Lateral view of the cranial muscles *Moringua edwardsi*. Dotted lines indicate parts of structures being covered by other elements. A: Skin is removed. B: Primordial ligament and A1 are removed, exposing the adductor mandibulae complex with dorsal (A2d), medial (A2m), ventral (A2v) and mandibular (Aω) part. C: The adductor mandibulae complex is removed, except for the A3. D: Opercular muscles are removed (after De Schepper, 2007).

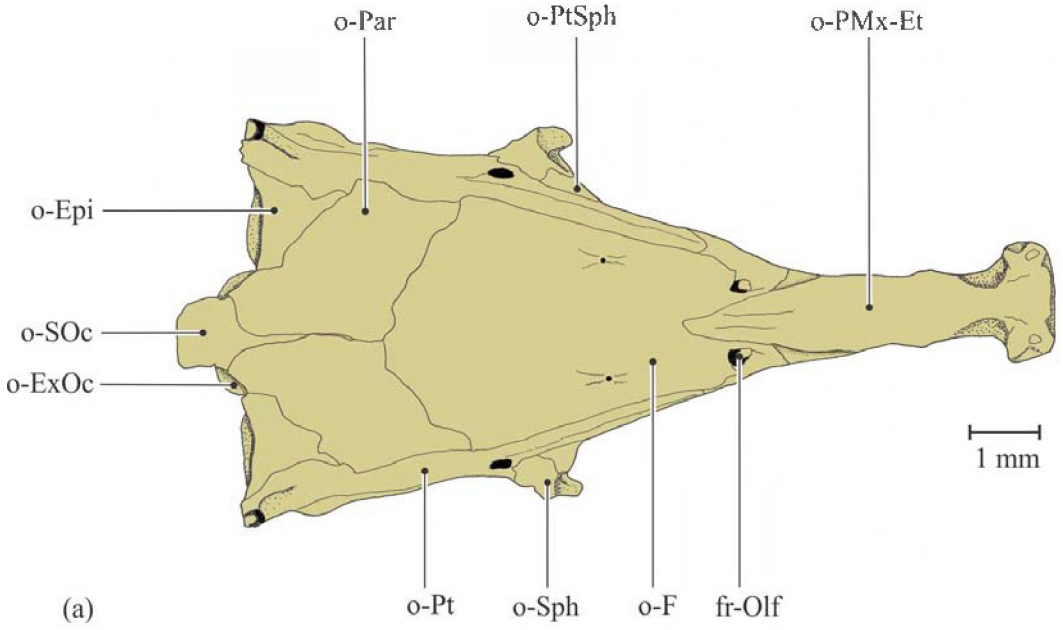
o-Par
o-PtSph
o-PMx-Et
o-Epi
o-SOc
o-ExOc
1 mm
(a)
o-Pt
o-Sph
o-F
fr-Olf

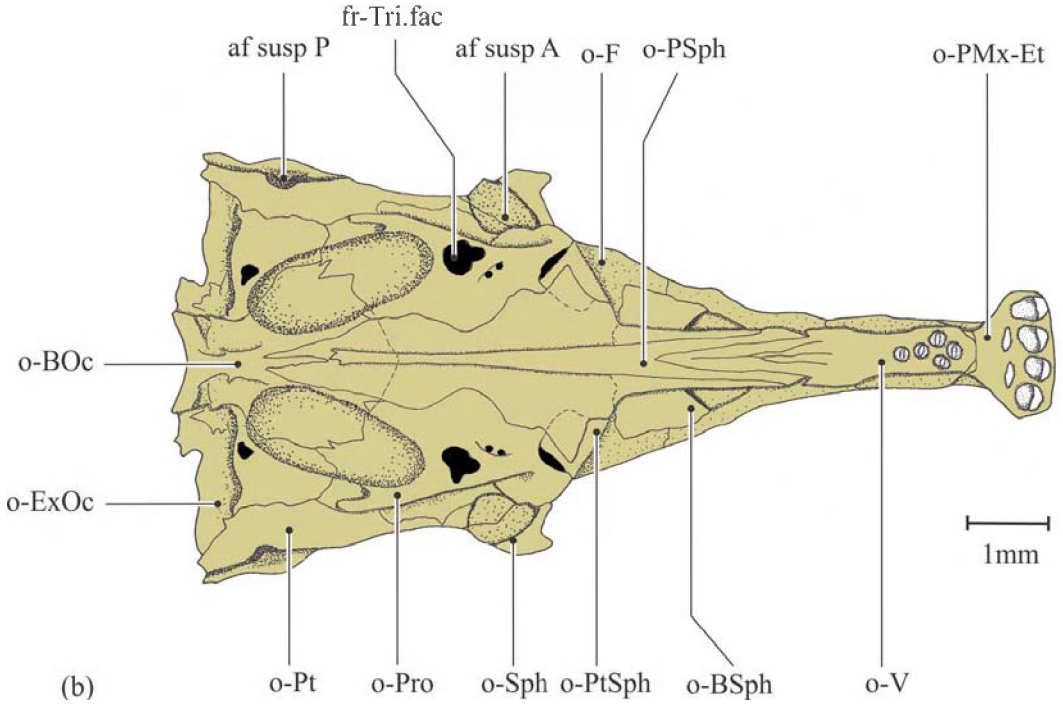
fr-Tri.fac
af susp P
af susp A
o-F
o-PSph
o-PMx-Et
o-BOc
o-ExOc
1mm
(b)
o-Pt
o-Pro
o-Sph
o-PtSph
o-BSph
o-V

Figure 5.1: Neurocranium of *Simenchelys parasiticus*. (A) Dorsal view, and (B) Ventral view. af susp A, anterior suspensorial articulation facet; af susp P, posterior suspensorial articulation facet; fr-Olf, foramen olfactorius; fr-Tri.fac, foramen trigemino-facialis; o-BOc, basioccipital; o-BSph, basisphenoid; o-Epi, epioccipital; o-ExOc, exoccipital; o-F, frontal; o-Par, parietal; o-PMx-Et, premaxillo-ethmoidal complex; o-Pro, prootic; o-PSph, parasphenoid; o-Pt, pterotic; o-PtSph, pterosphenoid; o-Soc, supraoccipital; o-Sph, sphenotic; o-V, vomer.

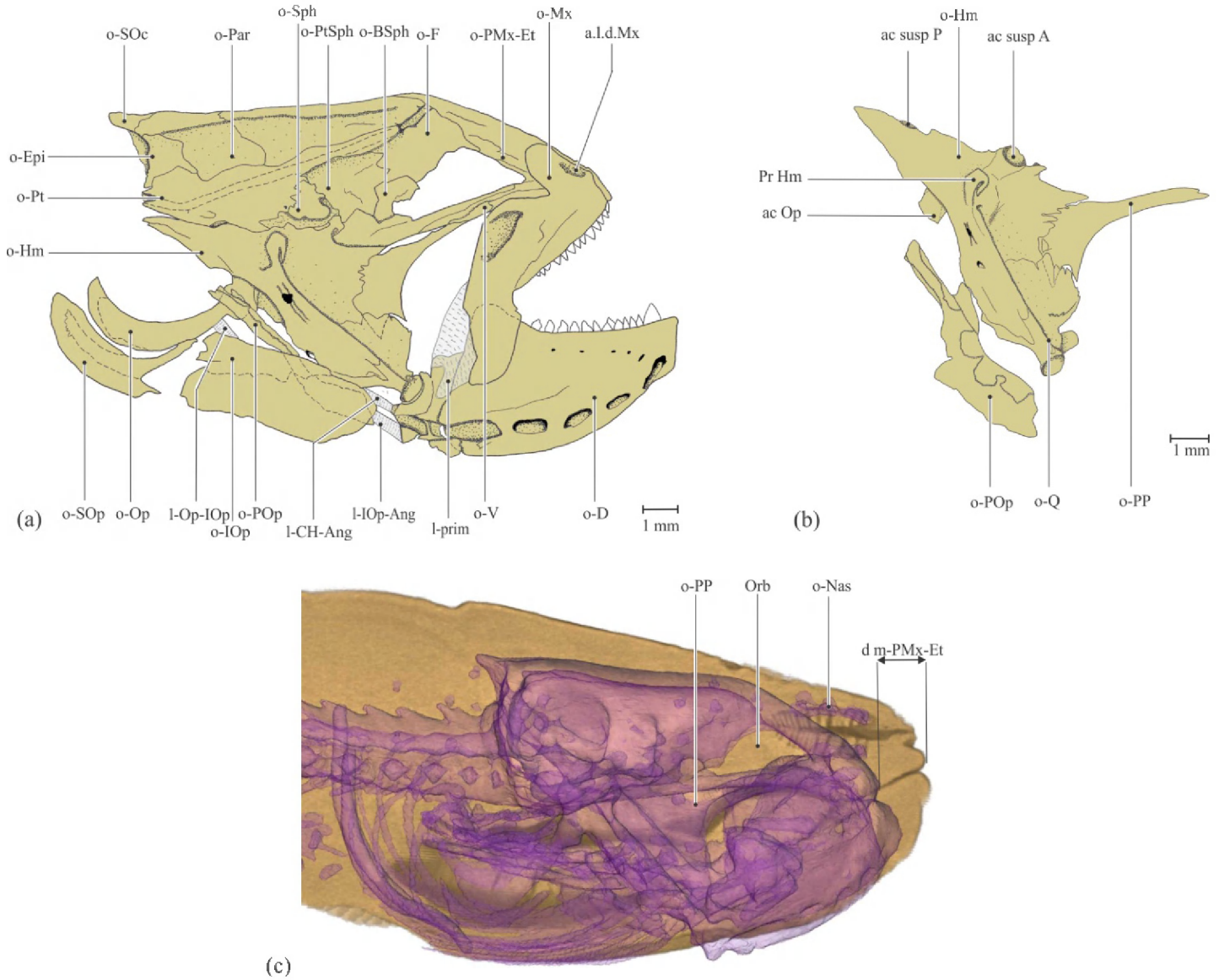
o-SOc
o-Par
o-Sph
o-PtSph
o-BSph
o-F
o-PMx-Et
o-Mx
a.l.d.Mx
o-Epi
o-Pt
o-Hm
o-SOp
o-Op
l-Op-IOp
o-IOp
o-POp
l-CH-Ang
l-IOp-Ang
l-prim
o-V
o-D
1 mm
(a)
o-Hm
ac susp P
ac susp A
Pr Hm
ac Op
o-POp
o-Q
o-PP
1 mm
(b)
o-PP
Orb
o-Nas
d m-PMx-Et
(c)

Figure 5.2: Cranial skeleton of *Simenchelys parasiticus* (lateral view). (a) Complete skull except the circumorbital bones (right side), (b) suspensorium (right side) and (c) position of the skull in the head. Cranial skeleton of *Simenchelys parasiticus* (lateral view). (A) Complete skull except the circumorbital bones (right side), (B) Suspensorium (right side) and (C) position of the skull in the head. ac Op, opercular articular condyle; ac susp A, anterior suspensorial condyle; ac susp P, posterior suspensorial condyle; a.l.d.Mx, anterolateral depression of maxillary; d m-PMx-Et, distance between anterior tip of mouth and premaxillo-ethmoidal complex (soft tissue); l-Iop-Ang, interoperculo-angular ligament; l-CH-Ang, ceratohyalo-angular ligament; l-Op-IOp, operculo-interopercular ligament; l-prim, primordial ligament; o-Nas, nasal; o-BSph, basisphenoid; o-D, dentary complex; o-Epi, epioccipital; o-F, frontal; o-Hm, hyomandibula; o-Iop, interopercle; o-Mx, maxillary; o-Op, opercle; o-Par, parietal; o-PMx-Et, premaxillo-ethmoidal complex; o-POp, preopercle; o-PP, palatopterygoid; o-PSph, parasphenoid; o-Pt, pterotic; o-PtSph, pterosphenoid; o-Q, quadrate; o-Soc, supraoccipital; o-SOp, subopercle; o-Sph, sphenotic; o-V, vomer; Orb, orbit; Pr Hm, hyomandibular lateral process.

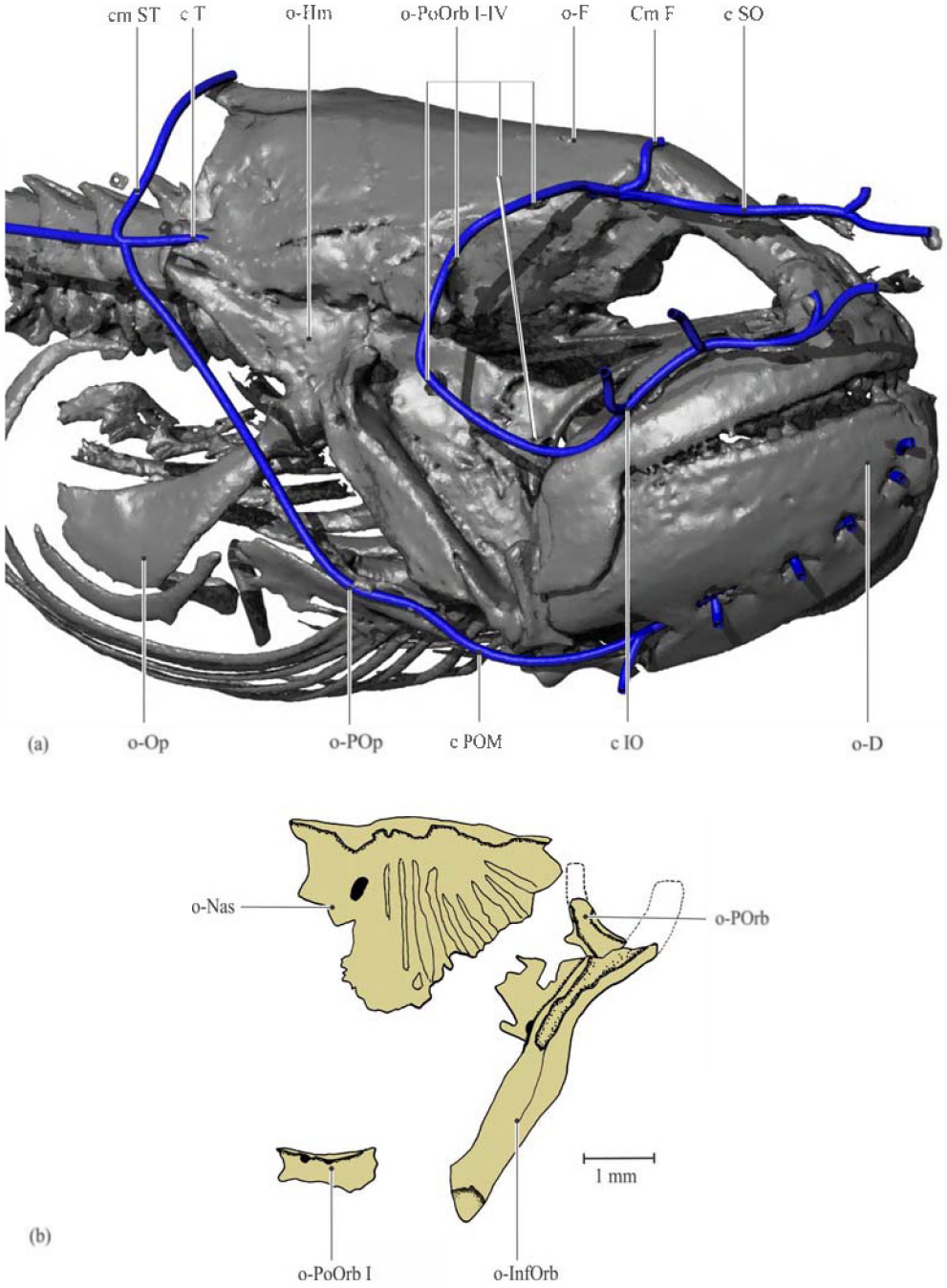

Figure 5.3: The cranial lateral line system of *Simenchelys parasiticus*. (a) Position of the composing canals in relation to the skull (right side, lateral view), and (b) lateral view of the nasal bone, preorbital bone, infraorbital bone and first postorbital bone (right side). c IO, infraorbital canal; c POM, preopercular mandibular canal; c SO, supraorbital canal; c T, temporal canal; cm F, frontal commissure; cm ST, supratemporal commissure; o-InfOrb, infraorbital; o-D, dentary complex; o-F, frontal; o-Hm, hyomandibula; o-Nas, nasal; o-Op, opercle; o-Porb, preorbital; o-PoOrb, postorbital, o-POp, preopercle.

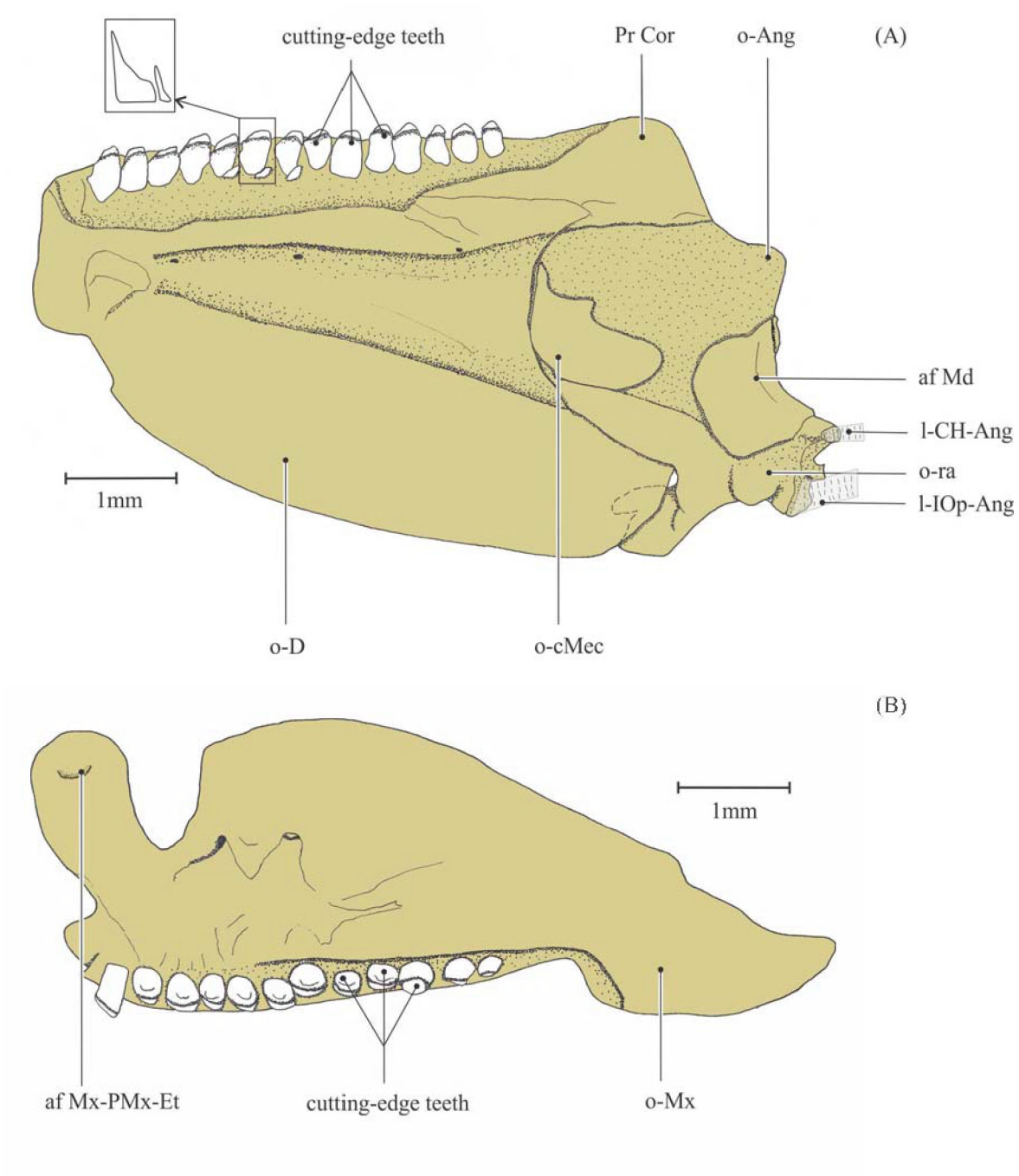

Figure 5.4: Jaws of *Simenchelys parasiticus* (right side). (a) Lower jaw; medial view, and (b) maxillary; medial view. af Md, mandibular articulation facet; af Mx-Et, maxillo-premaxillo-ethmoidal articular facet; l-Iop-Ang, interoperculo-angular ligament; l-CH-Ang, ceratohyalo-angular ligament; o-Ang, angular complex ; o-D, dentary complex; o-Mx, maxillary; o-cMec, coronomeckelian; pr Cor, coronoid process; o-ra, retroarticular.

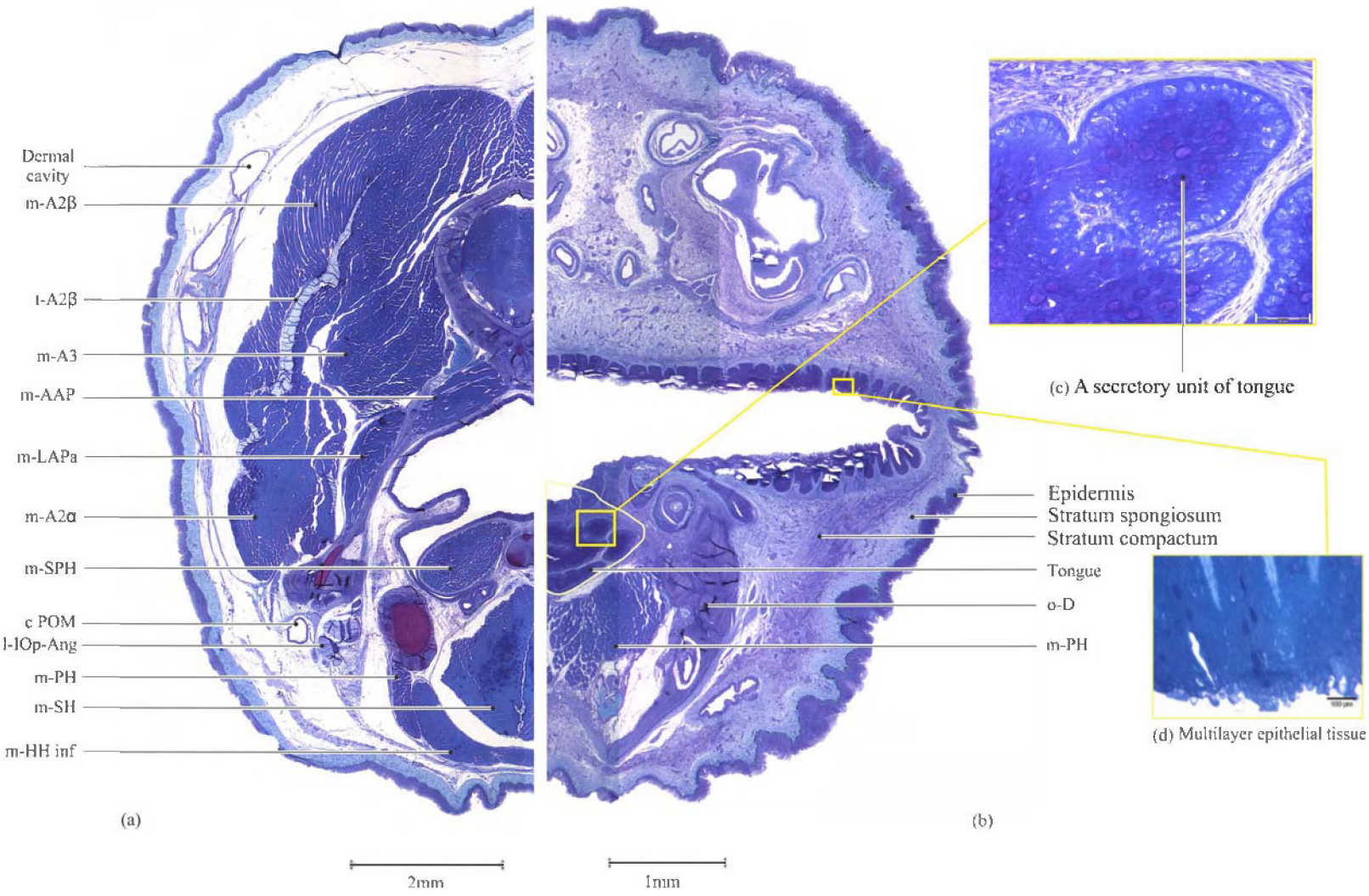
Dermal cavity
m-A2β
t-A2β
m-A3
m-AAP
m-LAPa
m-A2α
m-SPH
c POM
l-IOp-Ang
m-PH
m-SH
m-HH inf
(a)
2mm
(b)
1mm
(c) A secretory unit of tongue
Epidermis
Stratum spongiosum
Stratum compactum
Tongue
o-D
m-PH
(d) Multilayer epithelial tissue

Figure 5.5: (a): Cross section of the head of *Simenchelys parasiticus*: (a) at the level of the anterior part of the lower jaw: (b) at the level of the anterior part of the large tongue; (c) detail of the glandular tissue large in the tongue-like structure of *S. parasiticus*; and (d): multilayered epithelial tissue of the skin around the mouth. c POM, preopercular mandibular canal; l-IOp-Ang, interoperculo-angular ligament; m-A2α, ventral subsection of A2; m-A2β, dorsal subsection of A2; m-A3, A3 section of the adductor mandibulae muscle complex; m-AAP, adductor arcus palatini muscle; m-HH inf, hyohyoideus inferioris muscle; m-LAPa, anterior subsection of levator arcus palatini muscle; m-PH, protractor hyoidei muscle; m-SH, sternohyoideus muscle; m-SPH, pharyngocleithralis muscle; o-D, dentary complex; t A2β, tendon of A2β.

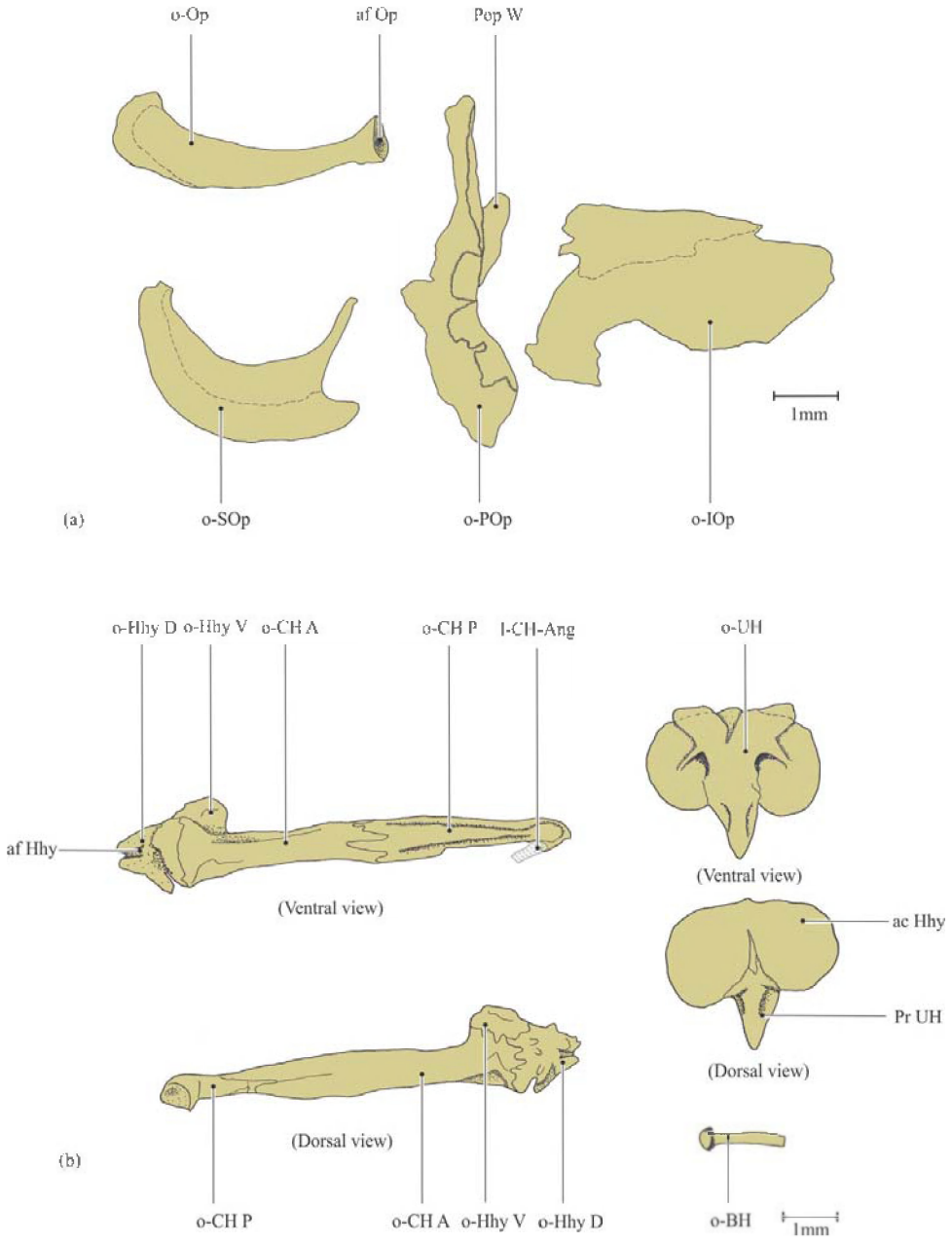

Figure 5.6: Opercular series and hyoid apparatus of *Simenchelys parasiticus*: (a) Opercular series; lateral view (right side), and (b) hyoid apparatus; ventral and dorsal views of the dorsal hypohyal, ventral hypohyal, anterior ceratohyal and posterior ceratohyal bones, ventral and dorsal views of urohyal, and dorsal view of basihyal. af Hhy, hypohyal articular facet; af Op, opercular articular facet; ac Hhy, hypohyal articular condyle ; l-CH-Ang, ceratohyalo-angular ligament; o-BH, basihyal; o-CH A, anterior ceratohyal bone; o-CH p, posterior ceratohyal bone; o-Hhy D, dorsal hypohyal bone; o-Hhy V, ventral hypohyal bone; o-Iop, interopercle; o-Op, opercle; o-POp, preopercle; o-SOp, subopercle; o; o-UH, urohyal; pr UH, urohyal process; Pop W, preopercular wing.

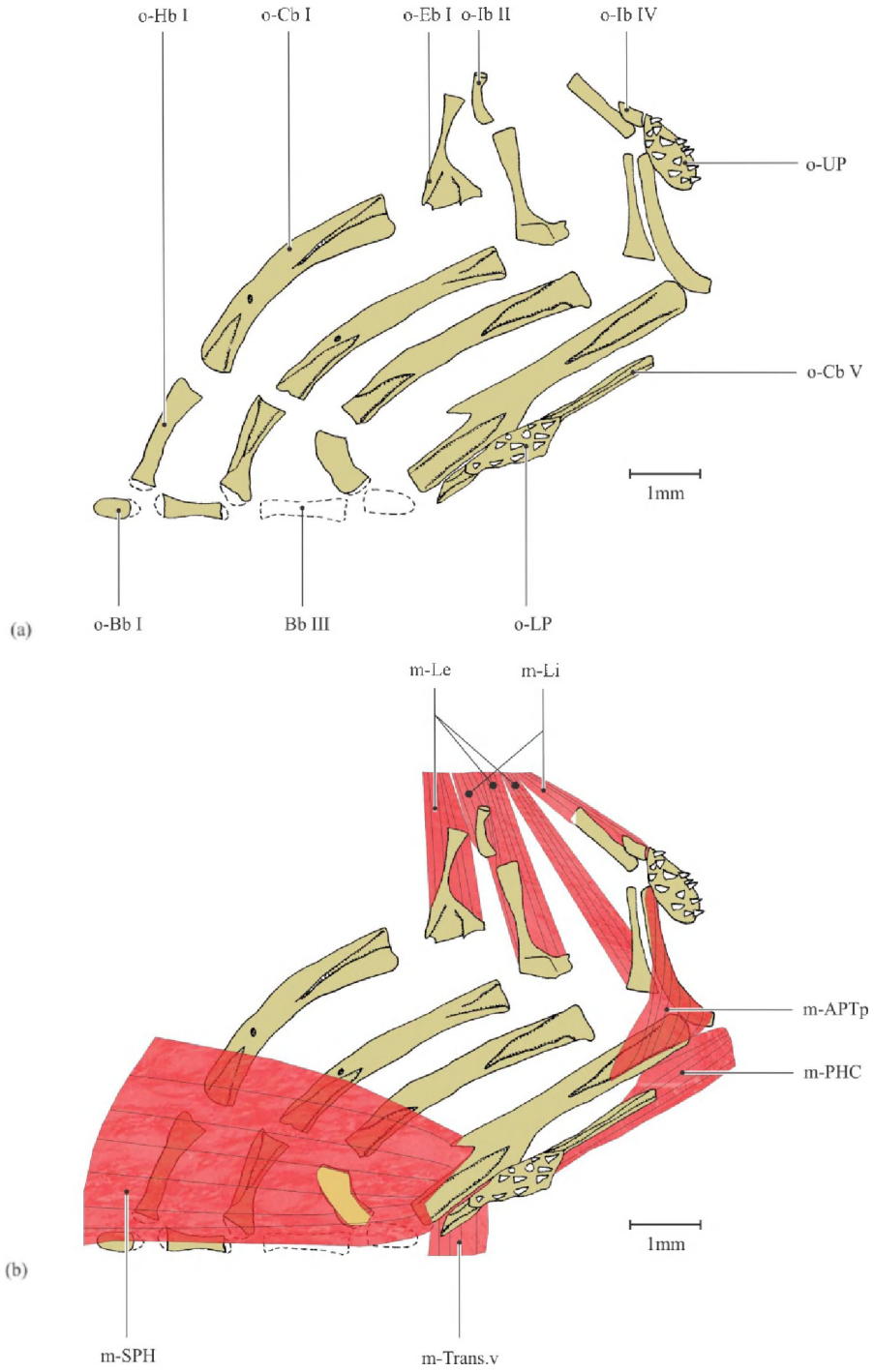

Figure 5.7: Gill arches of *Simenchelys parasiticus*. (a) Dorsal view of the ventral part and the ventral view of the dorsal part of the gill arch, and (b) gill arch muscles. o-Bb, basibranchial bone; o-Cb, ceratobranchial bone; o-Eb, epibranchial bone; o-Hb, hypobranchial bone; o-Ib, infrapharyngobranchial bone; o-LP, lower pharyngeal tooth plates; o-UP, upper pharyngeal tooth plates; m-APTp, pharyngeal tooth plate adductor muscle; m-Le, levator externus muscle; m-Li, levator internus muscle; m-PHC, pharyngocleithralis muscle; m-SPH, subpharyngealis muscle; m-Trans.v, transversus ventralis muscle.

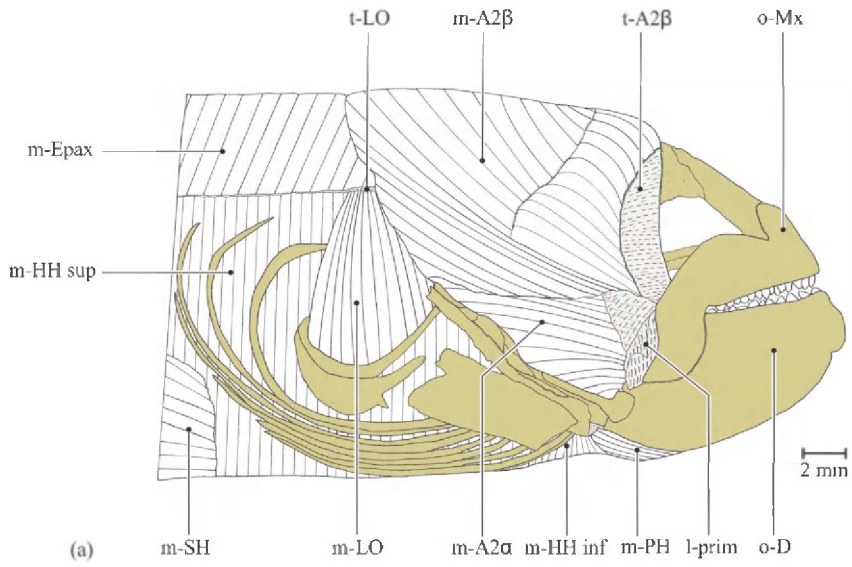
t-LO
m-A2β
t-A2β
o-Mx
m-Epax
m-HH sup
2 mm
(a)
m-SH
m-LO
m-A2α
m-HH inf
m-PH
l-prim
o-D

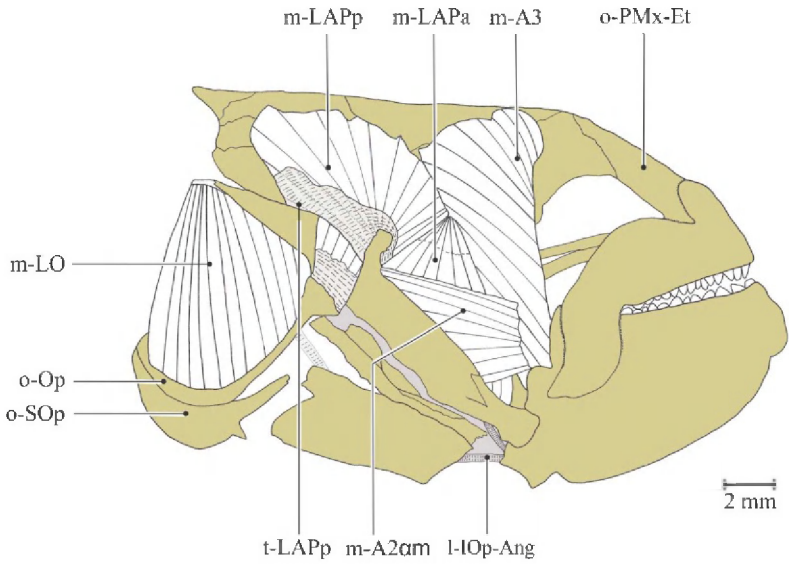
m-LAPp
m-LAPa
m-A3
o-PMx-Et
m-LO
o-Op
o-SOp
2 mm
t-LAPp
m-A2αm
l-IOp-Ang

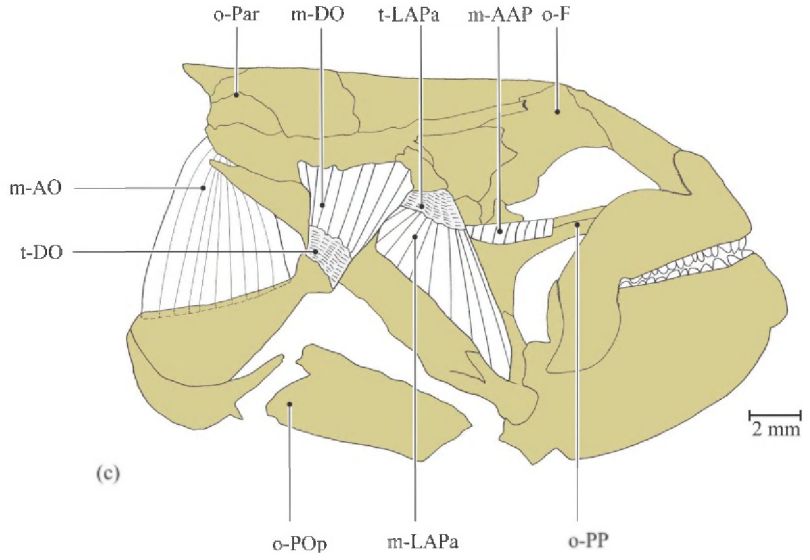
o-Par
m-DO
t-LAPa
m-AAP
o-F
m-AO
t-DO
2 mm
(c)
o-POp
m-LAPa
o-PP

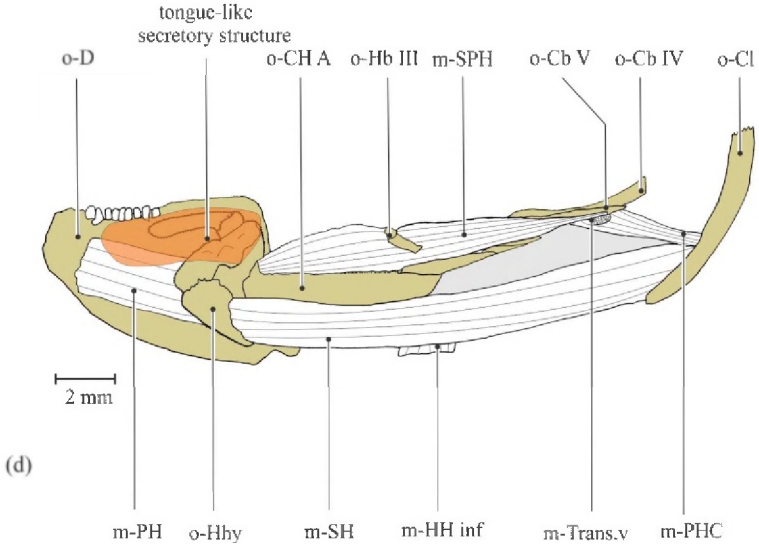
tongue-like
secretory structure
o-D
o-CH A
o-Hb III
m-SPH
o-Cb V
o-Cb IV
o-Cl
2 mm
(d)
m-PH
o-Hhy
m-SH
m-HH inf
m-Trans.v
m-PHC

Figure 5.8: The cranial muscles of *Simenchelys parasiticus*. (a) Skin removed (lateral view), (b) sections A2 except for the medial fibers of subsection A2α, hyohyoideus muscle, hyohyoideus inferioris muscle, epaxial muscles, hypaxial muscles, ventral muscles of the head and primordial ligament are removed (lateral view), (c) subsection A2α, section A3, lateral fibers of the levator arcus palatini muscle and levator operculi muscle are removed (lateral view), and (d) ventral muscles of head (sagittal left cut), hyohyoideus muscle is removed. l-Iop-Ang, interoperculo-angular ligament; l-prim, primordial ligament; m-A2α, ventral subsection of A2; m-A2β, dorsal subsection of A2; m-A2αm, medial fibers of vental subsection of A2; m-A3, A3 section of the adductor mandibulae muscle complex; m-AAP, adductor arcus palatini muscle; m-AO, adductor operculi muscle; m-DO, dilatator operculi muscle; m-Epax, epaxial muscles; m-HH inf, hyohyoideus inferioris muscle; m-HH sup, hyohyoideus superior muscle; m-LAPa, anterior subsection of levator arcus palatini muscle; m-LAPp, posterior subsection of levator arcus palatini muscle; m-LO, levator operculi muscle; m-PH, protractor hyoidei muscle; m-SH, sternohyoideus muscle; m-SPH, subpharyngealis muscle; m-Trans.v, transversus ventralis muscle; o-Cb, ceratobranchial bone; o-CH A, anterior ceratohyal bone; o-Cl, cleithrum bone; o-D, dentary complex; o-F, frontal bone; o-Hb, hypobranchial bone; o-Hhy V, ventral hypohyal bone; o-Mx, maxillary bone; o-Op, opercle; o-Par, parietal bone ; o-PMx-Et, premaxillo-ethmoidal complex; o-POp, preopercle; o-PP, palatopterygoid bone; t-A2β, tendon of A2β; t-DO, tendon of dilatator operculi muscle; t-LAPa, tendon of anterior subsection of levator arcus palatini; t-LAPp, tendon of posterior subsection of levator arcus palatini; t-LO, tendon of levator operculi.

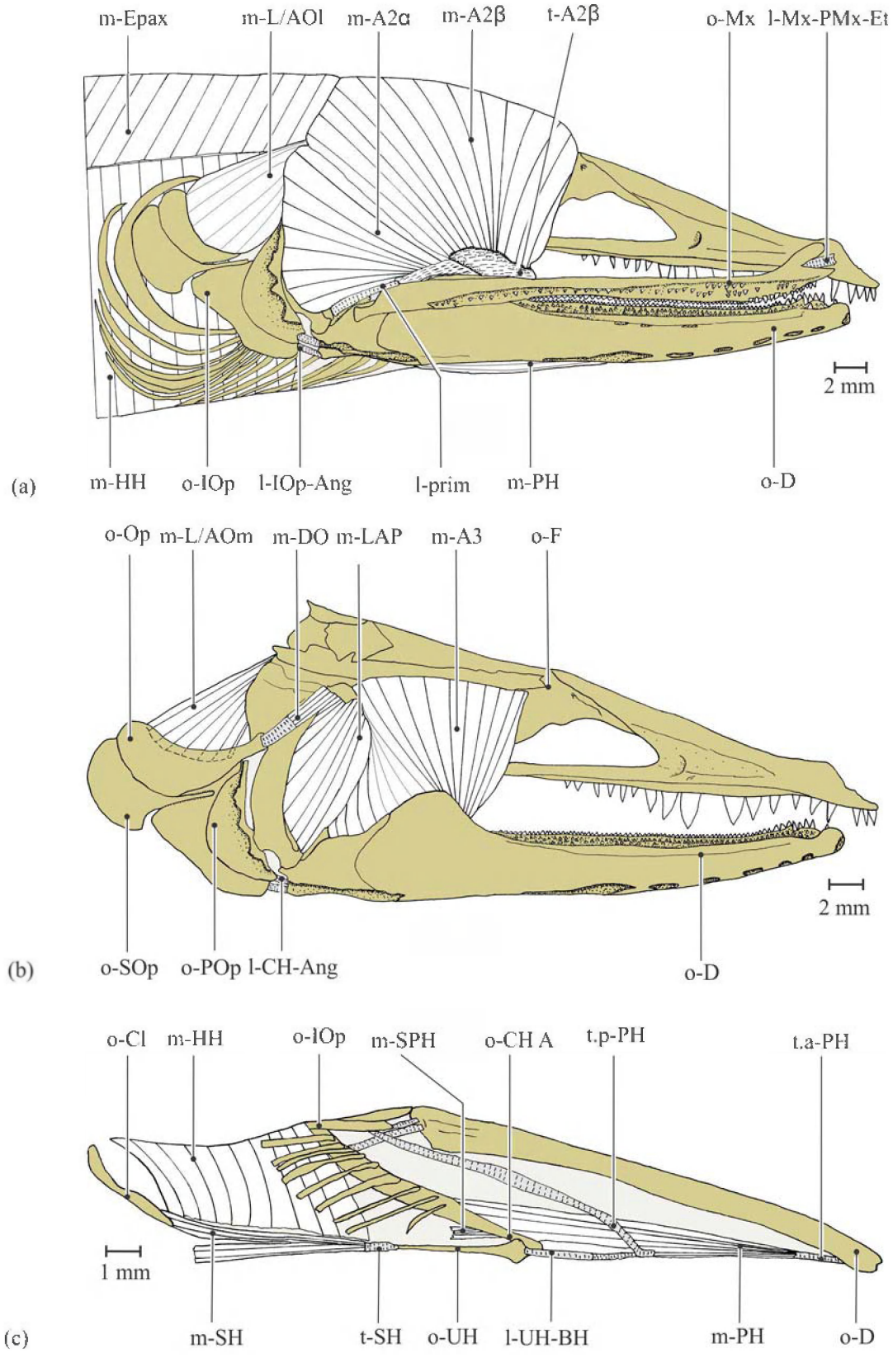
m-Epax
m-L/AOl
m-A2α
m-A2β
t-A2β
o-Mx
l-Mx-PMx-Et
2 mm
(a)
m-HH
o-IOp
l-IOp-Ang
l-prim
m-PH
o-D
o-Op
m-L/AOm
m-DO
m-LAP
m-A3
o-F
2 mm
(b)
o-SOp
o-POp
l-CH-Ang
o-D
o-Cl
m-HH
o-IOp
m-SPH
o-CH A
t.p-PH
t.a-PH
1 mm
(c)
m-SH
t-SH
o-UH
l-UH-BH
m-PH
o-D

Figure 5.9: The cranial muscles of *Ilyophis brunneus*. (a) Skin removed (lateral view); (b) sections A2, hyohyoideus muscle, lateral fibers of the levator/adductor operculi muscle, epaxial muscles, hypaxial muscles, maxillary bone, branchiostegal rays and primordial ligament are removed (lateral view); (c) ventral view of the right side of the cranial muscles (Skin is removed and subpharyngealis muscle is cut). l-Iop-Ang, interoperculo-angular ligament; l-CH-Ang, cratohyalo-angular ligament; l-prim, primordial ligament; l-Mx-PMx-Et, maxillo-premaxillo-ethmoidal ligament; l-UH-BH, urohyalo-basihyal ligament; m-A2α, ventral subsection of A2; m-A2β, dorsal subsection of A2; m-A3, A3 section of the adductor mandibulae muscle complex; m-DO, dilatator operculi muscle; m-Epax, epaxial muscles; m-HH, hyohyoideus muscle complex; m-LAP, levator arcus palatini muscle; m-L/AOl, lateral fibers of levator/adductor operculi muscle; m-L/AOm, medial fibers of levator/adductor operculi muscle; m-PH, protractor hyoidei muscle; m-SH, sternohyoideus muscle; m-SPH, subpharyngealis muscle; o-CH A, anterior ceratohyal bone; o-Cl, cleithrum bone; o-D, dentary complex; o-F, frontal bone; o-IOp, interopercle; o-Mx, maxillary bone; o-Op, opercle; o-POp, preopercle; o-SOp, subopercle; o-UH, urohyal bone; t-A2β, tendon of A2β; t.a-PH, anterior tendon of protractor hyoidei muscle; t.p-PH, posterior tendon of protractor hyoidei muscle; t-SH, tendon of sternohyoideus muscle.

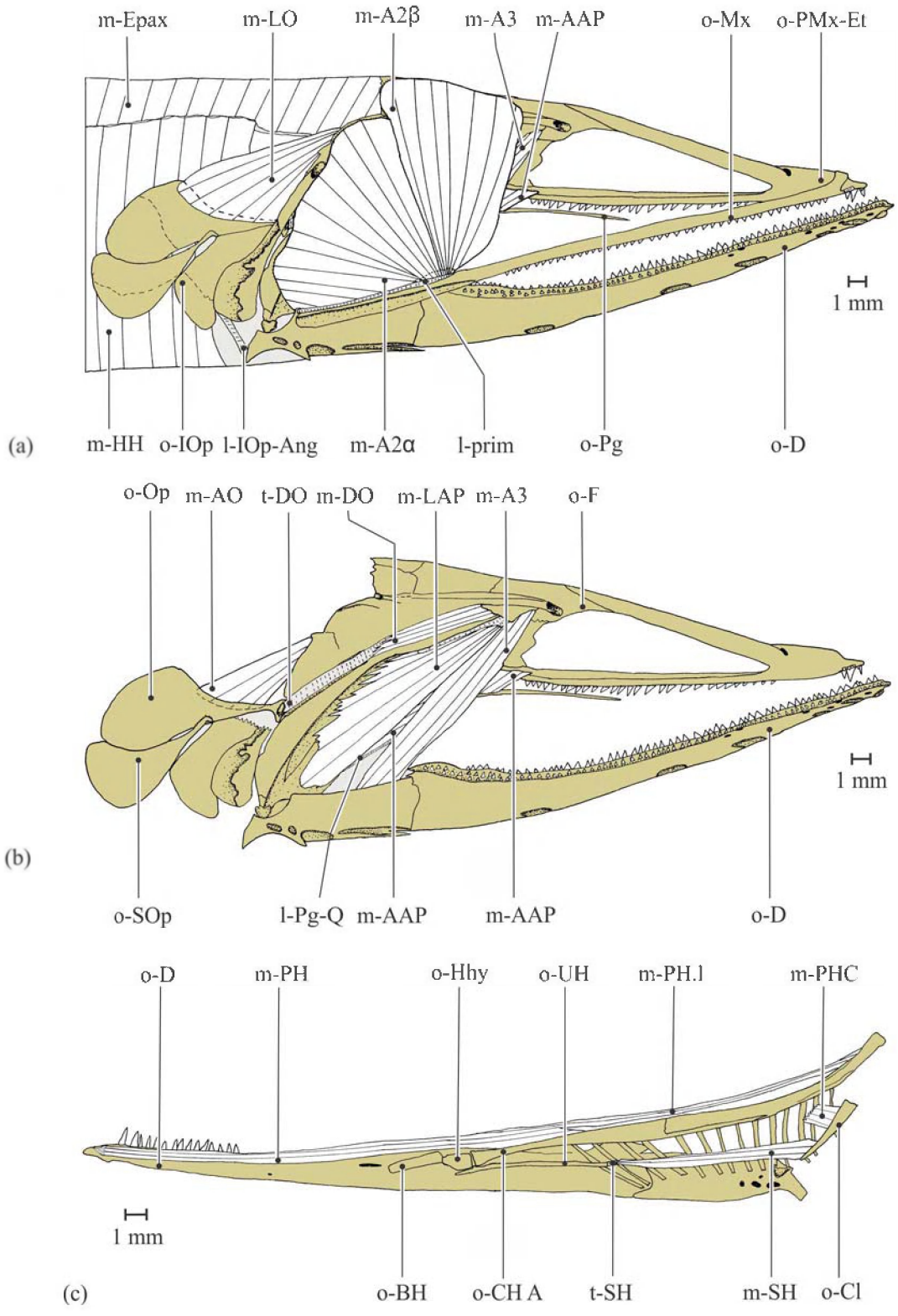
m-Epax
m-LO
m-A2β
m-A3
m-AAP
o-Mx
o-PMx-Et
1 mm
(a)
m-HH
o-IOp
l-IOp-Ang
m-A2α
l-prim
o-Pg
o-D
o-Op
m-AO
t-DO
m-DO
m-LAP
m-A3
o-F
1 mm
(b)
o-SOp
l-Pg-Q
m-AAP
m-AAP
o-D
o-D
m-PH
o-Hhy
o-UH
m-PH.l
m-PHC
1 mm
(c)
o-BH
o-CH A
t-SH
m-SH
o-Cl

Figure 5.10: The cranial muscles of *Synaphobranchus brevidorsalis*. (a) Skin removed (lateral view), (b) Sections A2, hyohyoideus muscle, levator operculi muscle, epaxial muscles, hypaxial muscles, maxillary bone and primordial ligament are removed (lateral view), and (c) ventral muscles of head; left lower jaw, anterior and posterior ceratohyal, and left muscle bundle of the protractor hyoidei (m-PH), and sternohyoideus (m-SH) are removed. l-Iop-Ang, interoperculo-angular ligament; l-prim, primordial ligament; l-Pg-Q, pterygoideo-quadrate ligament; m-AAP, adductor arcus palatini; m-A2α, ventral subsection of A2; m-A2β, dorsal subsection of A2; m-A3, A3 section of the adductor mandibulae muscle complex; m-DO, dilatator operculi muscle; m-Epax, epaxial muscles; m-HH, hyohyoideus muscle complex; m-LAP, levator arcus palatini muscle; m-AO, adductor operculi muscle; m-LO, levator operculi muscle; m-PH.l, lateral fibers of protractor hyoidei muscle; m-PHC, pharyngocleithralis; m-SH, sternohyoideus muscle; o-BH, basihyal; o-CH A, anterior ceratohyal bone; o-Cl, cleithrum bone; o-D, dentary complex; o-F, frontal bone; o-Hhy, hypohyal bone; o-IOp, interopercle; o-Mx, maxillary bone; o-Op, opercle; o-PMx-Et, premaxillo-ethmoidal complex; o-Pg, pterygoid bone; o-SOp, subopercle; o-UH, urohyal bone; t-DO, tendon of dilatator operculi muscle;t-SH, tendon of sternohyoideus muscle.

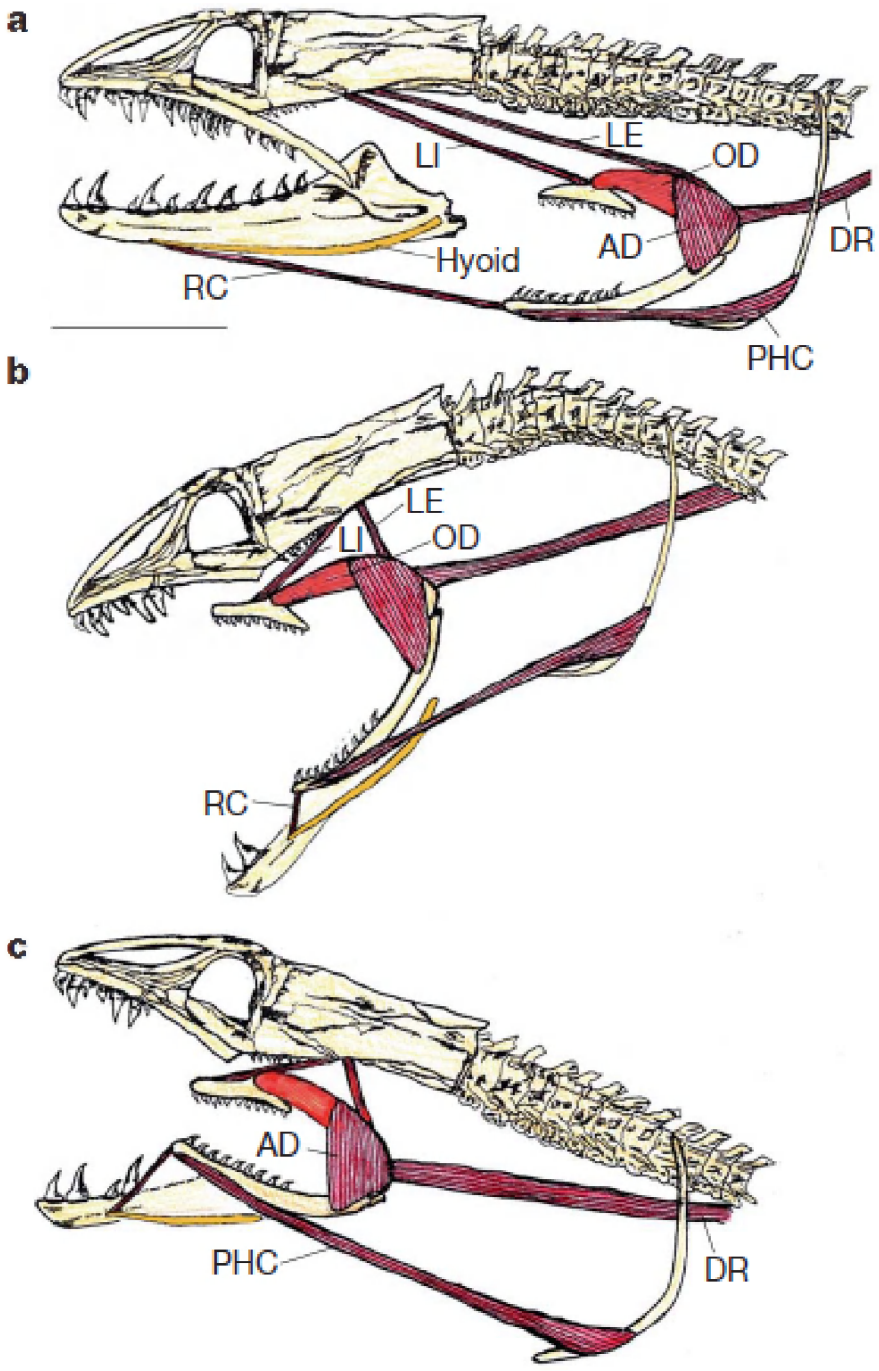
a
LE
LI
OD
AD
DR
Hyoid
RC
PHC
b
LE
LI
OD
RC
c
AD
PHC
DR

Figure 6.1. Functional morphological model of pharyngeal jaw movement in M. retifera. The left dentary has been removed in a–c, and the left maxilla has been removed in b and c. a, Pharyngeal jaw apparatus at rest. b, Pharyngeal jaw protracted: the levator internus (LI) and levator externus (LE) protract the upper jaw into the oral cavity, whereas the rectus communis (RC) protracts the lower jaw. During protraction, the upper pharyngobranchial is dorsally rotated by contraction of the LI and the obliqus dorsalis (OD). c, After prey contact, the adductor (AD) contracts to bring the upper and lower jaws together to deliver a second bite. The dorsal retractor (DR) and pharyngocleitheralis (PHC) retract the pharyngeal jaws back to their resting position behind the skull. Scale bar, 1 cm (after Mehta and Wainwright, 2007a).

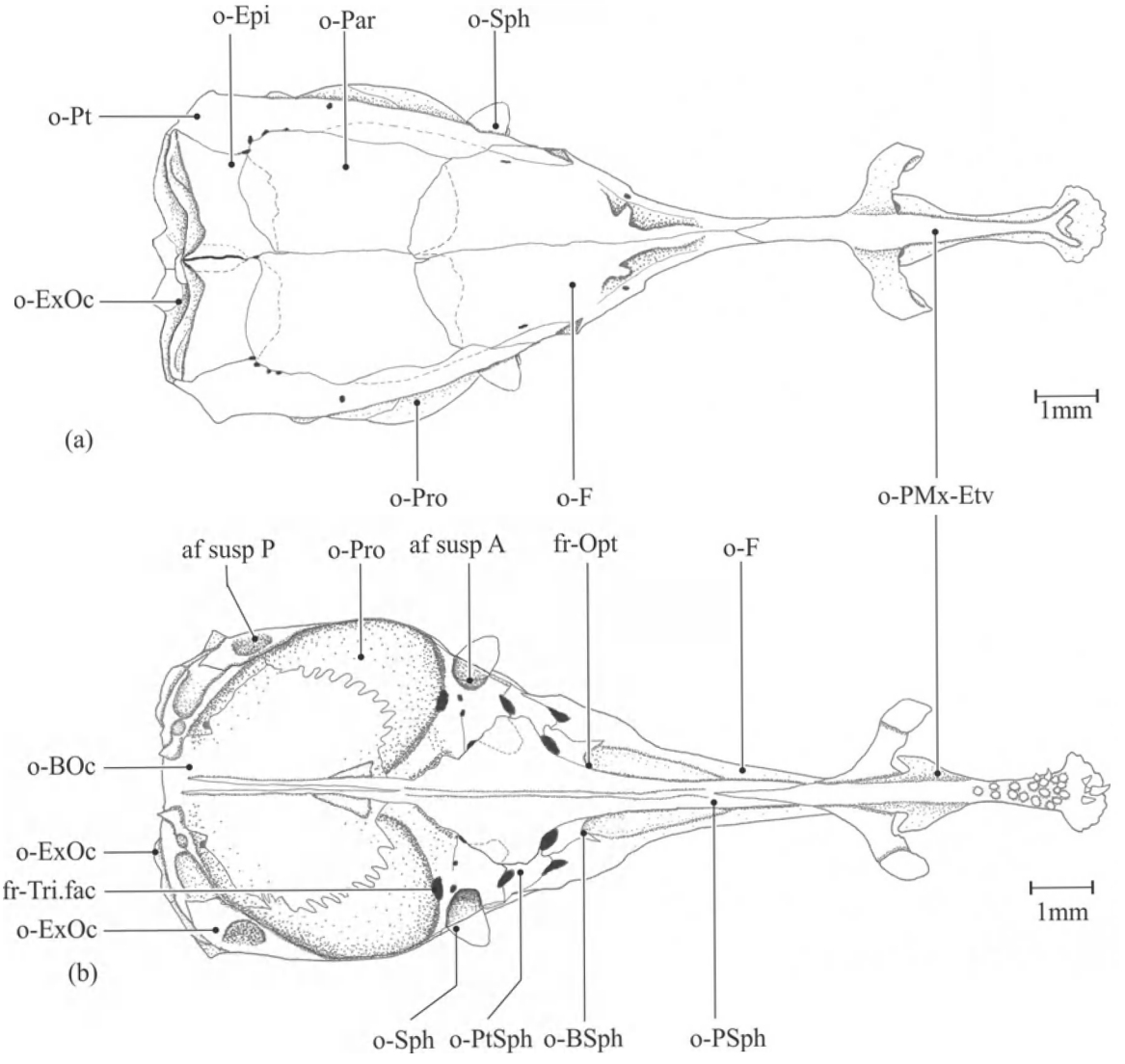

Figure 6.2: Neurocranium of *Ariosoma gilberti*. (a) Dorsal view and (b) ventral view. af susp A, anterior suspensorial articulation facet; af susp p, posterior suspensorial articulation facet; fr-Opt, foramen opticum;fr-Tri.fac, foramen trigemino-facialis; o-BOc, basioccipital bone; o-BSph, basisphenoid; o-Epi, epioccipital bone; o-ExOc, exoccipital bone; o-F, frontal bone; o-Par, parietal bone; o-PMx-Etv, premaxillo-ethmovomeral complex; o-Pro, prootic bone; o-PSph, parasphenoid; o-Pt, pterotic bone; o-PtSph, pterosphenoid; o-Sph, sphenotic bone.

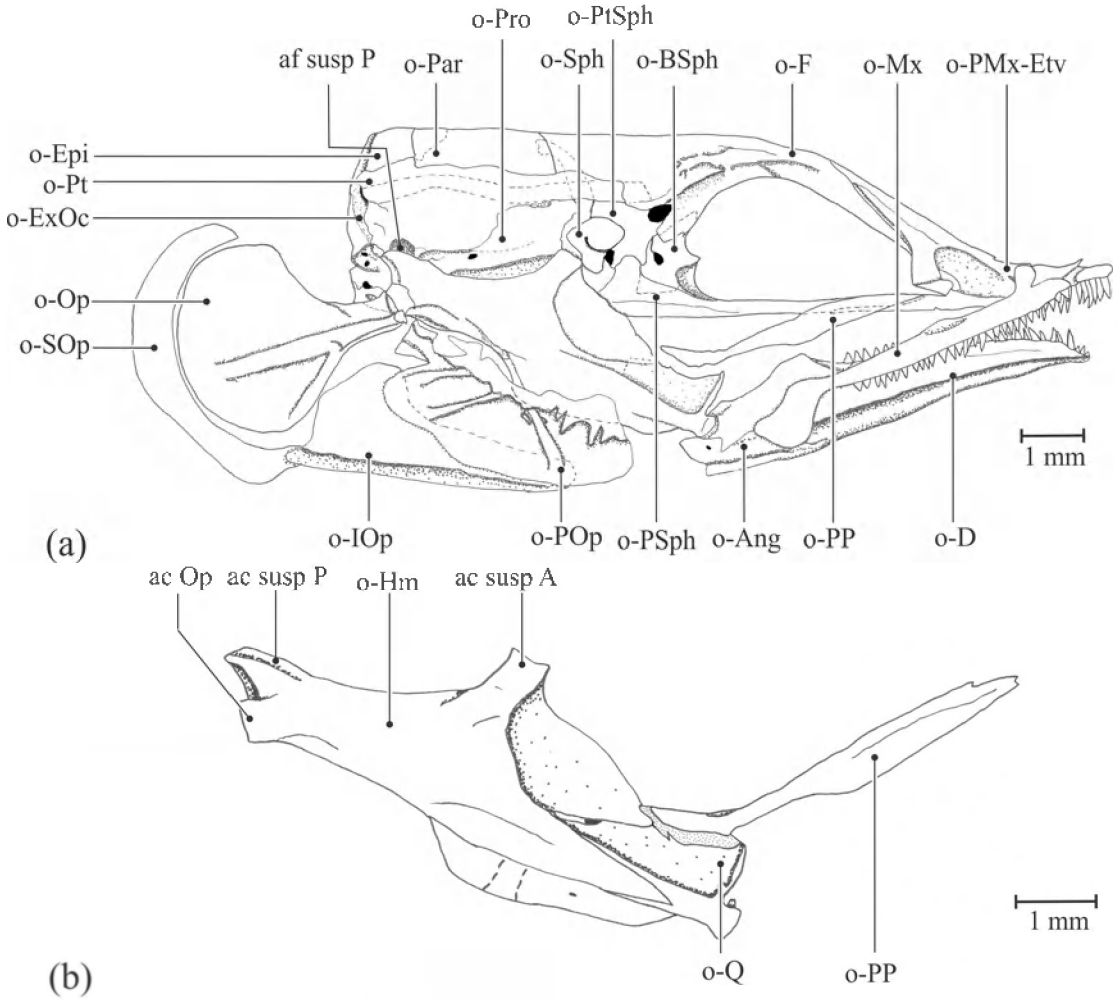

Figure 6.3: Cranial skeleton of *Ariosoma gilberti* (Lateral view). (a) Complete skull (right side) and (b) suspensorium (right side). ac Op, opercular articular condyle; af susp p, posterior suspensorial articulation facet; ac susp A, anterior suspensorial condyle; ac susp P, posterior suspensorial condyle; o-Ang, angular bony complex ; o-BSph, basisphenoid bone; o-D, dentary complex; o-Epi, epioccipital bone; o-ExOc, exoccipital bone; o-F, frontal bone; o-Hm, hyomandibular bone; o-Iop, interopercle; o-Mx, maxillary bone; o-Op, opercle; o-Par, parietal bone; o-PMx-Etv, premaxillo-ethmovomeral complex; o-POp, preopercle; o-PP, palatopterygoid; o-Pro, prootic bone; o-PSph, parasphenoid; o-Pt, pterotic bone; o-PtSph, pterosphenoid bone; o-Q, quadrate; o-SOp, subopercle; o-Sph, sphenotic bone.

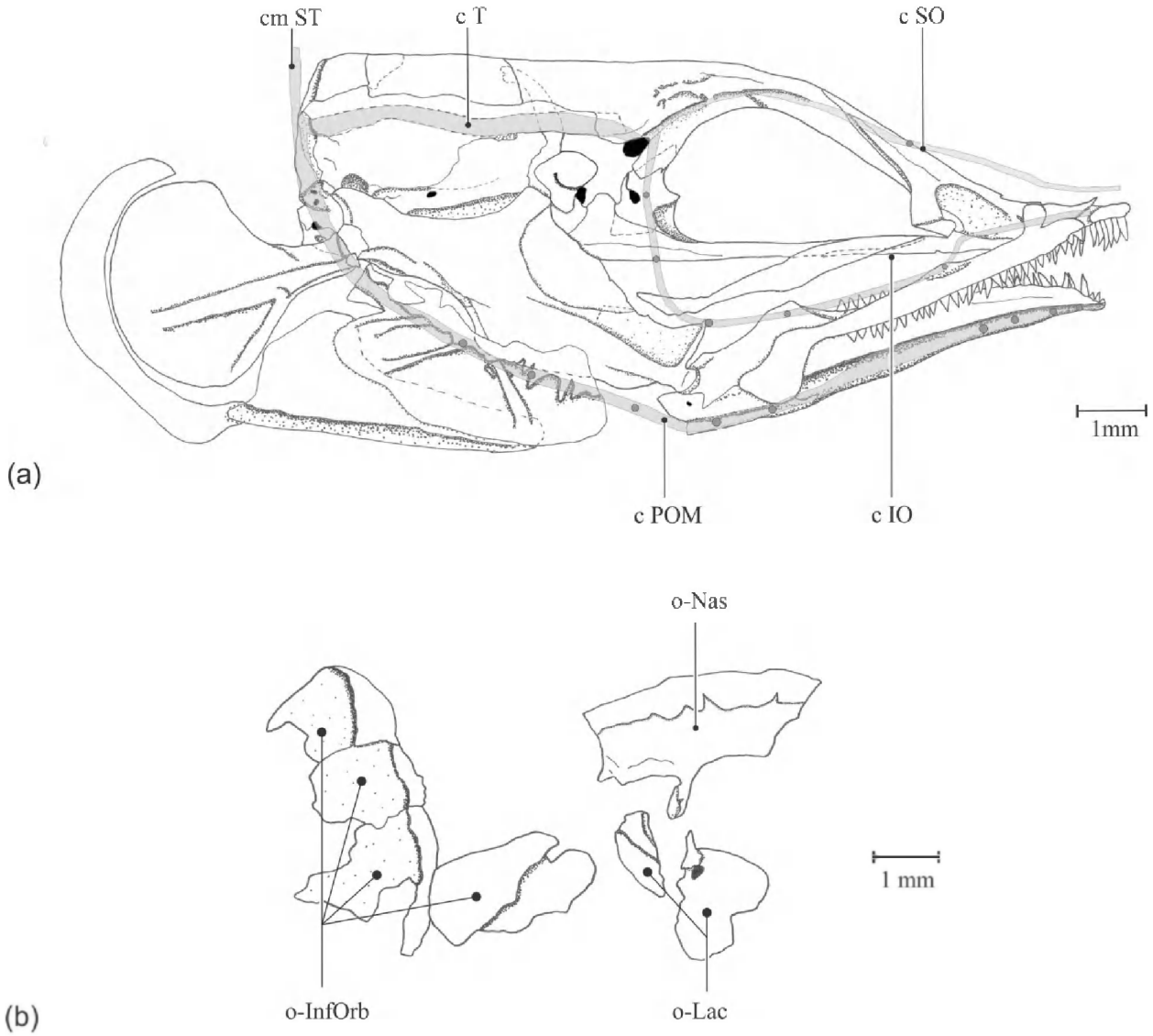

Figure 6.4: The cranial lateral line system of *Ariosoma gilberti*. (a) position of the composing canals in relation to the skull (right side, lateral view) and (b) lateral view of the nasal bone, lacrimal bones and infraorbital bones (right side) (relative position of bones do not correspond to their real position). c IO, infraorbital canal; c POM, preopercular mandibular canal; c SO, supraorbital canal; c T, temporal canal; cm ST, supratemporal commissure; o-Nas, nasal bone; o-InfOrb, infraorbital bone; o-Lac, lacrimal bone.

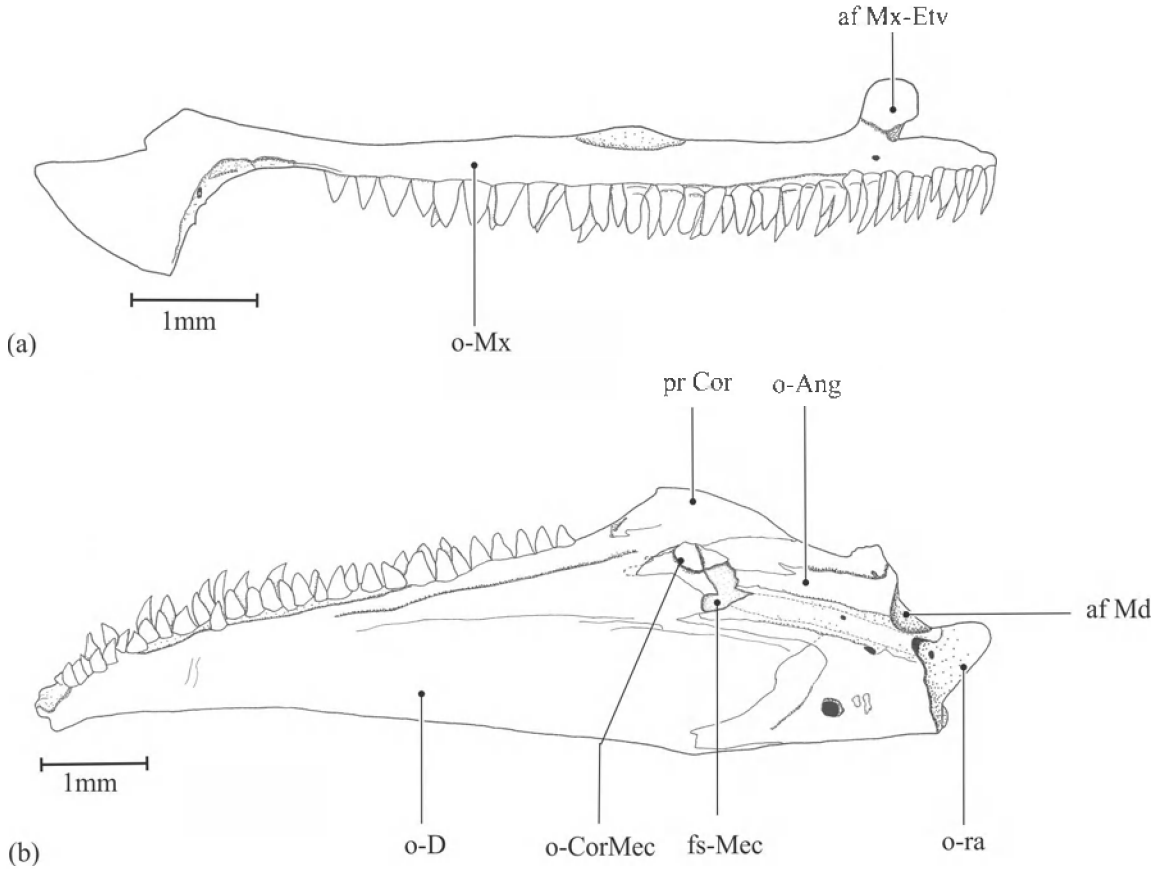

Figure 6.5: Jaws of *Ariosoma gilberti* (right side) (a-b), maxillary; medial view (a), and lower jaw; medial view (b). af Md, mandibular articulation facet; af Mx-Etv, maxillo-ethmovomeral articular facet; o-Ang, angular bony complex ; o-D, dentary complex; o-Mx, maxillary bone; o-CorMec, coronomeckelian bone; fs-Mec, meckelian fossa; pr Cor, coronoid process; o-ra, retroarticular bone.

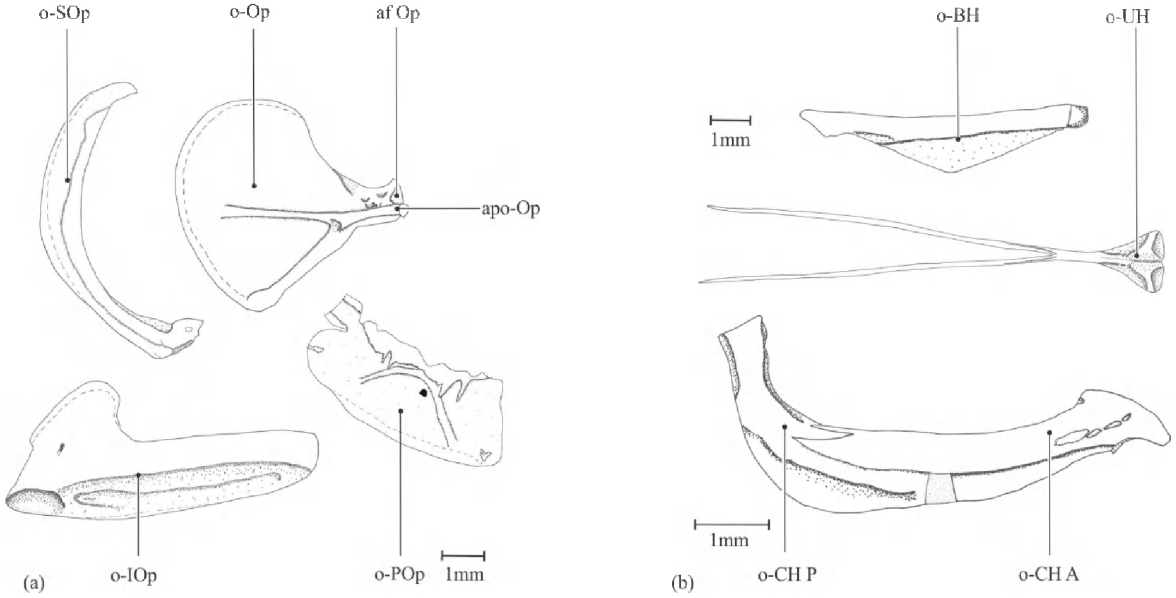

Figure 6.6: Opercular series and hyoid apparatus of *Ariosoma gilberti*. (a) Opercular series; lateral view (right side) and (b) hyoid apparatus; lateral views of the anterior ceratohyal and posterior ceratohyal bones, dorsal views of urohyal, and lateral view of basihyal (right side). af Op, opercular articular facet; apo-Op, apophysis of opercle; o-BH, basihyal bone; o-CH A, anterior ceratohyal bone; o-CH P, posterior ceratohyal bone; o-Iop, interopercle; o-Op, opercle; o-POp, preopercle; o-SOp, subopercle; o-UH, urohyal bone.

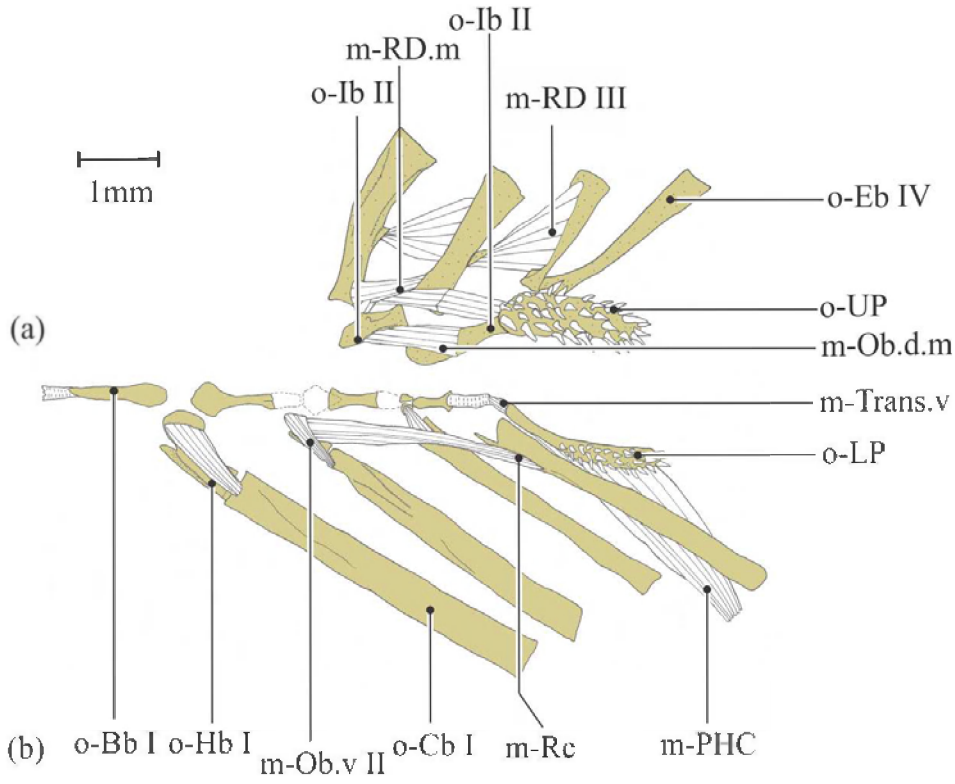

Figure 6.7: Gill arches and associated muscles of *Ariosoma gilberti*. (a) Dorsal view of the ventral part and (b) ventral view of the dorsal part of the gill arch. o-Bb, basibranchial bone; o-Cb, ceratobranchial bone; o-Eb, epibranchial bone; o-Hb, hypobranchial bone; o-Ib, infrapharyngobranchial bone; o-LP, lower pharyngeal tooth plates; o-UP, upper pharyngeal tooth plates; m-Ob.d.m, medial obliqus dorsalis muscle; m-Ob.v, ventral obliqus dorsalis muscle; m-PHC, pharyngocleithralis muscle; m-Rc, rectus communis muscle; m-RD, rectus dorsalis muscle; m-RD.m, medial rectus dorsalis muscle; m-Trans.v, transversus ventralis muscle.

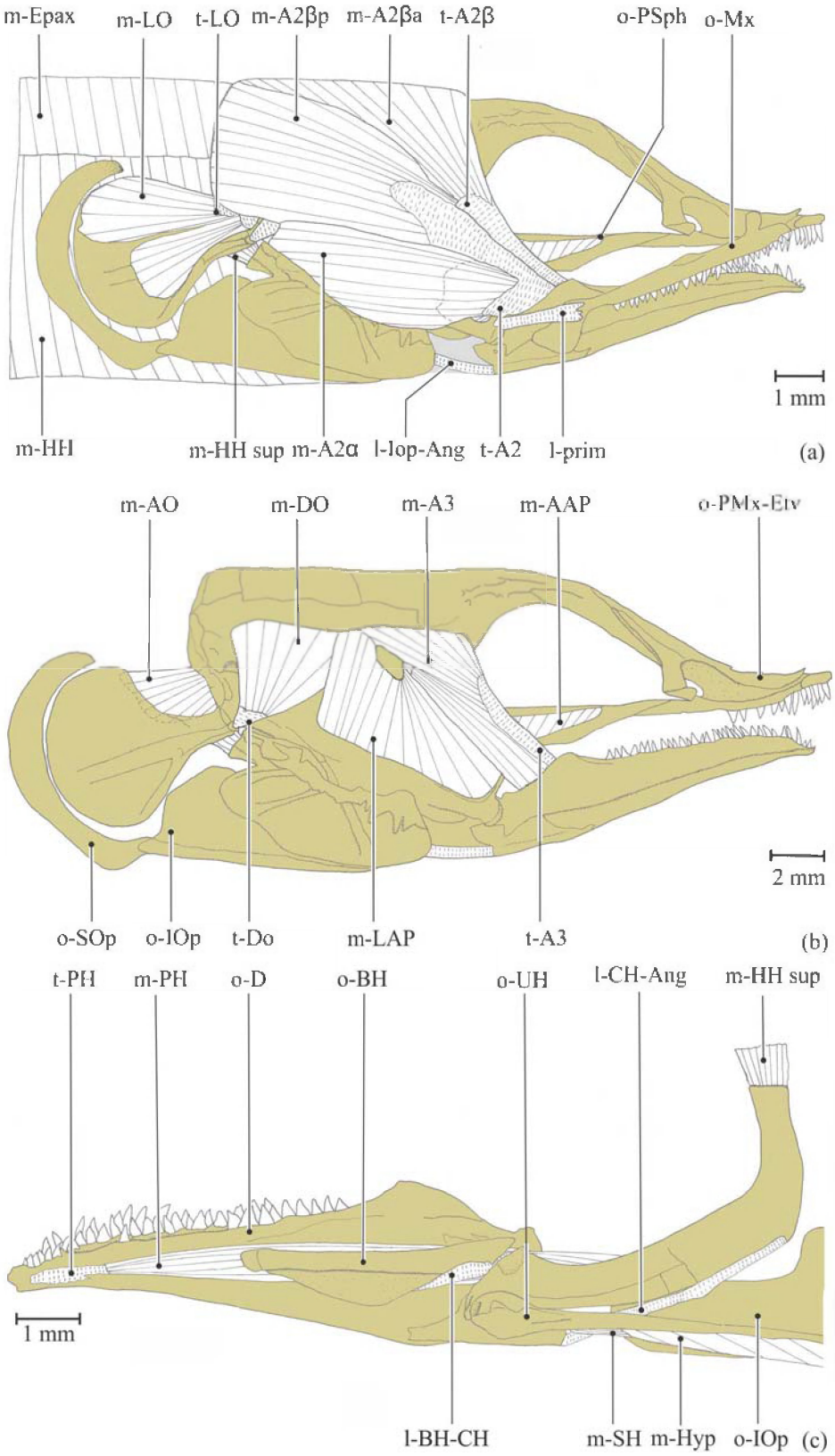
m-Epax
m-LO
t-LO
m-A2βp
m-A2βa
t-A2β
o-PSph
o-Mx
1 mm
m-HH
m-HH sup
m-A2α
l-Iop-Ang
t-A2
l-prim
(a)
m-AO
m-DO
m-A3
m-AAP
o-PMx-Etv
2 mm
o-SOp
o-IOp
t-Do
m-LAP
t-A3
(b)
t-PH
m-PH
o-D
o-BH
o-UH
l-CH-Ang
m-HH sup
1 mm
l-BH-CH
m-SH
m-Hyp
o-IOp
(c)

Figure 6.8: The cranial muscles of *Ariosoma gilberti*. (a) Skin removed (lateral view), (b) sections A2, hyohyoideus muscle complex, epaxial muscles, hypaxial muscles, ventral muscles of the head, branchiostegal rays and primordial ligament are removed (lateral view) and (c) ventral muscles of head (sagittal left cut), hyohyoideus muscle complex is removed and (d) Position of the muscles on the medial face of the suspensorium. l-CH-Ang, ceratohyalo-angular ligament; l-BH-CH, basihyalo-ceratohyal ligament; l-Iop-Ang, interoperculo-angular ligament; l-prim, primordial ligament; m-A2α, ventral subsection of A2; m-A2βa, anterior part of dorsal subsection of A2β; m-A2βp, posterior part of dorsal subsection of A2β; m-A3, A3 section of the adductor mandibulae muscle complex; m-AAP, adductor arcus palatini muscle; m-AO, adductor operculi muscle; m-DO, dilatator operculi muscle; m-Epax, epaxial muscles; m-HH, hyohyoideus muscle complex; m-HH sup, hyohyoideus superior muscle; m-Hyp, hypaxial muscles; m-LAP, levator arcus palatini muscle; m-LO, levator operculi muscle; m-PH, protractor hyoidei muscle; m-SH, sternohyoideus muscle; o-BH, basihyal bone; o-D, dentary complex; o-IOp, interopercle; o-Mx, maxillary bone; o-PMx-Etv, premaxillo-ethmovomeral complex; o-PSph, parasphenoid bone; o-SOp, subopercle; o-UH, urohyal bone ; t-A2, tendon of A2 ; t-A2β, tendon of A2β; t-A3, tendon of A3; t-DO, tendon of dilatator operculi muscle; t-LO, tendon of levator operculi; t-PH, tendon of protractor hyoidei.

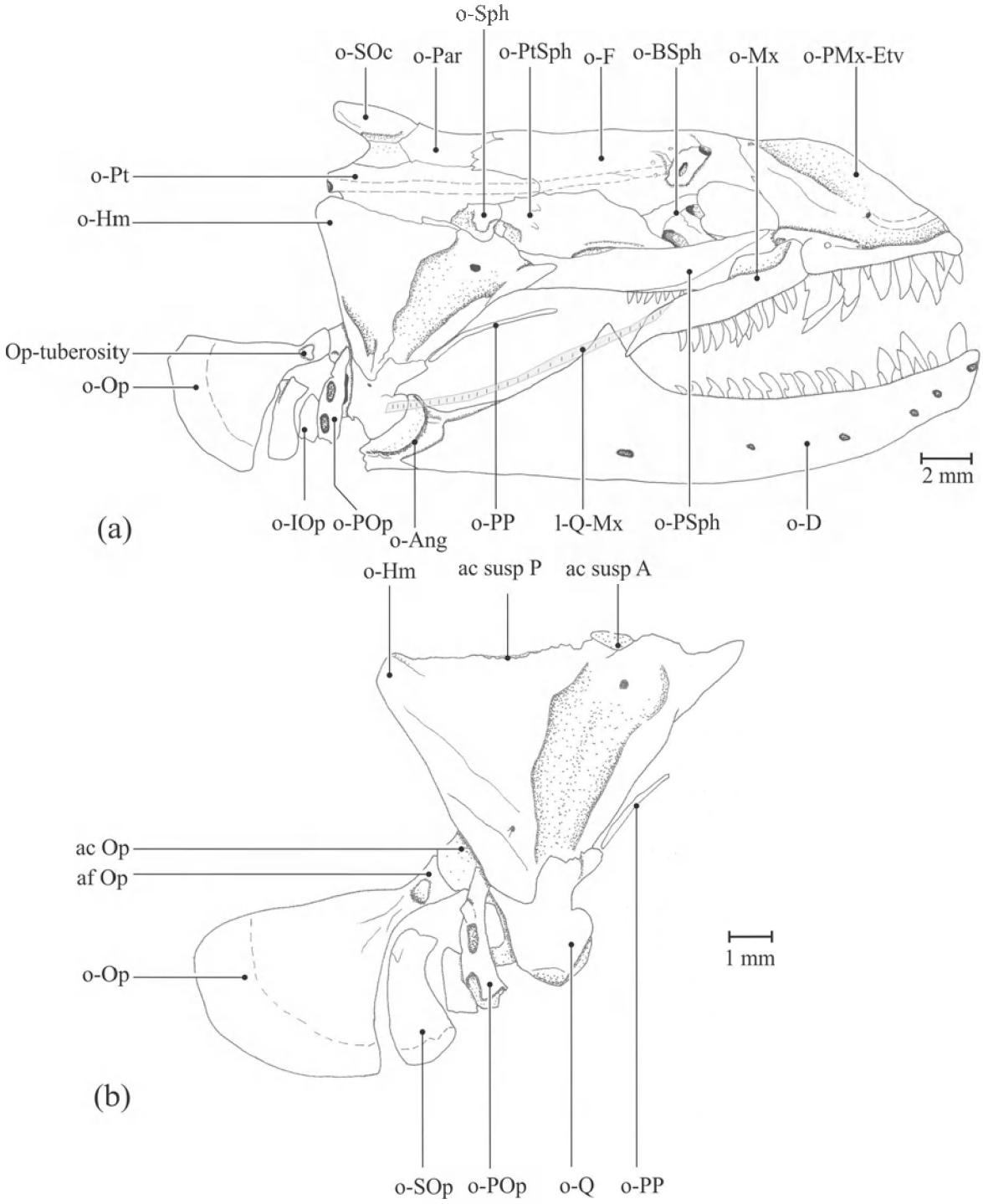
o-Sph
o-SOc
o-Par
o-PtSph
o-F
o-BSph
o-Mx
o-PMx-Etv
o-Pt
o-Hm
Op-tuberosity
o-Op
2 mm
(a)
o-IOp
o-POp
o-Ang
o-PP
l-Q-Mx
o-PSph
o-D
o-Hm
ac susp P
ac susp A
ac Op
af Op
o-Op
1 mm
(b)
o-SOp
o-POp
o-Q
o-PP

Figure 6.9: Cranial skeleton of *Gymnothorax prasinus* (lateral view). (a) Complete skull (right side) and (b) suspensorium (right side). ac Op, opercular articular condyle; af Op, opercular articular facet; ac susp A, anterior suspensorial condyle; ac susp P, posterior suspensorial condyle; l-Q-Mx, quadrato-maxillary ligament; o-Ang, Angular bony complex; o-BSph, basisphenoid bone; o-D, dentary complex; o-F, frontal bone; o-Hm, hyomandibular bone; o-Iop, interopercle; o-Mx, maxillary bone; o-Op, opercle; o-Par, parietal bone; o-PMx-Etv, premaxillo-ethmovomeral complex; o-POp, preopercle; o-PP, palatopterygoid; o-PSph, parasphenoid; o-Pt, pterotic bone; o-PtSph, pterosphenoid bone; o-Q, quadrate; o-SOp, subopercle; o-Soc, supraoccipital bone; o-Sph, sphenotic bone ; Op-tuberosity, opercular tuberosity.

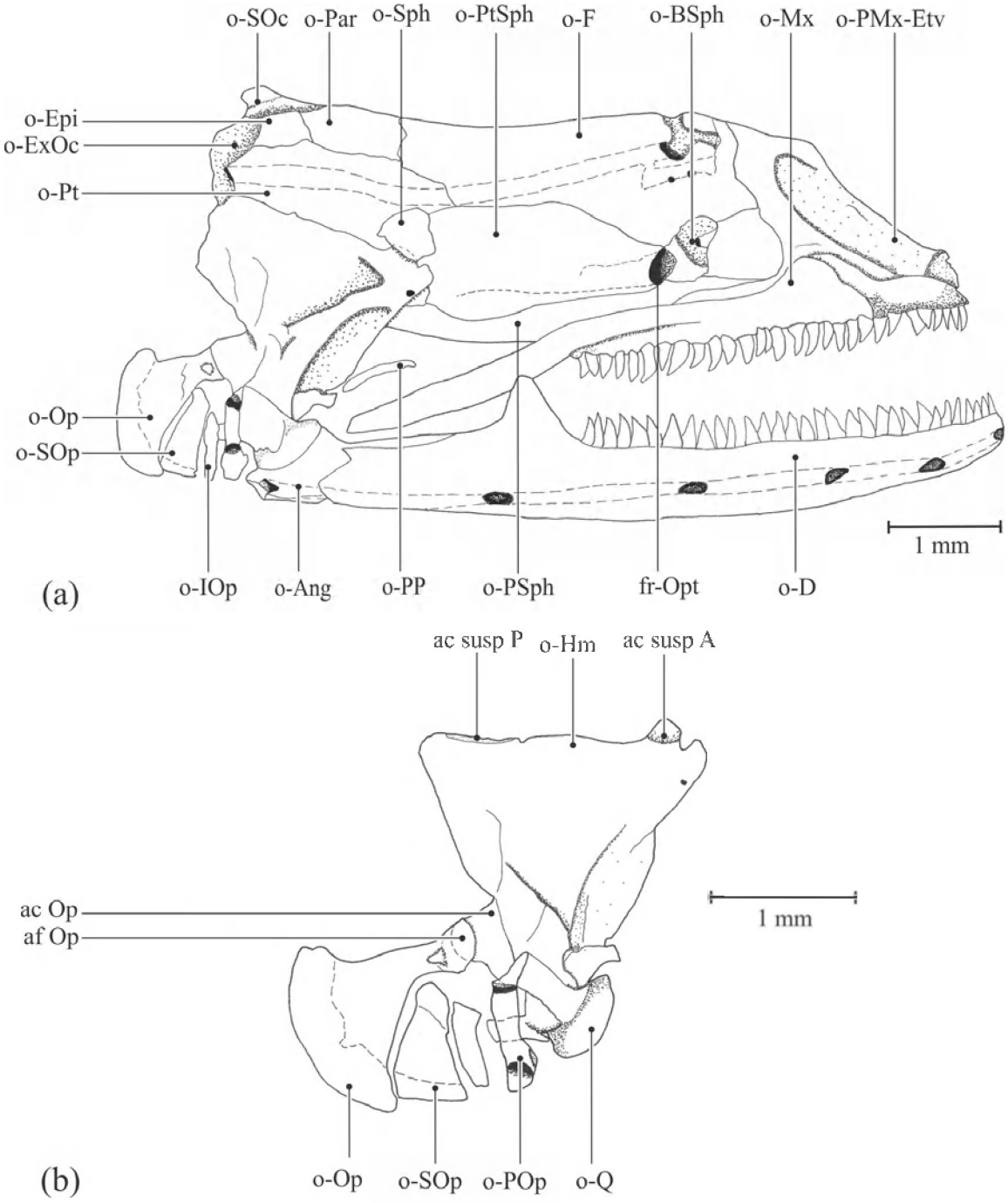
o-SOc
o-Par
o-Sph
o-PtSph
o-F
o-BSph
o-Mx
o-PMx-Etv
o-Epi
o-ExOc
o-Pt
o-Op
o-SOp
1 mm
(a)
o-IOp
o-Ang
o-PP
o-PSph
fr-Opt
o-D
ac susp P
o-Hm
ac susp A
ac Op
af Op
1 mm
(b)
o-Op
o-SOp
o-POp
o-Q

Figure 6.10: Cranial skeleton of *Anarchias allardicei* (lateral view). (a) Complete skull (right side) and (b) suspensorium (right side). ac Op, opercular articular condyle; af Op, opercular articular facet; ac susp A, anterior suspensorial condyle; ac susp P, posterior suspensorial condyle; fr-Opt, foramen opticum; o-Ang, angular bony complex ; o-BSph, basisphenoid bone; o-D, dentary complex; o-ExOc, exoccipital bone; o-F, frontal bone; o-Hm, hyomandibular bone; o-Iop, interopercle; o-Mx, maxillary bone; o-Op, opercle; o-Par, parietal bone; o-PMx-Etv, premaxillo-ethmovomeral complex; o-POp, preopercle; o-PP, palatopterygoid; o-PSph, parasphenoid; o-Pt, pterotic bone; o-PtSph, pterosphenoid bone; o-Q, quadrate; o-SOp, subopercle; o-Soc, supraoccipital bone; o-Sph, sphenotic bone.

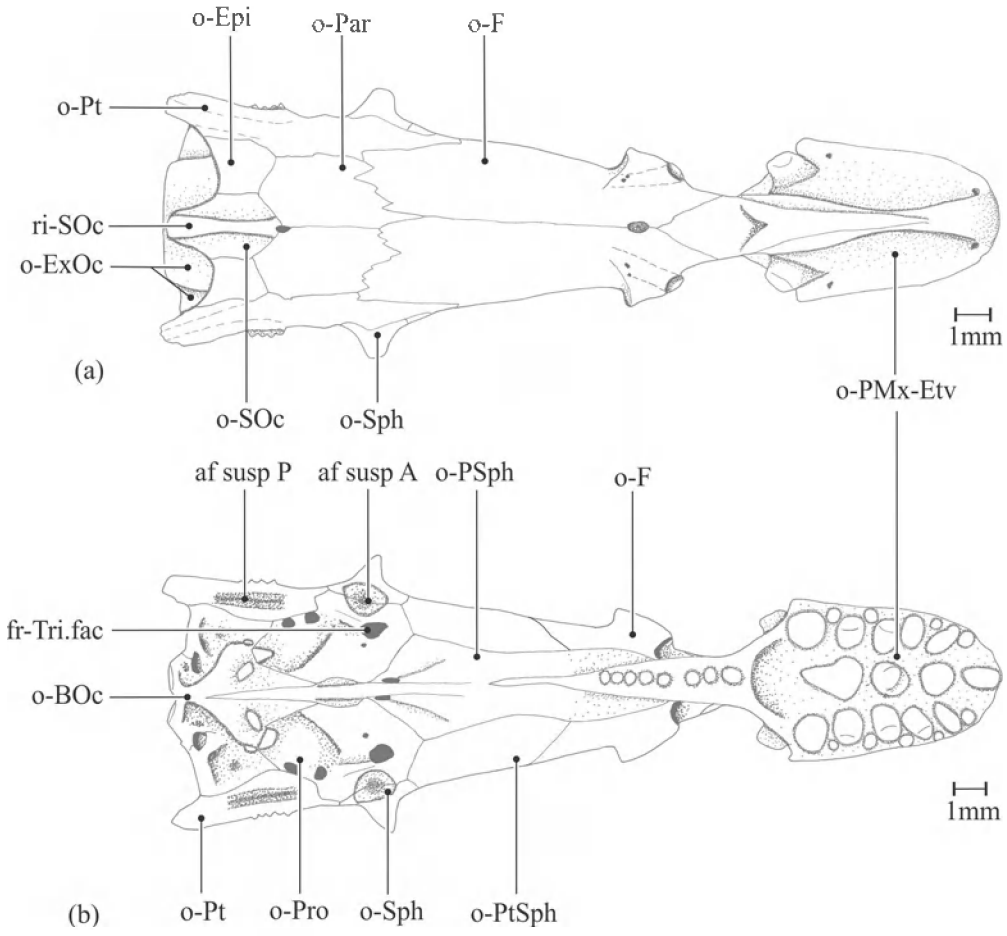

Figure 6.11: Neurocranium of *Gymnothorax prasinus*. (a) Dorsal view and (b) ventral view. af susp A, anterior suspensorial articulation facet; af susp p, posterior suspensorial articulation facet; fr-Tri.fac, foramen trigemino-facialis; o-BOc, basioccipital bone; o-Epi, epioccipital bone; o-ExOc, exoccipital bone; o-F, frontal bone; o-Par, parietal bone; o-PMx-Etv, premaxillo-ethmovomeral complex; o-Pro, prootic bone; o-PSph, parasphenoid; o-Pt, pterotic bone; o-PtSph, pterosphenoid; o-Soc, supraoccipital bone; o-Sph, sphenotic bone ; ri-Soc, supraoccipital crest.

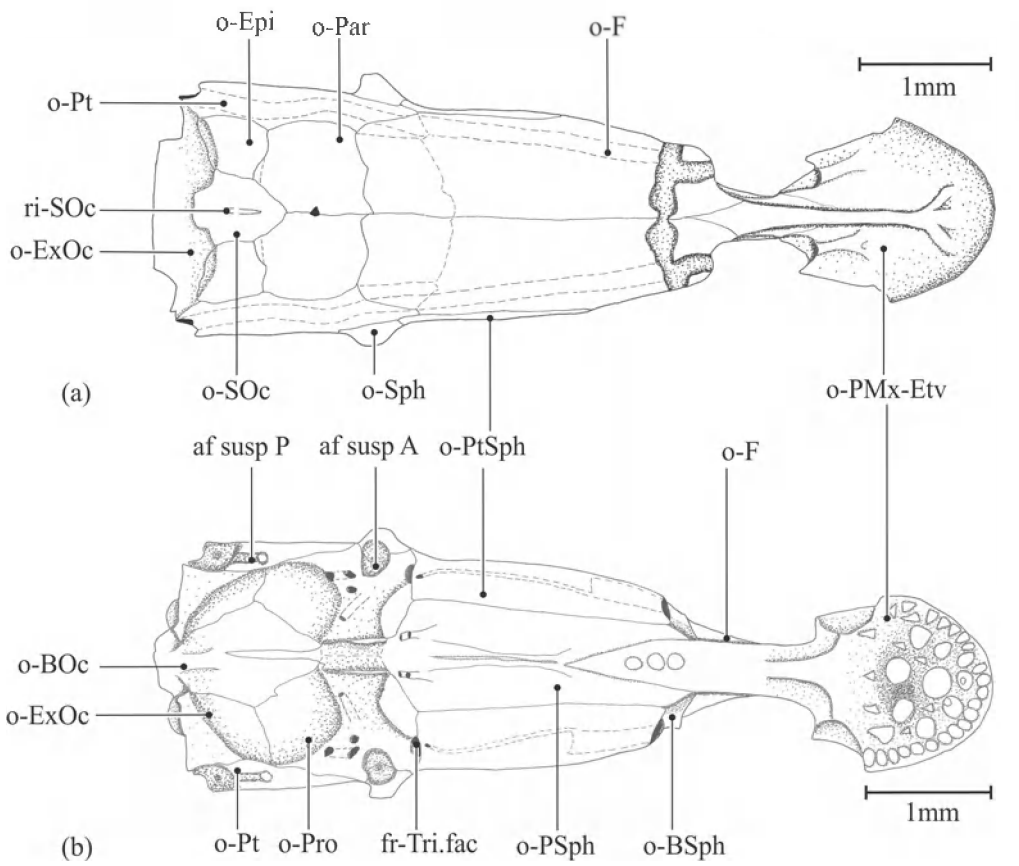

Figure 6.12: Neurocranium of *Anarchias allardicei*. (a) Dorsal view and (b) ventral view. af susp A, anterior suspensorial articulation facet; af susp p, posterior suspensorial articulation facet; fr-Tri.fac, foramen trigemino-facialis; o-BOc, basioccipital bone; o-BSph, basisphenoid; o-Epi, epioccipital bone; o-ExOc, exoccipital bone; o-F, frontal bone; o-Par, parietal bone; o-PMx-Etv, premaxillo-ethmovomeral complex; o-Pro, prootic bone; o-PSph, parasphenoid; o-Pt, pterotic bone; o-PtSph, pterosphenoid; o-Soc, supraoccipital bone; o-Sph, sphenotic bone ; ri-Soc, supraoccipital crest.

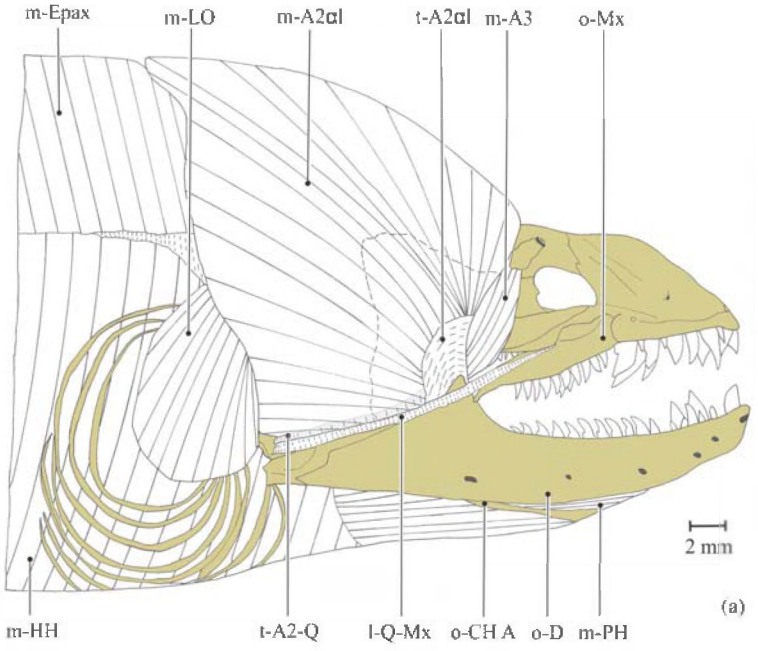
m-Epax
m-LO
m-A2αI
t-A2αI
m-A3
o-Mx
2 mm
m-HH
t-A2-Q
l-Q-Mx
o-CH A
o-D
m-PH
(a)

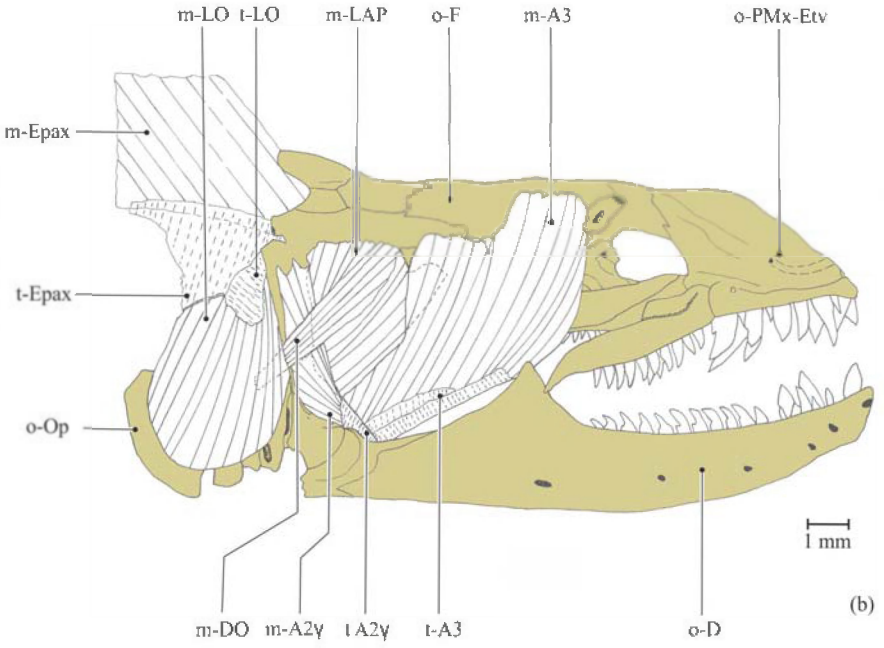
m-LO
t-LO
m-LAP
o-F
m-A3
o-PMx-Etv
m-Epax
t-Epax
o-Op
1 mm
m-DO
m-A2γ
t A2γ
t-A3
o-D
(b)

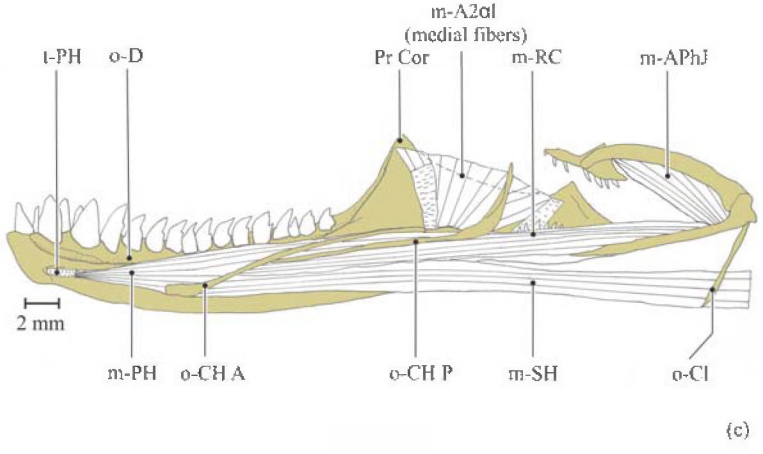
m-A2αI
(medial fibers)
t-PH
o-D
Pr Cor
m-RC
m-APhJ
2 mm
m-PH
o-CH A
o-CH P
m-SH
o-Cl
(c)

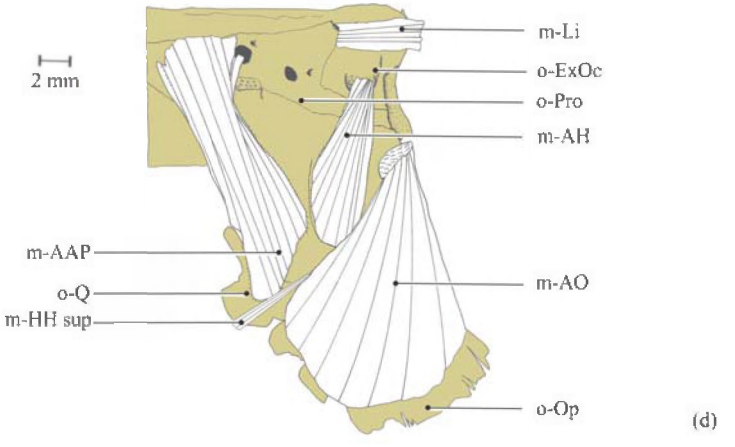
2 mm
m-Li
o-ExOc
o-Pro
m-AH
m-AAP
o-Q
m-HH sup
m-AO
o-Op
(d)

Figure 6.13: The cranial muscles of *Gymnothorax prasinus*. (a) Skin removed (lateral view), (b) sections A2 except the subsection A2m, hyohyoideus muscle complex, hypaxial muscles, ventral elements of the head and quadrate-maxillary ligament and branchiostegal rays are removed (lateral view), (c) Ventral muscles of head (sagittal left cut), hyohyoideus muscle complex is removed. l-Q-Mx, quadrato-maxillary ligament; m-A2αl, lateral subsection of A2α; m-A2γ, medial subsection of A2; m-A3, A3 section of the adductor mandibulae muscle complex; m-AAP, adductor arcus palatini muscle; m-AH, adductor hyomandibulae muscle; m-AO, adductor operculi muscle; m-APhJ, adductor muscle of the pharyngeal jaw; m-DO, dilatator operculi muscle; m-Epax, epaxial muscles; m-HH, hyohyoideus muscle complex; m-HH sup, hyohyoideus superior muscle; m-LAP, levator arcus palatini muscle; m-Li, levator internus muscle; m-LO, levator operculi muscle; m-PH, protractor hyoidei muscle; m-RC, rectus communis muscle; m-SH, sternohyoideus muscle; o-CH A, anterior ceratohyal bone; o-CH P, posterior ceratohyal bone; o-Cl, cleithrum; o-D, dentary complex; o-ExOc, exoccipital bone; o-F, frontal bone; o-Mx, maxillary bone; o-Op, opercle; o-PMx-Etv, premaxillo-ethmovomeral complex; o-Pro, prootic bone; o-Q, quadrate bone; t-A2αl, tendon of A2αl ; t-A2-Q, A2-quadrate tendon; t-A2γ, tendon of A2γ; t-A3, tendon of A3; t-Epax, tendon of epaxial muscles ; t-LO, tendon of levator operculi; t-PH, tendon of protractor hyoidei; pr Cor, coronoid process.

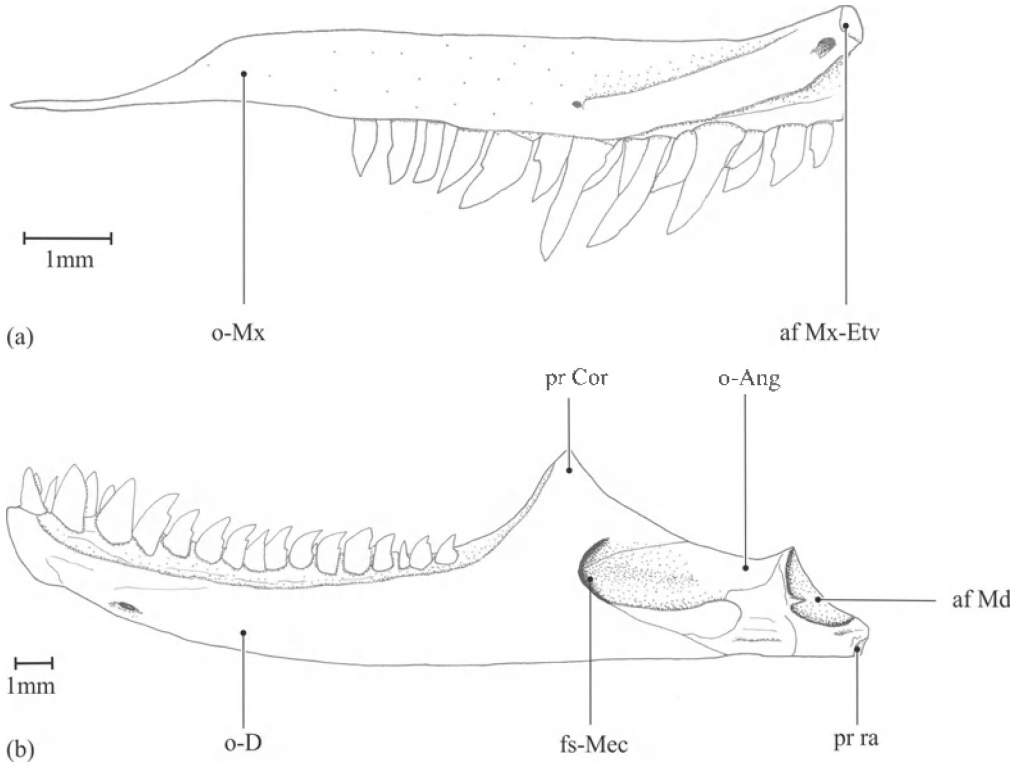

Figure 6.14: Jaws of *Gymnothorax prasinus* (right side) (a-b), maxillary; lateral view (a), and lower jaw; medial view (b). af Md, mandibular articulation facet; af Mx-Etv, maxillo-ethmovomeral articular facet; o-Ang, angular bony complex ; o-D, dentary complex; o-Mx, maxillary bone; fs-Mec, meckelian fossa; pr Cor, coronoid process; pr ra, retroarticular process.

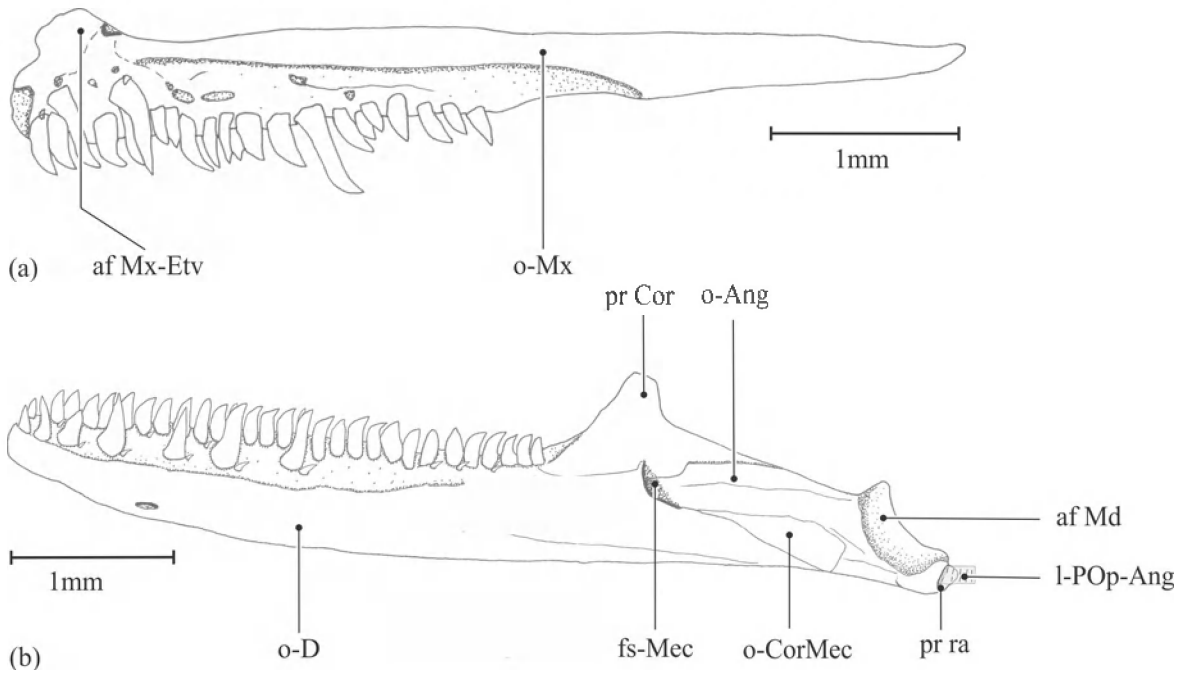

Figure 6.15: Jaws of *Anarchias allardicei* (right side) (a-b), maxillary; medial view (a), and lower jaw; medial view (b). af Md, mandibular articulation facet; af Mx-Etv, maxillo-ethmovomeral articular facet; l-Pop-Ang, preoperculo-angular ligament; o-Ang, angular bony complex ; o-D, dentary complex; o-CorMec, coronomeckelian bone; o-Mx, maxillary bone; fs-Mec, meckelian fossa; pr Cor, coronoid process; pr ra, retroarticular process.

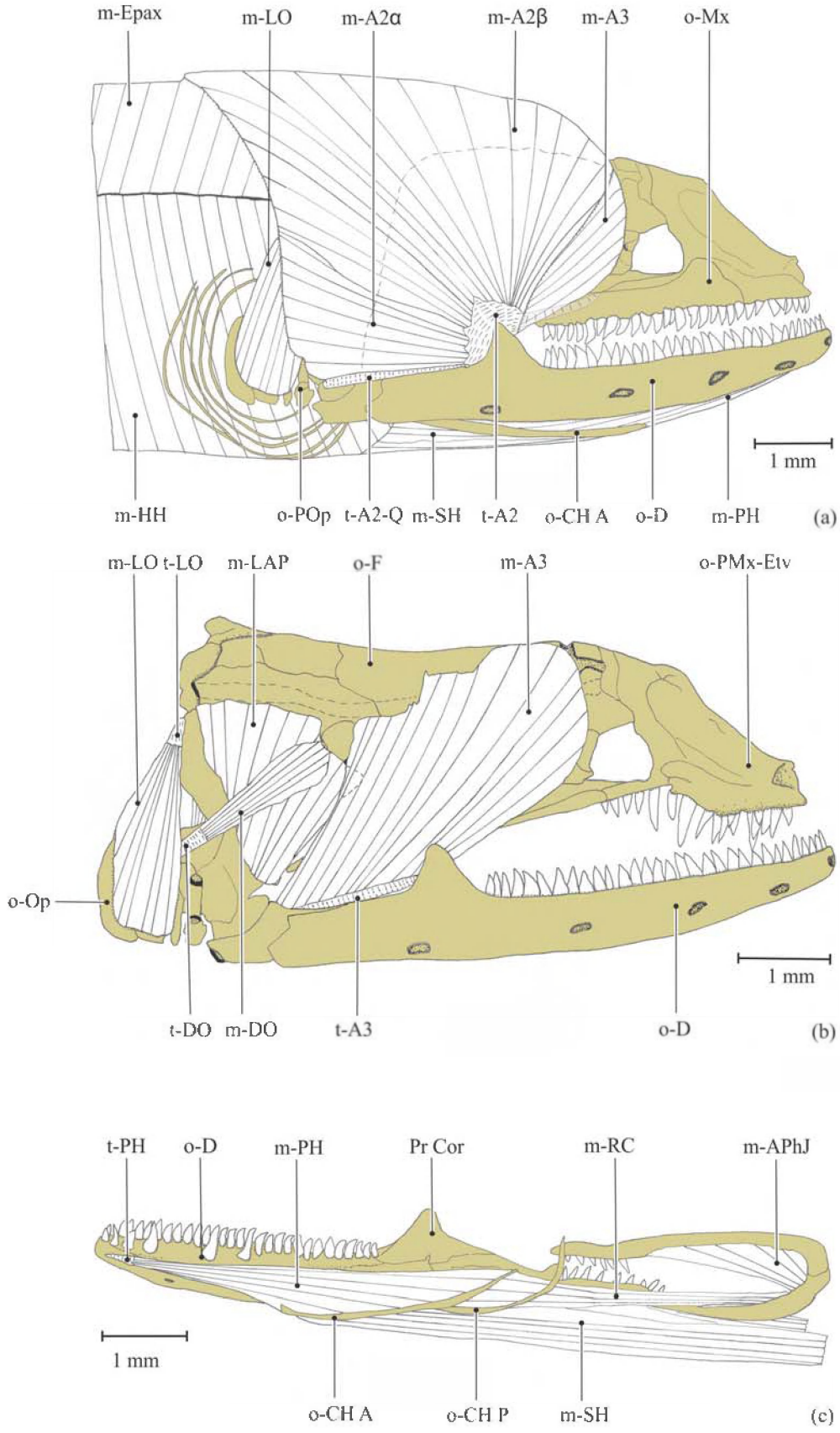
m-Epax
m-LO
m-A2α
m-A2β
m-A3
o-Mx
1 mm
m-HH
o-POp
t-A2-Q
m-SH
t-A2
o-CH A
o-D
m-PH
(a)
m-LO t-LO
m-LAP
o-F
m-A3
o-PMx-Etv
o-Op
1 mm
t-DO
m-DO
t-A3
o-D
(b)
t-PH
o-D
m-PH
Pr Cor
m-RC
m-APhJ
1 mm
o-CH A
o-CH P
m-SH
(c)

Figure 6.16: The cranial muscles of *Anarchias allardicei*. (a) Skin removed (lateral view), (b) sections A2, hyohyoideus muscle complex, epaxial muscles, hypaxial muscles, ventral elements of the head and quadrato-maxillary ligament and branchiostegal rays are removed (lateral view) and (c) ventral muscles of head (sagittal left cut) and position of the pharyngeal jaws in relation to the lower jaw and hyoid apparatus, hyohyoideus muscle complex is removed. m-A2α, ventral subsection of A2; m-A2β, dorsal subsection of A2; m-A3, A3 section of the adductor mandibulae muscle complex; m-APhJ, adductor muscle of the pharyngeal jaw; m-DO, dilatator operculi muscle; m-Epax, epaxial muscles; m-HH, hyohyoideus muscle complex; m-LAP, levator arcus palatini muscle; m-LO, levator operculi muscle; m-PH, protractor hyoidei muscle; m-RC, rectus communis muscle; m-SH, sternohyoideus muscle; o-CH A, anterior ceratohyal bone; o-CH P, posterior ceratohyal bone; o-D, dentary complex; o-F, frontal bone; o-Mx, maxillary bone; o-Op, opercle; o-PMx-Etv, premaxillo-ethmovomeral complex; o-POp, preopercle; t-A2, tendon of A2; t-A2-Q, A2-quadrate tendon; t-A3, tendon of A3; t-DO, tendon of dilatator operculi muscle; t-LO, tendon of levator operculi; t-PH, tendon of protractor hyoidei; pr Cor, coronoid process.

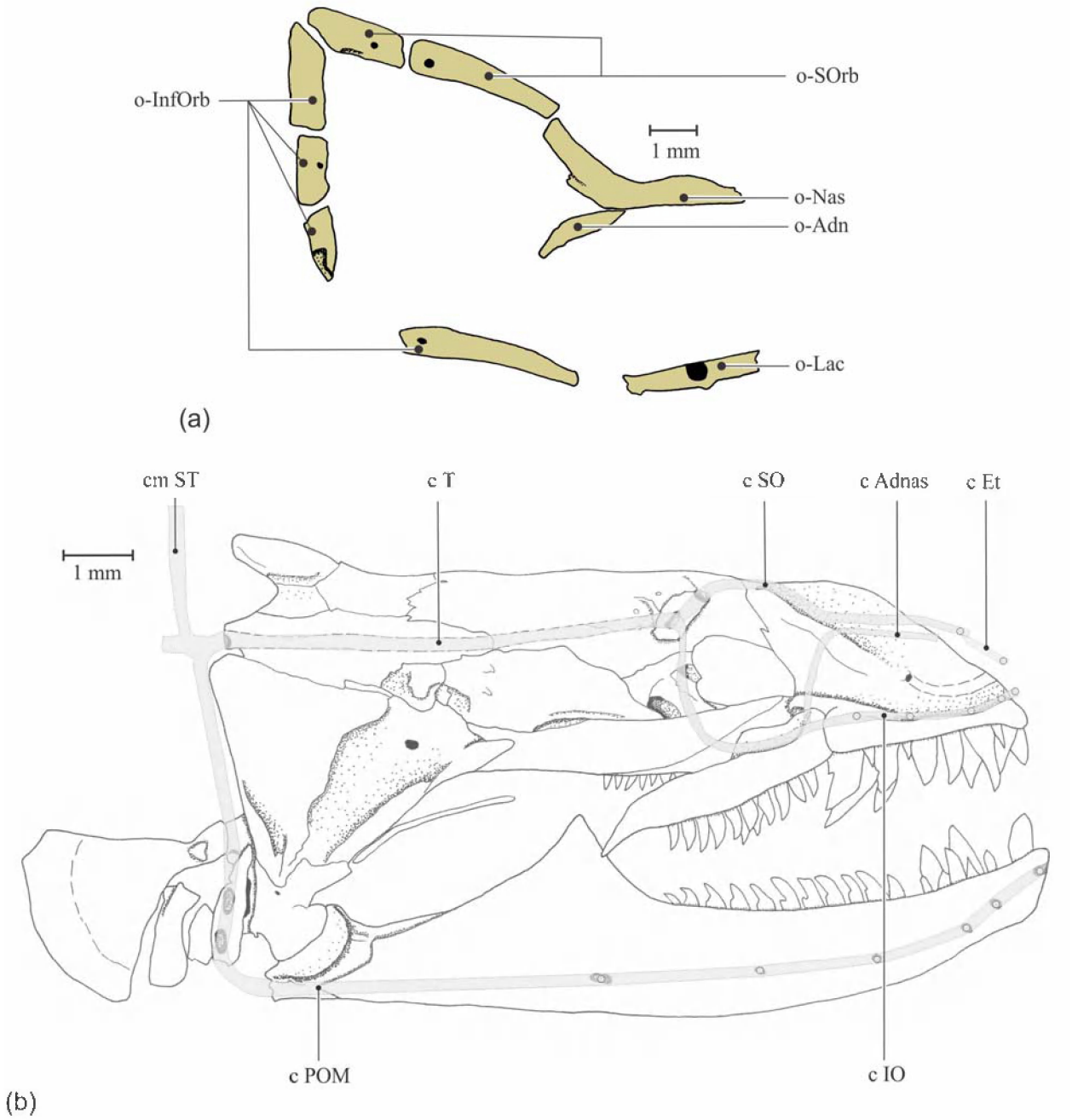

Figure 6.17: The cranial lateral line system and circumorbital bones of *Gymnothorax prasinus*. (a) Lateral view of the nasal bone, preorbital bones, infraorbital bone, postorbital bones and supraorbital bones (right side) and (b) position of the composing canals in relation to the skull (right side, lateral view). c Adnas, adnasal canal; c Et, ethmoid canal; c IO, infraorbital canal; c POM, preopercular mandibular canal; c SO, supraorbital canal; c T, temporal canal; cm ST, supratemporal commissure; o-Nas, nasal bone; o-Adn, adnasal bone; o-InfOrb, infraorbital bone; o-Lac, lacrimal bone; o-SOrb, supraorbital bone.

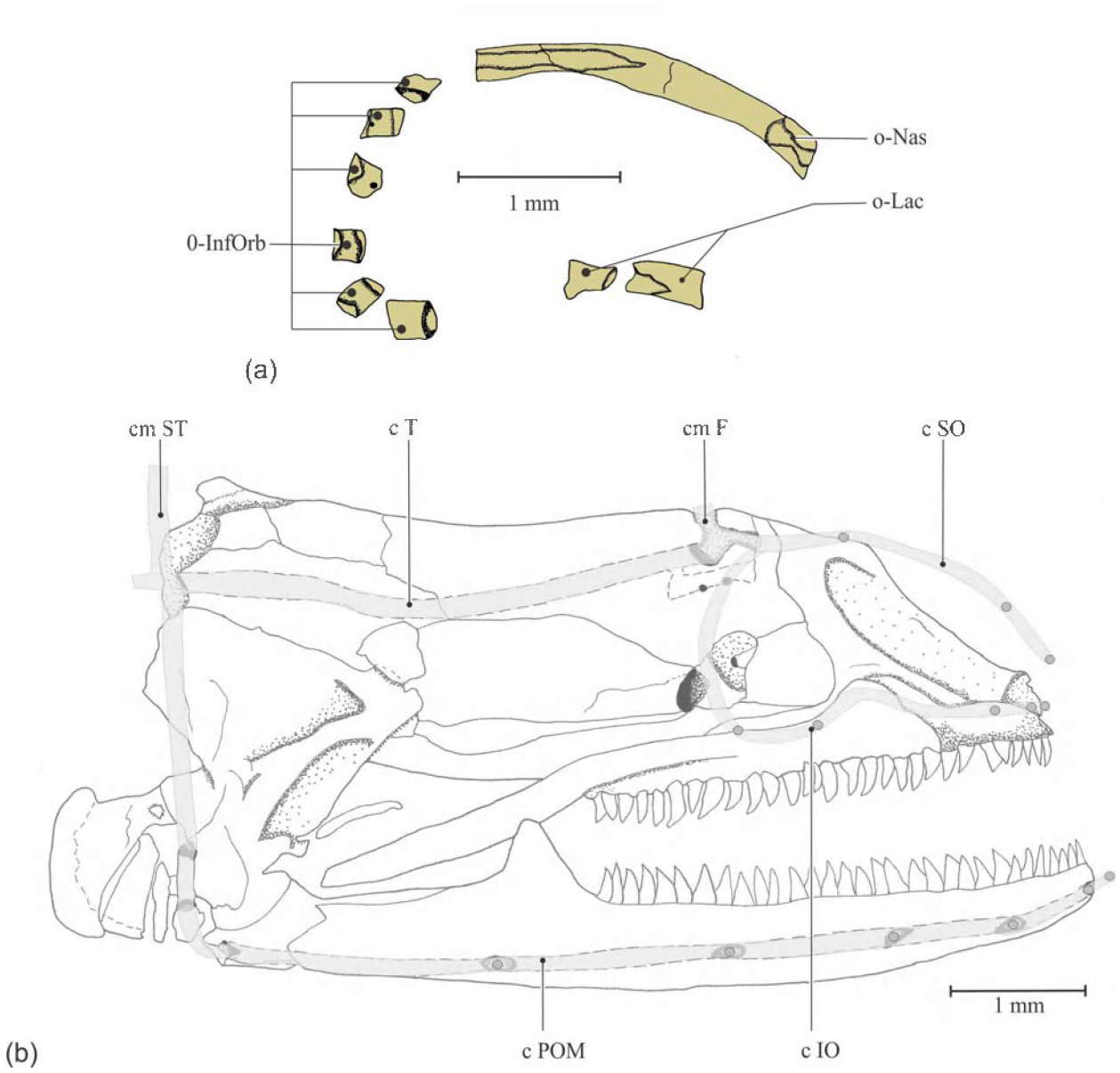

Figure 6.18: The cranial lateral line system and circumorbital bones of *Anarchias allardicei*. (a) lateral view of the nasal bone, preorbital bones and postorbital bones (right side) and (b) position of the composing canals in relation to the skull (right side, lateral view). c IO, infraorbital canal; c POM, preopercular mandibular canal; c SO, supraorbital canal; c T, temporal canal; cm F, frontal commissure; cm ST, supratemporal commissure; o-Nas, nasal bone; o-InfOrb, infraorbital bone; o-Lac, lacrimal bone.

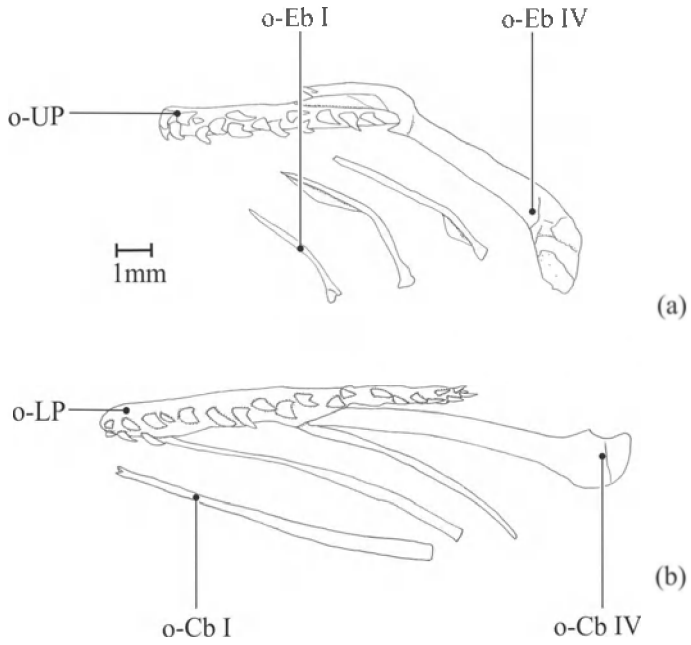

Figure 6.19: Gill arches of *Gymnothorax prasinus*. (a) Ventral view of the dorsal elements and (b) dorsal view of the ventral elements. o-Cb, ceratobranchial bone; o-Eb, epibranchial bone; o-LP, lower pharyngeal tooth plates; o-UP, upper pharyngeal tooth plates.

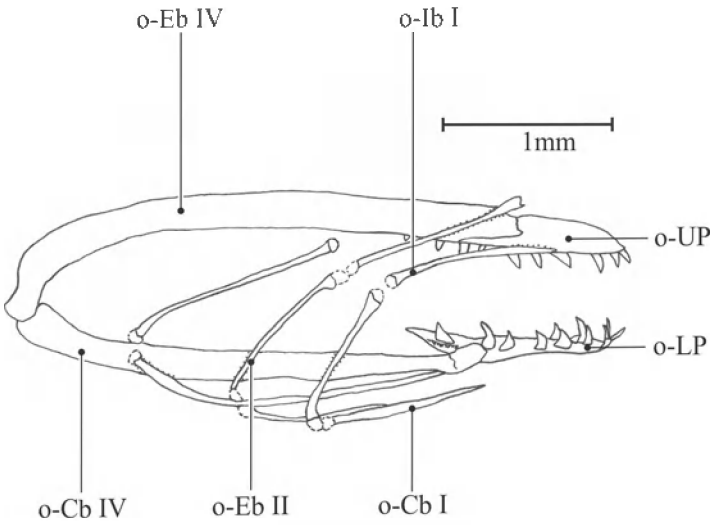

Figure 6.20: Gill arches of *Anarchias allardicei*. Lateral view of the ventral and dorsal part of the gill arches (right side). o-Cb, ceratobranchial bone; o-Eb, epibranchial bone; o-Ib, infrapharyngobranchial bone; o-LP, lower pharyngeal tooth plates; o-UP, upper pharyngeal tooth plates.

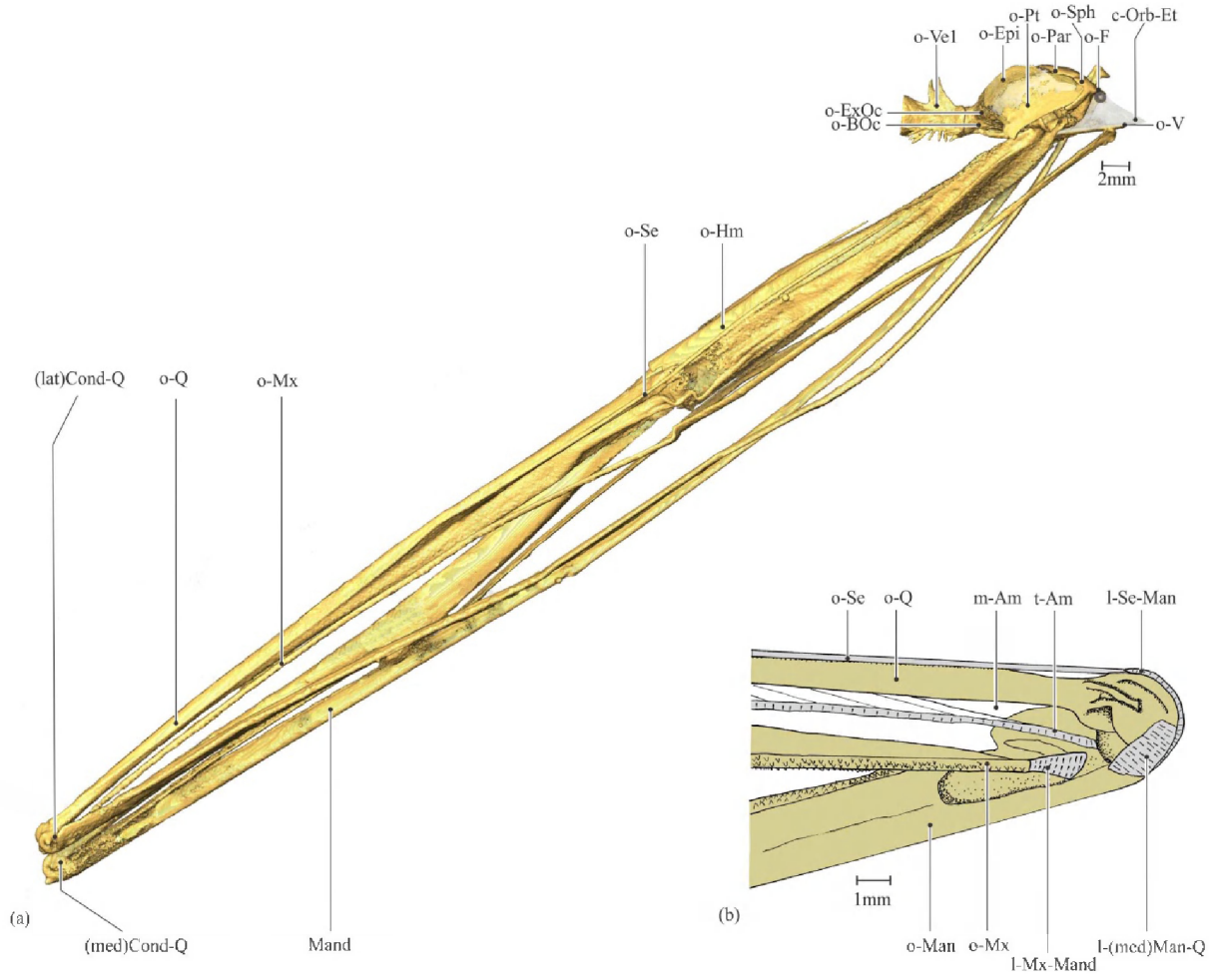

Figure 7.1: Cranial skeleton in *Eurypharynx pelecanoides* (Lateral view). (a) Complete scanned skull (right side), and (b) medial view the quadrato-mandibula joint (right side). c-orbito-ethmoid cartilage; (lat)Cond-Q, lateral condyle of quadrate; (med)Cond-Q, medial condyle of quadrate; l-(med)Man-Q, medial mandibulo-quadrate ligament; l-Se-Man, Sesamoid bone-mandibula ligament; o-BOc, basioccipital; o-Epi, epioccipital; o-ExOc, exoccipital; o-F, frontal; o-Hm, hyomandibula; Mand, mandibula; o-Mx, maxillary; o-Par, parietal; o-Pt, pterotic; o-Q, quadrate; o-Se, sesamoid bone; o-Sph, sphenotic; o-V, vomer; o-Ve1, first vertebra; m-Am, adductor mandibulae muscle; t-Am, tendon of the adductor mandibulae muscle.

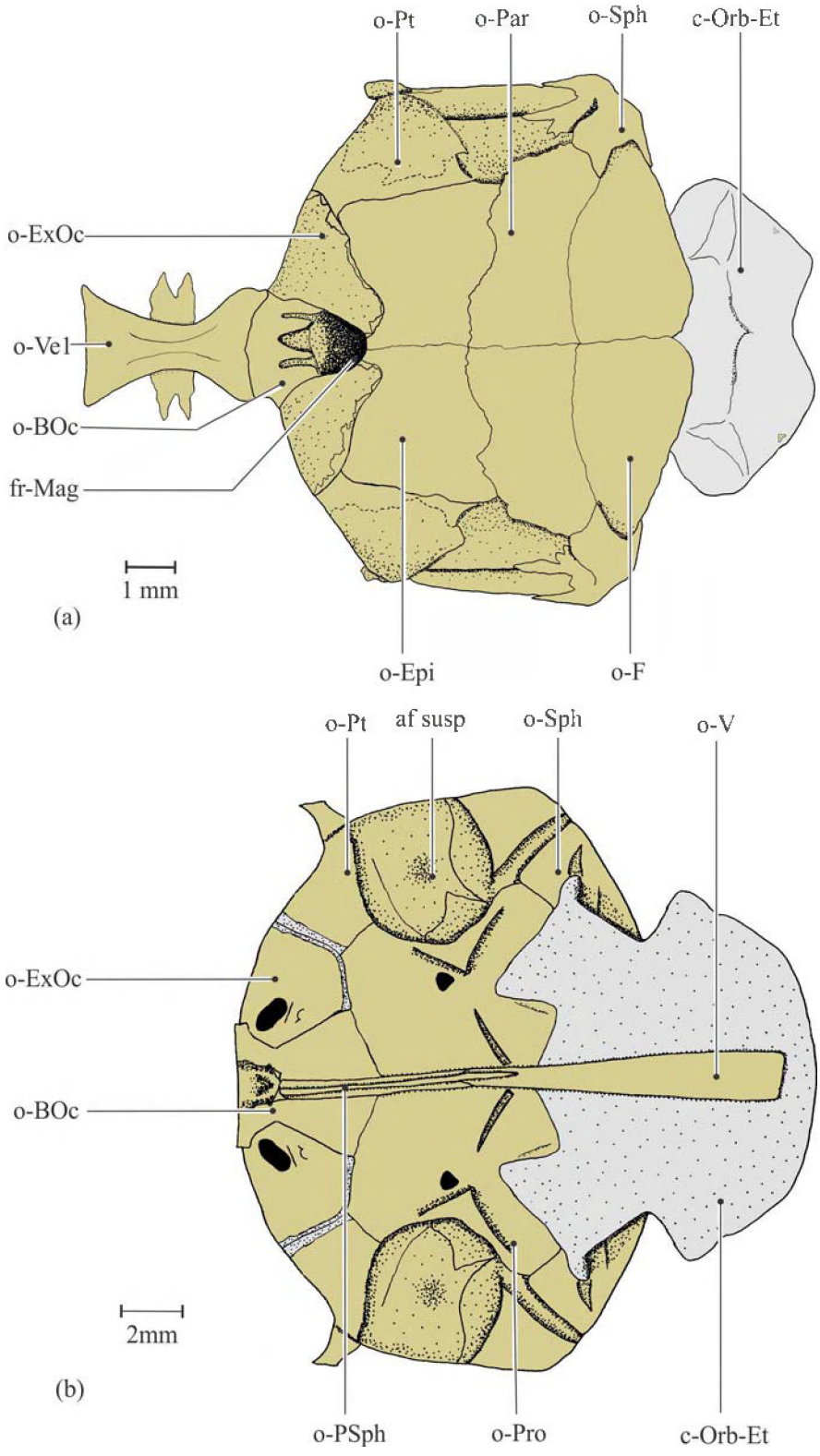
o-Pt
o-Par
o-Sph
c-Orb-Et
o-ExOc
o-Ve1
o-BOc
fr-Mag
1 mm
(a)
o-Epi
o-F
o-Pt
af susp
o-Sph
o-V
o-ExOc
o-BOc
2mm
(b)
o-PSph
o-Pro
c-Orb-Et

Figure 7.2: Neurocranium of *Eurypharynx pelecanoides*. (a) Dorsal view, and (b) Ventral view. af susp, suspensorial articulation facet; c-orbito-ethmoid cartilage; fr-Mag, foramen magnum; o-BOc, basioccipital; o-Epi, epioccipital; o-ExOc, exoccipital; o-F, frontal; o-Par, parietal; o-Pro, prootic; o-PSph, parasphenoid; o-Pt, pterotic; o-Sph, sphenotic; o-V, vomer; o-Ve1, first vertebra.

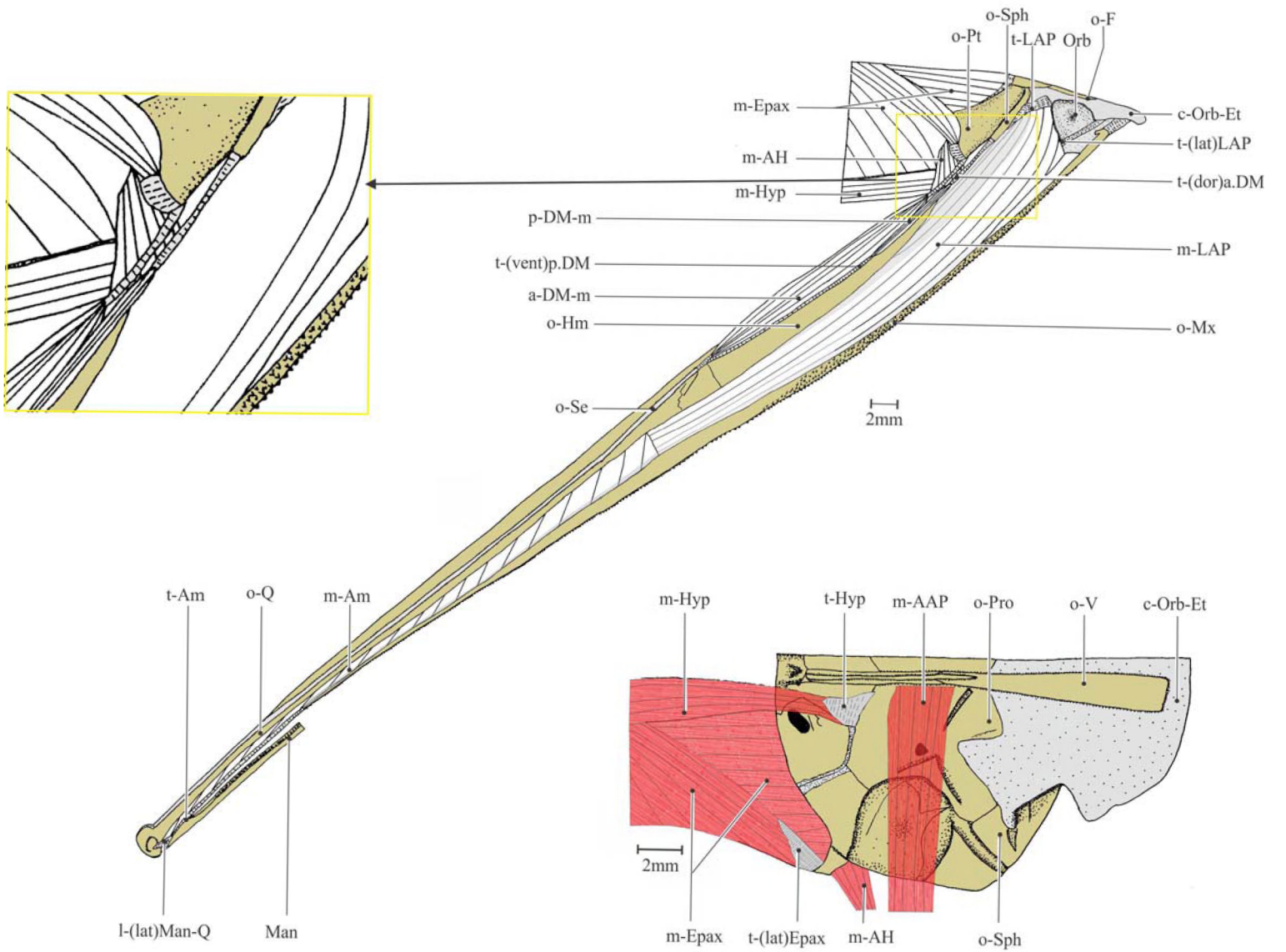
o-Sph
o-Pt
t-LAP
Orb
o-F
m-Epax
c-Orb-Et
t-(lat)LAP
m-AH
t-(dor)a.DM
m-Hyp
p-DM-m
m-LAP
t-(vent)p.DM
a-DM-m
o-Hm
o-Mx
o-Se
2mm
t-Am
o-Q
m-Am
l-(lat)Man-Q
Man
m-Hyp
t-Hyp
m-AAP
o-Pro
o-V
c-Orb-Et
2mm
m-Epax
t-(lat)Epax
m-AH
o-Sph

Figure 7.3: The cranial muscles of *Eurypharynx pelecanoides*. (a) Skin removed (lateral view) and does not show entire length of the mandibula, and (b) muscles of the ventral view of neurocranium. m-AAP, adductor arcus palatini muscle; m-Am, adductor mandibulae muscle; m-AH, adductor hyomandibulae muscle; a-DM-m, anterior depressor mandibulae muscle; p-DM-m, posterior depressor mandibulae muscle; m-Epax, epaxial muscles; m-Hyp, hypaxial muscles; m-LAP, levator arcus palatini muscle; c-orbito-ethmoid cartilage; o-BOc, basioccipital; o-Epi, epioccipital; o-ExOc, exoccipital; o-F, frontal; o-Hm, hyomandibular bone; Mand, mandibula; o-Mx, maxillary bone; o-Par, parietal; o-Pro, prootic; o-Pt, pterotic; o-Q, quadrate; o-Se, sesamoid bone; o-Sph, sphenotic; o-V, vomer; o-Ve1, first vertebra; Orb, orbit; t-Am, adductor mandibulae tendon; t(vent)p.DM, ventral tendon of posterior depressor mandibulae muscle; t(dor)p.DM, dorsal tendon of posterior depressor mandibulae muscle; t(lat)Epax, lateral tendon of epaxial muscles; t-Hyp, tendon of hypaxial; t-LAP, tendon of levator arcus palatini muscle.

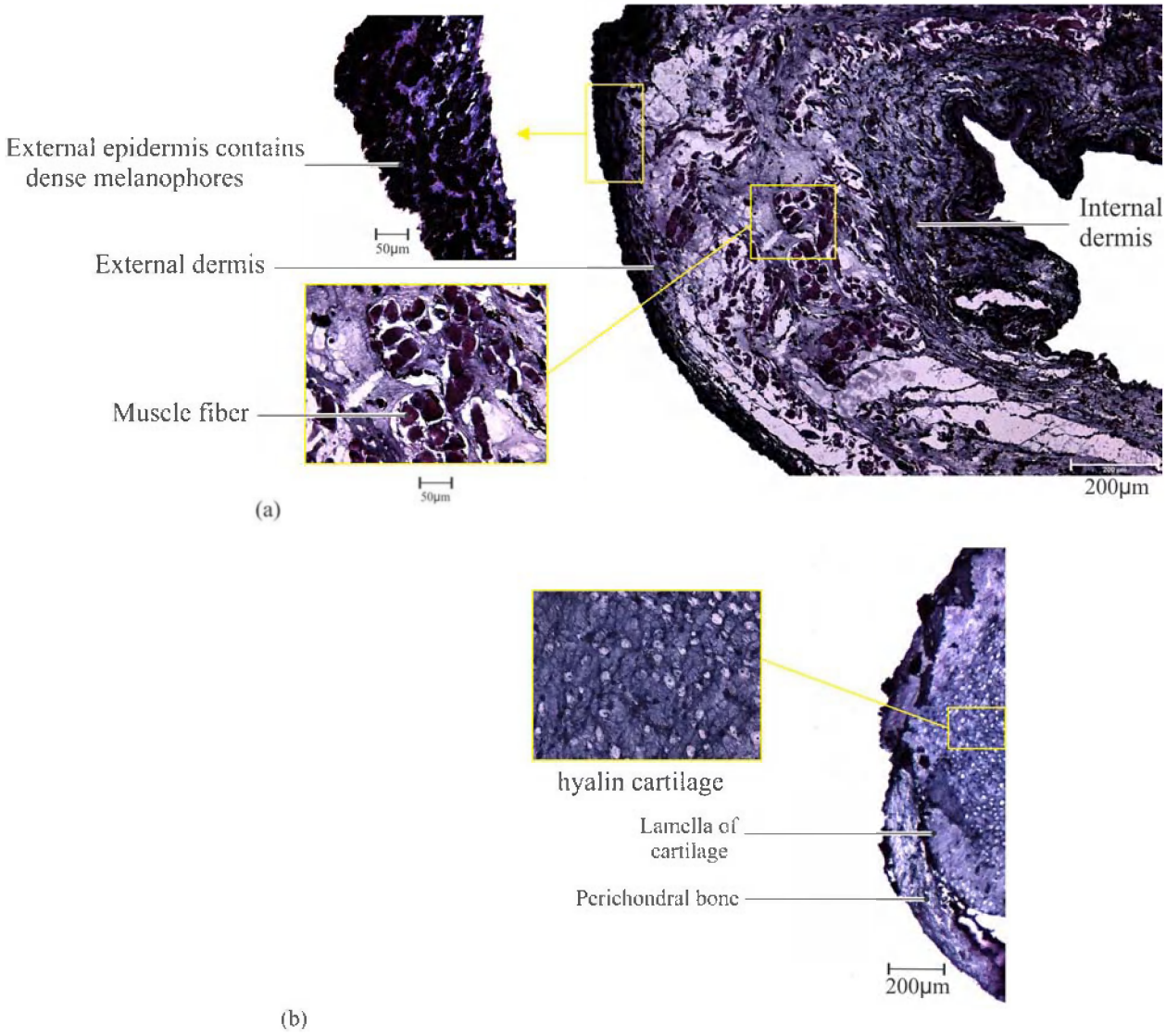

Figure 7.4: Histological section of the skin and bone in *Eurypharynx pelecanoides*: (a) cross section of the skin around the mouth, and (b) cross section of the hyomandibula.

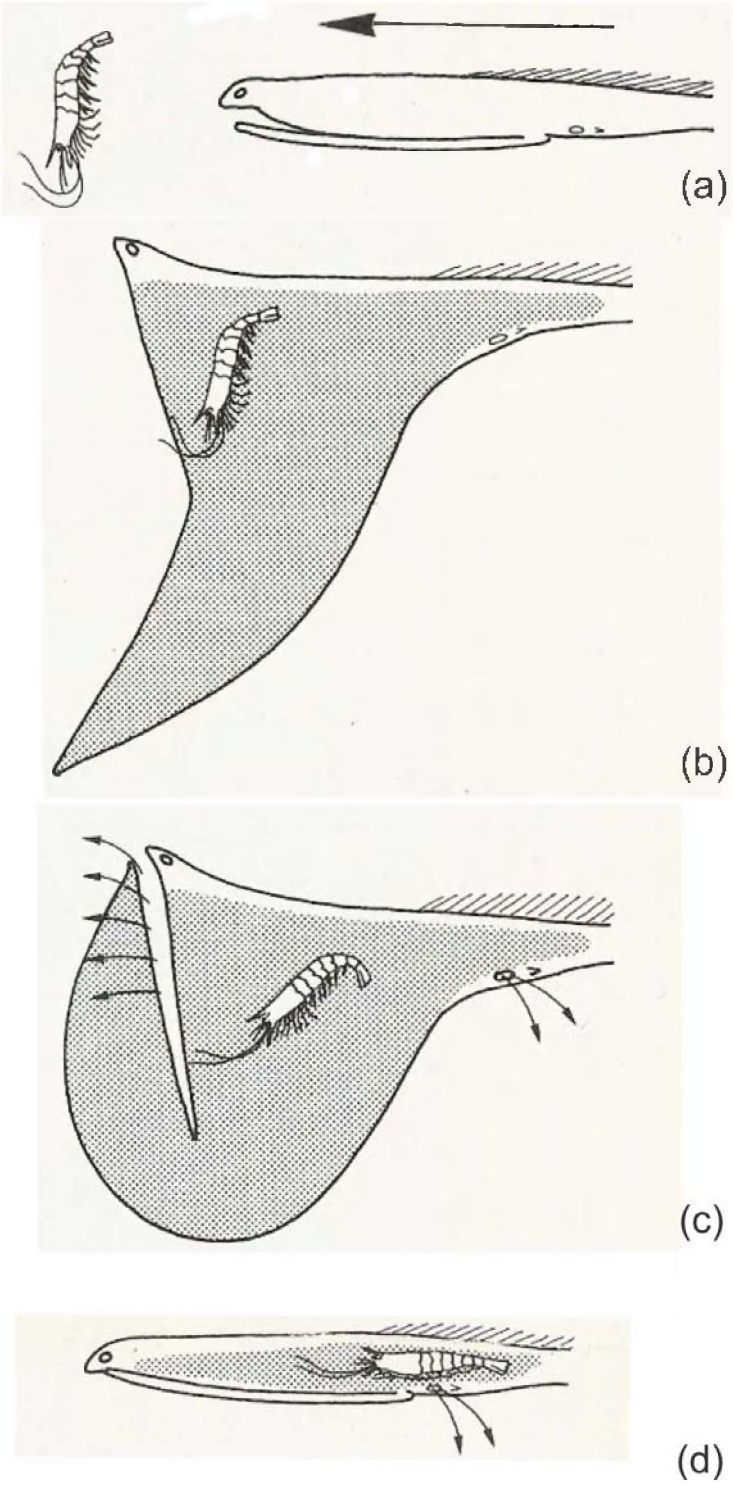

Figure 7.5: Stages of supposed feeding strategy by Nielsen et al. (1989) (after Nielsen et al. 1989).

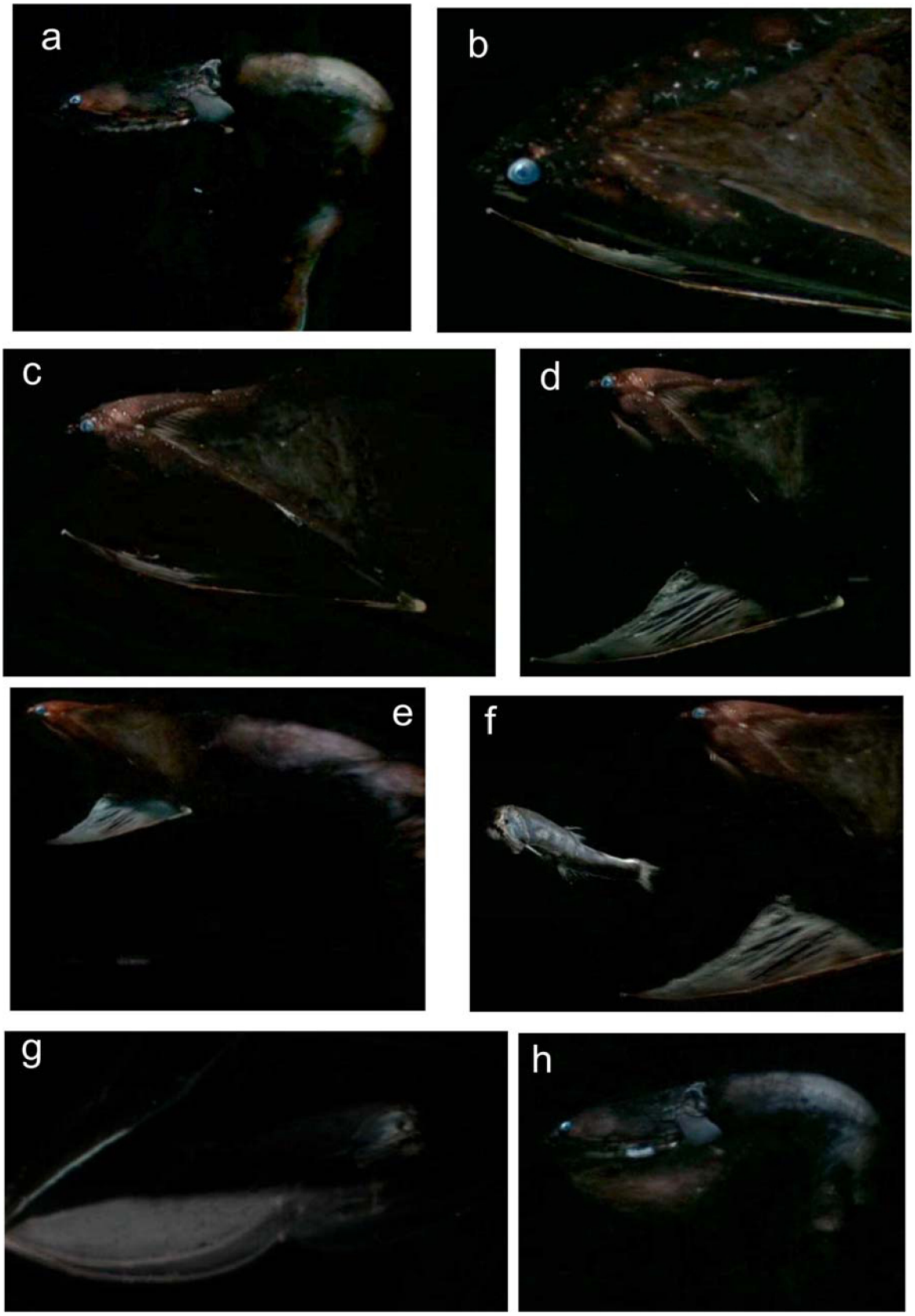
a
b
c
d
e
f
g
h

Figure 7.6: Stages of feeding in *Eurypharynx pelecanoides*: (a) Swimming, (b) detecting the prey and starting point of mouth opening, (c) first stage of mouth opening, (d) opened mouth at nearly a right angle, (e) moving towards the prey with the mouth opened, (f) engulfing of the prey, (g) closing mouth,(h) food items stay in the ventral pouch of the buccal cavity (after Blue planet: Eposid2 - The Deep, 2001).

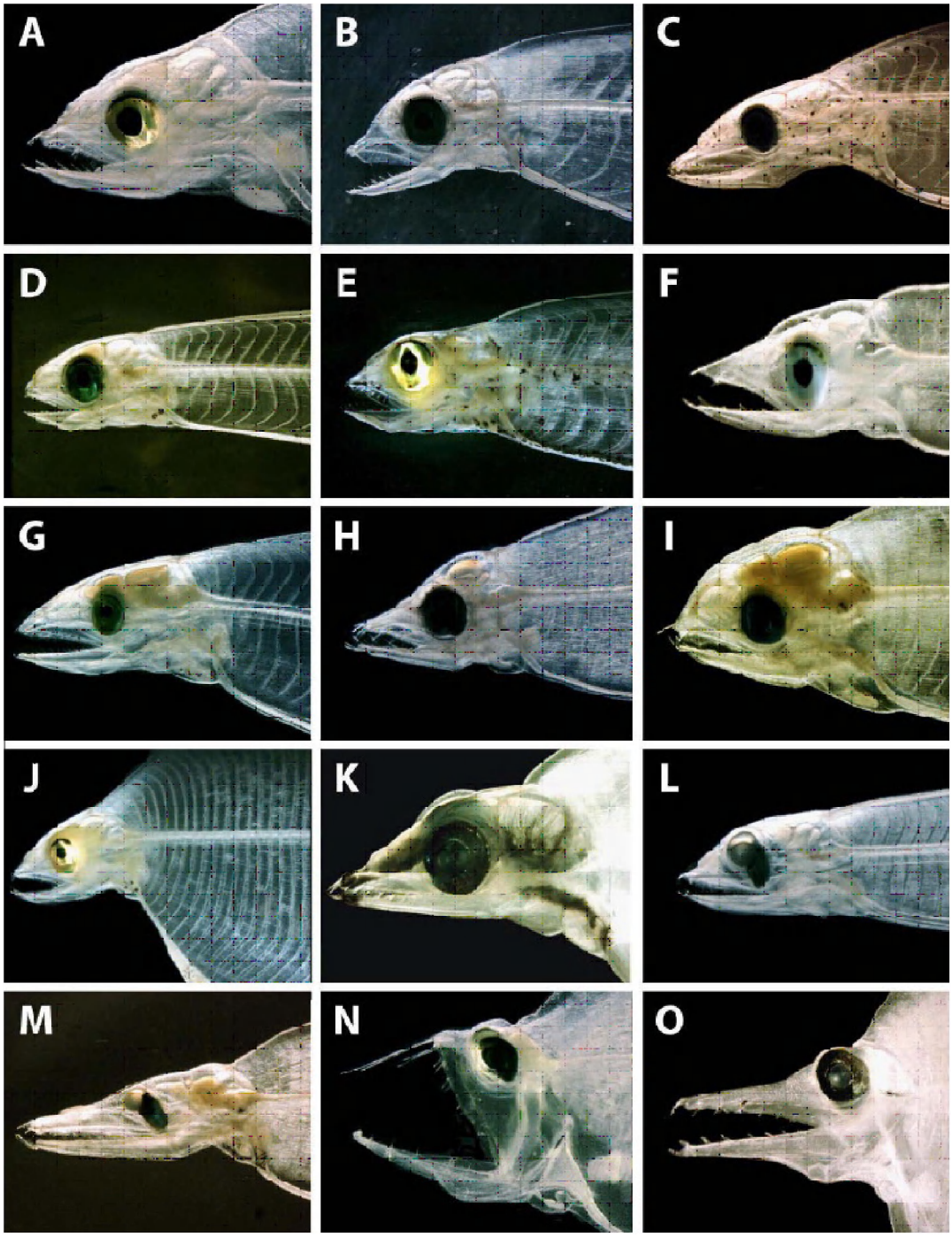

Figure. 8.1. Photographs showing typical head and jaw shapes of many types of anguilliform leptocephali. These taxa are *Anguilla marmorata* (A), *Ariosoma major* (B), *Heteroconger hassi* (C), *Conger* sp. (D), *Bathycongrus* sp. (E), *Gnathophis* sp. (F), *Muraenesox cinereus* (G), Serrivomeridae sp. (H), Muraenidae sp. (I), Chlopsidae sp. (J), *Nettenchelys* sp. (K), and Synaphobranchinae sp. (L), Ilyophinae, Synaphobranchidae (M), *Eurypharynx pelecanoides* (N), *Cyema atrum* (O). (after Miller and Tsukamoto, 2004).

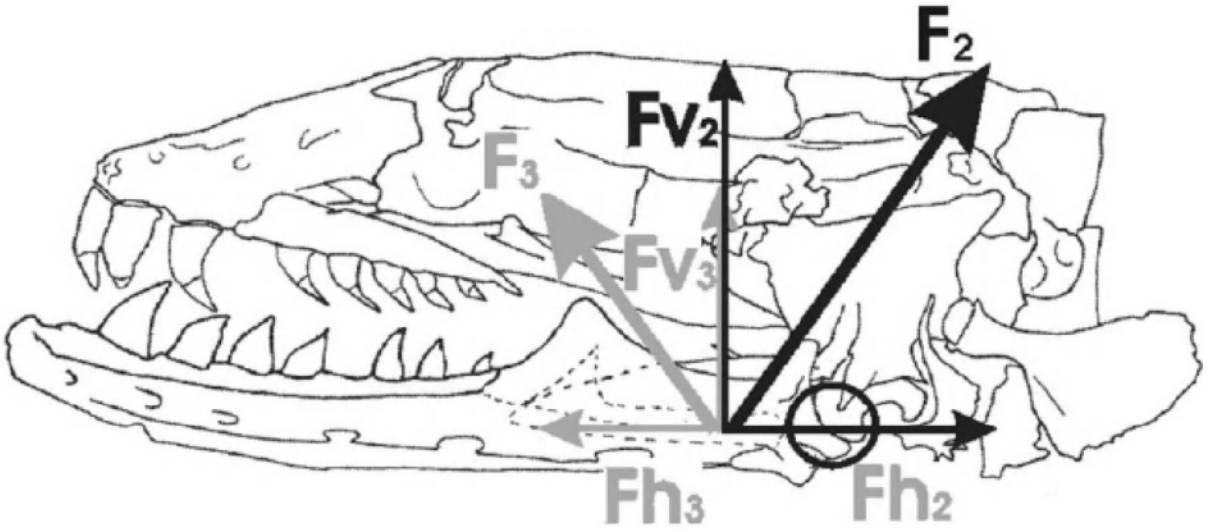

Figure. 8.2. Schematic illustration of the generated forces by the adductor mandibulae A2 (F2) and A2 (F3) with, respectively, their horizontal (Fh 2 and Fh 3) and vertical components (Fv 2 and Fv 3). The horizontal components run in the opposite direction, reducing the pressure in the joint between the lower jaw and the quadrate (encircled) (after De Schepper et al, 2005).